

TOWARDS A RAPID DIAGNOSTIC METHOD TO IDENTIFY BACTERIA ASSOCIATED WITH AOD

VICTORIA BUENO-GONZÁLEZ

A thesis submitted in partial fulfilment of the requirements of the University of the
West of England, Bristol for the degree of Doctor of Philosophy (PhD)

This research programme was carried out in collaboration with Forest Research and
Woodland Heritage

Faculty of Applied Sciences, University of the West of England, Bristol

July 2022

Word Count: 65,888

ABSTRACT

British oaks, *Quercus robur* and *Q. petraea* are threatened by Acute Oak Decline (AOD). Severe cases are lethal within five years. Symptoms include bleeding, longitudinal, necrotic cracks in the bark, from which a dark fluid emanates. AOD is caused by the interaction of several bacterial species, with *Brenneria goodwinii* and *Gibbsiella quercinecans* being the predominant pathogens. Species belonging to the *Enterobacterales* and *Pseudomonadaceae* are also routinely isolated from symptomatic trees.

To further investigate the bacteria associated with AOD, several novel species of *Pseudomonas* have been identified and described following a polyphasic approach. Their potential role in AOD was investigated through the genomic analysis of virulence factors, hypersensitive response tests in bean pods and tobacco leaves, and cell attachment assays. The study of the taxonomic relationships between the novel *Pseudomonas* and its neighbours led to a taxonomic reassessment of this polyphyletic genus. The polyphasic approach and phylogenetic analysis suggested that the phylogenetic boundaries within *Pseudomonas* and between *Pseudomonas* and neighbouring genera: *Azomonas*, *Azotobacter* and *Azorhizophilus* (collectively known as the “*Azotobacter* group”) were not well defined.

Three novel AOD-associated *Pseudomonas* were described in this project: *Pseudomonas daroniae* sp. nov. *Pseudomonas dryadis* sp. nov., and *Pseudomonas kirkliae* sp. nov. These novel *Pseudomonas* do not present a typical phytopathogenic set of genomic or phenotypic features. The phylogenetic study of the *Azotobacter* group suggested that *Pseudomonas*, *Azotobacter* and *Azomonas* should remain separated; and in turn, the polyphyletic *Pseudomonas* should be divided into several novel genera, conserving as *Pseudomonas* only those belonging to the *P. aeruginosa* lineage.

Many field samples of oaks affected by AOD must be processed on a daily basis, requiring a fast and cost-effective method of detection and identification. A multiplex high-resolution melt (HRM) analysis has been developed for the identification of AOD indicators: *B. goodwinii*, *G. quercinecans*, *Rahnella victoriana* and *Lonsdalea britannica*. HRM analysis is a real-time PCR-based technique in which single nucleotide polymorphisms can be identified in amplicons, without DNA sequencing. The multiplex HRM assay can identify up to four targets from field samples, in a single tube, in just 40 minutes per HRM run. For optimal detection, the sample must be incubated anaerobically in solid media to stimulate the growth of the targets, which are facultative anaerobes. The colonies can be used directly as a template for HRM without DNA extraction. Additionally, several tools designed to work with pure cultures were developed, including: a duplex-HRM assay of the genes *atpD* and *rpoD* for the identification of AOD-associated bacteria including the novel AOD-associated *Pseudomonas*; and three SNP-based HRM assays for the differentiation of species and subspecies of the AOD-associated genera *Gibbsiella*, *Brenneria* and *Rahnella*. The HRM-based diagnostic methods will potentially be useful tools for research institutions working with AOD and will save time and resources in the fight against the disease.

ACKNOWLEDGEMENTS

This acknowledgment section could be longer than the thesis itself, as I have been fortunate to be accompanied and supported by many excellent people. From family to friends, and without forgetting work colleagues or fellow PhD students, I want to thank all of them, who have made this journey from student to researcher a journey full of unconditional support, knowledge, and laughter.

First, I am grateful to my supervisors, Professor Dawn Arnold, Dr Carrie Brady, Dr Sandra Denman, and Associate Professor Joel Allainguillaume for giving me the opportunity to do this PhD, and for guiding, and supporting me throughout this research and personal journey. I am proud to have completed my thesis in an environment full of inspiring female figures with successful careers in STEM. I want to give special thanks to Carrie, an excellent scientist and role model from whom I have learned a lot. I would also like to thank the University of the West of England, Forest Research and Woodland Heritage for funding the project, and the researchers whose work I was able to build on.

Of course, I dedicate this work to my wonderful family (my parents Guillermo and María Victoria and my brother Guillermo) and to my friends. I would love to acknowledge the support received from my fellow PhD students and the rest of the lab group members (and friends), especially, Megan, and Helen. Thanks to my degree friends, it all started with them many (many) years ago. Our friendship and support remain today as strong as our love for science. I want to mention Chris Jones and Janet Tingle, they believed in me, and their wisdom and passion for Microbiology and Molecular Biology inspired me to follow these paths of knowledge. Thanks to the people who made Bristol even better, especially Sara. Finally, I want to thank the love of my life, Chuso, for his love and support during this time.

TABLE OF CONTENTS

ABSTRACT.....	II
ACKNOWLEDGEMENTS.....	III
TABLE OF CONTENTS.....	IV
LIST OF TABLES.....	XII
LIST OF FIGURES.....	XV
LIST OF ABBREVIATIONS	XXIII
CHAPTER 1. Introduction	1
1.1. Tree diseases in the United Kingdom	2
1.1.1. Oak decline.....	2
1.2. Acute Oak Decline (AOD)	5
1.2.1. Description and distribution of AOD.....	5
1.2.2. Host, symptoms and causes of AOD	6
1.2.3. Bacteria associated with AOD	10
1.2.4. Management of AOD	14
1.3. Plant-associated bacteria	14
1.4. Bacterial plant pathogen detection methods	15
1.5. Previous work in diagnosis of AOD	17
1.6. Taxonomic identification of bacteria	20
1.7. Aims, objectives and scope of the research project	22
CHAPTER 2. Materials and methods	23
2.1. Bacterial strains.....	24
2.2. Media and culture conditions	31
2.3. Revival of freeze-dried cultures	31
2.4. Formal classification of AOD-associated Pseudomonads	31
2.4.1. Genomic DNA extraction	31

2.4.2. Quantification of DNA purity and concentration.....	32
2.4.3. Polymerase chain reaction (PCR)	32
2.4.4. Agarose gel electrophoresis.....	35
2.4.5. DNA fingerprinting of AOD-associated Pseudomonads: BOX-PCR, ERIC-PCR and RAPD-PCR	35
2.4.6. ExoSAP Clean-up of PCR products prior to DNA sequencing.....	36
2.4.7. Preparation of PCR products for DNA sequencing	36
2.4.8. Genotypic characterisation of the AOD-associated Pseudomonads	36
2.4.8.1. 16S rRNA sequence analysis of the AOD-associated Pseudomonads...	36
2.4.8.2. Multilocus sequence analysis of the AOD-associated Pseudomonads.	37
2.4.8.3. Whole bacterial genome sequencing and analysis.....	38
2.4.8.3.1. Average Nucleotide Identity studies (ANI).....	38
2.4.8.3.2. <i>In silico</i> DNA-DNA hybridisation (<i>is</i> DDH).....	38
2.4.9. Description of cultural characteristics of AOD-associated Pseudomonads.	38
2.4.10. Description of cell characteristics of AOD-associated Pseudomonads.....	39
2.4.10.1. Transmission electron microscopy of AOD-associated Pseudomonads	39
2.4.11. Phenotypic characterisation of the AOD-associated Pseudomonads	39
2.4.11.1. API 20NE.....	40
2.4.11.2. API 50 CH.....	40
2.4.11.3. Biolog GN2 Microplates	40
2.4.11.4. Oxidase and catalase test	41
2.4.11.5. Studies of temperature, pH, and salt concentration tolerance ranges	41
2.4.12. Chemotypic characterisation of the AOD-associated Pseudomonads by fatty acid methyl esters (FAMES) profiling.....	41
2.4.13. Phylogenetic study of the relationships amongst <i>Pseudomonas</i> , <i>Azomonas</i> , <i>Azotobacter</i> and <i>Azorhizophilus</i>	42

2.5. Investigation of the potential pathogenicity traits of the AOD-associated <i>Pseudomonas</i>	42
2.5.1. Virulence factors in AOD-associated <i>Pseudomonas</i>	42
2.5.2. Hypersensitive response test of the AOD-associated <i>Pseudomonads</i> in bean pods.....	43
2.5.3. Hypersensitive response test of the combination of AOD-associated <i>Pseudomonads</i> and Bg, Gq and Rvi in bean pods.....	44
2.5.4. Hypersensitive response test of the AOD-associated <i>Pseudomonads</i> in tobacco leaves.....	45
2.5.5. Cell attachment assays.....	45
2.6. Rapid diagnostic method for the bacteria associated with AOD	46
2.6.1. High resolution melting analysis (HRM).....	46
2.6.2. HRM of the <i>atpD</i> gene (119 bp).....	48
2.6.2.1. HRM of the <i>atpD</i> gene (119 bp): Assessment of the effect of different sample preparation methods on HRM of the <i>atpD</i> gene	48
2.6.2.2. HRM of the <i>atpD</i> gene (119 bp): assessing the effects of strain combination on the HRM <i>atpD</i> assay	48
2.6.3. HRM of the <i>atpD</i> gene (320 bp): Assessment of increased amplicon length. HRM combined with agarose gel fingerprinting for the identification of AOD-associated bacteria, including AOD-associated <i>Pseudomonads</i>	49
2.6.3.1. Duplex-HRM assay of genes <i>atpD</i> (320 bp) and <i>rpoD</i> for the identification of AOD-associated bacteria including AOD-associated <i>Pseudomonads</i>	49
2.6.4. Multiplex-HRM assay for the detection and identification of Bg, Gq, Rvi and Lb.....	50
2.6.4.1. Multiplex-HRM assay specificity test	55
2.6.4.2. Multiplex-HRM assay sensitivity test	55
2.6.5. Single nucleotide polymorphism (SNP)-based HRM assay for the differentiation of species and subspecies of the genus <i>Brenneria</i>	55
2.6.5.1. SNP-based HRM assay for the differentiation of species of the genus <i>Rahnella</i>	56

2.6.5.2. SNP-based HRM assay for the differentiation of species of the genus <i>Gibbsiella</i>	57
2.7. Isolation, purification and identification of bacteria from field samples	57
2.7.1. Isolation, purification and identification of bacteria from oak stem and multiplex-HRM test.....	59
2.7.2. Isolation, purification and identification of epiphytic + endophytic bacteria and endophytic bacteria alone from oak leaves and multiplex-HRM test	60
2.8. Optimisation of processing of field samples for downstream HRM analysis: assessing the effect of sample preparation	62
2.8.1. Duplex-HRM assay for the detection and identification of Bg and Gq in initial stem suspensions.....	62
2.8.2. Duplex-HRM assay for the detection and identification of Bg and Gq in overnight LB broths.....	63
2.8.3. Duplex-HRM assay for the detection and identification of Bg and Gq in Kew 2: optimal temperature and atmosphere test.....	63
2.8.4. Duplex-HRM assay for the detection and identification of Bg and Gq in Kew 2: optimal media and atmosphere test	63
2.8.5. Duplex-HRM assay for the detection and identification of Bg and Gq in Kew 1, Kew 2, Kew 3, Kew 6 and Kew 11: optimal media and atmosphere test.....	64
2.8.6. Validation of the multiplex-HRM assay for the detection and identification of Bg, Gq, Rvi and Lb	65
CHAPTER 3. Taxonomic description of <i>Pseudomonas</i> associated with AOD.....	66
3.1. Introduction	67
3.2. Results.....	73
3.2.1. Genotypic characterisation of AOD-associated <i>Pseudomonas</i>	73
3.2.1.1. Phylogenetic analysis based on the partial 16S rRNA gene.....	73
3.2.1.2. MLSA study of the concatenated <i>gyrB</i> , <i>rpoB</i> and <i>rpoD</i> genes.....	78
3.2.1.3. DNA fingerprinting of AOD-associated <i>Pseudomonas</i>	83
3.2.1.4. Whole genome sequencing	85

3.2.1.5. Average Nucleotide Identity studies based on BLAST (ANiB) and <i>in silico</i> DNA-DNA hybridisation (<i>isDDH</i>)	86
3.2.2. Cultural characteristics of AOD-associated <i>Pseudomonas</i>	93
3.2.3. Cell characteristics of AOD-associated <i>Pseudomonas</i>	93
3.2.4. Phenotypic characterisation of the AOD-associated <i>Pseudomonas</i>	94
3.2.4.1. API 20NE and API 50 CH tests	94
3.2.4.2. Biolog GN2 microplates and catalase and oxidase activity.....	95
3.2.4.3. Studies of pH, salt concentration and temperature tolerance ranges	105
3.2.5. Chemotypic characterisation of the AOD-associated <i>Pseudomonas</i> by fatty acid methyl esters (FAMES) profiling	105
3.2.6. Phylogenetic study of the relationships amongst <i>Pseudomonas</i> , <i>Azomonas</i> , <i>Azotobacter</i> and <i>Azorhizophilus</i>	108
3.3. Discussion.....	114
CHAPTER 4. Investigation of the potential pathogenicity traits of the AOD-associated <i>Pseudomonas</i>	119
4.1. Introduction	120
4.2. Results.....	124
4.2.1. Virulence factors in AOD-associated <i>Pseudomonas</i>	124
4.2.2. Hypersensitive response test of the AOD-associated <i>Pseudomonas</i> in bean pods.....	132
4.2.3. Hypersensitive response test of the AOD-associated <i>Pseudomonas</i> in tobacco leaves.....	134
4.2.4. Cell attachment assays in AOD-associated <i>Pseudomonas</i>	134
4.2.4.1. Six-well plate assay of Pda, Pdr and Pki, performed in TSB	135
4.2.4.2. Tube-coverslip assay of Pda, Pdr and Pki, performed in LB: cell attachment in Falcon tubes	137
4.2.4.3. Tube-coverslip assay of Pda, Pdr and Pki, performed in LB: cell attachment in glass coverslips	138
4.2.4.4. Tube-coverslip assay of Pki, performed in LB and TSB: cell attachment in Falcon tubes and glass coverslips	140

4.3. Discussion.....	143
CHAPTER 5. Development of HRM-based tools for the identification and detection of AOD-associated bacteria	148
5.1. Introduction	149
5.2. Results.....	154
5.2.1. HRM of the <i>atpD</i> gene	154
5.2.1.1. HRM of the <i>atpD</i> gene: different sample preparation methods	154
5.2.1.2. HRM of the <i>atpD</i> gene: combined species test	155
5.2.2. HRM of the <i>atpD</i> gene: HRM combined with agarose gel fingerprinting for the identification of AOD-associated bacteria including <i>Pseudomonas</i>	158
5.2.3. Duplex-HRM assay of genes <i>atpD</i> and <i>rpoD</i> for the identification of AOD-associated bacteria including AOD-associated <i>Pseudomonas</i>	160
5.2.4. Multiplex-HRM assay for the detection and identification of Bg, Gq, Rvi, and Lb.....	163
5.2.4.1. Multiplex-HRM assay specificity test	166
5.2.4.2. Multiplex-HRM assay sensitivity test	168
5.2.5. SNP-based HRM assay for the differentiation of species and subspecies of the genus <i>Brenneria</i>	169
5.2.6. SNP-based HRM assay for the differentiation of species of the genus <i>Rahnella</i>	173
5.2.7. SNP-based HRM assay for the differentiation of species of the genus <i>Gibbsiella</i>	176
5.3. Discussion.....	179
CHAPTER 6. Optimisation of pre-HRM field sample processing, and validation of multiplex-HRM assay.....	185
6.1. Introduction	186
6.2. Results.....	189
6.2.1. Field sample processing optimisation studies	189
6.2.1.1. Duplex-HRM assay for the detection and identification of Bg and Gq in initial stem suspensions	190

6.2.1.2. Duplex-HRM assay for the detection and identification of Bg and Gq in overnight LB broths.....	190
6.2.1.3. Duplex-HRM assay for the detection and identification of Bg and Gq in Kew 2: optimal temperature and atmosphere test	192
6.2.1.4. Duplex-HRM assay for the detection and identification of Bg and Gq in Kew 2: optimal media and atmosphere test.....	193
6.2.1.5. Duplex-HRM assay for the detection and identification of Bg and Gq in Kew 1, Kew 2, Kew 3, Kew 6 and Kew 11: optimal media and atmosphere test	194
6.2.1.6. Multiplex-HRM assay for the detection and identification of Bg, Gq, Rvi and Lb in KP 1, KP 2 and KP 3: optimal atmosphere test	196
6.2.2. Validation of the multiplex-HRM assay for the detection and identification of Bg, Gq, Rvi and Lb. Isolation, purification and identification of bacteria from oak stem	197
6.2.3. SNP-based HRM assay for the differentiation of species of the genus <i>Rahnella</i>	207
6.2.4. Isolation, purification and identification of endophytic and epiphytic bacteria from oak leaves and multiplex-HRM test	209
6.3. Discussion.....	213
CHAPTER 7. Final discussion	220
7.1. Introduction	221
7.2. General overview	222
7.3. Conclusion.....	229
7.4. Future work.....	232
References	234
Appendix I: Bayesian 16S rRNA phylogenetic tree of the AOD-associated strains representatives of clusters A and B, 35 closest phylogenetic neighbours, and the outgroup <i>Acinetobacter baumannii</i>	261
Appendix II: Maximum likelihood 16S rRNA gene phylogenetic tree of the AOD-associated strain representative of cluster C, 38 closest phylogenetic neighbours, and the outgroup <i>Endozoicomonas elysicola</i>	262

Appendix III: Maximum likelihood MLSA phylogenetic tree of the concatenated gene sequences <i>gyrb</i> , <i>rpob</i> and <i>rpod</i> , obtained from the AOD-associated strains in cluster C, 25 closest phylogenetic neighbours, and the outgroup <i>Stenotrophomonas maltophilia</i>	263
Appendix IV: Bayesian MLSA phylogenetic tree of the concatenated gene sequences <i>gyrb</i> , <i>rpob</i> and <i>rpod</i> , obtained from AOD-associated strains in clusters A and B, 35 closest phylogenetic neighbours and the outgroup <i>Pseudomonas pertucinogena</i>	264
Appendix V: Maximum likelihood MLSA phylogenetic tree of the concatenated amino acid sequences <i>gyrb</i> , <i>rpob</i> and <i>rpod</i> , obtained from AOD-associated strains in clusters A and B, 35 closest phylogenetic neighbours and the outgroup <i>Pseudomonas pertucinogena</i>	265
Appendix VI: Maximum likelihood MLSA phylogenetic tree of the concatenated amino acid sequences <i>gyrb</i> , <i>rpob</i> and <i>rpod</i> , obtained from the AOD-associated strains in cluster C, 25 closest phylogenetic neighbours and the outgroup <i>Stenotrophomonas maltophilia</i>	266
Appendix VII: GenBank accession numbers for the MLSA trees of the aod-associated <i>Pseudomonas</i>	268
Appendix VIII: Phenotypic characteristics of the AOD-associated strains in cluster A, B and C, and their closest neighbours, obtained with the tests API 20NE, API CH 50 and BIOLOG GN2.	274
Appendix IX: ML 16S rRNA phylogenetic tree of selected <i>Pseudomonas</i> species, and all available members of <i>Azotobacter</i> , <i>Azomonas</i> and <i>Azorhizophilus</i>	282
Appendix X: ML MLSA phylogenetic tree of selected <i>Pseudomonas</i> species, and all available members of <i>Azotobacter</i> , <i>Azomonas</i> and <i>Azorhizophilus</i>	284
Appendix XI: ML MLSA phylogenetic tree of selected <i>Pseudomonas</i> species, and all available members of <i>Azotobacter</i> , <i>Azomonas</i> and <i>Azorhizophilus</i>	286
Appendix XII: Genbank accession numbers for the 16S rRNA genes used for the 16S rRNA sequence analysis, and for the housekeeping genes <i>gyrb</i> , <i>rpob</i> and <i>rpod</i> , used in the MLSA, performed to study the phylogenetic relationships amongst the genera: <i>Pseudomonas</i> , <i>Azotobacter</i> , <i>Azomonas</i> and <i>Azorhizophilus</i>	288
Appendix XIII: Presence/absence chart of phytopathogenic virulence factors in the genomes of AOD-associated <i>Pseudomonas</i> and other <i>Pseudomonas</i> species.	294
Appendix XIV: Optical density values obtained at 590 nm in the cell attachment assays..	299

LIST OF TABLES

Table 1: List of Pseudomonads isolated from AOD-symptomatic <i>Quercus robur</i> in the UK.	25
Table 2: List of bacterial species used in this project.	27
Table 3: Sequences of primers used for amplification and sequencing of 16S rRNA, <i>gyrB</i> , <i>rpoB</i> , and <i>rpoD</i> genes.	33
Table 4: PCR conditions used for amplification and sequencing of 16S rRNA, <i>gyrB</i> , <i>rpoB</i> , and <i>rpoD</i> genes.	34
Table 5: Primers designed for the multiplex-HRM assay for the detection and identification of Bg, Gq, Rvi and Lb from field samples and amplicons expected.	52
Table 6: Collection details of the field samples from Kew Gardens and Knole Park.	58
Table 7: Samples collected from oak leaves in the University of the West of England, for the characterisation of their microbiome.	61
Table 8: QCAST output of the genome assemblies obtained following the genome sequencing of the AOD-associated <i>Pseudomonas</i> and GenBank accession numbers.	86
Table 9: Heatmap of percentages of average nucleotide identity based on BLAST (ANIb, below the black cells), and <i>in silico</i> DNA-DNA hybridisation (<i>is</i> DDH, above the black cells).	88
Table 10: Heatmap of percentages of average nucleotide identity based on BLAST (ANIb, below the black cells), and <i>in silico</i> DNA-DNA hybridisation (<i>is</i> DDH, above the black cells).	90
Table 11: Distinguishing phenotypic characteristics of the AOD-associated strains in cluster A, B and their closest neighbours, obtained with the tests API 20NE, API CH 50 and Biolog GN2.	97

Table 12: Distinguishing phenotypic characteristics of the AOD-associated strains in cluster C, and their closest neighbours, obtained with the tests API 20NE, API CH 50 and Biolog GN2.....	101
Table 13: Percentages of cell fatty acid methyl esters (FAMES) in representative AOD-associated strains of clusters A and B.	106
Table 14: Percentages of cell fatty acid methyl esters (FAMES) in representative AOD-associated strains of cluster C.	107
Table 15: Presence/absence chart of phytopathogenic virulence factors in the genomes of AOD-associated <i>Pseudomonas</i> : <i>P. daroniae</i> sp. nov., <i>P. dryadis</i> sp. nov. and <i>P. kirkliae</i> sp. nov., the non-plant pathogen <i>Pseudomonas fluorescens</i> SBW25, and the phytopathogen <i>Pseudomonas syringae</i> pv. <i>phaseolicola</i> 1448A.	128
Table 16: Isolation frequency of Gq, Bg, Rvi and Lb in sites and trees with different health status.....	181
Table 17: Isolates from samples collected in Kew Gardens, and results of the duplex-HRM assay for the detection and identification of AOD-associated bacteria <i>Brenneria goodwinii</i> (Bg) and <i>Gibbsiella quercinecans</i> (Gq), in overnight LB broths.	192
Table 18: Isolates from samples collected in Kew Gardens, and results of the duplex-HRM assay for the detection and identification of AOD-associated bacteria <i>Brenneria goodwinii</i> (Bg) and <i>Gibbsiella quercinecans</i> (Gq), in optimal media and atmosphere test.	196
Table 19: Bacterial isolates from Kew Gardens and results of the multiplex-HRM assay for the detection and identification of AOD-associated bacteria <i>Brenneria goodwinii</i> (Bg), <i>Gibbsiella quercinecans</i> (Gq), <i>Rahnella victoriana</i> (Rvi) and <i>Lonsdalea britannica</i> (Lb).....	198
Table 20: Bacterial isolates from Knole Park and results of the multiplex-HRM assay for the detection and identification of AOD-associated bacteria <i>Brenneria goodwinii</i> (Bg), <i>Gibbsiella quercinecans</i> (Gq), <i>Rahnella victoriana</i> (Rvi) and <i>Lonsdalea britannica</i> (Lb).....	203

Table 21: Multiplex-HRM assay for the detection and identification of AOD-associated bacteria <i>Brenneria goodwinii</i> (Bg), <i>Gibbsiella quercinecans</i> (Gq), <i>Rahnella victoriana</i> (Rvi) and <i>Lonsdalea britannica</i> (Lb) in samples from the log tests.....	205
Table 22: Bacterial isolates from the log tests and results of the multiplex-HRM assay for the detection and identification of AOD-associated bacteria <i>Brenneria goodwinii</i> (Bg), <i>Gibbsiella quercinecans</i> (Gq), <i>Rahnella victoriana</i> (Rvi) and <i>Lonsdalea britannica</i> (Lb).....	206
Table 23: Multiplex-HRM assay for the detection and identification of AOD-associated bacteria <i>Brenneria goodwinii</i> (Bg), <i>Gibbsiella quercinecans</i> (Gq), <i>Rahnella victoriana</i> (Rvi) and <i>Lonsdalea britannica</i> (Lb), and single nucleotide polymorphism (SNP)-based HRM assay for the differentiation of species of the genus <i>Rahnella</i> of the isolates belonging to the genus <i>Rahnella</i> from the log tests.	209
Appendix VII: GenBank accession numbers for the housekeeping genes <i>gyrB</i> , <i>rpoD</i> and <i>rpoB</i> , used in the multilocus sequence analysis (MLSA) of the AOD-associated isolates belonging to the species <i>Pseudomonas daroniae</i> sp. nov., <i>Pseudomonas dryadis</i> sp. nov., <i>Pseudomonas kirkieae</i> sp. nov., and their closest related neighbours (Bueno-Gonzalez et al., 2019, 2020).....	268
Appendix VIII: Phenotypic characteristics of the AOD-associated <i>Pseudomonas</i> in cluster A, B and C, and their closest neighbours, obtained with the tests API 20NE, API CH 50 and Biolog GN2.....	274
Appendix XII: GenBank accession numbers for the 16S rRNA genes used for the 16S rRNA sequence analysis, and for the housekeeping genes <i>gyrB</i> , <i>rpoB</i> and <i>rpoD</i> , used in the MLSA performed to study the phylogenetic relationships amongst the genera: <i>Pseudomonas</i> , <i>Azotobacter</i> , <i>Azomonas</i> and <i>Azorhizophilus</i>	288
Appendix XIII: Presence/absence chart of phytopathogenic virulence factors in the genomes of AOD-associated <i>Pseudomonas</i> and other <i>Pseudomonas</i> species.	294
Appendix XIV: Optical density values obtained at 590 nm in the cell attachment assays.	299

LIST OF FIGURES

Figure 1: Spiral of the interacting set of factors associated with oak decline. Reproduced from Manion, 1981.....	3
Figure 2: <i>Quercus robur</i> in Bristol, United Kingdom, with symptoms of decline	4
Figure 3: Distribution of Acute Oak Decline cases, shown as red dots, in England as of March 2019.	6
Figure 4: Distribution of Acute Oak Decline cases, shown as red dots, in England as of March 2019.	8
Figure 5: Colonies of the Acute Oak Decline pathogen <i>Brenneria goodwinii</i> on eosin methylene blue agar.	11
Figure 6: Rapid identification of bacteria associated with Acute Oak Decline (AOD) by high resolution melt (HRM) analysis of the <i>atpD</i> gene.....	18
Figure 7: Graphical abstract of the paper of the multiplex Taqman-based diagnostic method for bacteria associated with Acute Oak Decline.	19
Figure 8: Layout of the hypersensitive response assays of the AOD-associated Pseudomonads in detached green pods (<i>Phaseolus vulgaris</i>).....	44
Figure 9: Layout of the hypersensitive response assays of the combination of AOD-associated Pseudomonads with <i>Brenneria goodwinii</i> , <i>Gibbsiella quercinecans</i> or <i>Rahnella victoriana</i> , in detached green pods (<i>Phaseolus vulgaris</i>).	45
Figure 10: Example of a whole genome alignment performed for the selection of targets for each of the species in the multiplex-HRM assay for the detection and identification of <i>Brenneria goodwinii</i> , <i>Gibbsiella quercinecans</i> , <i>Rahnella victoriana</i> and <i>Lonsdalea britannica</i>	51
Figure 11: Latest accepted intra-genus structure of <i>Pseudomonas</i> , according to the neighbour-joining MLSA phylogenetic study of the 16S rRNA, <i>gyrB</i> , <i>rpoB</i> and <i>rpoD</i> in 227 species and subspecies of <i>Pseudomonas</i> , (Lalucat et al., 2020).....	70

Figure 12: Maximum likelihood 16S rRNA gene phylogenetic tree of the 35 AOD-associated strains of <i>Pseudomonas</i> , 31 closest phylogenetic neighbours and the outgroup <i>Cellvibrio japonicus</i>	75
Figure 13: Maximum likelihood 16S rRNA gene phylogenetic tree of the AOD-associated strains representatives of clusters A and B, 35 closest phylogenetic neighbours and the outgroup <i>Acinetobacter baumannii</i>	77
Figure 14: Bayesian 16S rRNA phylogenetic tree of the AOD-associated strain representative of cluster C, 38 closest phylogenetic neighbours and the outgroup <i>Endozoicomonas elysicola</i>	78
Figure 15: Maximum likelihood MLSA phylogenetic tree of the concatenated gene sequences <i>gyrB</i> , <i>rpoB</i> and <i>rpoD</i> , obtained from AOD-associated strains in clusters A and B, 35 closest phylogenetic neighbours and the outgroup <i>Pseudomonas pertucinogena</i>	82
Figure 16: Bayesian MLSA phylogenetic tree of the concatenated gene sequences <i>gyrB</i> , <i>rpoB</i> and <i>rpoD</i> , obtained from the AOD-associated strains in cluster C, 25 closest phylogenetic neighbours and the outgroup <i>Stenotrophomonas maltophilia</i>	83
Figure 17: RAPD-PCR fingerprinting band patterns obtained with the primer OPA-04 from the AOD-associated strains included in clusters A and B, and the closest neighbours.	84
Figure 18: BOX-PCR fingerprinting band patterns obtained with the primer BOX-1AR from the AOD-associated strains included in cluster C, and the closest neighbours.	85
Figure 19: Transmission electron micrographs of cells of AOD-associated <i>Pseudomonas</i>	93
Figure 20: Bayesian 16S rRNA phylogenetic tree of selected <i>Pseudomonas</i> species, and all available members of <i>Azotobacter</i> , <i>Azomonas</i> and <i>Azorhizophilus</i>	111

Figure 21: Bayesian MLSA phylogenetic tree of selected <i>Pseudomonas</i> species, and all available members of <i>Azotobacter</i> , <i>Azomonas</i> and <i>Azorhizophilus</i>	112
Figure 22: Agglomerative hierarchical clustering (AHC) of the profiles of virulence factors (VFs) obtained from the genomes of AOD-associated <i>Pseudomonas</i> and other <i>Pseudomonas</i> species.	126
Figure 23: Phenotype of the controls used in the hypersensitive response tests. .	132
Figure 24: Hypersensitive response test of the AOD-associated <i>Pseudomonas</i> in bean pods.....	133
Figure 25: Hypersensitive response test of the AOD-associated <i>Pseudomonas</i> in tobacco leaves.....	134
Figure 26: Six-well plate assay of the AOD-associated <i>Pseudomonas</i> , performed in TSB.....	136
Figure 27: Tube-coverslip assay of the AOD-associated <i>Pseudomonas</i> , performed in LB: cell attachment in Falcon tubes.	138
Figure 28: Tube-coverslip assay of the AOD-associated <i>Pseudomonas</i> , performed in LB: cell attachment in glass coverslips.....	139
Figure 29: Tube-coverslip assay of the AOD-associated <i>Pseudomonas</i> , performed in LB and TSB: cell attachment in Falcon tubes.	140
Figure 30: Tube-coverslip assay of the AOD-associated <i>Pseudomonas</i> , performed in LB and TSB: cell attachment in Falcon tubes and glass coverslips.....	142
Figure 31: Example of a single nucleotide polymorphism-based high resolution melting analysis of three different bacterial species.	151
Figure 32: Workflow followed by the Rotor-Gene ScreenClust HRM software.	153
Figure 33: Melting temperatures of the amplicons obtained from the HRM assay of the <i>atpD</i> gene (119 bp) of the bacterial species <i>Gibbsiella quercinecans</i> (Gq), <i>Brenneria goodwinii</i> (Bg) and <i>Rahnella victoriana</i> (Rvi), prepared following three different methods.	155

Figure 34: Melting temperatures of the amplicons obtained from the HRM assay of the <i>atpD</i> gene (119 bp) of the bacterial species <i>Gibbsiella quercinecans</i> (Gq), <i>Brenneria goodwinii</i> (Bg) and <i>Rahnella victoriana</i> (Rvi), for the combined species test.	156
Figure 35: Unsupervised ScreenClust cluster analysis of the data set obtained in the HRM assay of the <i>atpD</i> gene (119 bp) of the bacterial species <i>Gibbsiella quercinecans</i> (Gq), <i>Brenneria goodwinii</i> (Bg) and <i>Rahnella victoriana</i> (Rvi), for the combined species test.....	157
Figure 36: Derivative melt plot of the HRM of the 320 bp fragment of the <i>atpD</i> gene (a), and agarose gel electrophoresis of the DNA fragments amplified in the HRM assay of the 320 bp fragment of the <i>atpD</i> gene (b).	159
Figure 37: Derivative (a) and normalised (b) fluorescence plots of the duplex-HRM assay of genes <i>atpD</i> and <i>rpoD</i> for the identification of AOD-associated bacteria including <i>Pseudomonas</i>	161
Figure 38: Unsupervised ScreenClust cluster analysis of the data set obtained in the duplex-HRM assay of genes <i>atpD</i> and <i>rpoD</i> for the identification of AOD-associated bacteria including <i>Pseudomonas</i>	162
Figure 39: Derivative (a) and normalised (b) fluorescence plots of the multiplex-HRM assay for the detection and identification of AOD-associated bacteria <i>Brenneria goodwinii</i> (Bg), <i>Gibbsiella quercinecans</i> (Gq), <i>Rahnella victoriana</i> (Rvi) and <i>Lonsdalea britannica</i> (Lb).	164
Figure 40: Unsupervised ScreenClust cluster analysis of the data set obtained in the multiplex-HRM assay for the detection and identification of AOD-associated bacteria <i>Brenneria goodwinii</i> (Bg), <i>Gibbsiella quercinecans</i> (Gq), <i>Rahnella victoriana</i> (Rvi) and <i>Lonsdalea britannica</i> (Lb).....	165
Figure 41: Derivative fluorescence plot of the multiplex-HRM assay for the detection and identification of AOD-associated bacteria <i>Brenneria goodwinii</i> (Bg), <i>Gibbsiella quercinecans</i> (Gq), <i>Rahnella victoriana</i> (Rvi) and <i>Lonsdalea britannica</i> (Lb).	167

Figure 42: Derivative fluorescence plot of the multiplex-HRM assay for the detection and identification of AOD-associated bacteria *Brenneria goodwinii* (Bg), *Gibbsiella quercinecans* (Gq), *Rahnella victoriana* (Rvi) and *Lonsdalea britannica* (Lb).168

Figure 43: Derivative fluorescence plot of the sensitivity study of the multiplex-HRM assay for the detection and identification of AOD-associated bacteria *Brenneria goodwinii* (Bg), *Gibbsiella quercinecans* (Gq), *Rahnella victoriana* (Rvi) and *Lonsdalea britannica* (Lb).169

Figure 44: Amplification (a), derivative (b) and normalised (c) fluorescence plots of the single nucleotide polymorphism (SNP)-based HRM assay for the differentiation of species and subspecies of the genus *Brenneria*.171

Figure 45: Unsupervised ScreenClust cluster analysis of the data set obtained in the single nucleotide polymorphism (SNP)-based HRM assay for the differentiation of species and subspecies of the genus *Brenneria*.....172

Figure 46: Derivative (a) and normalised (b) fluorescence plots of the single nucleotide polymorphism (SNP)-based HRM assay for the differentiation of species of the genus *Rahnella*.174

Figure 47: Unsupervised ScreenClust cluster analysis of the data set obtained in the single nucleotide polymorphism (SNP)-based HRM assay for the differentiation of species of the genus *Rahnella*.....175

Figure 48: Amplification (a), derivative (b) and normalised (c) fluorescence plots of the single nucleotide polymorphism (SNP)-based HRM assay for the differentiation of species of the genus *Gibbsiella*.....177

Figure 49: Unsupervised ScreenClust cluster analysis of the data set obtained in the single nucleotide polymorphism (SNP)-based HRM assay for the differentiation of species of the genus *Gibbsiella*.178

Figure 50: Trees sampled in Kew Gardens and Knole Park.187

Figure 51: Derivative fluorescence plot of the duplex-HRM assay for the detection and identification of AOD-associated bacteria <i>Brenneria goodwinii</i> (Bg) and <i>Gibbsiella quercinecans</i> (Gq), in overnight LB broths.....	191
Figure 52: Derivative fluorescence plot of the duplex-HRM assay for the detection and identification of AOD-associated bacteria <i>Brenneria goodwinii</i> (Bg) and <i>Gibbsiella quercinecans</i> (Gq), in sample Kew 2: optimal temperature and atmosphere test. 193	193
Figure 53: Derivative fluorescence plot of the duplex-HRM assay for the detection and identification of AOD-associated bacteria <i>Brenneria goodwinii</i> (Bg) and <i>Gibbsiella quercinecans</i> (Gq), in sample Kew 2: optimal media and atmosphere test.....	194
Figure 54: Derivative fluorescence plot of the multiplex-HRM assay for the detection and identification of AOD-associated bacteria <i>Brenneria goodwinii</i> (Bg), <i>Gibbsiella quercinecans</i> (Gq), <i>Rahnella victoriana</i> (Rvi) and <i>Lonsdalea britannica</i> (Lb) in samples from Knole Park: optimal atmosphere test.	197
Figure 55: Derivative fluorescence plot of the multiplex-HRM assay for the detection and identification of AOD-associated bacteria <i>Brenneria goodwinii</i> (Bg), <i>Gibbsiella quercinecans</i> (Gq), <i>Rahnella victoriana</i> (Rvi) and <i>Lonsdalea britannica</i> (Lb) in samples from Kew Gardens.	202
Figure 56: Derivative fluorescence plot of the multiplex-HRM assay for the detection and identification of AOD-associated bacteria <i>Brenneria goodwinii</i> (Bg), <i>Gibbsiella quercinecans</i> (Gq), <i>Rahnella victoriana</i> (Rvi) and <i>Lonsdalea britannica</i> (Lb) in samples from Knole Park.....	204
Figure 57: Derivative fluorescence plot of the single nucleotide polymorphism (SNP)-based HRM assay for the differentiation of species of the genus <i>Rahnella</i>	208
Figure 58: Bacterial endophytes and epiphytes isolated from leaves of sapling and mature <i>Quercus robur</i>	212
Figure 59: Initial stem suspension. Samples collected from stem bleeds in Acute Oak Decline-affected oaks, submerged in Ringers solution.....	214
Figure 60: Optimal pre-HRM assay sample processing.	218

Figure 61: Flowchart of the optimized Acute Oak Decline molecular diagnostic workflow protocol according to the sample type.....	230
Appendix I: Bayesian 16S rRNA phylogenetic tree of the AOD-associated strains representatives of clusters A and B, 35 closest phylogenetic neighbours and the outgroup <i>Acinetobacter baumannii</i>	261
Appendix II: Maximum likelihood 16S rRNA gene phylogenetic tree of the AOD-associated strain representative of cluster C, 38 closest phylogenetic neighbours and the outgroup <i>Endozoicomonas elysicola</i>	262
Appendix III: Maximum likelihood MLSA phylogenetic tree of the concatenated gene sequences <i>gyrB</i> , <i>rpoB</i> and <i>rpoD</i> , obtained from the AOD-associated strains in cluster C, 25 closest phylogenetic neighbours and the outgroup <i>Stenotrophomonas maltophilia</i>	263
Appendix IV: Bayesian MLSA phylogenetic tree of the concatenated gene sequences <i>gyrB</i> , <i>rpoB</i> and <i>rpoD</i> , obtained from AOD-associated strains in clusters A and B, 35 closest phylogenetic neighbours and the outgroup <i>Pseudomonas pertucinogena</i>	264
Appendix V: Maximum likelihood MLSA phylogenetic tree of the concatenated amino acid sequences <i>gyrB</i> , <i>rpoB</i> and <i>rpoD</i> , obtained from AOD-associated strains in clusters A and B, 35 closest phylogenetic neighbours and the outgroup <i>Pseudomonas pertucinogena</i>	265
Appendix VI: Maximum likelihood MLSA phylogenetic tree of the concatenated amino acid sequences <i>gyrB</i> , <i>rpoB</i> and <i>rpoD</i> , obtained from the AOD-associated strains in cluster C, 25 closest phylogenetic neighbours and the outgroup <i>Stenotrophomonas maltophilia</i>	266
Appendix IX: ML 16S rRNA phylogenetic tree of selected <i>Pseudomonas</i> species, and all available members of <i>Azotobacter</i> , <i>Azomonas</i> and <i>Azorhizophilus</i>	283
Appendix X: ML MLSA phylogenetic tree of selected <i>Pseudomonas</i> species, and all available members of <i>Azotobacter</i> , <i>Azomonas</i> and <i>Azorhizophilus</i>	284

Appendix XI: ML MLSA phylogenetic tree of selected *Pseudomonas* species, and all available members of *Azotobacter*, *Azomonas* and *Azorhizophilus*.....286

LIST OF ABBREVIATIONS

AOD	Acute Oak Decline
COD	Chronic Oak Decline
AHC	Agglomerative hierarchical clustering
ANI	Average Nucleotide Identity
ANlb	Average nucleotide identity studies based on BLAST
ANIm	Average nucleotide identity studies based on MUMmer tools
<i>avr</i>	Avirulence gene
Ba	<i>Brenneria alni</i>
BCCM	Belgian Co-ordinated Collection of Micro-organisms
Bco	<i>Brenneria corticis</i>
Bg	<i>Brenneria goodwinii</i>
BI	Bayesian Inference
BLAST	basic local alignment search tool
Bn	<i>Brenneria nigrifluens</i>
bp	Base pairs
Bra	<i>Brenneria roseae</i> subsp. <i>americana</i>
Brr	<i>Brenneria roseae</i> ssp. <i>roseae</i>
Bru	<i>Brenneria rubrifaciens</i>
Bsa	<i>Brenneria salicis</i>
C	Cytosine
CFU	Colony forming units
DDH	DNA–DNA hybridisation
DSMZ	Deutsche Sammlung von Mikroorganismen und Zellkulturen (German collection of microorganisms and cell cultures)
EMB	Eosin methylene blue
ERIC-PCR	Enterobacterial repetitive intergenic consensus PCR
FAME	Fatty acid methyl ester
G	Guanine
Gd	<i>Gibbsiella dentisursi</i>
Gg	<i>Gibbsiella greigii</i>
GGDC	Genome to genome distances comparison
GPR	Ground penetrating radar
Gq	<i>Gibbsiella quercinecans</i>
GTR	General time reversible model
HGT	Horizontal gene transfer
HR	Hypersensitive response
HRM	High resolution melting
I+G	Invariable sites and gamma distribution

<i>is</i> DDH	<i>In silico</i> DNA-DNA hybridisation
KB	King's B
Lb	<i>Lonsdalea britannica</i>
LB	Luria Bertrani
LPS	Lipopolysaccharide
M9	Minimal media
MIDI	Microbial Identification System
ML	Maximum likelihood
MLSA	Multilocus sequence analysis studies
NGS	Next generation sequencing
NIC	Non-inoculum control
NPP	Non-plant pathogenic control
nt	Nucleotides
NTC	Non-template control
OD	Optical density
Pa	<i>Pantoea agglomerans</i>
PCA	Principal component analysis
PCR	Polymerase chain reaction
Pda	<i>Pseudomonas daroniae</i> sp. nov.
Pdr	<i>Pseudomonas dryadis</i> sp. nov.
Pki	<i>Pseudomonas kirkiae</i> sp. nov.
PP	Posterior probabilities
<i>Pph</i>	<i>Pseudomonas syringae</i> pv. <i>phaseolicola</i>
Psv	<i>Pseudomonas savastanoi</i> pv. <i>savastanoi</i>
qPCR	Quantitative PCR
QS	Quorum sensing
QUAST	QUality assessment tool
R	Resistance gene
RAPD-PCR	Random amplification of polymorphic DNA PCR
Raq	<i>Rahnella aquatilis</i>
Rbru	<i>Rahnella bruchi</i>
rep-PCR	Repetitive element sequence-based PCR
Rinu	<i>Rahnella inusitata</i>
Rva	<i>Rahnella variigena</i>
Rvi	<i>Rahnella victoriana</i>
Rwo	<i>Rahnella woolbedingensis</i>
SDW	Sterile distilled water
SNP	Single nucleotide polymorphism
T	Type strain
T3SS	Type III secretion systems
TAE	Tris-acetate-ethylenediamine tetraacetic acid

TEM	Transmission electron microscopy
TIM	Transitional model
T _m	Melting temperature
TMV	Transversional model
TSA	Tryptone soy agar
VF	Virulence factor
VOC	Volatile organic compounds

CHAPTER 1. Introduction

1.1. Tree diseases in the United Kingdom

Tree diseases are caused by a wide range of pests and pathogens including insects, fungi, and bacteria. The most predominant emerging infectious tree diseases in Europe are ash dieback, the diseases caused by *Xylella fastidiosa* and Acute Oak Decline (AOD) (Broome et al., 2019; Giannakis et al., 2019; Janse and Obradovic, 2010). Specifically, in the UK, conifers are threatened by fungal species of *Phytophthora*, *Sirococcus* or *Dothistroma* and by insects such as the great spruce bark beetle, the pine processionary moth, and the eight-toothed spruce bark beetle (<https://www.woodlandtrust.org.uk/trees-woods-and-wildlife/tree-pests-and-diseases/key-tree-pests-and-diseases/>). In Scotland, the European mountain ash ringspot-associated virus affects trees in the *Sorbus* family like the rowan. Fungi like *Cryphonectria* affect broad-leaved trees such as the chestnut tree, which also suffers from a bleeding canker caused by the bacterium *Pseudomonas syringae* pv. *aesculi*. For the last 40 years, the devastating Dutch elm disease, caused by the fungus *Ophiostoma novo-ulmi* has killed millions of elm trees in the UK. A major concern in the UK is ash dieback, caused by the fungal pathogen *Hymenoscyphus fraxineus*. It is estimated that 95-99 % of ashes in the UK will die due to this disease (Coker et al., 2019; Hill et al., 2019). Several pests and diseases endanger oak trees in UK, including the complex disease, Acute Oak Decline. Insects such as the caterpillars of the oak processionary moth (*Thaumetopoea processionea*), and the caterpillars of the moth *Tortrix viridana* feed on the leaves of the oak. These caterpillars can completely defoliate the oak, leaving it more prone to other pests and stresses such as drought (Tomlinson, Potter and Bayliss, 2015). The wasp *Andricus quercuscalicis* causes knopper galls in the growing acorns, and the fungus *Erysiphe alphitoides* causes oak mildew (Lonsdale, 2015). Some of the diseases might not be lethal but they weaken the oak, predisposing it to a potential decline.

1.1.1. Oak decline

The combination of climatic and edaphological conditions in the United Kingdom is ideal for the growth of broadleaved trees. However, climate change will be a challenge for tree populations as warmer temperatures are expected to damage their health through water stress, heat stress, and the increasing pressure of displaced populations of insects (Denman and Webber, 2009; Petr et al., 2014). Oaks are the second most common broadleaved tree in the UK after birch and their health is a main concern in the country and in mainland

Europe. Forty years ago, evidence of oak decline appeared in countries such as USA, UK, Spain, Russia, and Italy (Denman and Webber, 2009; Thomas, Blank and Hartmann, 2002; Brady *et al.*, 2014a; Denman *et al.*, 2014; Gallego, Perez De Algaba and Fernandez-Escobar, 1999; Oleksyn and Przybyl, 1987; Ragazzi, Fedi and Mesturino, 1989). Oak decline is a complex syndrome in which the combination of abiotic and biotic factors causes the serious deterioration of the oak's health (Sinclare, 1967). The most common factors that damage the tree's health in the forest ecosystems are shortages (i.e. water or nutrients) and fungi, and they can act simultaneously or sequentially (Manion, 1981) (**Figure 1**).

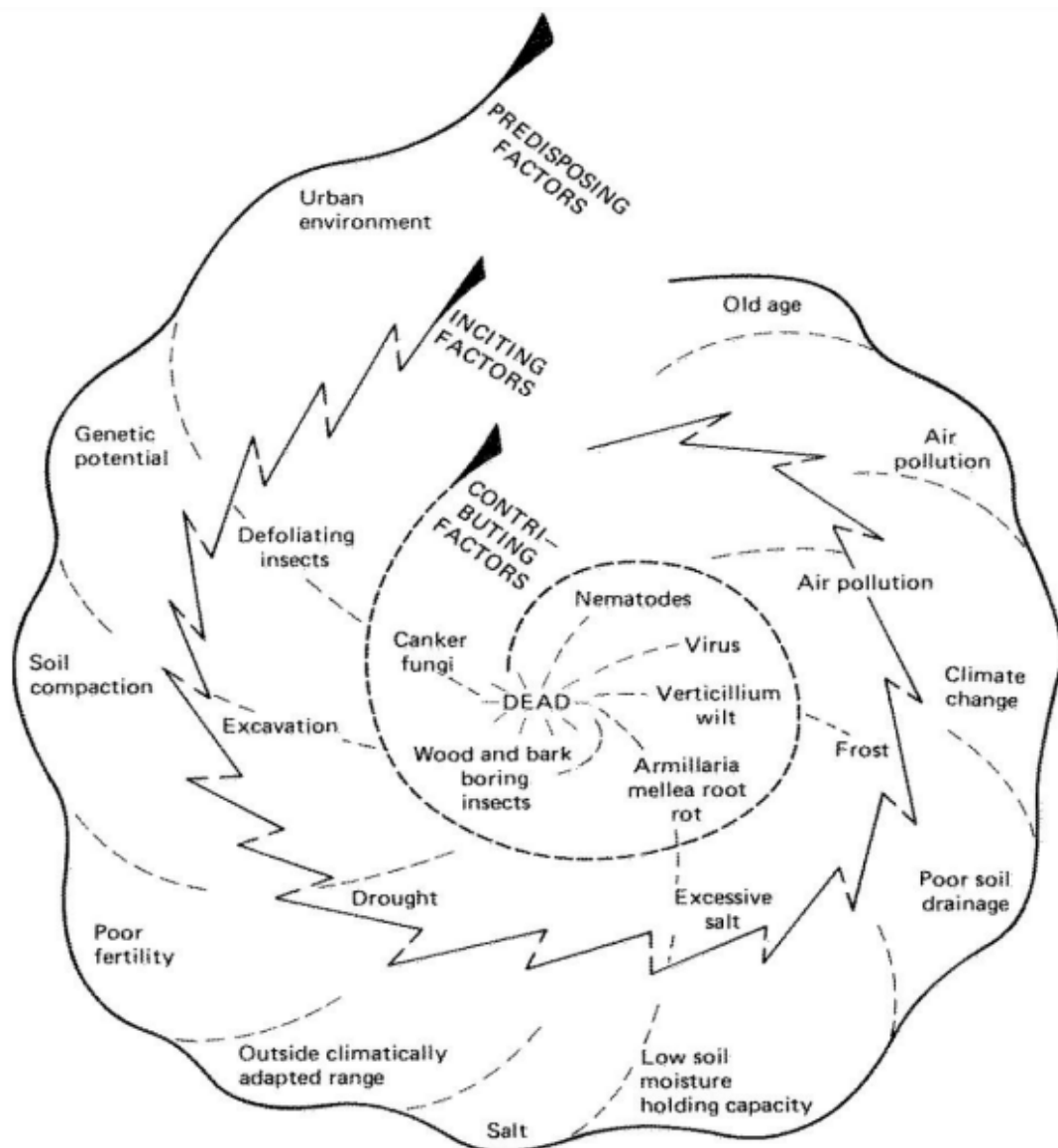


Figure 1: Spiral of the interacting set of factors associated with oak decline. Reproduced from Manion, 1981.

The decline can sometimes be lethal, but trees can also recover from it. The symptoms of decline include poor growth, foliage issues (chlorosis, small or fewer leaves, premature drop) and branch dieback, amongst others (**Figure 2**). Also known as oak dieback, there are several types of oak decline in the UK, including Chronic Oak Decline (COD) and Acute Oak Decline (AOD). COD is characterised by a slow progression of 10 to 50 years, as opposed to AOD, which in severe cases can kill the tree in three to five years. The characteristic symptoms of COD are mainly related to the deterioration of the foliage and crown (Denman and Webber, 2009). Forest Research does not currently consider COD a threat in the UK.



Figure 2: *Quercus robur* in Bristol, United Kingdom, with symptoms of decline, such as poor leaf growth.

1.2. Acute Oak Decline (AOD)

1.2.1. Description and distribution of AOD

A distinctive form of oak decline, the disease known as AOD threatens oak tree species, particularly those native to the United Kingdom. The syndrome is believed to have first appeared in the UK two to three decades ago (Denman and Webber, 2009). The geographical distribution is spreading across the southeast of England and the Midlands, and slowly spreading west- and north-wards (**Figure 3**) (Brown et al., 2016; Denman et al., 2013; Denman, Kirk and Webber, 2010). The estimation is that about a third of the forests in England and Wales are now affected by AOD (Brown et al., 2017). As of 2021, AOD has not been observed in Scotland or Northern Ireland. Similar symptoms to AOD have also been noted in several other countries, including Spain (Biosca et al., 2003; González and Ciordia, 2020), Germany (Hartmann and Blank, 1992), Belgium (Vansteenkiste et al., 2004), France (Jacquot *et al.*, 1950), Switzerland (Ruffner et al., 2020), Poland (Moraal and Hilszczanski, 2000). Other oak species affected by AOD abroad are Bali oak (*Q. fabri*), holm oak (*Q. ilex*), oriental white oak (*Quercus aliena* var. *accuserrata*), pin oak (*Q. palustris*), Pyrenean oak (*Q. pyrenaica*), red oak (*Q. rubra*), scarlet oak (*Q. coccinea*), Turkey oak (*Q. cerris*), and water oak (*Q. nigra*). Recently, AOD-associated bacterial species have been also isolated from trees displaying AOD-like symptoms in Iran (Moradi-Amirabad et al., 2019). The species affected in Iran were *Quercus castaneifolia* (chestnut-leaved oak), *Q. brantii* (Persian oak) and *Carpinus betulus* (hornbeam).

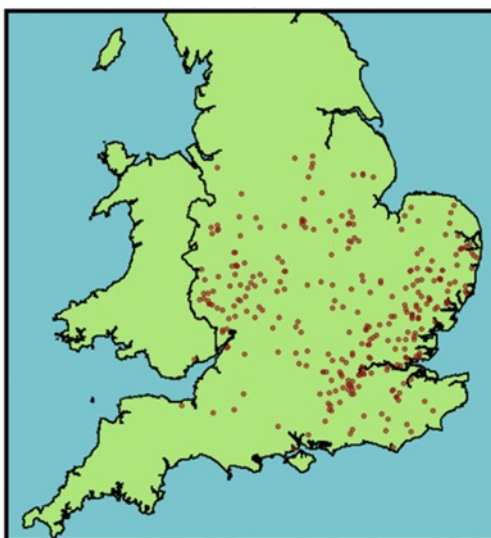


Figure 3: Distribution of Acute Oak Decline cases, shown as red dots, in England as of March 2019. Image adapted from <https://www.forestresearch.gov.uk/tools-and-resources/fthr/pest-and-disease-resources/acute-oak-decline/acute-oak-decline-aod-incidence-and-distribution/>.

1.2.2. Host, symptoms and causes of AOD

The natural hosts associated with symptoms of AOD in UK are *Quercus robur* (English or pedunculate oak) and *Q. petraea* (sessile oak), as well as other non-native species of oak. The disease can be lethal in less than five years although some oaks have been observed to recover from AOD (Denman, Kirk and Webber, 2010). Oaks are a national treasure and a keystone species to British ecosystems. Oak species are representative of the forests of the UK, and they possess an important economic value for the timber industry, as well as a strong historical, cultural and ecological significance. Compared to other tree species, oaks are especially supportive of biodiversity; 2300 species of birds, mammals, fungi, lichens, invertebrates and bryophytes (mosses and liverworts) are linked to pedunculate and sessile oak in the UK (Mitchell et al., 2019). Of the 2300 species, 326 are exclusively associated with pedunculate and sessile oak. The species directly associated with oak can suffer a direct impact due to the decline of the tree, particularly if they are obligate associated species (those are species that are only found in oak), because specialists are generally less resilient to change than generalist species. Mature oak forests are more likely to support a wider range of taxa than younger forests, therefore in terms of biodiversity protection, older trees

are more valuable (Mitchell et al., 2019). AOD symptoms appear mainly on mature oaks (older than 50 years) and include:

1. Vertical cracks between the outer bark plates (**Figure 4a**).
2. Stem bleeding from the cracks and tissues underlying the bleeding patches (**Figure 4b**). This symptom can normally be spotted in spring and autumn (Denman et al., 2014).
3. The weeping patches are stained and necrotic, leading to the formation of cavities in the inner bark (**Figure 4b**).
4. Larval galleries of the bark boring buprestid beetle *Agrilus biguttatus* are frequently found near the necrotic tissue (**Figure 4c**).

Distinctive D-shaped emergence holes are created by the beetle in the bark (Brown et al., 2015; Denman et al., 2014) (**Figure 4d and 4e**). Some cases of complete recovery have been observed in AOD lesions, evidenced by the presence of calluses formed by lignified tissue on top of the lesion (Denman, Kirk and Webber, 2010), (**Figure 4f**). Dendrochronological studies have observed that oaks that have been through an episode of AOD and other forms of decline are less able to take advantage of the benign growing periods (spring and autumn) and this can be correlated to a reduced stem growth and a reduced resilience to change (Reed et al., 2020). The spread of AOD is still under study. It is still unknown if *A. biguttatus* plays a role in the disease or in its dispersion. What it is known so far is that there is evidence of the presence of its larvae in more than 95 % of the trees affected by AOD (Brown et al., 2017). The distribution of AOD in the UK coincides with the distribution of the beetle, both restricted to the warmer part of the country (the South). In a study of the life cycle of the beetle and its thermal requirements for growth and development, evidence was found of a thermal limitation to the distribution of the beetle. This implies that in a climate change scenario, the distribution of the beetle might expand to colder regions in the UK and AOD with it (Reed et al., 2018).



Figure 4: Distribution of Acute Oak Decline cases, shown as red dots, in England as of March 2019. Image adapted from <https://www.forestresearch.gov.uk/tools-and-resources/fthr/pest-and-disease-resources/acute-oak-decline/acute-oak-decline-aod-incidence-and-distribution/>.

As for other decline diseases of forest trees, it is believed that the appearance of AOD is facilitated by a series of abiotic factors (Brown et al., 2016, 2018). Abiotic predisposition factors including environmental pollution, soil type, annual rainfall and nutrient imbalance will affect the resilience of the oaks, increasing their susceptibility to AOD, and therefore triggering graver outbreaks (Brown et al., 2018; Thomas, Blank and Hartmann, 2002). The ways that each abiotic factor weaken the trees are variable, for instance, a drought might lead to wilt and poor growth of the plant, as water availability is essential for several metabolic processes such as nutrient assimilation, photosynthesis and transpiration. Water availability depends greatly on the soil type the trees are growing in (Thomas, 2008). Studies revealed that AOD sites were most commonly found in places with environmental factors

that influence water availability, like higher temperatures or lower rainfall, however, no correlation was observed between soil type and AOD (Brown et al., 2018). AOD sites were linked to excess of nitrogen, which can cause more growth, but can also contribute to nutrient imbalance, detrimentally impacting the health of the tree and the ectomycorrhizal fungal communities associated with the roots (Brown et al., 2018). The excess of nitrogen in the soil has more indirect effects upon the health of the oak such as the potential acidification of the soil through nitrification (Robson, Yeates and Porter, 1989). The acidification of forest soils might lead to the inhibition of the nutrient intake by the roots and therefore, deficiency of elements like calcium, magnesium or potassium (Thomas and Büttner, 1998). All these factors affect the resilience of the oak and make it more prone to disease.

In addition to the abiotic predisposition factors, it is common to find biotic factors associated with AOD-affected oaks that contribute to the rapid deterioration of the tree health. Two key examples are the buprestid beetle *A. biguttatus* or the root decay fungi, *Armillaria sp.*, whose role in the decline is still undetermined (Brown et al., 2015; Denman et al., 2017, 2014). The opportunists associated with AOD contribute to the rapid deterioration of tree health in several ways, for example, the larval galleries that *A. biguttatus* creates in the phloem of the host, limit the flux of sap around the tree; if the phloem is destroyed, non-photosynthetic parts of the plant starve. *A. biguttatus* lays its eggs between the bark plates of the stem. The beetles are inclined to choose trees that are already under abiotic or biotic stress, as they are attracted by volatile organic compounds emitted by the weakened tree (Vuts et al., 2016). When the eggs hatch, the larvae enter the trunk tissues beneath the bark and create the sinuous galleries in the phloem. The larval galleries normally appear in close proximity to necrotic tissues. There is a relationship between presence of larval galleries and an increased size of necrotic AOD patches, therefore it is known that *A. biguttatus* has a role in spreading the disease within the tree, as the larvae spread the pathogen around the inner bark (Denman et al., 2018). The distribution of *A. biguttatus* in UK is overlapping with the distribution of AOD cases, and the galleries are highly concurrent with the necrotic lesions (Brown et al., 2017).

1.2.3. Bacteria associated with AOD

AOD is caused by a consortium of bacterial species. Over the past decade, numerous Gram-negative bacterial strains have been isolated from necrotic lesions on AOD symptomatic oaks, at several sites in UK. Many of these strains have been identified as belonging to the order Enterobacterales, and have been classified as novel species or subspecies in the genera *Gibbsiella*, *Brenneria*, *Lonsdalea* and *Rahnella* (Brady *et al.* 2010; Denman *et al.* 2012; Brady *et al.* 2012). The taxonomic arrangement of these four genera have changed often and currently *Gibbsiella* and *Rahnella* belong to the family *Yersiniaceae* and *Brenneria* and *Lonsdalea* belong to *Pectobacteraceae* (Soutar and Stavrinides, 2020). Additionally, bacteria included in the family *Pseudomonadaceae* have been isolated from symptomatic trees, but their involvement in the disease has yet to be elucidated, although the general consensus is that they are endophytes (Sapp *et al.*, 2016).

Several studies of the bacterial communities in oak, related to AOD, have been performed over the years. The traditional idea that describes a disease as the interaction between host, pathogen and the environment is being questioned the more we know about microbial communities, their interactions, and the role of endophytes (Feau and Hamelin, 2017). Culture-dependent and culture-independent techniques have been used to analyse the microbiome of oaks in studies related to AOD. Studies in the composition of the cultivatable bacterial communities isolated from diseased and healthy oaks at different sites in UK have been performed. Denman *et al.*, (2016) observed that the most frequently isolated species from symptomatic oak in UK include the pathogens *Gibbsiella quercinecans* (Gq), *Brenneria goodwinii* (Bg) (**Figure 5**), *Rahnella victoriana* (Rvi), as well as unclassified *Pseudomonas* species and two undescribed Gram-positive species (Broberg *et al.*, 2018). In parallel, Sapp *et al.*, (2016) performed culture-independent studies of the bacteria in healthy and diseased oaks in five sites in the UK. The study was the metabarcoding of the microbiome, based on a 454 base pairs long amplicon contained in the 16S rRNA gene. According to the results, the composition of the microbiome was more strongly influenced by geographical location of the tree than for health status or the tissue type analysed. Generally, the most abundant species in the oaks were Gammaproteobacteria (such as *Enterobacteraceae* and *Pseudomonadaceae*), and Firmicutes. The *Enterobacteraceae* could be Bg as this species was part of this family at the time the study was published (currently *Pectobacteriaceae*) (Adeolu *et al.*, 2016). Other species of *Enterobacteraceae* were found in diseased oaks, such as the known phytopathogens *Erwinia*, and it was suggested that they could possess a role in AOD.

No difference was observed between the composition of the *Pseudomonadaceae* in healthy and diseased oaks, indicating that they were common members of the oak's microbiome. Some Firmicutes are able to degrade cellulose, and undertake a saprophytic lifestyle, suggesting that these Gram-positives could play a role in AOD (Cotta et al., 2009). In addition, in healthy oaks *Halomonadaceae*, *Shewanella* sp., *Achromobacter* sp., and *Stenotrophomonas* sp. were found.

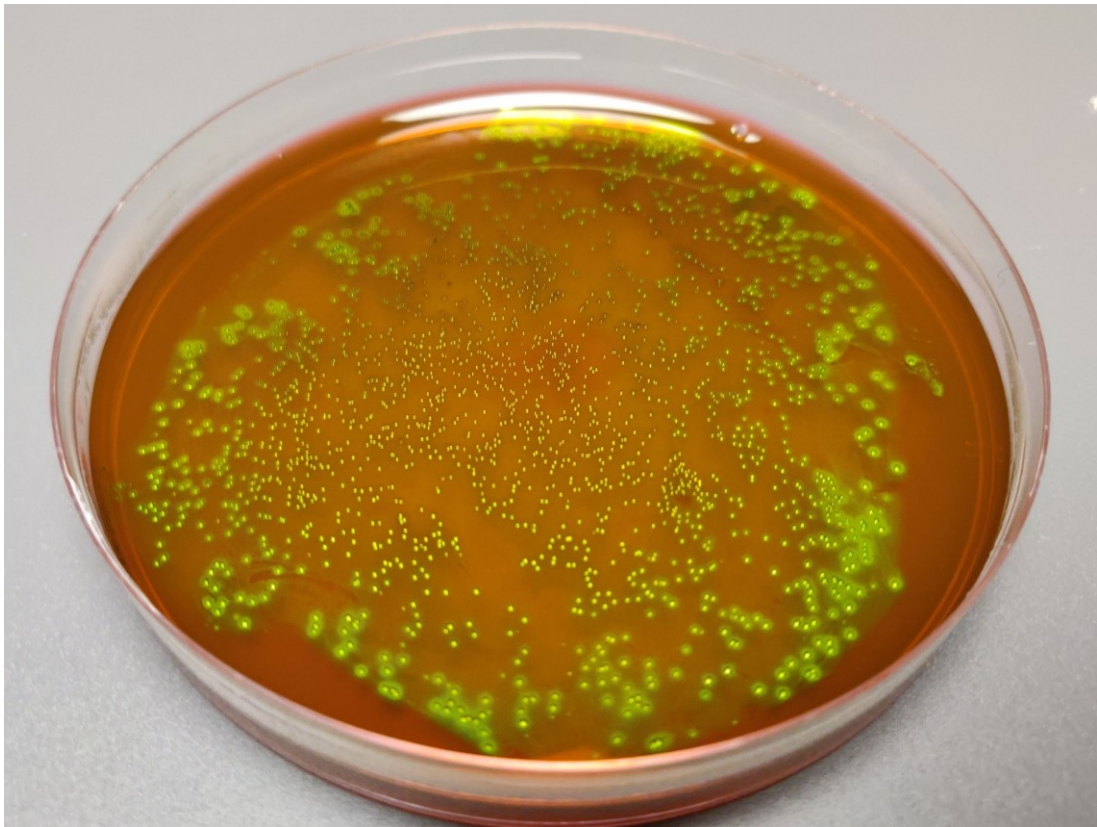


Figure 5: Colonies of the Acute Oak Decline pathogen *Brenneria goodwinii* on eosin methylene blue agar. The bacterial colonies show a distinctive metallic green colouration.

Studies of the microbiome associated with lesions (also known as pathobiome) and classical infectivity studies in oak logs showed that Bg, Gq and Rvi are abundant in the lesion and that they have genes that code for virulence factors typical of a phytopathogen (Denman et al., 2018). Denman *et al.* (2018) demonstrated that Bg, Gq and Rvi fulfilled the Koch's postulates with traditional infection/re-isolation procedures in logs. Koch's postulates are four principles conceived to determine a connecting association between a causal agent and a

disease. Posterior studies compared the pangenomes of the members of the AOD pathobiome with putative phytopathogens and the results suggested that Bg and *Lonsdalea britannica* (Lb) (occasionally isolated in the AOD necrotic tissue), are the primary pathogens (Doonan et al., 2019). According to Doonan *et al.* (2019), Gq and Rvi might be collaborating with the primary pathogens in the necrosis as opportunistic pathogens.

Where do Bg and Gq come from? The survival of these species has been tested in rainwater and forest soil, which are the main niches of plant pathogenic bacteria in forests. Bg survival was very low in the reservoirs studied, suggesting that Bg is unable to live in these ecological niches, and therefore could be an endosymbiont of oak. However, greater viability was observed in the case of Gq, which suggests that this species could survive in soil and rainwater in forest ecosystems (Pettifor et al., 2020). Are the bacteria brought to the oak by *A. biguttatus*? Recently, differential gene expression analyses were performed in log inoculation studies. Amongst other combinations, inoculations of Bg and of Bg + *A. biguttatus* eggs were compared. Co-inoculation of Bg + *A. biguttatus* eggs showed an upregulation of genes related to pathogenicity and detoxification (such as the genes encoding catalase peroxidase or glutathione reductase, which are enzymes used by bacteria to neutralize plant defences) in Bg, suggesting an increase of virulence of Bg when inoculated with the beetle's eggs. This study also showed that the oak upregulates more genes related to defence when *A. biguttatus* was present (Doonan et al., 2020). However, the question as to whether the beetle is a vector for the AOD bacteria is still under study (Brown et al., 2015, 2017; Denman et al., 2018, 2014; Moraal, Achterberg and van Achterberg, 2001; Vansteenkiste et al., 2004).

Due to the polybacterial character of AOD, an in-depth investigation is needed to describe the roles of all bacterial species isolated from AOD lesions, including the undescribed Pseudomonads. This is because bacterial infections in plants do not always meet Koch's postulates. There are several reasons why polymicrobial diseases sometimes challenge the Koch postulates. For instance, the postulates require a causal agent to be isolated in diseased tissue, but never in healthy tissue, and this presents an issue in plant diseases because an asymptomatic status of the plant can easily be erroneously classified as healthy, and vice versa, and because an endophyte can turn pathogenic. In addition to this, another way in which plant diseases sometimes challenge Koch's postulates is if a pathogen causes the disease in synergy with other pathogens or endophytes. In this case, the re-inoculation of this pathogen in the host will not necessarily cause the disease, as the microorganism is lacking the cooperation of the other bacteria (Bass et al., 2019; Lamichhane and Venturi,

2015). One example of this is the olive knot disease, which was initially believed to be caused by *Pantoea agglomerans* (Pa), because it satisfied the Koch's postulates. Savastano, (1886), managed to infect healthy olive plants with the knot disease using pure cultures of Pa, and to isolate afterwards the same bacterial strain from the infected tissue. However, the olive knot disease was subsequently demonstrated to be caused by *Pseudomonas savastanoi* pv. *savastanoi* (Psv) (Petri, 1907). In this study, it was suggested that the incorrect role assignment was due to some contamination of the Pa inoculum with the authentic pathogen, Psv. It has also been revealed that Psv causes greater damage when it is accompanied by endophytes of the olive tree (Marchi et al., 2006). Endophytes are bacterial species considered harmless or even beneficial, living in the plant tissues. In the case of the olive tree, the endophytes are mainly *Erwiniaceae* (formerly of the *Enterobacteriaceae*) belonging to the genera *Pantoea* and *Erwinia* (da Silva et al., 2014). It has been observed that when co-inoculating both bacteria Pa and Psv, the knots produced on olive were bigger than the knots produced when inoculating Psv alone, (Fernandes and Marcelo, 2002). Furthermore, several studies have proven that Pa forms stable communities with other non-pathogenic *Enterobacteriaceae*. These communities facilitate the establishment and development of Psv, and therefore collaborate in increasing the progression and severity of the disease (Buonaurio et al., 2015). Thus, non-pathogenic bacteria can benefit the activity of pathogenic strains in several ways, including through the exchange secondary metabolic products, release of substances that facilitate the creation of biofilms, or production of compounds that suppress the defence responses of the plant (Harwood and Parales, 1996).

1.2.4. Management of AOD

Oak trees displaying symptoms of AOD are reported by the public to the Tree Health Diagnostic Advisory Service of Forest Research. Forest Research's recommendations regarding trees affected by AOD are generally to do nothing with them, unless the symptoms appear only in a few trees among numerous other trees who appear healthy. In that case, the recommendation may be to cut down the infected trees. No pruning or composting the plant materials of infected trees is advised.

1.3. Plant-associated bacteria

Important symbiotic relationships exist between plants and their specific associated microbiome. Bacteria associated with plants are classified as endophytic, rhizospheric or phyllospheric depending on the location of their habitat in the plant (Hardoim et al., 2015; Reinhold-Hurek et al., 2015; Vorholt, 2012). Most rhizospheric bacteria approach the plant horizontally, from the soil, but can also be transferred vertically through seeds (Fierer, 2017; Hardoim et al., 2012). Endophytes normally reach the different parts of the plant through its xylem (Compant, Clément and Sessitsch, 2010). Phyllospheric and endophytic bacteria come generally from the soil and the profile of the community is highly dependent on environmental conditions (Vorholt, 2012; Zarraonaindia et al., 2015). The bacteria that make up the microbial communities associated with plants interact with each other and with the plant. Strategies of plant-associated bacteria to invade, colonise and establish themselves within the plant tissues include motility and the ability to secrete plant wall-degrading enzymes and lipopolysaccharides (Liu et al., 2017). Plant-associated bacteria also generally have the capacity to avoid plant defence mechanisms such as the production of reactive oxygen species, secreting enzymes to scavenge them (Apel and Hirt, 2004). Plant-associated bacteria can have a beneficial effect in the plant such as growth promotion or inhibition of pathogen activity. Bacteria promote plant growth with mechanisms such as fixing atmospheric nitrogen, solubilizing phosphorus from the soil, providing iron with the help of bacterial siderophores and altering phytohormone balances to alleviate plant biotic and abiotic stresses (Glick, 2004, 2012). Endophytic bacteria can inhibit pathogen activity with mechanisms such as the production of antibiotics or lytic enzymes. Endophytes can also compete with the pathogen for resources, for example by using siderophores that chelate the iron, decreasing its availability for the pathogens (Frankowski et al., 2001; Innerebner,

Knief and Vorholt, 2011; O'Sullivan and O'Gara, 1992; Singh et al., 1999; Whipps, 2001). There are also approximately 150 known bacterial species that are pathogenic to plants. Plant pathogenic bacteria have a huge impact on agriculture, food supply, and the environment. These pathogens are sometimes able to attack a wide variety of plant hosts and their dispersion is nearly impossible to control as they generally disperse through air, soil, or vectors like insects.

1.4. Bacterial plant pathogen detection methods

Plant diseases caused by bacteria are often difficult to diagnose, particularly at early stages of the disease, when management and treatment are more effective. The traditional cultured-based methods of diagnosis of phytopathogenic bacteria were based on time consuming morphological and biochemical analyses. Nowadays there are a wide range of molecular biology techniques applied to plant pathogen detection. The diagnostic methods can be classified by the compound they target, i.e. nucleotide sequences, volatile organic compounds (VOC), and proteins. The methods based on the DNA amplification of specific sequence targets are highly specific and sensitive. These techniques can be grouped as those related to polymerase chain reaction (PCR), and those that employ isothermal nucleic acid amplification. PCR-based procedures rely on thermal cyclers that allow thermostable DNA polymerases to perform amplification of the specific target sequence. Some examples of PCR based methods of detection for plant pathogens are sequence characterized amplified region (Paran and Michelmore, 1993), DNA microarray (Boonham et al., 2003), high resolution melting (HRM) (Gori, Cerboneschi and Tegli, 2012), and next generation sequencing (NGS) (Al Rwahnih et al., 2015). They are robust procedures (Sankaran et al., 2010), but require prior knowledge of the targeted sequence. Multiplex PCR (López et al., 2009), HRM and DNA microarray allow simultaneous amplification and analysis of multiple target sequences. Another nucleic acid-based assay related to PCR is DNA fingerprinting, first described by Sir Alec Jeffreys in 1985 (Jeffreys, Wilson and Thein, 1985). This technique compares unique DNA patterns or polymorphisms of the individuals to assess the genetic diversity. Some examples of DNA fingerprinting techniques are: amplified fragment length polymorphism (Clerc, Manceau and Nesme, 1998), repetitive element sequence-based PCR or rep-PCR (Versalovic, Koeth and Lupski, 1991), including BOX-PCR (Martin et al., 1992), enterobacterial repetitive intergenic consensus, abbreviated as ERIC-PCR (Hulton, Higgins and Sharp, 1991), and RAPD-PCR, that stands for random amplification of polymorphic DNA

(Williams et al., 1990). Fingerprinting methods do not need previous knowledge of the genomic fragments amplified.

Isothermal DNA amplification methods are very time-efficient and do not require a thermocycler, as the amplification reaction occurs at a constant temperature. Some isothermal amplification techniques are strand displacement methods such as strand displacement amplification (Walker et al., 1992), loop-mediated amplification (Mori et al., 2001; Ward and Harper, 2012), and Smart Amplification process version 2 (Lezhava et al., 2010). Helicase-dependent amplification method (Vincent, Xu and Kong, 2004), and the recombinase polymerase amplification (Piepenburg et al., 2006) are isothermal DNA amplification techniques. Nucleic acid sequence-based amplification is an isothermal RNA amplification assay (Compton, 1991) that has been used to detect bacterial pathogens in citrus (Scuderi et al., 2010).

Another approach for pathogen identification is the detection of proteins associated with the microorganisms or their activity in the plant tissues with serological techniques such as enzyme-linked immunosorbent assay, flow cytometry or immunofluorescence (Alarcon et al., 1990; Caruso et al., 2002). There are other DNA-independent plant disease diagnostic methods such as spectroscopy and imaging techniques or methods based on volatile organic compound (VOC) detection. These are also called remote sensing technology. The aim of imaging techniques such as hyperspectral imaging technology (Okamoto et al., 2009) is to remotely sense spectral changes of the plant, due to physiological changes related to the disease, such as the reduction of the photosynthesis rate in the leaves. Electronic-nose devices (Laothawornkitkul et al., 2008) can target VOCs generated by the phytopathogens themselves or by changes in the metabolism of the plant, this can be very helpful to determine plant disease in early stages when the symptoms are still not apparent. Gas chromatography–mass spectrometry is also commonly used for profiling of VOCs in plant diseases (Kushalappa et al., 2002).

In recent years nanotechnology-based diagnostic methods are emerging for the detection of plant pathogens. Most of the nanotechnologies were initially developed for medical research and they have been applied to plant disease management afterwards. The nanodiagnostic techniques can be divided between those that use tools on a nanoscale, and those that use nanoparticles (structures with one dimension smaller than 100 nm). Examples of “nanotools”-based techniques are those that include devices such as microneedle patches and nanopore sequencing platforms; examples of nanoparticle-based techniques are array-

based nanosensors such as the “electronic nose” (Li et al., 2020) and gold nanoparticles. A microneedle patch combined with traditional real-time PCR has been used for the detection of DNA of the pathogen *Phytophthora infestans* in tomato leaves (Paul et al., 2019). The single-molecule sequencing technology, nanopore platform, has also been successfully used for the detection of several inoculated plant pathogens in plants and seeds (Chalupowicz et al., 2019). As nanoparticle-based diagnostic techniques, electronic noses have been used to detect plant pathogens, food pathogens and chemicals related to food spoilage. They work because VOCs induce physicochemical changes in the electronic nose's gas sensors, and the changes are translated into electrical signals, which, in turn, are interpreted through pattern recognition analysis. The detected gas patterns are interpreted as the corresponding diagnoses (Bhattacharya et al., 2007; Srivastava, Dev and Karmakar, 2018). Other nanoparticle-based diagnostic techniques rely on the physicochemical properties of gold nanoparticles. These properties allow them to bond with nucleic acids or proteins, thus, becoming target-specific probes that are used for the molecular pathogen detection and identification, amongst other uses (Thaxton, Georganopoulou and Mirkin, 2006).

1.5. Previous work in diagnosis of AOD

More than 200 swabs from symptomatic oaks, suspected to have AOD, were processed by Forest Research in 2019 alone (Crampton et al., 2020). This ongoing effort is combined with a constant improvement of the diagnostic methods used for this disease. Using the large database of acquired sequence information generated by the multilocus sequence analysis studies (MLSA) of the bacteria associated with AOD in UK, a rapid identification technique was developed (Brady et al., 2016). The technique was based on HRM analysis of the *atpD* gene and it identified four of the most frequently isolated bacterial species. HRM analysis is a real-time PCR technique, whereby single nucleotide polymorphisms (SNPs) can be identified in amplification products without DNA sequencing. HRM analysis provides the melting profile of a PCR product depending mainly on its GC composition, length, sequence, and the SNPs, using DNA-intercalating dyes, that lose fluorescent signal when the double stranded DNA denatures. This SNP detection tool is rapid, accurate, and is non-destructive of the amplification products, while also being cost-effective. Using HRM analysis of the *atpD* gene, it has been possible to assign isolates to either Gq, Bg, *Brenneria roseae* ssp. *roseae* (Brr) or Lb (four of the most frequently isolated species associated with AOD in UK) in a single assay, greatly reducing the time taken to identify these species from pure cultures (Brady et

al., 2016, 2017). However, this assay has only been successfully implemented on pure cultures of the four AOD bacterial species. Environmental samples can contain hundreds of bacterial species, therefore a diagnostic method for AOD must be able to detect bacteria from mixed cultures. The HRM analysis of the *atpD* gene required the “spiking” of the sample following the amplification of the partial *atpD* and prior to the HRM analysis to find enough differentiation between strains (**Figure 6**). The spike was a PCR probe of the *atpD* gene, belonging to the type strain of Gq. Another challenge in the diagnosis of AOD is that the species of bacteria associated with AOD are strongly phylogenetically related, and the discriminating power of the HRM analysis of the *atpD* gene is often not enough to separate the strains.

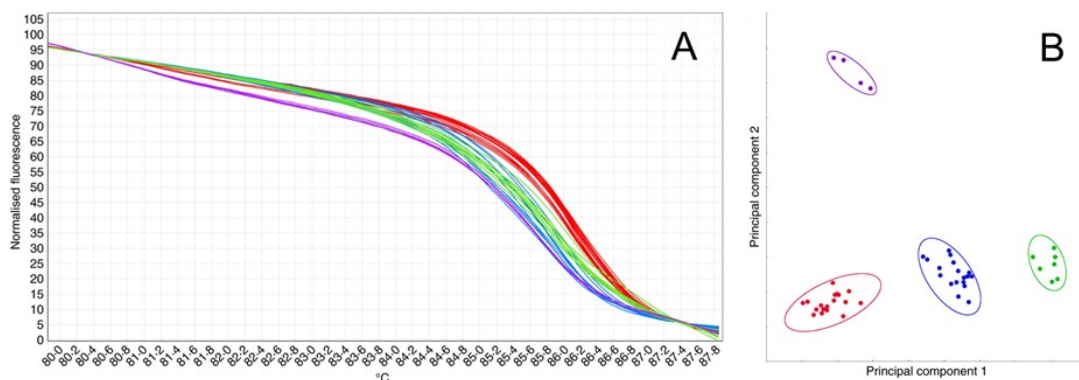


Figure 6: Rapid identification of bacteria associated with Acute Oak Decline (AOD) by high resolution melt (HRM) analysis of the *atpD* gene. **A:** HRM curves generated for species associated with AOD in UK. *Gibbsiella quercinecans* n=10 (—), *Brenneria goodwinii* n=9 (—), *Brenneria roseae* subsp. *roseae* n=5 (—) and *Lonsdalea britannica* n=2 (—). **B:** Scatter plot of the data set obtained in the HRM assay of the *atpD* gene in figure A, each dot represents a single strain in duplicate. Figure adapted from (Brady et al., 2016), and used under agreement with John Wiley and Sons (press with the license no. 5003801129021).

Recently a multiplex real-time PCR assay was developed for the detection and quantification of Gq, Bg Rvi and Lb (Crampton et al., 2020). The method can do so from swabs obtained from the bleeding cracks in the stem, and it is specific to species-level for Bg and genus-level for the other three targets. The assay is based on TaqMan probes and primers that were designed using the beta subunit of the gyrase gene (*gyrB*) and the beta subunit of the RNA polymerase gene (*rpoB*) as template. The swabs are collected from stem bleeds, stored at 4

°C and then cells in the swabs are rinsed in PBS, filtered (5 µm pore hydrophilic filter) and washed four times (**Figure 7**). The assay is highly sensitive, detecting values below 100 cells for the four targets, but poorly specific, as only the assay for one of the targets, Bg, was species-specific.

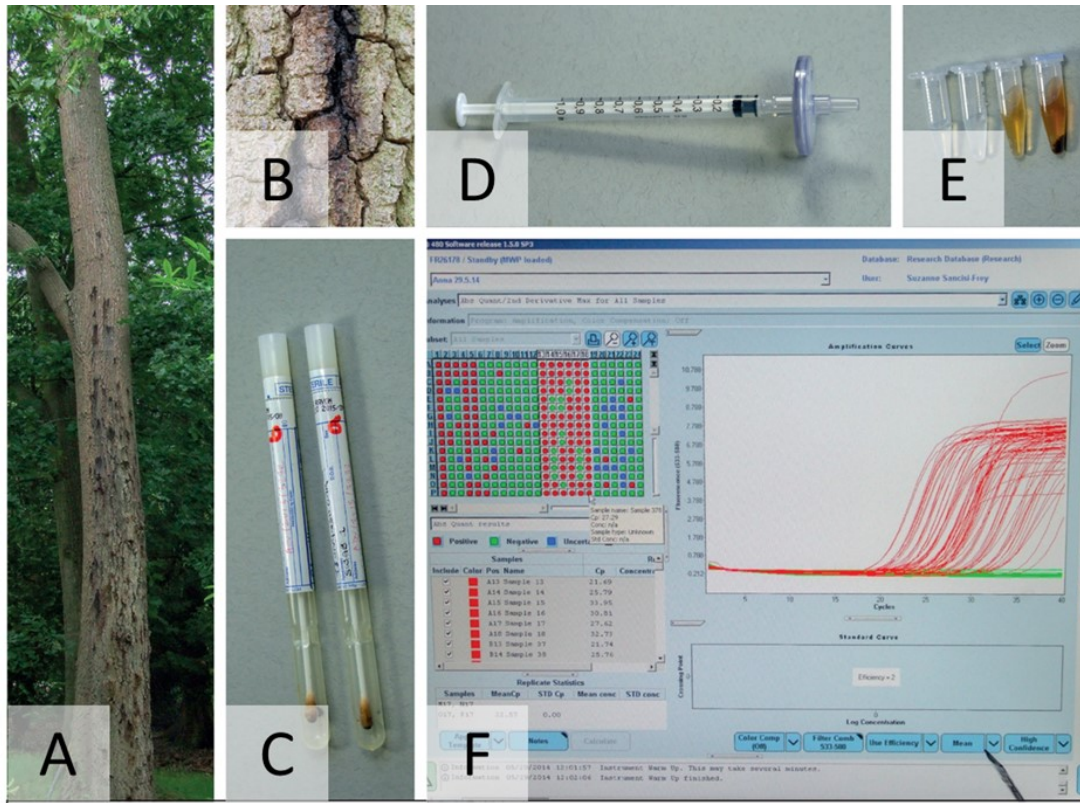


Figure 7: Graphical abstract of the paper of the multiplex Taqman-based diagnostic method for bacteria associated with Acute Oak Decline. **A:** Stem of an oak tree displaying symptoms of AOD, vertical cracks from which dark fluid emanates. **B:** Closer image of a stem bleed. **C:** Swabs used for the collection of the sample (exudate from the stem). **D:** Syringe used for filtering the cells detached from the swab into PBS. **E:** Sample after each of the four washing steps that are part of the sample processing prior to the analysis. **F:** Real-time PCR reactions of the AOD samples. Figure adapted from (Crampton et al., 2020), and used under agreement with John Wiley and Sons (press with the license no. 5003810819101).

Ground penetrating radar (GPR) technology has also been proposed for the diagnosis of AOD (Giannakis et al., 2019). Giannakis *et al.*, (2019) simulated the main symptoms of AOD-decay,

the vertical cracks in the bark filled with dark fluid. Holes were drilled in cross sections of dead oak logs and they were filled with sawdust mixed with water to simulate the bleeding of the tree. Simulated symptoms of AOD were successfully diagnosed under laboratory conditions and GPR has been proposed as a commercially appealing way to detect the main symptom of AOD-decay. However, the technique has not been tested in the field yet. Additionally, in the field, the bleeding of the tree will not be in a cross section of oak logs, but in the outer bark, whose background is more irregular than a cross section of a tree.

1.6. Taxonomic identification of bacteria

Several undescribed species belonging to the family *Pseudomonadaceae* were consistently isolated along with the key AOD-associated species. In environmental microbiology it is common to isolate undescribed species of bacteria. An essential step for the precise knowledge of a bacterial disease is the accurate profiling of the species present in the affected tissues, in the case of AOD, the bacteria present in the vertical necrotic patches between the bark plates. Establishing a clear profile of the species present in the infected area is essential to proceed with pathogenicity studies and studies of interactions between different species. Once the roles of each bacterium in the disease are clear, targets can be chosen for the development of diagnostic methods or possible treatments. The field of microbiology dealing with the formal description of novel bacterial species is bacterial taxonomy.

For the last several decades the preferred method for prokaryotic taxonomic classification is the polyphasic approach (Colwell, 1970). The polyphasic approach is the collection of a standardised list of features of the novel bacterium, including genotypic, phenotypic and chemotaxonomic features. The characterisation allows the comparison of the novel species with already described species, and specifically, the identification of the differences between the novel bacterium and its closest known relatives. The information obtained through the polyphasic approach creates a reliable and well-defined phylogenetic framework for the microorganism under analysis. The phylogenetic relationships are usually inferred by comparing molecular markers (homologous nucleic acid or amino acid sequences). More than fifty years ago, nucleotide sequences were described as evolutionary indicators (Zuckerkindl and Pauling, 1965). The study of rRNA gene sequences for phylogenetic purposes was first proposed four decades ago (Woese and Fox, 1977), and since then, the

genes encoding for the 16S ribosomal RNA, a structural component of the 30S subunit of the ribosomes in prokaryotes, have been widely used as genetic markers for taxonomic identification. It is generally accepted that when a strain differs more than 3% in its 16S rRNA sequence with the closest related neighbour, this strain can tentatively be considered a new species (Konstantinidis and Tiedje, 2005). However, the 97% 16S rRNA sequence similarity threshold does not determine a new species by itself; it only indicates the possibility, as it is known that the 16S rRNA gene is too conserved to provide sufficient resolution as molecular marker in very related species (Mignard and Flandrois, 2006; Reller, Weinstein and Petti, 2007). To perform a more robust taxonomic analysis of the phylogenetic relationships of the taxa it is necessary to combine the study of the 16S rRNA gene with the study of other molecular markers (Dahllof, Baillie and Kjelleberg, 2000). Protein-coding genes such as gyrase beta subunit (*gyrB*), RNA polymerase 70 sigma factor (*rpoD*) and beta subunit of the RNA polymerase (*rpoB*) are less evolutionary preserved and several studies have selected them to be used in MLSA, specifically in *Pseudomonas* species (Mulet, Lalucat and García-Valdés, 2010; Yamamoto et al., 2000). Protein-coding molecular markers are preferred to the widely used 16S rRNA marker, because while being widely distributed among prokaryotic lineages, the rate of evolutionary conservation is lower than for the 16S rRNA gene, allowing a better prediction of the phylogenetic relationships between taxa (Lan, Rosen and Hershberg, 2016). Due to the advances in DNA sequencing technology which have made the sequencing of whole bacterial genomes not only possible but affordable in laboratories worldwide, the genotypic characterisation of novel species of bacteria now generally includes the sequencing of its complete genome. Tools are available for inferring the phylogenetic relationships amongst taxa using not only genes, but the complete genomes. This avoids some issues such as any potential bias caused by the choice of gene in the phylogenetic analysis (Shakya et al., 2020). Due to its reliability, the phylogenetic analysis of the complete genomes is likely to become the next gold standard in bacterial taxonomy. In addition to the genotypic characterisation of the novel bacterium, the polyphasic approach must include the collection of a set of phenotypic features (e.g. pigment production, carbohydrate utilisation or colony morphology) and chemotypical features such as fatty acid methyl esters profiling. These features support the description of the novel species and help distinguish the novel bacterium from its closest phylogenetic neighbours.

Bacterial taxonomy is in constant change, the names and groups of taxa suffer constant alterations when novel species are described, and more phylogenetic studies are performed. It could be said that taxonomy is a fluid science that never really settles. The microbial tree

of life is incomplete, hundreds of novel bacterial species are described every year. Every time a novel species is described, the shape of the tree can potentially be modified, since each addition is a piece of the puzzle that was not available before. The International Code of Nomenclature of Prokaryotes and its successors regulate the nomenclature of bacteria, although there is not an official classification system in bacterial taxonomy. For the validation of novel bacterial names, the author must designate a type strain, deposit it into two different culture collections, located in different countries, and perform a polyphasic approach of bacterial classification.

1.7. Aims, objectives and scope of the research project

The rapid detection of affected oaks is crucial for developing management strategies to reduce the spread of AOD. The overall aim of this project was to optimize the identification and diagnosis of the bacteria isolated from symptomatic oaks suspected of AOD infection. The idea is to create a simple and cost-efficient diagnostic method for AOD-associated bacteria, based on the HRM technique, as well as to describe the different *Pseudomonads* isolated frequently from diseased oak, and investigate their implication in the disease. To achieve these aims, three objectives were defined:

Objective 1

Formally describe the novel *Pseudomonads* species consistently isolated from AOD lesions, and study their potential pathogenicity traits. To perform this part of the project the *Pseudomonads* will be formally described following the polyphasic approach of bacterial classification. Their potential pathogenicity traits will be studied through pathology tests.

Objective 2

Develop an HRM diagnostic assay to allow detection and identification of AOD-associated bacteria from swabs taken from trees, as well as directly from plant material. Investigate multiplex HRM including several diagnostic loci.

Objective 3

Expand the bacteria that can be identified by the HRM technique to include other species of the genera commonly found in AOD symptomatic plants.

CHAPTER 2. Materials and methods

2.1. Bacterial strains

Bacterial strains, isolated from AOD symptomatic oaks were obtained from Forest Research, UK. They were collected from AOD-affected sites in the South of England: Great Monk Wood, Bisham Woods, Send and Stratfield Brake. The isolates were tentatively identified by partial *gyrB* gene sequencing as members of the family *Pseudomonadaceae* at Forest Research, and additional strains collected in Kew Gardens were included in this study (**Table 1**). In addition to AOD-associated Pseudomonads, other relevant strains were used for the development and validation of diagnostic methods for AOD-associated bacteria (**Table 2**).

Table 1: List of Pseudomonads isolated from AOD-symptomatic *Quercus robur* in the UK. The list of strains contains various types of nomenclature. The twenty-eight strains whose name begins with “P”, participated in this study from the beginning, they were named like this to simplify the name. The strains that kept their isolate name were incorporated into the study afterwards, and their name was not changed.

Isolate	Strain	Isolation source	Location	Coordinates
PW134 a	P1	<i>Q. robur</i> , AOD-symptomatic inner bark	Bisham Woods, UK	51.54911° N, 0.77071° W
PW134 b	P2	<i>Q. robur</i> , AOD-symptomatic inner bark	Bisham Woods, UK	51.54911° N, 0.77071° W
PW135 b	P3	<i>Q. robur</i> , AOD-symptomatic inner bark	Bisham Woods, UK	51.54911° N, 0.77071° W
PW138 aii	P5	<i>Q. robur</i> , AOD-symptomatic inner bark	Bisham Woods, UK	51.54911° N, 0.77071° W
PW147	P7	<i>Q. robur</i> , AOD-symptomatic inner bark	Bisham Woods, UK	51.54911° N, 0.77071° W
PW148 b	P8	<i>Q. robur</i> , AOD-symptomatic inner bark	Bisham Woods, UK	51.54911° N, 0.77071° W
PW150 aii	P9	<i>Q. robur</i> , AOD, symptomatic sapwood	Bisham Woods, UK	51.54911° N, 0.77071° W
PW169 b	P18	<i>Q. robur</i> , larval galleries created by <i>A. biguttatus</i> in phloem	Bisham Woods, UK	51.54911° N, 0.77071° W
PW184 b	P20	<i>Q. robur</i> , larval galleries created by <i>A. biguttatus</i> in phloem	Bisham Woods, UK	51.54911° N, 0.77071° W
PW187 b	P21	<i>Q. robur</i> , larval galleries created by <i>A. biguttatus</i> in phloem	Bisham Woods, UK	51.54911° N, 0.77071° W
PW188 ci	P22	<i>Q. robur</i> , larval galleries created by <i>A. biguttatus</i> in phloem	Bisham Woods, UK	51.54911° N, 0.77071° W
PW208	P23	<i>Q. robur</i> , AOD-symptomatic inner bark	Bisham Woods, UK	51.54911° N, 0.77071° W
PW141 biiiaib	P6	<i>Q. robur</i> , AOD-symptomatic inner bark	Bisham Woods, UK	51.54911° N, 0.77071° W
GM35b	P26	<i>Q. robur</i> , larval galleries created by <i>A. biguttatus</i> in phloem	Great Monk Wood, UK	51.89955 °N, 000.64606 °E
GM36b	P27	<i>Q. robur</i> , larval galleries created by <i>A. biguttatus</i> in phloem	Great Monk Wood, UK	51.89955 °N, 000.64606 °E
GM38b	GM38b	<i>Q. robur</i> , larval galleries created by <i>A. biguttatus</i> in phloem	Great Monk Wood, UK	51.89955 °N, 000.64606 °E
GM48c	GM48c	<i>Q. robur</i> , larval galleries created by <i>A. biguttatus</i> in phloem	Great Monk Wood, UK	51.89955 °N, 000.64606 °E
GM50b	GM50b	<i>Q. robur</i> , larval galleries created by <i>A. biguttatus</i> in phloem	Great Monk Wood, UK	51.89955 °N, 000.64606 °E

I151	I151	<i>Q. robur</i> , outer bark, dry AOD lesion	Kew Gardens, UK	Ref. n. tree: 19017, D.O.B.: 1973
I160	I160	<i>Q. robur</i> , AOD-symptomatic sapwood	Kew Gardens, UK	Ref. n. tree: 19017, D.O.B.: 1973
I163	I163	<i>Q. robur</i> , AOD-symptomatic sapwood	Kew Gardens, UK	Ref. n. tree: 19017, D.O.B.: 1973
I166	I166	<i>Q. robur</i> , AOD-symptomatic sapwood	Kew Gardens, UK	Ref. n. tree: 19017, D.O.B.: 1973
PW136	P4	<i>Q. robur</i> , AOD-symptomatic inner bark	Bisham Woods, UK	51.54911° N 0.77071° W
PW153	P10	<i>Q. robur</i> , AOD-symptomatic sapwood	Bisham Woods, UK	51.54911° N 0.77071° W
PW155 ai	P11	<i>Q. robur</i> , larval galleries created by <i>A. biguttatus</i> in phloem	Bisham Woods, UK	51.54911° N 0.77071° W
PW158 a	P14	<i>Q. robur</i> , larval galleries created by <i>A. biguttatus</i> in phloem	Bisham Woods, UK	51.54911° N 0.77071° W
PW160 bib	P16	<i>Q. robur</i> , larval galleries created by <i>A. biguttatus</i> in phloem	Bisham Woods, UK	51.54911° N 0.77071° W
PW164 bia	P17	<i>Q. robur</i> , larval galleries created by <i>A. biguttatus</i> in phloem	Bisham Woods, UK	51.54911° N 0.77071° W
PW214	P24	<i>Q. robur</i> , non-AOD-symptomatic sapwood	Bisham Woods, UK	51.54911° N 0.77071° W
PW211 b	P25	<i>Q. robur</i> , AOD-symptomatic sapwood	Bisham Woods, UK	51.54911° N 0.77071° W
S40	P28	<i>Q. robur</i> , non-AOD-symptomatic sapwood	Send, UK	51.287756° N 0.52787875° W
SB22b	P29	<i>Q. robur</i> , larval galleries created by <i>A. biguttatus</i> in phloem	Stratfield Brake, UK	51.80306° N 001.28274° W
SB60b	P30	<i>Q. robur</i> , AOD-symptomatic inner bark	Stratfield Brake, UK	51.80306° N 001.28274° W
SB61b	P31	<i>Q. robur</i> , AOD-symptomatic inner bark	Stratfield Brake, UK	51.80306° N 001.28274° W
SB65	P32	<i>Q. robur</i> , larval galleries created by <i>A. biguttatus</i> in phloem	Stratfield Brake, UK	51.80306° N 001.28274° W

AOD: Acute Oak Decline.

Table 2: List of bacterial species used in this project.

Species	Strain	Culture collection	Isolation source	Location
<i>Brenneria alni</i>	DSM 11811 ^T	DSMZ	Bark cancer of alder	Tuscany, Italy
<i>Brenneria goodwinii</i>	FRB 141 ^T	FR	<i>Q. robur</i> exhibiting symptoms of AOD	UK
<i>Brenneria goodwinii</i>	BH 1/28a	FR	<i>Q. robur</i> exhibiting symptoms of AOD	UK
<i>Brenneria goodwinii</i>	FRB 171	FR	<i>Q. robur</i> exhibiting symptoms of AOD	UK
<i>Brenneria goodwinii</i>	FRB 186	FR	<i>Q. robur</i> exhibiting symptoms of AOD	UK
<i>Brenneria goodwinii</i>	BH 4/25a	FR	<i>Q. robur</i> exhibiting symptoms of AOD	UK
<i>Brenneria nigrifluens</i>	DSM 30175 ^T	DSMZ	Bark canker in Persian (English) walnut tree	California, USA
<i>Brenneria roseae</i> ssp. <i>americana</i>	FRB 223 ^T	FR	<i>Q. kelloggii</i>	USA
<i>Brenneria roseae</i> ssp. <i>roseae</i>	FRB 222 ^T	FR	<i>Q. cerris</i>	UK
<i>Brenneria roseae</i> ssp. <i>roseae</i>	BH1/58	FR	<i>Q. robur</i>	UK
<i>Brenneria roseae</i> ssp. <i>roseae</i>	BH1/40b	FR	<i>Q. robur</i>	UK
<i>Brenneria rubrifaciens</i>	DSM 4483 ^T	DSMZ	Persian walnut tree	Unknown
<i>Brenneria salicis</i>	DSM 30166 ^T	DSMZ	Willow	Unknown
<i>Erwinia billingiae</i>	BH1/33	FR	<i>Q. robur</i>	UK
<i>Erwinia rhapontici</i>	A3 P19	FR	<i>A. biguttatus</i> , gut	UK
<i>Erwinia rhapontici</i>	Outwood 149	FR	<i>Q. robur</i>	UK
<i>Ewingella americana</i>	LMG 7869 ^T	FR	Throat sample	USA
<i>Ewingella americana</i>	FOD 24/3b	FR	<i>Q. robur</i> , AOD-symptomatic inner bark	Gloucestershire, UK
<i>Gibbsiella dentisursi</i>	DSM 23818 ^T	FR	Bear, oral cavity	Japan

<i>Gibbsiella dentisursi</i>	JCM 18389 ^T (=DSM 23818 ^T)	FR	Chinese bushbrown butterfly (<i>Mycalesis gotama</i>), intestinal tract	Seoul, Republic of Korea
<i>Gibbsiella gregii</i>	FRB 224 ^T	FR	<i>Q. kelloggii</i>	California, USA
<i>Gibbsiella gregii</i>	USA 42	FR	<i>Q. kelloggii</i>	California, USA
<i>Gibbsiella gregii</i>	R-52b	FR	<i>Q. kelloggii</i>	California, USA
<i>Gibbsiella gregii</i>	R-54a	FR	<i>Q. kelloggii</i>	California, USA
<i>Gibbsiella gregii</i>	R-66a	FR	<i>Q. kelloggii</i>	California, USA
<i>Gibbsiella quercinecans</i>	FRB 97 ^T	FR	<i>Q. petraea</i> , inner bark	Hoddesdon Park, UK
<i>Gibbsiella quercinecans</i>	BH 1/65b	FR	<i>Q. robur</i>	Essex, UK
<i>Gibbsiella quercinecans</i>	AT 18b	FR	<i>Quercus. sp.</i>	Shropshire, UK
<i>Gibbsiella quercinecans</i>	BH 1/86	FR	<i>Q. robur</i>	Essex, UK
<i>Gibbsiella quercinecans</i>	BER 12	FR	<i>Quercus. sp.</i>	Warwickshire, UK
<i>Gibbsiella quercinecans</i>	BW 2/28	FR	<i>Q. robur</i>	Essex, UK
<i>Gibbsiella quercinecans</i>	FOD 9/25	FR	<i>Quercus. sp.</i>	Gloucestershire, UK
<i>Gibbsiella quercinecans</i>	CH 214	FR	<i>Quercus. sp.</i>	Leicestershire, UK
<i>Gibbsiella quercinecans</i>	BH 1/44b	FR	<i>Q. robur</i>	Essex, UK
<i>Gibbsiella quercinecans</i>	FRB 24	FR	<i>Q. robur</i>	Booth Wood, UK
<i>Gibbsiella quercinecans</i>	FRB 124	FR	<i>Q. robur</i>	Outwood, UK
<i>Gibbsiella quercinecans</i>	N79	FR	<i>Quercus. sp.</i>	Spain
<i>Lonsdalea britannica</i>	LMG 26267 ^T (=FRB 18 ^T)	FR	<i>Q. robur</i>	Booth Wood, United Kingdom
<i>Lonsdalea iberica</i>	LMG 26264 ^T	FR	<i>Q. ilex</i>	Madrid, Spain
<i>Lonsdalea quercina</i>	LMG 2724 ^T	FR	<i>Quercus. sp.</i>	USA
<i>Pantoea sp.</i>	DI 19b	FR	<i>Quercus. sp.</i>	Netherlands

<i>Pantoea</i> sp.	DI 7a	FR	<i>Quercus</i> sp.	Netherlands
<i>Pseudomonas argentinensis</i>	LMG 22563 ^T	BCCM/LMG	<i>Chloris ciliata</i> , rhizosphere	Cordoba, Argentina
<i>Pseudomonas azotifigens</i>	LMG 23662 ^T	BCCM/LMG	Hyperthermal compost material	Japan
<i>Pseudomonas balearica</i>	LMG 18376 ^T	BCCM/LMG	Wastewater treatment plant	Mallorca, Spain
<i>Pseudomonas flavescens</i>	LMG 18387 ^T	BCCM/LMG	English walnut tree, canker tissue	Orinda, California, United States of America
<i>Pseudomonas fulva</i>	LMG 11722 ^T	BCCM/LMG	Japanese paddy	Japan
<i>Pseudomonas punonensis</i>	LMG 26839 ^T	BCCM/LMG	Grasses (<i>Poaceae</i>) straw in which potato are dried	Puno, Peru
<i>Pseudomonas seleniipraecipitans</i>	LMG 25475 ^T	BCCM/LMG	Soil	Fresno County, California, United States of America
<i>Pseudomonas straminea</i>	LMG 21615 ^T	BCCM/LMG	Japanese unhulled rice	Japan
<i>Pseudomonas stutzeri</i>	LMG 11199 ^T	BCCM/LMG	Human spinal fluid	American Type Culture Collection
<i>Pseudomonas syringae</i> pv. <i>phaseolicola</i> , race 4	1302A	University of the West of England	<i>Phaseolus vulgaris</i>	Ethiopia
<i>Pseudomonas syringae</i> pv. <i>phaseolicola</i> , race 6	1448A	University of the West of England	<i>Phaseolus vulgaris</i>	Ethiopia
<i>Pseudomonas xanthomarina</i>	LMG 23572 ^T	BCCM/LMG	Ascidian (<i>Halocynthia aurantium</i>)	Troitsa Bay, Sea of Japan, Russia
<i>Rahnella aquatilis</i>	DSM 4594 ^T	FR	Drinking water	France
<i>Rahnella bruchi</i>	FRB 226 ^T	FR	Gut of an <i>A. biguttatus</i> beetle	Shropshire, UK
<i>Rahnella inusitata</i>	DSM 30078 ^T	FR	Unknown	Unknown
<i>Rahnella variigena</i>	CIP 105588 ^T	FR	Human burn	USA
<i>Rahnella variigena</i>	SOT 2/10	FR	<i>Q. robur</i> , AOD-symptomatic inner bark	Norfolk, UK

<i>Rahnella variigena</i>	Pfk1-1C2a	FR	<i>Q. robur</i> , AOD-symptomatic inner bark	Sussex, UK
<i>Rahnella variigena</i>	GC 165b	FR	<i>Q. robur</i> , healthy root	Leicestershire, UK
<i>Rahnella variigena</i>	FOD 20/8	FR	<i>Q. robur</i> , wound response fluid	Gloucestershire, UK
<i>Rahnella variigena</i>	SOT 2/16	FR	<i>Q. robur</i> , AOD-symptomatic inner bark	Norfolk, UK
<i>Rahnella victoriana</i>	FRB 225 ^T	FR	<i>Q. robur</i> , AOD-symptomatic inner bark	Suffolk, UK
<i>Rahnella victoriana</i>	BRK18a	FR	<i>Q. robur</i> , AOD-symptomatic outer bark	Worcestershire, UK
<i>Rahnella victoriana</i>	USA 3	FR	<i>Q. kelloggii</i>	California, USA
<i>Rahnella victoriana</i>	BRK 3	FR	<i>Q. robur</i> , AOD-symptomatic outer bark	Worcestershire, UK
<i>Rahnella victoriana</i>	AT 15Ab	FR	<i>Q. robur</i> , AOD-symptomatic outer bark	Shropshire, UK
<i>Rahnella victoriana</i>	USA 13	FR	<i>Q. kelloggii</i>	California, USA
<i>Rahnella victoriana</i>	USA 39	FR	<i>Q. kelloggii</i>	California, USA
<i>Rahnella victoriana</i>	USA 47	FR	<i>Q. kelloggii</i>	California, USA
<i>Rahnella victoriana</i>	GC 176	FR	<i>Q. robur</i> , AOD-symptomatic inner bark	Leicestershire, UK
<i>Rahnella woolbedingensis</i>	DSM 27399 ^T	DSMZ	<i>Alnus glutinosa</i> , inner bark	Surrey, UK

DSMZ: Leibniz Institute DSMZ-German Collection of Microorganisms. BCCM/LMG: Belgian co-ordinated collections of microorganisms. FR: Forest Research.

AOD: Acute Oak Decline. ^T = type strain.

2.2. Media and culture conditions

Strains were isolated on potato yeast glucose agar by Forest Research and were received on nutrient agar plates. Upon receipt, agar plates containing bacterial isolates were incubated at 25 °C for 24 hours. Routinely, the bacteria were streaked out on to either King's B agar (KB, Oxoid), Luria Bertrani agar (LB, Fisher Bioreagents), eosin methylene blue agar (EMB) or tryptone soy agar (TSA, Oxoid). The plates were incubated in a static incubator (LT2J, LEEC) at 25 °C for 48 hours. Bacterial liquid cultures were grown overnight in LB broth at 25 °C in a shaking incubator (Innova 4230, New Brunswick Scientific). Unless otherwise stated, bacteria were cultured aerobically, but when bacterial cultures were incubated anaerobically, the temperature in the chamber (Whitley A95 TG) was 35 °C. Glycerol stocks of bacterial strains were prepared for long-term bacterial storage. A single colony from each strain was stored in 20% (w/v) glycerol at -80 °C (U57085, New Brunswick Scientific).

2.3. Revival of freeze-dried cultures

The reference strains for the phenotypic tests of the Pseudomonads were obtained from the Belgian Co-ordinated Collection of Micro-organisms (BCCM). Additional *Rahnella* and *Brenneria* species were obtained from the DSMZ (German Collection of Microorganisms and Cell Cultures). The strains were received freeze-dried and were revived following manufacturer's instructions. Liquid and agar cultures were incubated at 25 °C for 16 hours and 48 hours respectively. Glycerol stocks were saved from all strains after two passages on solid media, to ensure purity.

2.4. Formal classification of AOD-associated Pseudomonads

2.4.1. Genomic DNA extraction

Genomic DNA was extracted from fresh colonies grown on TSA for 24 hours by following an alkali lysis method (Niemann et al., 1997). For the extraction, a single colony was re-suspended in 20 µl of alkaline lysis buffer (0.05 M NaOH, 0.25 % sodium dodecyl sulphate). The cell suspension was incubated at 95 °C for 15 minutes. After incubation, the lysate was diluted 10-fold in HyPure™ molecular biology grade water (HyClone™), and centrifuged at 12,000 × g to pellet the cell debris. DNA was stored at -20 °C. One µL of the resulting lysate

was used per PCR unless otherwise stated. DNA for HRM work was extracted using the kit Quick-gDNA™ MiniPrep (Zymo Research) as per manufacturer's instructions.

2.4.2. Quantification of DNA purity and concentration

Nanodrop 1000 (Thermo Scientific) was used for the quantification of DNA purity and concentration of the DNA extracted with the kit Quick-gDNA™ MiniPrep. The purity of the DNA sample was assessed by looking at the ratios of absorbance 260/280 and 260/230. A DNA sample was classed as pure, if the 260/280 ratio was equal or greater to 1.8 and if the 260/230 ratio was between 2.0 and 2.2. Concentration of DNA extracted by alkali lysis was also measured with the Nanodrop, although because this is a raw method, the purity readings could not be trusted and the purpose was exclusively to standardize all samples in terms of concentration.

2.4.3. Polymerase chain reaction (PCR)

The standard individual reaction mixture volume for PCR amplifications was 25 µL. Each 0.2 mL PCR tube contained 12.5 µL of 2x Taq PCR Master Mix (QIAGEN; final concentration of 1x), a final concentration of 0.4 µM of each forward and reverse primers (Eurofins), and 9.5 µL of molecular biology grade water. The DNA template used was one µL of DNA (typical conc. 50 ng/µL). A non-template control consisting in 24 µL of master mix and one µL of molecular biology grade water was included to all PCRs performed. PCR amplifications were performed in a TC-412 Thermal Cycler (Flexigene), using different sets of primers and thermal profiles (**Table 3** and **Table 4**). The genes amplified by PCR for the MLSA were the 16S rRNA (a component of the 30S small subunit of bacterial ribosomes); *gyrB*, encoding the beta-subunit of gyrase, responsible for negative supercoiling of DNA during replication; *rpoB*, encoding the DNA-directed RNA polymerase subunit beta, and *rpoD*, encoding the sigma 70 subunit of RNA polymerase.

Table 3: Sequences of primers used for amplification and sequencing of 16S rRNA, *gyrB*, *rpoB*, and *rpoD* genes.

Gene	Primer	Sequence 5'-3'	Reference
16S rRNA	16F27	AGAGTTTGATCMTGGCTCAG	(Lane, 1991)
16S rRNA	16R1492	TACGGYTACCTTGTTACGACTT	(Lane, 1991)
16S rRNA	PAF	AGAGTTTGATCCTGGCTCAG	(Edwards et al., 1989)
16S rRNA	PHR	AAGGAGGTGATCCAGCCGCA	(Edwards et al., 1989)
<i>gyrB</i>	BAUP2	GCGGAAGCGGCCNGSNATGTA	(Santos and Ochman, 2004)
<i>gyrB</i>	APrU	TGTAAACGACGGCCAGTGCNNGRTCYTTYTCYTGRCA	(Yamamoto et al., 2000)
<i>gyrB</i>	M13(-21)	TGTAAAACGACGGCCAGT	(Messing, 1983)
<i>rpoB</i>	LAPS5	TGGCCGAGAACCAGTTCCGCGT	(Ait Tayeb et al., 2005)
<i>rpoB</i>	LAPS27	CGGCTTCGTCCAGCTTGTTCA	(Ait Tayeb et al., 2005)
<i>rpoB</i>	VIC4	GCGCAAATGGCDGARAACCA	(Tayeb et al., 2008)
<i>rpoD</i>	PsEG30F	ATYGAAATCGCCAARCG	(Mulet et al., 2009)
<i>rpoD</i>	PsEG790R	CGGTTGATKTCCTTGA	(Mulet et al., 2009)

Table 4: PCR conditions used for amplification and sequencing of 16S rRNA, *gyrB*, *rpoB*, and *rpoD* genes.

Gene	PA	PS	C	ID	D	A	E	FE	Reference
16S rRNA	16F27/16R1492	16F27/	30	94 °C, 5 min	94 °C, 1 min	55 °C, 1 min	72°, 1.5 min	72 °C, 10 min	(Gomila et al., 2005)
16S rRNA	PAF/PHR	PAF/PHR	30	94 °C, 1 min	94 °C, 1 min	55 °C, 1 min	72 °C, 1 min	72 °C, 5 min	(Edwards et al., 1989)
<i>gyrB</i>	BAUP2/AprU	M13(-21)	30	94 °C, 5 min	94 °C, 1 min	55 °C, 1 min	72 °C, 1.5 min	72 °C, 10 min	(Beiki et al., 2016)
<i>rpoB</i>	LAPS5/LAPS27	LAPS5	40	94 °C, 1 min	94 °C, 10 sec	60 °C, 20 sec	72 °C, 50 sec	72 °C, 5 min	(Ait Tayeb et al., 2005)
<i>rpoB</i>	VIC4/LAPS27	VIC4	40	94 °C, 1 min	94 °C, 10 sec	60 °C, 20 sec	72 °C, 50 sec	72 °C, 5 min	(Tayeb et al., 2008)
<i>rpoD</i>	PsEG30F/PsEG790R	PsEG30F	40	94 °C, 5 min	94 °C, 1 min	45 °C, 1 min	72 °C, 1.5 min	72 °C, 10 min	(Mulet et al., 2009)

PA = primers used for the PCR amplification; PS = primers used for sequencing; C = number of cycles; ID = initial denaturation; D = denaturation; A = annealing temperature; E = extension; FE = final extension.

2.4.4. Agarose gel electrophoresis

Agarose gels were prepared by dissolving agarose powder (Fisher Scientific) in 1× Tris-acetate-EDTA (TAE) buffer (40 mM Tris, 20 mM acetic acid, 1 mM EDTA) and heating. The agarose concentration used in the gels was typically 1 % (w/v). The nucleic acid staining reagent SYBR™ Safe (Qiagen) was added to a final concentration of 1x before pouring the gel to allow visualisation of DNA under UV light. DNA loading buffer Blue (1x; Bioline) was added to the DNA samples before loading them into the gel. Amplicons were visualised under UV light with a NuGenius gel documentation workstation (Syngene). Electrophoresis was performed at 100 V in 1x TAE buffer. DNA amplicon size and concentration was estimated by comparison to the Hyperladder 1Kb (Bioline).

2.4.5. DNA fingerprinting of AOD-associated Pseudomonads: BOX-PCR, ERIC-PCR and RAPD-PCR

Three PCR-based DNA fingerprinting techniques including BOX, ERIC and RAPD were used to study the genetic diversity of the AOD-associated Pseudomonads. DNA fingerprinting amplification was performed on all AOD-associated Pseudomonads strains, and their genetically closest neighbours, according to the published protocols (Versalovic, Koeuth and Lupski, 1991; Versalovic et al., 1994; Williams et al., 1990) for BOX, ERIC and RAPD-PCR respectively. Primers BOX-A1R (5' CTACGGCAAGGCGACGCTGACG 3', Martin *et al.*, 1992), ERIC-2 (5' AAGTAAGTGACTGGGGTGAGCG 3') and ERIC-1R (5' ATGTAAGCTCCTGGGGATTAC 3', Versalovic, Koeuth and Lupski, 1991), and OPA-04 (5' AATCGGGCTG 3') were used for the BOX, ERIC, and RAPD PCR reactions, respectively. The total reaction volume for fingerprinting assays was 25 µL and contained 50 ng of genomic bacterial DNA and 12.5 µL of 2x Taq PCR Master Mix (final concentration 1x). Each BOX-PCR reaction contained a final concentration of 2 µM of BOX-A1R. Each ERIC-PCR reaction contained 2 µM of each ERIC2 and ERIC1R primers. RAPD-PCR reactions contained 0.2 µM of OPA-04 primer. PCR settings for BOX and ERIC-PCR were a denaturation step of 7 minutes at 95 °C, followed by 30 cycles of 30 seconds at 90 °C, 1 minute at 52 °C, 8 minutes at 65 °C and a unique final extension step of 16 minutes at 65 °C. PCR conditions for RAPD-PCR comprised a 5 minutes denaturation step at 94°C, followed by 45 cycles of 1 minute at 94 °C, 1 minute at 36 °C and 2 minutes at 72 °C. The amplicons generated were resolved in 1.5 % (w/v) agarose gel at 50 V for 3 to 4 hours.

2.4.6. ExoSAP Clean-up of PCR products prior to DNA sequencing

PCR products were cleaned-up enzymatically before sequencing using the two enzymes Exonuclease I (Thermo Scientific) and Shrimp Alkaline Phosphatase (GE Healthcare) (ExoSAP). Each 25 μ L PCR amplification product was added 10 μ L of ExoSAP master mix (2.5 μ L Exonuclease I, 25 μ L SAP, 972.5 μ L molecular biology grade water), and incubated at 37 °C for 30 minutes and 95 °C for 5 minutes. Treated PCR products were stored at -20 °C when necessary.

2.4.7. Preparation of PCR products for DNA sequencing

PCR fragments cleaned by ExoSAP were prepared for Sanger sequencing using the Mix2Seq kit (Eurofins Genomics) as per manufacturer's protocol. Two μ L of the forward sequencing primer (10 μ M) were added to 15 μ L of the PCR products (150-300 bp: 1 ng/ μ L; 300-1000 bp: 5 ng/ μ L; > 1000 bp: 10 ng/ μ L) to obtain the mixture that was then sent for automated cycle DNA sequencing (on ABI 3730XL capillary sequencers) by Eurofins Genomics.

PCR products with sequences expected to be longer than 900 bp were sequenced with the forward primer (to obtain the beginning of the gene) and also, separately, with the reverse primer (to obtain the end of the gene). Resulting forward and reverse nucleotide sequences for each gene were then assembled in contigs using the software DNA Dragon 1.6.0 (Sequentix).

2.4.8. Genotypic characterisation of the AOD-associated Pseudomonads

To identify the AOD-associated Pseudomonads, 16S rRNA gene phylogenetic analysis and MLSA were performed. In addition, whole genomes of the AOD-associated Pseudomonads were analysed and compared to whole genomes of the genetically closest species.

2.4.8.1. 16S rRNA sequence analysis of the AOD-associated Pseudomonads

For taxonomic comparison, 16S rRNA gene sequences of the closest neighbours of the AOD-associated Pseudomonads were downloaded from EzBioCloud 16S rRNA database (Yoon et

al., 2017). These sequences were aligned with the sequences obtained for the AOD-associated Pseudomonads and manually trimmed with the sequence alignment application ClustalW (Larkin et al., 2007; Thompson, Higgins and Gibson, 1994) included in the software Bioedit 7.2.5. (Hall, 1999). Maximum likelihood (ML) and Bayesian Inference (BI) phylogenetic trees were constructed in PhyML (Guindon et al., 2010) and MrBayes (Huelsenbeck and Ronquist, 2001), respectively. BI phylogeny was estimated using Markov chain Monte Carlo methods; four Markov chains were run simultaneously 10,000,000 times, one in every 1,000 trees was sampled, and the first 1,000 trees were discarded whilst the other 9,000 were used to calculate the posterior probabilities (PP). The best-fit nucleotide substitution model – based on the Akaike information criterion – was selected by the software Smart Model Selection (Lefort, Longueville and Gascuel, 2017) for the ML tree, and by JModelTest (Darriba et al., 2012) for the BI tree. Phylogenetic inference was tested by the bootstrap method (Felsenstein, 1985) in the ML tree; and with PP values in the BI tree. Percentages of bootstrap or PP lower than 50 % or 0.5, respectively, were removed from the dendrograms.

2.4.8.2. Multilocus sequence analysis of the AOD-associated Pseudomonads

MLSA of the housekeeping, protein-encoding genes *gyrB*, *rpoB* and *rpoD* was performed to complete the phylogenetic analysis of the AOD-associated Pseudomonads. Species used in the 16S rRNA analysis were added to the MLSA, as well as the taxa that achieved the highest sequence similarity in basic local alignment search tool (BLASTn), (Morgulis et al., 2008; Zhang et al., 2000), and the closest relatives in the All Species Living Tree project (Yarza et al., 2008). Nucleotide sequences were downloaded from GenBank database, aligned and trimmed as for the 16S rRNA analysis, and then checked for concordance to translated amino acid sequences. Each gene alignment was analysed individually in JModelTest to select the best nucleotide substitution model. All housekeeping gene datasets were concatenated in the following order: *gyrB*, *rpoB* and *rpoD*, using the program SequenceMatrix 1.8. (Vaidya, Lohman and Meier, 2011). ML and BI trees were constructed using the concatenated nucleotide sequences and using the translated amino acid sequences. Phylogenetic analysis of the nucleotide and amino acid sequences were performed as described in **section 2.4.8.1.**

2.4.8.3. Whole bacterial genome sequencing and analysis

Bacterial strains P2, P4, P6, P9, P17, P18, P23, P26, P27, P28 and P30 sequenced by Illumina next-generation whole genome sequencing in MicrobesNG (Birmingham, UK). The reads obtained were trimmed using Trimmomatic (Bolger, Lohse and Usadel, 2014), and aligned using in-house scripts combined with the alignment tools, Samtools, BedTools and bwa-mem, used to map reads back to a reference genome or de novo assembled contigs (Li and Durbin, 2010; Li et al., 2009; Quinlan and Hall, 2010). The genome assembler SPAdes (version 3.10.1) was used for the *de novo* genome assembly of the reads. The assembly metrics were calculated using QUAST (Gurevich et al., 2013). Annotation of the draft genomes was performed with RAST (Aziz et al., 2008; Brettin et al., 2015; Overbeek et al., 2014).

2.4.8.3.1. Average Nucleotide Identity studies (ANI)

The JSpecies web service was used to perform pairwise genome calculations (Richter et al., 2015). Genome-wide average nucleotide identity studies based on BLAST (ANiB) and MUMmer tools (ANIm), as well as statistical analysis of tetranucleotide usage patterns were performed. Whole genomes of representative strains and reference closest related species, available in NCBI, were uploaded and compared. Threshold for species delimitation in ANI values of 95 % has been shown to correspond to the DNA-DNA hybridisation value of 70 % (Goris et al., 2007).

2.4.8.3.2. *In silico* DNA-DNA hybridisation (*is* DDH)

Is DDH, based on genome-to-genome distances comparison (GGDC), was performed using the distance calculator service GGDC 2.1 (Meier-Kolthoff et al., 2013). GGDC 2.1 transformed intergenomic distances into values analogous to DNA-DNA hybridisation using a generalized linear model. The cut off value for species delimitation in *is* DDH is 70 %.

2.4.9. Description of cultural characteristics of AOD-associated Pseudomonads

Isolates P1, P2, P3, P4, P5, P6, P7, P8, P9, P10, P11, P14, P16, P17, P18, P20, P21, P22, P23, P24, P25, P26, P27, P28, P29, P30, P31, P32, GM38b, GM48c, GM50b, I151, I160, I163 and

1166 were grown on KB agar plates to study their culture characteristics. The shape, colour, texture, elevation and margin type of the colonies were observed, and colony diameter was measured. Strains were incubated for 48 hours on KB agar at 25 °C for fluorescent pigment production analysis. The pigmented colonies were visualised under ultraviolet light (UV) using the benchtop UV transilluminator (model UPV TM-40).

2.4.10. Description of cell characteristics of AOD-associated Pseudomonads

Gram staining of the bacteria was performed on all the isolates after growing them on KB agar (Doetsch, 1981). Cell size and motility were measured in living bacterial cells using light microscopy after growing the strains on KB agar. For living cell imaging, a colony was re-suspended in a 10 µL drop of sterile water, placed on top of a glass slide, and the prepared slide was covered with a cover slip. Images of the prepared samples were captured, and cell sizes were measured using the microscopy imaging software CellSens version 1.11 (Olympus Life Science). An average of the length and width of the cells was calculated.

2.4.10.1. Transmission electron microscopy of AOD-associated Pseudomonads

Transmission electron microscopy (TEM) was used to image bacterial cells. Bacterial strains were grown overnight in tryptone soy broth in shaking conditions. Cell cultures with an optical density at 600 nm (OD_{600}) of 1.3 were centrifuged at $3000 \times g$ for 10 minutes. The supernatant was discarded and pellets were re-suspended in 200 µL of Tris-saline buffer (50mM Tris pH 8.0, 130mM NaCl). This washing step was performed twice. Five µL of the samples were applied to glow-discharged carbon coated copper grids (Cu 300 mesh). Grids were washed and stained for a minute with 2 % (w/v) uranyl acetate. Digital images were acquired using a Tecnai T12 TEM microscope with a CETA 16M camera (ThermoFisher Scientific) at a nominal magnification of 2900 \times .

2.4.11. Phenotypic characterisation of the AOD-associated Pseudomonads

Isolates P2, P4, P6, P9, P18, P26, P27, P28 and P30 were chosen as representative strains on the basis of the genotypic characterisation of the strains. The closest related bacterial species

to the AOD-associated Pseudomonads, obtained from BCCM, were selected for phenotypic characterisation studies as reference strains. The reference species were *Pseudomonas flavescens* (LMG 18387^T), *Pseudomonas seleniipraecipitans* (LMG 25475^T), *Pseudomonas argentinensis* (LMG 22563^T), *Pseudomonas straminea* (LMG 21615^T), *Pseudomonas punonensis* (LMG 26839^T), *Pseudomonas stutzeri* (LMG 11199^T), *Pseudomonas azotifigens* (LMG 23662^T), *Pseudomonas balearica* (LMG 18376^T) and *Pseudomonas xanthomarina* (LMG 23572^T).

2.4.11.1. API 20NE

Metabolic profiles were obtained using Analytical Profile Index identification strips, API 20NE (BioMérieux). The tests were inoculated following the instructions provided by the manufacturer, and incubated at 30 °C for 24 hours. The assimilation tests were interpreted as positive if the strains had changed the turbidity of the cupule of the microtube from clear to opaque. An opaque cupule indicated that the strain had grown with the nutrient contained in the microtube.

2.4.11.2. API 50 CH

Carbohydrate fermentation patterns were obtained with API 50 CH galleries. All tests were performed according to the manufacturer's instructions. The phenol red pH indicator present in the medium turned from red to yellow when the substrate was fermented, due to the subsequent drop in pH, indicating a positive result. The esculin test microtube turned black if positive. Tests were incubated at 30 °C for 48 hours. Isolates P4, P28, P30 and references *Pseudomonas stutzeri*, *Pseudomonas azotifigens*, *Pseudomonas balearica* and *Pseudomonas xanthomarina* were incubated for five days, as a low reactivity was observed for these strains.

2.4.11.3. Biolog GN2 Microplates

Carbon utilization-based metabolic fingerprints were studied using Biolog GN2 Microplates (Biolog) as per manufacturer's specifications. Microplates were incubated at 30 °C and two readings were taken after 6 and 20 hours of incubation. In positive results the inoculum

oxidised the substrate, changing the well colour from transparent to purple, due to the tetrazolium redox dye chemistry. The metabolic fingerprint patterns were compared using the MicroLog™ 4.20.05 database software.

2.4.11.4. Oxidase and catalase test

Oxidase tests were performed using the wet filter paper method: scraping some fresh growth with a plastic sterile inoculation needle and rubbing it into a piece of filter paper soaked in the oxidase reagent (BioMérieux). The positive control added was strain SBW25 of *Pseudomonas fluorescens* and the negative control was strain FRB 97^T of *Gibbsiella quercinecans*.

Catalase presence was studied by placing 50 µL of 3 % (w/w) H₂O₂ in a petri dish. Twenty-four hours old colonies were spread in the H₂O₂ drops with plastic sterile inoculation needles. The generation of O₂ bubbles indicated a positive result for catalase presence.

2.4.11.5. Studies of temperature, pH, and salt concentration tolerance ranges

The ability of the bacterial strains to grow in different ranges of pH, temperature and salt concentration was investigated on TSA plates. The temperatures tested were 4 – 10 °C, 33 °C, 37 °C, 39 °C and 41 °C. The pH tested were 6.0, 7.0, 8.0 and 9.0, plates were prepared as in Zhang et al., (2015). TSA plates have a pH of 7.3 (± 0.2). To increase the pH, 0.1 M Tris - HCl buffer (0.1M Tris, HCl to adjust pH) was added to the media to reach pH, 8 and 9, and 0.1 M acetate buffer was added for pH 6 (0.07 M sodium acetate, 0.03 M acetic acid, HCl to adjust pH). Plates were inspected for bacterial growth for 6 days.

2.4.12. Chemotypic characterisation of the AOD-associated Pseudomonads by fatty acid methyl esters (FAMES) profiling

Bacterial fatty acid methyl esters (FAMES) profiles were obtained by Fera Science Ltd. (York, UK) from strains P2, P4, P6, P9, P17, P18, P23, P26, P27, P28 and P30. Bacterial strains were

analysed by gas chromatography using the MIDI microbial identification system Sherlock Version 6.2. The results obtained were compared against the library TSBA6 6.10.

2.4.13. Phylogenetic study of the relationships amongst *Pseudomonas*, *Azomonas*, *Azotobacter* and *Azorhizophilus*

16S rRNA analysis and MLSA were performed as described in **section 2.4.8.1**, to explore the phylogenetic relationship amongst the genera *Pseudomonas*, *Azomonas*, *Azotobacter* and *Azorhizophilus*. Nucleotide sequences and translated amino acid sequences of *gyrB*, *rpoB* and *rpoD* genes (in this order) were used for the MLSA. Bayesian and maximum likelihood trees were constructed using a dataset that comprised the representative species from each of the *Pseudomonas* groups according to Gomila et al. (Gomila et al., 2015), *Pseudomonas* outliers (species which cannot be assigned to an existing *Pseudomonas* group), and all available *Azotobacter*, *Azomonas* and *Azorhizophilus* species.

2.5. Investigation of the potential pathogenicity traits of the AOD-associated *Pseudomonas*

2.5.1. Virulence factors in AOD-associated *Pseudomonas*

Identification of virulence factors (VF) in the bacterial chromosome of AOD-associated *Pseudomonas* was performed in the online platform VFAnalyzer (Liu et al., 2019). Pre-annotated draft genomes of *P. daroniae* sp. nov. P2, *P. dryadis* sp. nov. P27 and *P. kirkieae* sp. nov. P4 were uploaded to the VFAnalyzer (accession numbers: QJUH00000000, QJUN00000000, and QJUO00000000, respectively). The genomes were screened and the known/potential VFs were identified. The VFs in the genomes of AOD-associated *Pseudomonas* were then compared to the VFs present in two *Pseudomonas* species, available in the VFAnalyzer platform. The *Pseudomonas* used for the comparison were the non-plant pathogen *Pseudomonas fluorescens* SBW25, and the phytopathogen *Pseudomonas syringae* pv. *phaseolicola* 1448A (accession numbers: NC_012660 and NC_005773, respectively). Agglomerative hierarchical clustering of the data obtained was performed using XLSTAT 2020.2.3.65347. The dissimilarity was calculated using Euclidean distance, and the agglomeration method used was Ward's method. Data was scaled and

centred. The truncation was left automatic to let the software choose the number of clusters. The output was a dendrogram.

2.5.2. Hypersensitive response test of the AOD-associated Pseudomonads in bean pods

Inoculation in triplicate of the AOD-associated Pseudomonads in detached bean pods (dwarf French beans, *Phaseolus vulgaris*) was performed to assess if they elicit hypersensitive response (HR). In each pod, a colony of the strain SBW25 of *Pseudomonas fluorescens* (non-plant pathogen control) was inoculated, as well as colonies of both strains 1302A (HR control) and 1448A (disease control) of *Pseudomonas syringae* pv. *phaseolicola* (**Figure 8**). The strains of AOD-associated Pseudomonads inoculated were P1, P2, P3, P4, P5, P6, P7, P8, P9, P10, P11, P14, P16, P17, P18, P20, P21, P22, P23, P24, P25, P26, P27, P28, P29, P30, P31, and P32.

Sterile toothpicks were used to pick up a single colony from the KB plates and stab it into the bean pods. The bean pods were placed in plastic square Petri dishes with moist paper on the bottom, and glass rods separating the paper and the pods. The Petri dishes were incubated at 25 °C and photographs of the symptoms were taken every 24 hours for 3 days. This study was performed in triplicate.

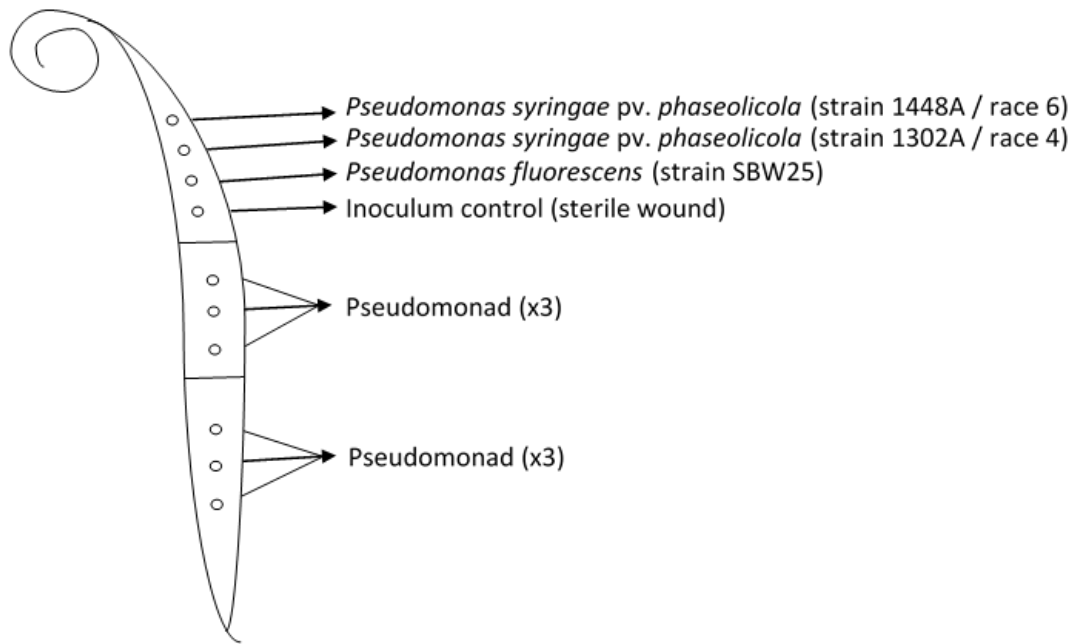


Figure 8: Layout of the hypersensitive response assays of the AOD-associated *Pseudomonads* in detached green pods (*Phaseolus vulgaris*). A single pure colony of each of the species was inoculated in the pods.

2.5.3. Hypersensitive response test of the combination of AOD-associated *Pseudomonads* and Bg, Gq and Rvi in bean pods

Two colonies instead of one were inoculated in each stabbing point, in detached green pods (dwarf French beans, *Phaseolus vulgaris*). All possible combinations between Bg, Gq or Rvi, and P2, P4 or P27 were tested in triplicate. Controls were as in **section 2.5.2** and individual inoculations for each of the species tested were also included, (**Figure 9**). Sterile toothpicks were used to pick up a single colony from the KB plates and stab it into the bean pods. This study was performed in triplicate.

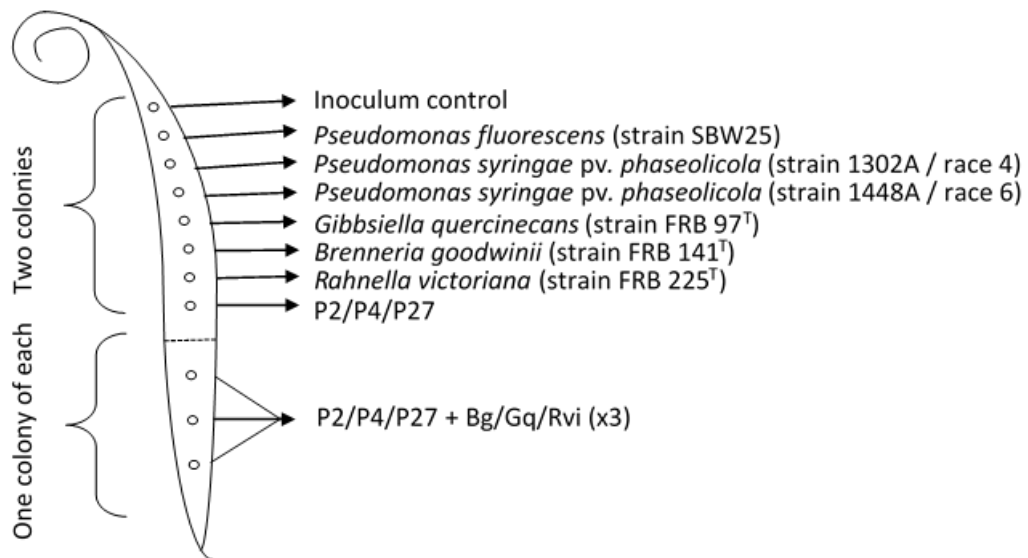


Figure 9: Layout of the hypersensitive response assays of the combination of AOD-associated *Pseudomonads* with *Brenneria goodwinii*, *Gibbsiella quercinecans* or *Rahnella victoriana*, in detached green pods (*Phaseolus vulgaris*).

2.5.4. Hypersensitive response test of the AOD-associated *Pseudomonads* in tobacco leaves

Tobacco plants (*Nicotiana benthamiana*, variety White Burley) were grown from seed until the leaves were approximately 15 cm long. The inoculum was prepared by washing overnight cultures of the *Pseudomonads* and the controls and adjusting them to OD₆₀₀ of 0.1. The *Pseudomonads* tested were P2, P4, and P27. The controls added were HR control *Pseudomonas syringae* pv. *phaseolicola* strain 1302A, and a sterile water control. The leaves were surface disinfected with 70 % (w/v) ethanol. The inoculation was performed using hypodermic needles, injecting the liquid in the leaf blade, between the upper surface (epidermis) and the lower surface (lower epidermis). The phenotype of the plant tissue inoculated was recorded daily for 4 days.

2.5.5. Cell attachment assays

The ability of bacteria to attach themselves to abiotic surfaces was studied with a cell attachment assay. The tests were 6-well plate assays and Falcon tube-coverslip assays

adapted from Merritt, Kadouri and O'Toole, (2011). The species studied were the AOD-associated Pseudomonads, Pda (strains P2^T, P9 and P18), Pdr (strains P27^T, P6 and P26) and Pki (strains P4^T, P28 and P30). The closest neighbours to the AOD-associated Pseudomonads were also added to the assay as well as the positive control *Pseudomonas fulva* LMG 11722^T. In addition, a non-inoculum control was introduced in the assay. Inoculums were prepared for both assays by growing the strains in overnight TSB broths, at 25 °C, with gentle agitation. Overnight cultures were adjusted to an OD_{600nm} of 0.1 and 100 µL added to each well containing 4 mL of fresh media. Four mL of fresh media were added to each of the wells, before adding the inoculum. In the case of the tube-coverslip assays, 50 mL Falcon tubes were filled with 25 mL of fresh media (LB or TSB depending on the experiment), before adding the inoculum. Additionally, a glass coverslip was sterilised (by immersion in 70 % ethanol and flaming with fire) and introduced in each Falcon tube.

The 6-well plates and the Falcon tubes were incubated statically at 25 °C, for 6 days. After incubation, the media and planktonic cells were discarded by inversion followed by a rinse through gentle immersion in a beaker with distilled water. Plates, tubes and coverslips were stained for 30 minutes with 1 % crystal violet and then gently submerged in distilled water a second time to remove excess dye. After visual inspection, the coverslips were removed from the tubes.

The wells were filled with 4 mL of 95 % ethanol to dilute the crystal violet-stained cells attached to the well walls. The tubes were filled with 25 mL of 95 % ethanol to dilute the crystal-violet-stained cells attached to the interior of the tubes. Spectrophotometer readings were then taken at OD_{590nm} from the stained cells suspended in ethanol, to obtain a semi quantitative assessment of the cell attachment. The experiment was performed on three independent occasions.

2.6. Rapid diagnostic method for the bacteria associated with AOD

2.6.1. High resolution melting analysis (HRM)

Several HRM assays for the work with AOD-associated bacteria have been developed in this project:

- A duplex-HRM assay of genes *atpD* and *rpoD* for the identification of pure cultures of AOD-associated bacteria including AOD-associated Pseudomonads.

- A multiplex-HRM assay for the detection and identification of Bg, Gq, Rvi and Lb from field samples.

- Three assays (designed to work with pure cultures) for the discrimination between species and subspecies of the genus *Brenneria*; and the discrimination between species of the genera *Rahnella* and *Gibbsiella*.

Unless otherwise indicated, all strains of the species tested are the type strains (**Table 1** and **Table 2**). All experiments were performed in the Rotor-Gene (Qiagen) in triplicate. The sample tested was one μL of a single pure colony re-suspended in 750 μL of molecular biology grade water. The total HRM reaction volume was 15 μL , containing 2x SensiFAST HRM mix (Bioline, 1x final concentration) and a final concentration of 0.67 μM of each primer used. PCR was followed by melt curve analysis. A non-template control containing the master mix and one μL of molecular biology grade water was added in triplicate to all assays performed. Custom designed primers were obtained from Eurofins, lyophilized, diluted with molecular biology grade water to 100 μM and stored at $-20\text{ }^{\circ}\text{C}$ until needed.

Changes in fluorescence were recorded in the instrument, and the data obtained was plotted. The same set of data was plotted in two types of graphs: normalised fluorescence curves (normalised fluorescence vs. temperature), and derivative melting curves (derivate of the fluorescence by the derivate of the temperature vs. temperature). In the derivative melting curves, the melting temperature (T_m) of the products appeared as peaks. The HRM runs were visualised virtually with the software Rotor-Gene 4.4.1 (Qiagen). The statistical analysis of the files generated on the Rotor-Gene instrument was performed with the Rotor-Gene Screen-Clust HRM Software 1.10.1.3 (Qiagen). ScreenClust normalised the curves, generated a residual plot, analysed the plot by principal component analysis (PCA), and then clustered the samples accordingly. DNA amplicons were resolved in agarose gel electrophoresis as indicated in **section 2.4.4**.

Validation of results obtained by HRM: To verify the results obtained by the HRM analysis, a selection of the amplicons generated by HRM were sequenced. The amplicons were cleaned-up before sequencing using the ExoSAP method (**section 2.4.6**). The DNA was sequenced as described in **section 2.4.7** using the same primers as for the amplification. The HRM results were also verified by the identification by partial 16S rRNA gene sequencing of the isolates present in the sample tested.

2.6.2. HRM of the *atpD* gene (119 bp)

The HRM assay in Brady *et al.* (2016) was replicated using fresh samples of Bg, Gq, and Rvi as well as the original samples used on the publication. PCR followed by HRM analysis was performed using the primers Gq6bF (5' GGCAACCCATCGACATGAA 3') and Gq6bR (5' CTTGATACCGTTTCCAGCAG 3'). PCR settings used were as in the publication, a hold step at 95 °C for 10 minutes, 45 cycles of 5 seconds of denaturation at 95 °C, 30 seconds of annealing at 58 °C. Fluorescence data points were recorded from 50 to 99 °C every 0.5 °C.

2.6.2.1. HRM of the *atpD* gene (119 bp): Assessment of the effect of different sample preparation methods on HRM of the *atpD* gene

The melt profiles obtained by strains Bg, Gq and Rvi, but prepared using different methods (pure DNA, cell suspension in water, and LB broth) were compared to study whether the pre-HRM sample preparation could be done without the DNA extraction step.

The strains used were Bg, Gq and Rvi. Each strain was prepared in three different ways: (I) DNA of the strain was purified by alkaline lysis (15 ng/μL); (II) a single colony of the strain was re-suspended in 750 μL of molecular biology grade water, and (III) a colony was grown overnight in LB broths whose turbidity was adjusted after incubation to an OD_{600nm} of 0.1. The primers used were Gq6bF-Gq6bR. PCR conditions were made more astringent (increased annealing temperature and a lower number of cycles) to avoid the appearance of non-specific amplification events observed in previous assays. PCR settings were a hold step at 95 °C for 10 minutes, 40 cycles of 10 seconds of denaturation at 95 °C, 30 seconds of annealing at 68 °C, and 10 seconds of extension at 72 °C. Fluorescence data points were recorded from 65 to 99 °C every 0.1 °C. Melting profiles of samples were compared visually, in ScreenClust and in Excel. Average T_{ms} (°C) were plotted in bar charts for each of the species, and sample formats, and standard errors were added.

2.6.2.2. HRM of the *atpD* gene (119 bp): assessing the effects of strain combination on the HRM *atpD* assay

To assess if the set of primers Gq6bF-Gq6bR were able to discriminate amongst more than one species in the same reaction (mixed samples), an assay was designed by preparing

titrations of the species Bg, Gq and Rvi, and comparing the T_{ms} of the amplicons. The samples combined were a suspension of a single colony in 750 μ L of molecular biology grade water. PCR conditions were performed as in **section 2.6.2.1**. The samples tested were as it follows: 100 % Gq, 75 % Gq – 25 % Rvi, 50 % Gq – 50 % Rvi, 25 % Gq – 75 % Rvi, 25 % Bg – 75 % Gq, 50 % Bg – 50 % Gq, 75 % Bg – 25 % Gq, 100 % Bg, 25 % Rvi – 75 % Bg, 50 % Rvi – 50 % Bg, 75 % Rvi – 25 % Bg and 100 % Rvi. Average T_{ms} ($^{\circ}$ C) were plotted as bar charts with standard errors.

2.6.3. HRM of the *atpD* gene (320 bp): Assessment of increased amplicon length. HRM combined with agarose gel fingerprinting for the identification of AOD-associated bacteria, including AOD-associated Pseudomonads

To prevent non-specific amplification, a novel HRM assay was designed. A reverse primer (AOD1R: 5' ACGTTGGATTCGGTCATTC 3') was designed for the use in combination with Gq6bF. The region targeted was a larger fragment of the *atpD* gene (320 bp), which contained the 119 bp amplicon in the 5' end. To design the AOD1R primer, published *atpD* nucleotide sequences of the AOD-associated bacteria Bg, Brr, Gq, Rvi, Rva and Lb were downloaded from NCBI and aligned in Bioedit.

Primers Gq6bF-AOD1R were used in HRM assays of the *atpD* gene of strains Bg, Brr, Gq, Rvi, Rva, Lb, P2, P18, P6, P27, P4, and P28, using 25 ng of genomic DNA extracted by alkaline lysis. PCR settings were 5 minutes at 95 $^{\circ}$ C, followed by 40 cycles of 10 seconds at 95 $^{\circ}$ C, 30 seconds at 53 $^{\circ}$ C and 10 seconds at 72 $^{\circ}$ C. HRM fluorescence data was collected from 82 to 95 degrees at 0.5 $^{\circ}$ C intervals. Reactions were analysed by 2 % (w/v) agarose gel electrophoresis, comparing the amplicon size to the marker Hyperladder 100 bp.

2.6.3.1. Duplex-HRM assay of genes *atpD* (320 bp) and *rpoD* for the identification of AOD-associated bacteria including AOD-associated Pseudomonads

PCR settings and primer concentrations were optimised until no primer-dimers or non-specific amplification events were observed in the reaction as verified by gel electrophoresis. To detect also Pseudomonads, the assay was complemented with a second pair of degenerate primers specific to *Pseudomonas*: PsEG30F (5' ATYGAAATCGCCAARCG 3') and

PsEG790R (5' CGGTTGATKTCCTTGA 3') (Mulet et al., 2009). PsEG30F-PsEG790R targeted a 746 bp long fragment of the *rpoD* gene. The species Bg, Brr, Gq, Rvi, Rva, Lb, P2, P4 and P27 were tested with PsEG30F-PsEG790R and with Gq6bF-AOD1R in single HRM reactions. The PCR settings were a hold step of 95 °C for 5 minutes, followed by 30 cycles of 10 seconds at 95 °C, 30 seconds at 62 °C and 5 seconds at 72 °C. Amplicons were melted, and fluorescence data was recorded from 82 to 96 °C every 0.05 °C steps. Following singleplex HRMs for each primer pair, Bg, Brr, Gq, Rvi, Rva, Lb, P2, P4 and P27 were tested again in a duplex-HRM assay, using the primer combination PsEG30F-PsEG790R-Gq6bF-AOD1R under the same PCR conditions. For all tests in this section, the final concentration of each of the primers was 0.33 µM, and 25 ng of DNA per sample were the tested.

2.6.4. Multiplex-HRM assay for the detection and identification of Bg, Gq, Rvi and Lb

To design the multiplex-HRM assay, whole genomes of the species Bg (strain FRB141^T, accession: MJLX01000000), Gq (strain FRB 97^T, accession: CP014136); Rvi (strain DSM 27397^T, accession: SJOJ01000000) and Lb (strain LMG 26267^T, accession: LUTN00000000) were analysed. Multiple whole genome alignment was performed using the multiple genome comparison tool Mauve (Darling et al., 2004) and the alignments were visualised in Bioedit. To ensure for maximum specificity, DNA inserts only present in one of the species and absent in the rest were selected (**Figure 10**). Several DNA inserts were selected for each of the species targeted.

Gibbsiella quercinecans	GTCTTCCTT	CGGCAACAG
Brenneria goodwinii	GCCTCTTTTATAACGGGTTTATCGCCCGAAATCGCTCCAGGCGATTGTAAAG	CGGCAACAG
Rahnella victoriana	GTCTTTTGTG	CGGCAACAG
Lonsdalea britannica	GTCTTCCTT	CGGCAACAG

Figure 10: Example of a whole genome alignment performed for the selection of targets for each of the species in the multiplex-HRM assay for the detection and identification of *Brenneria goodwinii*, *Gibbsiella quercinecans*, *Rahnella victoriana* and *Lonsdalea britannica*. Specific inserts, present only in the genome of one of the targets and absent from the rest were selected as targets for the multiplex-HRM. The figure shows an insert present in *B. goodwinii*.

Primers for these markers or DNA inserts were designed manually, and their quality was checked with the tool Multiple Primer Analyzer by Thermo Fisher Scientific to minimise the possibility of self-dimers and cross primer-dimers events. Five sets of primers were created for Bg, four for Gq, five for Rvi and three for Lb, (**Table 5**). All primers and resulting amplicons were compared to the BLAST database, to ensure they did not possess significant sequence similarity with any other known bacterial species. The primers were created with similar T_{ms} , to allow combining in the same PCR tube, and at the same annealing temperature. The software tool uMelt batch (Dwight, Palais and Wittwer, 2011) was used for *in silico* prediction of the melting behaviour of the amplicons, generated with each primer set designed. The primer pairs for each marker were tested independently and in combinations. Primers Bgi2F-Bgi2R-Gqi3F-Gqi3R-Rvii1F-Rvii1R-Lbi2F-Lbi2R were selected for the multiplex-HRM assay. Optimisation of the PCR settings was performed by testing different annealing temperatures and durations, the most stringent conditions were selected to avoid potential false positives. PCR amplification conditions were a hold step at 95 °C for 5 minutes, 30 cycles of denaturation at 95 °C for 5 seconds and annealing at 75 °C for 7 seconds. HRM was measured from 73-91 °C, and fluorescence was recorded every 0.5 °C. This assay was routinely used with cell suspension samples, but was also tested with 25 ng of pure DNA, to compare the amplification efficiency of the four reactions.

Table 5: Primers designed for the multiplex-HRM assay for the detection and identification of Bg, Gq, Rvi and Lb from field samples and amplicons expected.

Primer/ amplicon	Tm (°C)	G + C mol %	Length (nt)	Sequence 5'-3'
Bgi1F	66.3	44.4	27	GGTACGCTATACCCAATAGATTTGAG
Bgi1R	70.6	55	20	GGATTCGTTGTTTGGCGCT
Amplicon	86	46.4	56	GGTACGCTATACCCAATAGATTTGAGTTGCAGAAAAGCGGCAAACGAACGAATCC
Bgi2F	70.8	46.2	26	CGTCAAACATTTGCTTCCACCCATC
Bgi2R	70.4	57.1	21	CGGTATGGGTCTGGGACATTTG
Amplicon	89.6	49.2	59	CGTCAAACATTTGCTTCCACCCATCCGCTGAATACATCAAATGTCCCGACCCATACCG
Bgi3F	70	66.7	18	CATCGCGTCCAGCGTCTG
Bgi3R	70.9	50	26	GCCTATTGCGTGAACGAACGGATAG
Amplicon	95	54.2	96	CATCGCGTCCAGCGTCTGGACTCTGCAACTTACCATCCGGCGCATTGAGCTGATAAACATCCACCGAGCTATCCA GTTTCGTTACGCAATAGGC
Bgi4F	71.8	57.1	21	CCATCATTGAGCGCGGCTATG
Bgi4R	71.3	54.2	24	CTCACGATCCAACCTCTCGCATCTG
Amplicon	91.7	50	64	CCATCATTGAGCGCGGCTATGGTTTACAGATGCGAGAGTTGGATCGTGAGTTTGGCGATTTGAG
Bgi5F	71.3	50	24	GCTGACAAACGATTAATCTGCGCC
Bgi5R	69.8	54.5	22	GTCGGCAAACATCTCGATTCTCGT
Amplicon	95	52.5	118	GCTGACAAACGATTAATCTGCGCGCTAATCGCCATATCTACAAAAGCGATATCTTCCCGCGCAAGCAGATCCCATCC CCGCACAGTCGGGGATGACGAGAATCGAGATGTTTGGCGAC
Gqi1F	70.3	61.9	21	GACGTGCCGCTGTTAGAAGCC
Gqi1R	70.2	52.2	23	GTTAAGCCCTGTATGCGGCAATG

Amplicon	85.9	54.3	46	GACGTGCCGCTGTTAGAAGCCTACATTGCCGCATACAGGGCTTAAC
Gqi2F	71.1	63.2	19	CAGCGATCGGCGGTTATCG
Gqi2R	71.1	65	20	GCCAGGCCGTGGTCGTTAAG
Amplicon	95	67.1	73	GCCGGCCAGCGATCGGCGGTTATCGCAAACCAATCGGTATCGCGGCTGCGCCCCTTAACGACCACGGCCTGGC
Gqi3F	70.2	65	20	GCATACGCCTGGTACAGCGC
Gqi3R	71.6	65	20	CCTTGGCGGGACAGTCTTGC
Amplicon	95	67.1	76	GCATACGCCTGGTACAGCGCCTCATAGTCGCGTTCCGGCTCCAGCGGCTCCAGCCGGCAAGACTGTCCCGCCAAGG
Gqi4F	71.9	54.2	24	GTGCTGGGCGATATAACAACGGATG
Gqi4R	71.8	57.1	21	GCGAACATTCGCCGCTGTATG
Amplicon	95	61	59	GTGCTGGGCGATATAACAACGGATGCAGGCCAAGGGCGGCATACAGCGGCGAATGTTTCGC
Rvii1F	70.5	54.5	22	GCATCTCGCAGATCGTGAAAC
Rvii1R	71.7	70.6	17	TGGAAGCGGCGGCTGAC
Amplicon	91.9	57.7	52	GCATCTCGCAGATCGTGAAACGGGTAATAGAGACGTCAGCCGCCGCTTCCA
Rvii2F	69.6	63.2	19	GTTGAGATCACCCGTCGCG
Rvii2R	70.2	56.5	23	TGCGTCAGTTTAGCACAGCCAG
Amplicon	89.1	59.5	42	GTTGAGATCACCCGTCGCGCTGGCTGTGCTAAACTGACGCAC
Rvii4F	71.2	52.2	23	CCATGGCTCATTATCCAACGGTG
Rvii4R	71.4	48	25	GATCGTTTCTGCAATTGACCGTCAC
Amplicon	94.3	53.2	62	CCATGGCTCATTATCCAACGGTGACGGTCAATTGCAGAAACGATC
Rvii5F	70.1	60	20	CGTCATACGCATGGCACAGG
Rvii5R	70.9	60	20	CCAGTGCCGCAGAAAGCGTA
Amplicon	92.6	56.9	51	TCAACACCCGTCATACGCATGGCACAGGATGTACGCTTTCTGCGGCACTGG
Rvii6F	70.9	50	22	CTGCGCATTGATCAACACCATG
Rvii6R	70.1	54.2	24	CCACGACTGACAGGAAATGACCTC

Amplicon	94.5	54.1	61	CTGCGCATTGATCAACACCATGACCACCGATCACCGTGAGGTCATTTCTGTGTCAGTCGTGG
Lbi2F	70.1	50	24	GGAATCGCTTTACCGTCGCTATTG
Lbi2R	71.9	56.5	23	CAAGGTGGTGATGGTGGTCGATC
Amplicon	95	52.7	93	GGAATCGCTTTACCGTCGCTATTGATGACGAACATTTTGTAGTGCCTGGCGTCCTGCGCATAGAGCGGATCGAC CACCATCACCACCTTG
Lbi3F	71.3	52.2	23	TCAGCAGGAGCGGAATGAATACG
Lbi3R	70.8	61.9	21	CGTCGTCTCCATGAGCGTGTC
Amplicon	92.3	56.6	53	TCAGCAGGAGCGGAATGAATACGGCGATTAGCGACACGCTCATGGAGACGACG
Lbi4F	71.6	58.3	24	ACGCTAACTCTGGCTTGAGGCTCC
Lbi4R	71.3	52.2	23	GGTGTCAAATGCCAGCGTTATGG
Amplicon	94.3	57.1	63	ACGCTAACTCTGGCTTGAGGCTCCGATGGATGCCCGTCTGCCATAACGCTGGCATTGACACC

T_m°C = melting temperature, C + G mol % = percentage of cytosine (C) or guanine (G), nt = nucleotides.

2.6.4.1. Multiplex-HRM assay specificity test

The specificity of the multiplex-HRM assay was studied testing type strains of species belonging to the genera *Brenneria*, *Gibbsiella*, *Rahnella* and *Lonsdalea*. In addition, species routinely isolated in AOD lesions in lower numbers, which were closely related to these four genera, were also tested by multiplex-HRM. The species analysed were: *Brenneria roseae* subsp. *americana*, *Brenneria roseae* subsp. *roseae*, *Brenneria alni*, *Brenneria salicis*, *Brenneria nigrifluens*, *Brenneria rubrifaciens*, *Gibbsiella dentisursi*, *Gibbsiella greigii*, *Rahnella bruchi*, *Rahnella variigena*, *Rahnella woolbedingensis*, *Rahnella inusitata*, *Rahnella aquatilis*, *Lonsdalea iberica*, *Lonsdalea quercina*. *Erwinia billingiae* (strains 119, 157, R-45), *Pantoea* sp. (strains 120, 121, 124, DI 19b and DI 7a), *Enterobacter* sp. (strain 123), *Serratia proteamaculans* (strain 126.2), *Ewingella americana* (strains LMG 7869^T and FOD 24/3b), and *Erwinia rhapontici* (strains A3 P19 and Outwood 149). Positive controls Bg, Gq, Rvi and Lb were included.

2.6.4.2. Multiplex-HRM assay sensitivity test

To assess the sensitivity of the multiplex-HRM assay, the lower limit of detection was investigated. To study the lower limit of detection, a colony of each targeted species Bg, Gq, Rvi and Lb was re-suspended in 750 µL of ¼ Ringers solution. Ten-fold serial dilutions were made from these cell suspensions. Serial dilutions were then tested with the multiplex-HRM assay. Fifty µL of each dilution were plated out on LB following the spread plate technique and colony forming units (CFU) were counted to estimate the minimum number of viable cells that the multiplex-HRM method was capable of detecting.

2.6.5. Single nucleotide polymorphism (SNP)-based HRM assay for the differentiation of species and subspecies of the genus *Brenneria*

Melt curve predictions were performed on the amplicons generated by species and subspecies of *Brenneria*, using primers originally designed for the multiplex HRM assay. Gene sequences of *Brenneria goodwinii* (strain FRB 141^T, accession CP014137), *Brenneria roseae* subsp. *americana* (abbreviation: Bra, strain LMG 27715^T, accession QDKJ01000004), *Brenneria roseae* subsp. *roseae* (abbreviation: Brr, strain LMG 27714^T, accession QDKI01000011), *Brenneria alni* (abbreviation: Ba, strain NCPPB 3934^T, accession

MJLZ01000035), *Brenneria nigrifluens* (abbreviation: Bn, strain LMG 2694^T, accession CP034036), *Brenneria salicis* (abbreviation: Bsa, strain ATCC 15712^T, accession MJMA01000001), *Brenneria rubrifaciens* (abbreviation: Bru, strain: 6D370^T, accession CP034035) and *Brenneria corticis* (abbreviation: Bco, strain CFCC 11842^T, accession QDKH01000027) were downloaded from NCBI and aligned in Bioedit. Primers Bgi3F and Bgi3R were designed to amplify a 96 bp long portion of a single copy gene, encoding the enzyme 6-phosphogluconolactonase which catalyses the hydrolysis of 6-phosphogluconolactone to 6-phosphogluconate. Bgi3F and Bgi3R were designed for the multiplex-HRM assay. The quality of the primers was checked and the melting behaviour of amplicons was predicted as described in **section 2.6.4**.

The PCR conditions were a denaturation step of 95 °C for 5 minutes, and 40 cycles of denaturation at 95 °C for 5 seconds and annealing at 55 °C for 7 seconds. HRM data was recorded from 78 to 91 °C every 0.3 °C. Samples tested were cell suspensions (a single pure bacterial colony in 750 µL of molecular biology grade water) of Bg, Brr, Bra, Ba, Bn, Bsa and Bru.

2.6.5.1. SNP-based HRM assay for the differentiation of species of the genus *Rahnella*

Nucleotide sequences of *Rahnella victoriana* (Rvi, strain DSM 27397^T, accession SJOJ01000016), *Rahnella variigena* (Rva, strain CIP 105588^T, accession RAHI01000008), *Rahnella bruchi* (Rbru, strain DSM 27398^T, accession QZWI01000008), *Rahnella woolbedingensis* (Rwo, strain DSM 27399^T, accession RAHH01000004) *Rahnella aquatilis* (Raq, strain ATCC 33071^T, accession CP003244) and *Rahnella inusitata* (Rinu, strain DSM 30078^T, accession RAHG01000008) were retrieved from NCBI and aligned in Bioedit. The marker, originally created for the multiplex-HRM assay, was a 52 bp nucleotide sequence, which was part of a gene that codes for an acyltransferase. Primers Rvii1F (5' GCATCTCGCAGATCGCTGAAAC 3') and Rvii1R (5' TGGAAGCGGCGGCTGAC 3') were manually designed for this region. The PCR conditions used were a denaturation step of 95 °C for 5 minutes, and 30 cycles of denaturation at 95 °C for 5 seconds and annealing at 68 °C for 7 seconds. HRM data was recorded from 75 to 95 °C every 0.5 °C.

2.6.5.2. SNP-based HRM assay for the differentiation of species of the genus *Gibbsiella*

Primers Gqi4F (5' GTGCTGGGCGATATACAACGGATG 3') and Gqi4R (5' GCGAACATTCGCCGCTGTATG 3'), originally designed for the multiplex-HRM assay, were tested in several strains of all three species of the genus *Gibbsiella*. The amplicon was a 59 bp long fragment of a gene whose product is a deoxyribonuclease YjjV. Strains tested were: FRB 97^T, BH 1/65b, AT 18b, BH 1/86 and Kew 224 of *Gibbsiella quercinecans*; strains FRB 224^T, USA 42, R 52b, R 54a and R66a of *Gibbsiella gregii*; strain DSM 23818^T of *Gibbsiella dentisursi* and strain JCM 18389^T of *Gibbsiella papillionis*. *Gibbsiella papillionis* was proposed as a later heterotypic synonym of *Gibbsiella dentisursi*, but strains of both synonyms (firstly described as different species but later discovered as belonging to a single taxon) were included in the assay because they were available (Brady et al., 2015).

PCR conditions were a denaturation step of 95 °C for 5 minutes, and 35 cycles of denaturation at 95 °C for 5 seconds and annealing at 71 °C for 7 seconds. HRM data was recorded from 75 to 89 °C every 0.5 °C.

2.7. Isolation, purification and identification of bacteria from field samples

Bacterial isolation, purification and identification by 16S rRNA gene sequencing was performed from several field samples. Samples were collected from stems of *Quercus robur* suspected to be affected by AOD in Kew Gardens and in Knole Park, UK (**Table 6**). In Kew Gardens, samples were also collected from the stem of a *Quercus nigra*, this oak species has never been reported to be affected by AOD but the tree presented longitudinal, dark cracks in the bark, similar to those in AOD symptomatic trees. In addition, 98 samples from the polybacterial inoculation studies in oak logs, performed by Denman *et al.* (2018) were used in this study. Leaves were collected from a mature and sapling oak at the University of the West of England, UK.

Table 6: Collection details of the field samples from Kew Gardens and Knole Park.

Name	D.O.B. host	Ref. no. host	Beetle exit holes	Isolation source	Location
Kew 1	1969	16775	None observed	<i>Quercus nigra</i> , outer bark, dry injury	Kew Gardens, UK
Kew 2	2000	10550	Circular: <i>Platypus cylindrus</i>	<i>Quercus robur</i> , outer bark, dry injury	Kew Gardens, UK
Kew 3	2000	10550	Circular: <i>Platypus cylindrus</i>	<i>Q. robur</i> , outer bark, dry injury	Kew Gardens, UK
Kew 4	1973	19017	Circular and D-shaped: PC + AB	<i>Q. robur</i> , outer bark, dry injury	Kew Gardens, UK
Kew 5	1973	19017	Circular and D-shaped: PC + AB	<i>Q. robur</i> , outer bark, dry injury	Kew Gardens, UK
Kew 6	1973	19017	Circular and D-shaped: PC + AB	<i>Q. robur</i> , outer bark, dry injury	Kew Gardens, UK
Kew 7	1973	19017	Circular and D-shaped: PC + AB	<i>Q. robur</i> , sapwood	Kew Gardens, UK
Kew 8	1973	19017	Circular and D-shaped: PC + AB	<i>Q. robur</i> , sapwood	Kew Gardens, UK
Kew 9	1973	19017	Circular and D-shaped: PC + AB	<i>Q. robur</i> , inner bark	Kew Gardens, UK
Kew 10	1973	19017	Circular and D-shaped: PC + AB	<i>Q. robur</i> , inner bark	Kew Gardens, UK
Kew 11	1973	19017	Circular and D-shaped: PC + AB	<i>Q. robur</i> , larval galleries created by <i>Agrilus biguttatus</i> in phloem	Kew Gardens, UK
KP 1	1700-1800	901	None observed	<i>Q. robur</i> , outer bark, exudate	Knole Park, UK
KP 2	1700-1800	901	None observed	<i>Q. robur</i> , outer bark, exudate	Knole Park, UK
KP 3	1700-1800	901	None observed	<i>Q. robur</i> , outer bark, exudate	Knole Park, UK
KP4	1700-1800	901	None observed	<i>Q. robur</i> , outer bark, exudate	Knole Park, UK

PC + AB = *Platypus cylindrus* + *Agrilus biguttatus*.

2.7.1. Isolation, purification and identification of bacteria from oak stem and multiplex-HRM test

Oak stem samples collected in Kew Gardens, Knole Park and from the log tests were processed prior to HRM as follows: samples were collected with sterile swabs from stem exudates and from stem layers removed with a chisel (disinfected with 70 % ethanol) at approximately 150 cm from the ground. Outer bark, inner bark, sapwood and larval galleries created by *Agrilus biguttatus* were the tissue types sampled. The head of each swab was cut into a 1.5 mL tube with 750 µL of sterile ¼ Ringers solution, and referred to as initial stem suspension. Glycerol stocks were saved from the initial stem suspension. Ten µL of the initial stem suspension or 50 µL of the glycerol stock obtained from the initial stem suspension were spread on EMB or LB plates. Plates were incubated anaerobically at 35 °C for 48 hours.

A maximum of one loopful was scraped from each plate. The loopful contained bacterial growth belonging to each different colony type that had grown on the plate. The loopful, which contained growth from several colony types, was re-suspended in a single tube with molecular biology grade water. Each multiplex-HRM reaction contained one µL of this suspension. Multiplex-HRM was performed as in **section 2.6.4**.

For the identification of bacterial isolates, 20 µL of glycerol stocks created from the initial stem suspension were spread on LB or EMB agar plates, as well as 10^{-1} and 10^{-2} dilutions, and incubated at 25 °C for 72 hours. Samples Kew 1, Kew 2, Kew 6 and Kew 8 were also spread on plates and incubated anaerobically at 35 °C for 72 hours. Different morphology colonies were sub-cultured twice in fresh plates. One colony of each pure isolate was re-suspended in 750 µL of molecular biology grade water and kept at -20 °C. PCR and sequencing of the 16S rRNA genes were performed as in **section 2.4.8.1**. Each PCR reaction contained one µL of the colony suspension and the primers used were PAF/PHR. Identification of the isolates to genus and, in some cases, to species level was obtained by comparing the sequenced 16S rRNA sequences to those in EzBioCloud database; sequences with less than 99 % of sequence similarity were also identified using BLAST. Isolates identified by 16S rRNA as Pseudomonads were further studied by MLSA of the *gyrB*, *rpoB* and *rpoD* genes as performed in **section 2.4.8.2**.

2.7.2. Isolation, purification and identification of epiphytic + endophytic bacteria and endophytic bacteria alone from oak leaves and multiplex-HRM test

To determine whether Bg and Gq were present in the leaves of healthy oaks in a non AOD-affected site, the microbiomes of oak leaves from a mature tree and from leaves from a sapling were studied. Leaves were processed, prior to multiplex-HRM, as it follows: two leaves from mature oak tree and two leaves from sapling were collected from two pedunculate oaks in the University of the West of England, United Kingdom. In a paired analysis for each tree performed with and without surface sterilisation, a leaf of each tree was surface sterilised by submersion for 30 seconds in sterile distilled water, 10 % bleach, 70 % ethanol and sterile distilled water again. All leaves were crushed separately in four sterile mortars with sterile pestles along with three mL of ¼ Ringers solution. Twenty µL of the liquid crushed leaves (referred to as initial leaf suspension) were spread on LB plates and incubated aerobically, at 25 °C for 72 hours, and anaerobically, at 35 °C for 72 hours. Glycerol stocks were saved from the initial leaf suspension. Samples were enriched by inoculating LB broths with 100 µL of the initial leaf suspension and incubating overnight in shaking conditions at 28 °C. Glycerol stocks were saved from the LB broths after incubation. Aliquots of the initial leaf suspension, and of the enriched LB broths were stored at -20 °C for HRM studies (**Table 7**).

Table 7: Samples collected from oak leaves in the University of the West of England, for the characterisation of their microbiome.

Name	Sample	Tree age	Surface sterilised?
R1	Initial leaf suspension in 1/4 Ringers	Sapling	Yes
R2	Initial leaf suspension in 1/4 Ringers	Sapling	Yes
R3	Initial leaf suspension in 1/4 Ringers	Mature	Yes
R4	Initial leaf suspension in 1/4 Ringers	Mature	Yes
R5	Initial leaf suspension in 1/4 Ringers	Sapling	No
R6	Initial leaf suspension in 1/4 Ringers	Sapling	No
R7	Initial leaf suspension in 1/4 Ringers	Mature	No
R8	Initial leaf suspension in 1/4 Ringers	Mature	No
L1	Overnight LB broth inoculated with R1	Sapling	Yes
L2	Overnight LB broth inoculated with R2	Sapling	Yes
L3	Overnight LB broth inoculated with R3	Mature	Yes
L4	Overnight LB broth inoculated with R4	Mature	Yes
L5	Overnight LB broth inoculated with R5	Sapling	No
L6	Overnight LB broth inoculated with R6	Sapling	No
L7	Overnight LB broth inoculated with R7	Mature	No
L8	Overnight LB broth inoculated with R8	Mature	No

For the identification of bacterial isolates, 20 µL of samples R1, R2, R3, R4, R5, R6, R7 and R8, and 20 µL of serial dilutions 10^{-1} , 10^{-2} and 10^{-3} of samples L1, L2, L3, L4, L5, L6, L7 and L8 were spread in LB plates and incubated at 25 °C for 72 hours. Each colony type was sub-cultured twice in LB plates. Pure isolates were then identified by partial 16S rRNA gene sequencing, as described in **section 2.7.1**.

All leaf samples were tested in multiplex-HRM as in **section 2.6.4** as well as the type strains of Bg, Gq, Rvi and Lb, that were added as positive controls.

2.8. Optimisation of processing of field samples for downstream HRM analysis: assessing the effect of sample preparation

To determine the optimal sample preparation for downstream HRM analysis, a paired analysis for each sample was performed using several methods to prepare it for HRM. Derivative profiles were compared using a duplex-HRM that targeted Bg and Gq, with the primers Bgi3F-Bgi3R-Gqi1F-Gqi1R (final concentration of each primer 0.33 μM).

The samples were prepared in several ways:

1. Initial stem suspension (description in **section 2.7.1**). Each duplex/HRM assay contained one μL of this suspension as DNA template.
2. Broths containing 10 mL of LB were inoculated with 50 μL of glycerol stocks and incubated overnight with and without agitation and inside and outside of the anaerobic chamber. Each duplex/HRM assay contained one μL of this suspension as DNA template.
3. Ten μL of the initial stem suspension, incubated anaerobically at 35 $^{\circ}\text{C}$ for 48 hours on EMB or LB plates. A loopful containing growth from several colony types scrapped from the plate, was re-suspended in a single tube with 750 μL of molecular biology grade water. Each duplex/HRM assay contained one μL of this suspension as DNA template.

Duplex-HRM conditions were: denaturation at 95 $^{\circ}\text{C}$ for 5 minutes, followed by 30 cycles of 5 seconds at 95 $^{\circ}\text{C}$ and 7 seconds at 71 $^{\circ}\text{C}$. HRM data was collected every 0.5 $^{\circ}\text{C}$ from 74 to 88 $^{\circ}\text{C}$. A non-template control was added to all the HRM assays performed.

2.8.1. Duplex-HRM assay for the detection and identification of Bg and Gq in initial stem suspensions

Duplex-HRM assay with the primers Bgi3F-Bgi3R-Gqi1F-Gqi1R was performed in the initial stem suspensions. The samples tested were all of those collected in Kew Gardens (Kew 1, Kew 2, Kew 3, Kew 4, Kew 5, Kew 6, Kew 7, Kew 8, Kew 9, Kew 10 and Kew 11), as well as the controls Bg and Gq. One μL of each initial stem suspension was used as DNA template for the duplex-HRM assay.

2.8.2. Duplex-HRM assay for the detection and identification of Bg and Gq in overnight LB broths

The second assay performed towards the optimisation of the sample processing was a duplex-HRM analysis of overnight LB broths of all the samples from Kew. The 10 mL broths were inoculated with 50 μ L of glycerol stocks and incubated at 25 °C, for 20 hours, in shaking conditions. The controls Bg and Gq were prepared in the same way, and the control and Bg + Gq was LB broth inoculated with 25 μ L of Bg and 25 μ L of Gq. After incubation, 1 μ L of each broth was used as DNA template for the duplex-HRM assay. The thermocycling conditions used were as described in **section 2.8**.

2.8.3. Duplex-HRM assay for the detection and identification of Bg and Gq in Kew 2: optimal temperature and atmosphere test

The third assay performed towards the sample processing optimisation studies was designed to find the optimal temperature of incubation. LB plates were inoculated with 50 μ L of the glycerol stock of Kew 2 and incubated aerobically for 72 hours at 25, 35 and 41 °C and anaerobically at 35 °C. The species Bg and Gq were added as controls. A loopful of bacterial growth from each plate was re-suspended in 750 μ L of molecular grade water and one μ L of these samples was used as DNA template for the duplex-HRM assay. The thermocycling conditions used were as described in **section 2.8**.

2.8.4. Duplex-HRM assay for the detection and identification of Bg and Gq in Kew 2: optimal media and atmosphere test

To find the best atmosphere and media type for the sample processing a fourth assay performed towards the sample processing optimisation studies was performed. Fifty μ L of the glycerol stock, saved from the same sample (Kew 2), were inoculated in 10 mL LB broths and in LB plates. The broths were incubated for 20 hours and the plates for 72 hours, all of them at 35 °C. The broths were incubated in static conditions as opposed to the shaking conditions tested above. Some broths were incubated aerobically, others in the anaerobic chamber and others in microaerophilic conditions (a layer of sterile mineral oil was carefully placed on top of the broths after inoculation, to avoid the gas exchange between the liquid

and the air). The species Bg and Gq were added as controls. A loopful of bacterial growth from each plate was re-suspended in 750 μL of molecular grade water and one μL of these samples was used as DNA template for the duplex-HRM assay. In the case of the broths, one μL of the culture was used as a DNA template for the duplex-HRM. The thermocycling conditions used were as described in **section 2.8**.

2.8.5. Duplex-HRM assay for the detection and identification of Bg and Gq in Kew 1, Kew 2, Kew 3, Kew 6 and Kew 11: optimal media and atmosphere test

Once the optimal sample enrichment method was selected, extra samples from Kew were prepared using different methods and tested using the duplex-HRM assay. Fifty μL of the glycerol stocks saved from samples Kew 1, Kew 2, Kew 3, Kew 6 and Kew 11 and controls Bg, and Gq were inoculated in LB broths and in LB plates. The broths were incubated for 20 hours, aerobically and in shaking conditions at 25 °C and at 35 °C. The plates were incubated at 25, 35 and 41 °C aerobically, and at 35 °C anaerobically. The species Bg and Gq were added as controls. A loopful of bacterial growth from each plate was re-suspended in 750 μL of molecular grade water and one μL of these samples was used as DNA template for the duplex-HRM assay. In the case of the broths, one μL of the culture was used as a DNA template for the duplex-HRM. The thermocycling conditions used were as described in **section 2.8**.

A multiplex-HRM assay of the samples from Knole Park was performed to compare the melting profiles obtained after incubating the same samples aerobically and anaerobically. Fifty μL of the glycerol stocks from samples KP 1, KP 2 and KP 3 were spread on plates and incubated aerobically and anaerobically at 35 °C for 72 hours. The species Bg, Gq, Rvi and Lb were added as controls. A loopful of bacterial growth from each plate was re-suspended in 750 μL of molecular grade water and one μL of these samples was tested by multiplex-HRM, following the conditions described in **section 2.6.4**.

2.8.6. Validation of the multiplex-HRM assay for the detection and identification of Bg, Gq, Rvi and Lb

The validation of the multiplex-HRM assay was performed testing 84 field samples: five from Kew Gardens, four from Knole Park and 75 from the log tests. The samples from Kew Gardens and Knole Park were prepared as follows. Fifty μL of the glycerol stocks obtained from the initial stem suspensions were plated out on LB or EMB agar plates. The plates were incubated anaerobically at 35 °C for 72 hours. A loopful of bacterial growth was collected from each plate ensuring that all the colony types were included. The bacterial growth was suspended in 750 μL of molecular grade water. One μL of the cell suspension was used as DNA template for the multiplex-HRM assay. The samples from the log tests performed at Forest Research are termed “mass isolates”. The sterile swab soaked in the lesion fluids was directly rubbed onto the nutrient agar plate. Glycerol stocks were collected from the 98 mass isolates. The glycerol stocks were plated out on EMB and incubated for 72 hours, anaerobically at 35 °C. A loopful of bacterial growth was collected from each place ensuring all colony types were included. The bacterial growth was suspended in 750 μL of molecular grade water. One μL of the cell suspension was used as DNA target for the multiplex-HRM assay.

CHAPTER 3. Taxonomic description of
Pseudomonas associated with AOD

3.1. Introduction

Botanist Walter Migula named the genus *Pseudomonas* (from the Greek pseudo = false and monas = unit) in 1894. *Pseudomonas* are a large and heterogeneous group of Gram-negative bacteria, placed in the *Gammaproteobacteria* class (Woese et al., 1984). *Pseudomonas* belong to the family *Pseudomonadaceae* and the order *Pseudomonadales*. The genus has more than 220 species and the type species is *Pseudomonas aeruginosa*, an important opportunistic pathogen (Schroeter, 1872). *Pseudomonas* do not form spores and they are characterised for being short bacilli, chemoorganotrophic, and most of them are aerobic and motile by means of polar flagella. Their mol % G + C DNA content is variable within the range 58 to 69 (Palleroni, 2015). *Pseudomonas* are ubiquitous microbes present in every ecosystem, from the deserts to the poles, and they have also been described as saprophytes, symbionts or pathogens of animals, fungi and plants (Peix, Ramírez-Bahena and Velázquez, 2009). Some species are currently used as biocontrol agents such as *P. fluorescens*, known to suppress crop pathogens (Haas and Défago, 2005), and bioremediation agents, such as *P. putida* and *P. alcaligenes*, able to metabolise chemical contaminants like toluene or polycyclic aromatic hydrocarbons, respectively (Marqués and Ramos, 1993; O'Mahony et al., 2006). Plant-associated *Pseudomonas* have been found as saprophytes, symbionts or pathogens in all the plant structures from root to leaf and from the inside to the surface of the plant.

One hundred and twenty-seven years have passed since the genus *Pseudomonas* was first described. The molecular tools available to microbiologists have evolved enormously and bacterial taxonomy with it. The current accepted method to formally classify novel bacterial species is the polyphasic approach for bacterial classification (Prakash et al., 2007). The polyphasic approach includes several tests to establish the differences amongst the novel strains and the closest related neighbours by comparing their genotypic, phenotypic and chemotypic features.

The phenotypic characterisation of the bacteria is generally performed by analysing the novel strain and the closest phylogenetic neighbours with commercial tests such as API 20NE, API 50 CH and Biolog GN2 microplates. The results of the phenotypic commercial tests are the metabolic responses of the strains to different compounds, and the combination of the results creates strain-specific phenotypic profiles that can be easily compared. Phenotypic characterisation also includes Gram stain, colony and cell morphology analysis, the study of growth requirements and ranges of tolerance.

Some tools for the chemotypic characterisation of bacteria are the profiling of FAMES, present in the bacterial cell membrane; polar lipid analysis, and respiratory quinones content analysis. In addition to the phenotypic and chemotypic characterisation, the polyphasic approach of bacterial classification requires the genotypic characterisation of the bacterium.

In the early days of microbiology, bacterial systematics used to be based exclusively on the phenotypic characteristics of the microbe. However, with the scientific advances of the last decades, systematics began to focus on the genotypic characterization of microbes. (Moore et al., 1987; Stackebrandt et al., 2002). In the last 50 years, besides the investigation of the phenotypic and chemotypic features of the bacterium, analysis of the 16S rRNA gene, combined with DNA–DNA hybridisation (DDH) were the gold standards for bacterial classification (Moore et al., 1996, 1987; Verhille et al., 1999; Woese, Kandler and Wheelis, 1990). However, some disadvantages pushed taxonomists to search for alternatives to complement or substitute these methods. DDH had the disadvantage of being a time and labour-consuming method as well as not being very accurate or reproducible. The analysis of the 16S rRNA gene is not discriminative enough for species delimitation due to the slow evolutionary rates of the gene; but it is still useful for genus delineation, (Adékambi, Drancourt and Raoult, 2009; Ait Tayeb et al., 2005; Yamamoto et al., 2000).

16S rRNA analysis was later complemented with a rapid and robust method for bacterial classification, MLSA, which is still in use (Gomila et al., 2015; Maiden et al., 1998; Mulet, Lalucat and García-Valdés, 2010). MLSA is in the phylogenetic analysis of multiple concatenated sequences of generally protein-encoding genes or amino acids. Protein-encoding genes provide higher species delimitation power than the 16S rRNA gene due to their faster evolutionary rates. Commonly used protein-encoding genes for the description of novel *Pseudomonas* species are *gyrB*, *rpoD*, and *rpoB* genes (Ait Tayeb et al., 2005; Yamamoto and Harayama, 1998; Yamamoto et al., 2000). Other genes such as *atpD* (encoding for F-ATPase, beta-subunit), *carA* (coding the predicted small chain of carbamoylphosphate synthetase), and *recA* (coding a DNA recombination protein) have also been used for *Pseudomonas* description (Hilario, Buckley and Young, 2004). In some cases, 16S rRNA gene has also been added to MLSA of *Pseudomonas* (Gomila et al., 2015; Mulet et al., 2012; Mulet, Lalucat and García-Valdés, 2010). A correlation was observed between MLSA and genome-based methods such as tetranucleotide usage patterns (TETRA), average nucleotide identity (ANIm, based on MUMmer and ANIb, based on BLAST) and genome-to-genome distance (GGDC), for *Pseudomonas* species delineation, (Gomila et al., 2015).

Technically, the more genes are added to the MLSA, the less possibility of a bias, however, the optimal method, would be the comparison of the complete bacterial genomes. Nowadays, whole genome sequencing has become affordable and it yields a huge amount of comparable information. Due to the increase on the public availability of whole genomes and the facility to sequence new strains, *in silico* comparison of whole genomes are the new gold standards for bacterial classification and have replaced techniques like DDH. The digital comparison of complete genomes uses tools based on average nucleotide identities (ANI) or genome-to-genome-distance calculations (GGDC) (Auch et al., 2010; Goris et al., 2007; Konstantinidis and Tiedje, 2005). ANI compares coding regions of two prokaryotic genomes and it has been observed that values of 95% of ANI are comparable to the 70% threshold for species delimitation in DDH (Goris et al., 2007). GGDC performs genome-based species delineation by calculating intergenomic distances between two genomes and translating them into similarity values comparable to those in DDH (Meier-Kolthoff et al., 2013; Meier-Kolthoff, Klenk and Göker, 2014).

A percentage of 98.7–99% of 16S rRNA gene sequence similarity is the threshold for *Pseudomonas* species delimitation (Stackebrandt and Ebers, 2006). The species threshold is 97% in the 4-gene MLSA for *Pseudomonas*, and 70% in GGDC (Auch, Klenk and Göker, 2010; Gomila et al., 2015; Goris et al., 2007; Meier-Kolthoff et al., 2013; Mulet et al., 2012). ANI of 95% is the cut-off value for species delimitation (Lalucat et al., 2020), although the range 94–96% is the ANI threshold in other studies (Richter and Rosselló-Móra, 2009). A percentage of 94.5% of sequence similarity of the 16S rRNA gene is the general threshold to genus delimitation, and the cut-off ANI value for genus delimitation is <93% (Beye et al., 2018; Rosselló-Móra and Amann, 2015).

With the refining of molecular techniques for species delimitation, *Pseudomonas* has gone through and it is still going under intra-genus modifications. Fifty years ago the genus was subdivided into five rRNA subgroups according to the measurements of RNA–DNA relatedness (Palleroni et al., 1973). From those five rRNA subgroups, only the rRNA subgroup I would remain as *Pseudomonas*, the rest of the subgroups were excluded from *Pseudomonas* and relocated in other genera (De Vos and De Ley, 1983; De Vos et al., 1985, 1989). Ten years ago two intra-genus groups called lineages were described within *Pseudomonas* using MLSA. The lineages were *P. aeruginosa* lineage and *P. fluorescens* lineage; each lineage contained three and six groups respectively, and some of the groups contained subgroups (Mulet, Lalucat and García-Valdés, 2010). Some of the species analysed

by Mulet and colleagues were characterised as outliers of the genus because they did not fit into any described category. Since 2010, many authors have updated the phylogenetic diversity of *Pseudomonas*. Currently, *Pseudomonas* counts with three lineages: *Pseudomonas aeruginosa*, *Pseudomonas fluorescens* and *Pseudomonas pertucinogena*. Each lineage is divided into groups and subgroups according to MLSA studies (**Figure 11**) (García-Valdés and Lalucat, 2016; Garrido-Sanz et al., 2016; Gomila et al., 2015, 2017; Lalucat et al., 2020; Martínez-Carranza et al., 2019; Mulet et al., 2012; Parks et al., 2018; Peix, Ramírez-Bahena and Velázquez, 2018, 2009). Commonly, studies that revise the intra-genus structure on *Pseudomonas*, suggest that a rearrangement of the genus, and possible split will have to be performed (Peix, Ramírez-Bahena and Velázquez, 2018).

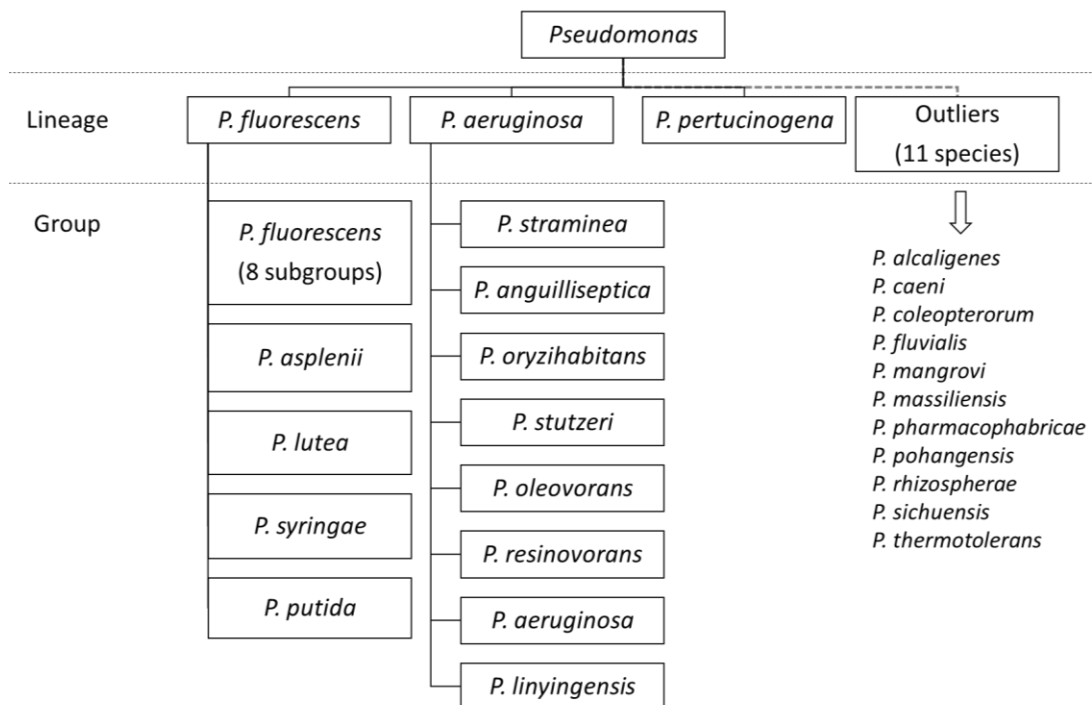


Figure 11: Latest accepted intra-genus structure of *Pseudomonas*, according to the neighbour-joining MLSA phylogenetic study of the 16S rRNA, *gyrB*, *rpoB* and *rpoD* in 227 species and subspecies of *Pseudomonas*, (Lalucat et al., 2020).

The internal structure of the genus *Pseudomonas* is not the only concern of taxonomists as the family *Pseudomonadaceae* is also likely to need a taxonomic revision. In the 1980s, the close relationship of the aerobic, nitrogen-fixing, and free-living genera *Azomonas* and *Azotobacter*, and the genus *Pseudomonas* was observed in a study based on rRNA/DNA hybridization experiments (De Vos et al., 1985). In the following decade, Anzai *et al.* (2000) pointed this close relationship out again, but they did not study it further because of the insufficient sequence data available for *Azotobacter* and *Azomonas* species (Anzai et al., 2000). Since then, several studies have considered the relationships amongst the genera *Pseudomonas*, and *Azotobacter*, *Azomonas* and *Azorhizophilus* (collectively called the *Azotobacter* group). Synonymy between taxa like *Azorhizophilus* and *Azotobacter*, *Azotobacter* and *Azomonas* and between *Azotobacter* and *Pseudomonas* has been suggested (García-Valdés and Lalucat, 2016; Lalucat et al., 2020; Martínez-Carranza et al., 2019; Özen and Ussery, 2012; Peix, Ramírez-Bahena and Velázquez, 2009; Rediers, Vanderleyden and De Mot, 2004; Young and Park, 2007).

Bacterial communities isolated from Acute Oak Decline (AOD) affected trees show a significantly similar composition pattern, where *Brenneria goodwinii* and *Gibbsiella quercinecans* appear to be the predominant pathogens (Brady et al., 2010; Denman et al., 2018, 2012, 2014; Doonan et al., 2019). In addition to these, other species of the genus *Brenneria*, and members of *Lonsdalea*, *Rahnella*, *Erwinia* and *Ewingella* have been isolated in AOD lesions and they could contribute to the symptoms. Several undescribed species included in the family *Pseudomonadaceae*, have also been consistently isolated from AOD affected trees (Denman et al., 2016b, 2018, 2014; Sapp et al., 2016).

It is essential for establishing disease management strategies and designing diagnostic methods to obtain a detailed profile of the bacteria present in the AOD lesions, and therefore to determine the phylogenetic position of the undescribed *Pseudomonas* and to study the potential roles they play in the disease. In this chapter, three *Pseudomonas* species associated with AOD have been formally described. In addition, a simplified overview of the taxonomical relationships amongst a selection of species within the genera *Pseudomonas*, *Azotobacter*, *Azomonas* and *Azorhizophilus* is described in this chapter.

Thirty-one bacterial strains isolated by Forest Research, tentatively classified as *Pseudomonas fulva* by *gyrB* sequencing, were sent to the University of the West of England for complete identification (**Table 1**). Later during the project, four additional strains were

collected from Kew Gardens and added to the polyphasic approach of bacterial classification (Table 1).

3.2. Results

3.2.1. Genotypic characterisation of AOD-associated *Pseudomonas*

3.2.1.1. Phylogenetic analysis based on the partial 16S rRNA gene

Three different phylogenetic analyses of the 16S rRNA gene of the AOD-associated *Pseudomonas* were performed to verify their genus and lineage. The first analysis contained all the 35 AOD-associated Pseudomonads and their closest neighbours, according to EzBioCloud (**Figure 12**). For the construction of all the 16S rRNA phylogenetic trees, the best nucleotide substitution model was the general time reversible model with invariable sites and gamma distribution (GTR+I+G). Clade-credibility values are called bootstraps in maximum likelihood method (ML) and posterior probabilities (PP) in Bayesian method (BI). Bootstrap values below 50 % and PP values below 0.95 are considered low support.

This 16S phylogenetic analysis showed that the AOD-associated strains grouped in three well-defined clusters within *Pseudomonas*, and each of the clusters were referred to as cluster A, cluster B and cluster C (**Figure 12**). Cluster A contained strains P1, P2, P3, P5, P7, P8, P9, P18, P20, P21, P22 and P23, which grouped together with 94 % bootstrap support. Cluster B contained strains P6, P26, P27, GM38b, GM48c, GM50b, I151, I160, I163 and I166, which grouped together in 75 % of the bootstrap replicates. Cluster C comprised strains P4, P10, P11, P14, P16, P17, P24, P25, P28, P29, P30, P31 and P32; these strains grouped in 100 % of the bootstrap replicates. Clusters A and B were closely related with bootstrap support of 83 %, and the taxonomic position of cluster C was far away from the other two clusters. The initial identification of the strains confirmed that they belonged to the genus *Pseudomonas*, and that the closest related species, based on percentage of sequence similarity seen in EzBioCloud, were *Pseudomonas flavescens* (98.73 - 99.23 %), *Pseudomonas seleniipraecipitans* (98.66 - 99.23 %), *Pseudomonas argentinensis* (97.96 - 98.66 %), *Pseudomonas straminea* (98.1 - 98.73 %), and *Pseudomonas punonensis* (98.31 - 98.87 %) to clusters A and B. The closest related species to cluster C were *Pseudomonas nosocomialis* (>96.3 %), *Pseudomonas mangiferae* (>95.7 %), *Pseudomonas stutzeri* (> 95.4 %), and percentages of sequence similarity of 95.0 – 95.3 % were observed to species *Pseudomonas xanthomarina*, *Pseudomonas aeruginosa*, *Pseudomonas stutzeri*, *Pseudomonas furukawaii*, *Pseudomonas composti* and *Azotobacter chroococcum*.

Clusters A and B belonged to the *P. straminea* group, contained in the *P. fluorescens* lineage, and cluster C belonged to the *P. stutzeri* group, located in the *P. aeruginosa* lineage. From

this point, and due to the evidence that clusters A and B were taxonomically distant to cluster C, all the following phylogenetic studies were performed in parallel, one for both clusters A and B and another one for cluster C. One strain per cluster was selected as representative for the following 16S rRNA phylogenetic studies. The representative strains chosen were P2, P27 and P4 for clusters A, B and C, respectively.

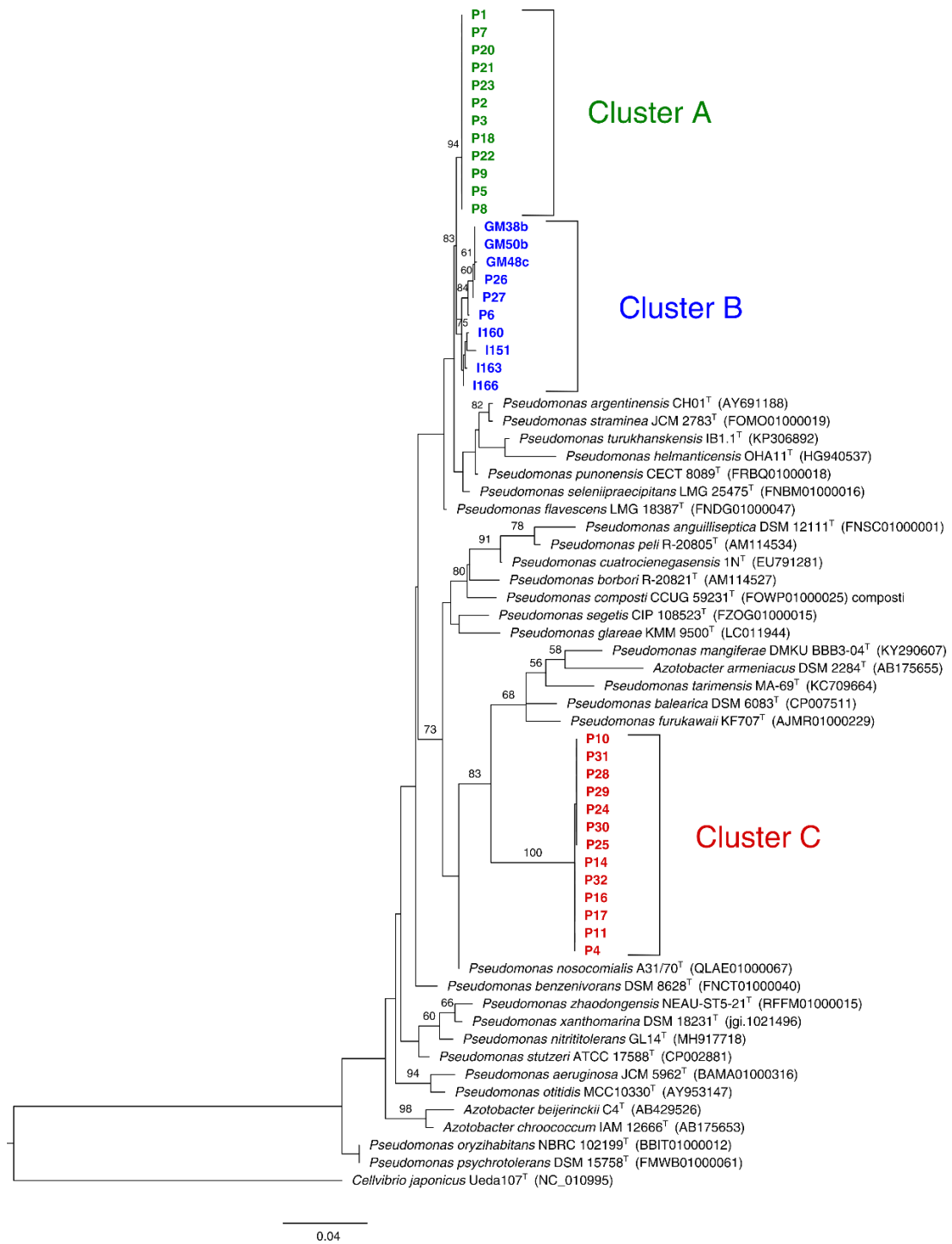


Figure 12: Maximum likelihood 16S rRNA gene phylogenetic tree of the 35 AOD-associated strains of *Pseudomonas*, 31 closest phylogenetic neighbours and the outgroup *Cellvibrio japonicus*. Phylogenetic relationships amongst the strains were inferred from a dataset of partial 16S rRNA gene nucleotide sequences (1399 bp), using the program PhyML. Bootstrap values were obtained from 1000 replicates and values below 50 % are considered low support and were removed from the branches. The scale bar indicates the nucleotide substitutions per site. Species names, strain numbers and GenBank accession numbers are

shown next to the branches. Clusters A, B, and C in green, blue, and red, respectively. ^T = type strain.

Phylogenetic analyses of the 16S rRNA gene was performed for clusters A, B, and their closest neighbours, using ML and BI methods (**Figure 13** and **Appendix I**); and the analysis of cluster C, and its closest neighbours, using BI and ML methods (**Figure 14** and **Appendix II**).

It was observed that BI and ML methods estimated similar tree topologies, but clade-credibility values for the same clusters were generally higher in BI. In the case of the 16S trees constructed specifically for clusters A and B, similar topologies were observed in the phylogenies computed using ML and BI methods (**Figure 13** and **Appendix I**). Representative strains of clusters A and B formed their own independent clade in both ML and BI 16S trees, with confidence values of 83 % in the ML tree and without clade confidence in the BI tree, (PP value of 0.62). The closest phylogenetic neighbour to this clade was *P. flavescens*, without clade confidence.

The topologies of BI and ML trees computed for cluster C were less congruent between each other than the BI and ML trees performed for clusters A and B (**Figure 14** and **Appendix II**). Amongst the closest neighbours for cluster C there were species of different genera (*Pseudomonas*, *Azomonas*, *Azotobacter* and *Azorhizophilus*), which suggested that cluster C is located on the taxonomic edge of the genus. The clade where cluster C was located in the ML tree also contained *Azomonas*, *Azotobacter* and *Azorhizophilus* species (as well as *Pseudomonas*), whereas in the BI tree, the clade that included cluster C only contained *Azomonas* species as well as *Pseudomonas*. The closest neighbour without clade support was *P. balearica* in the BI tree. Cluster C did not cluster with any neighbour with confidence in any of the 16S trees, behaving like an outlier (a species that does not fit into any described group).

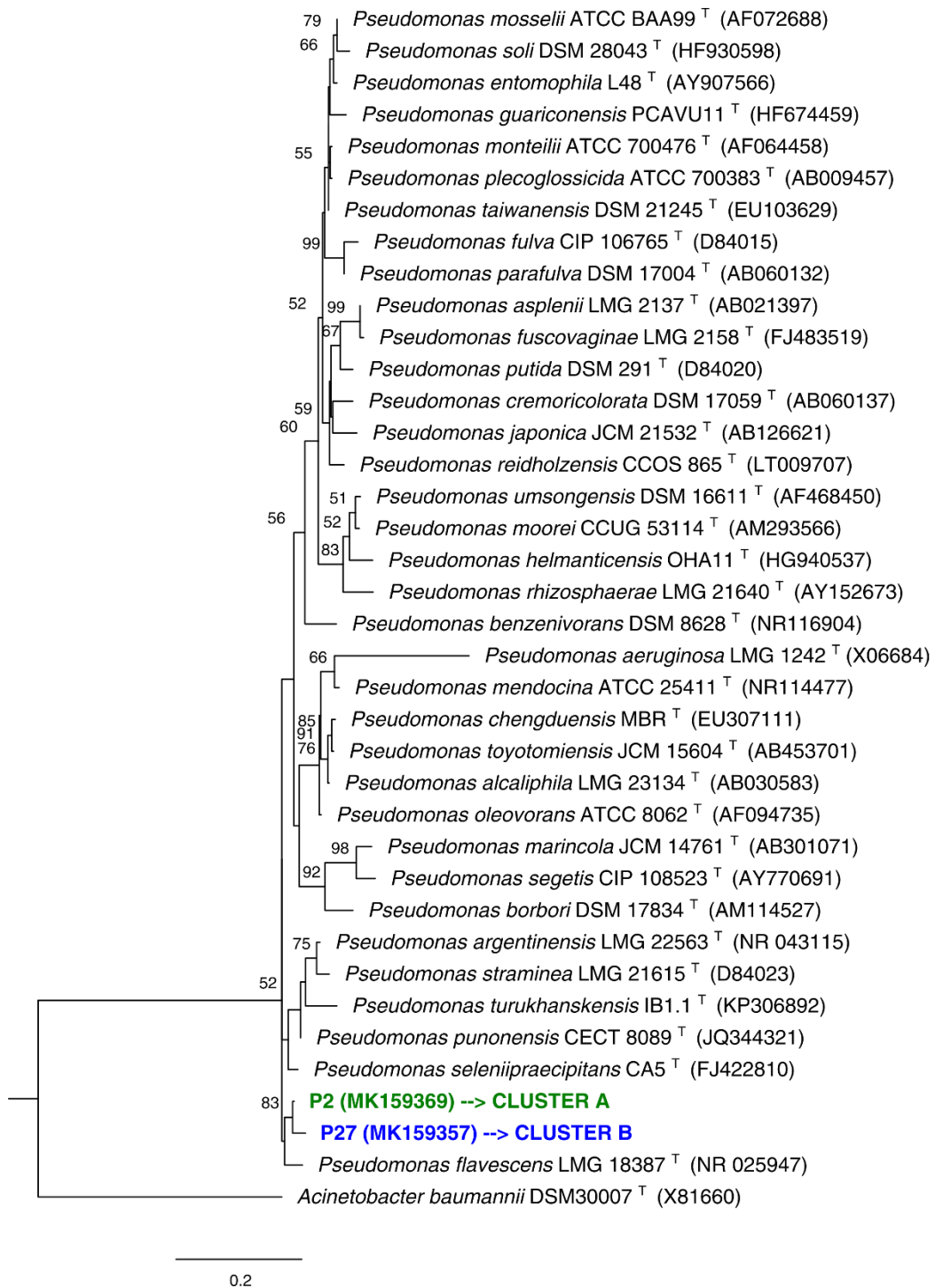


Figure 13: Maximum likelihood 16S rRNA gene phylogenetic tree of the AOD-associated strains representatives of clusters A and B, 35 closest phylogenetic neighbours and the outgroup *Acinetobacter baumannii*. Phylogenetic relationships amongst the strains were inferred from a dataset of partial 16S rRNA gene nucleotide sequences (1399 bp), using the program PhyML. Bootstrap values were obtained from 1000 replicates and values below 50 % are considered low support and were removed from the branches. The scale bar indicates the nucleotide substitutions per site. Species names, strain numbers and GenBank accession

numbers are shown next to the branches. Strains representative of clusters A and B in green and blue respectively. ^T = type strain.

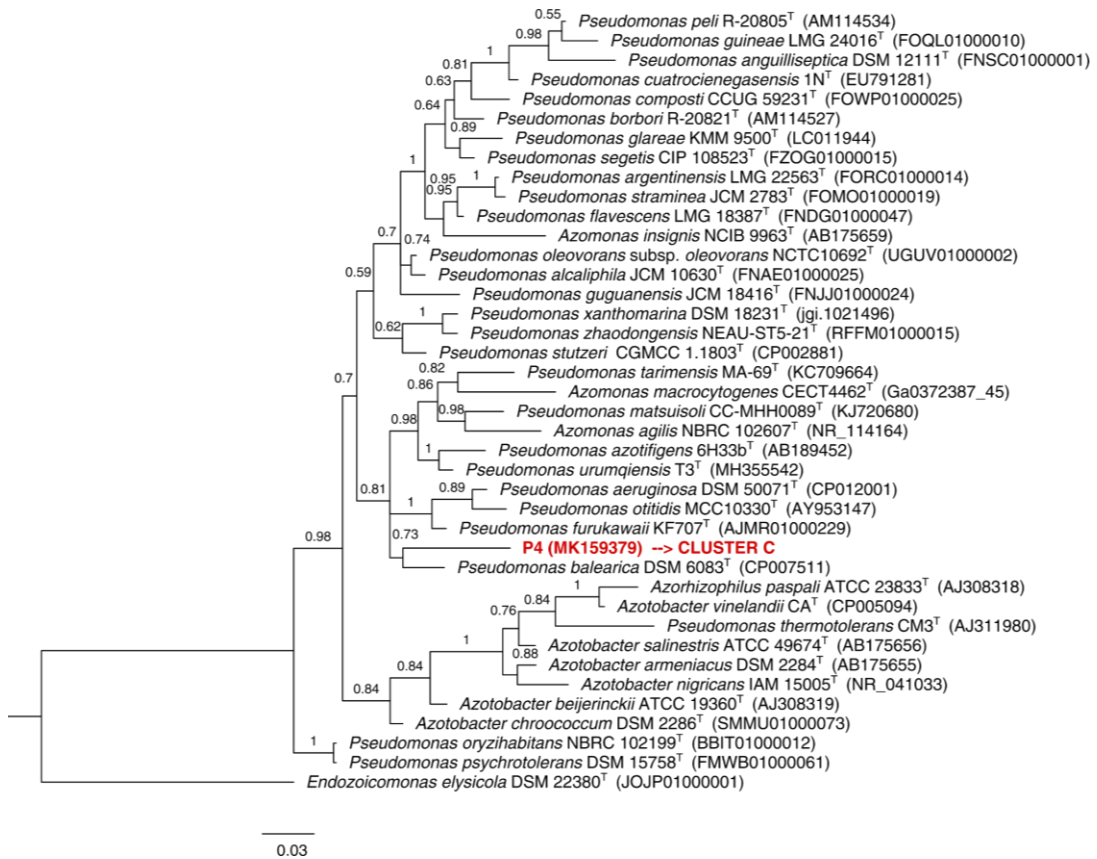


Figure 14: Bayesian 16S rRNA phylogenetic tree of the AOD-associated strain representative of cluster C, 38 closest phylogenetic neighbours and the outgroup *Endozoicomonas elysicola*. Phylogenetic relationships amongst the strains were inferred from a dataset of partial 16S rRNA gene nucleotide sequences (1367 bp), using the program MrBayes. Posterior probabilities lower than 0.95 are considered low support. Values lower than 0.5 were removed from the branches. The scale bar indicates the nucleotide substitutions per site. Species names, strain numbers and GenBank accession numbers are shown next to the branches. Strain representative of cluster C in red. ^T = type strain.

3.2.1.2. MLSA study of the concatenated *gyrB*, *rpoB* and *rpoD* genes

To further explore the taxonomic position of the AOD-associated strains, phylogenetic analyses of the individual and concatenated nucleotide and translated amino acid sequences

of the genes *gyrB*, *rpoB* and *rpoD* were performed. The phylogenies inferred from the individual genes (data not shown) were mostly congruent with those inferred for the concatenated sequences. The best nucleotide substitution model for all the ML phylogenetic trees was GTR+I+G, for both the tree for the clusters A and B (**Figure 15**), and the ML tree for the cluster C (**Appendix III**). The best nucleotide substitution model for BI trees was the transitional model with invariable sites and gamma distribution (TIM2+I+G in the tree for clusters A and B (**Appendix IV**), and TIM1+I+G in the tree for cluster C, (**Figure 16**). The fittest amino acid substitution model used for the amino acid trees, (**Appendix V** and **Appendix VI**), was LG+G+I+F, model with invariable sites and gamma distribution. “F” indicates the use of the empirical amino acid distribution in the analysed alignment, instead of the model default distribution; and “LG” is the name of the model, given after the authors (Le and Gascuel, 2008). Accession numbers in **Appendix VII**.

Similar topologies were obtained when computing the trees using ML with nucleotide and amino acid sequences. However, comparing ML to BI trees, the branching varied slightly. In all the phylogenies inferred in this section, strains from each of the clusters A, B and C, grouped in three different clusters. In the trees performed using nucleotide sequences, the intra-cluster clade support values obtained for each of the clusters A, B and C was 100 % bootstrap support or PP of 1. In the phylogenies computed from the translated amino acid sequences, the intra-cluster clade support values obtained from each of the clusters was also the maximum except for the clade support value obtained for the strains in cluster B, which clustered together in 79 % of the replicates instead of 100 %.

The novel strains formed their own three clusters, and none of the closest neighbours clustered within any of the novel clusters A, B or C. The structures of the MLSA trees generated in this section supported the 16S analysis findings, indicating that each of the three clusters belong to three different taxa.

In all the MLSA trees computed for clusters A and B, (ML nucleotide tree, BI nucleotide tree and ML amino acid tree, (**Figure 15**, **Appendix IV** and **Appendix V**), the neighbours *P. seleniipraecipitans*, *P. flavescens*, *P. argentinensis*, *P. punonensis* and *P. straminea* were closely related. *P. seleniipraecipitans*, *P. flavescens*, *P. argentinensis*, *P. punonensis* and *P. straminea*, clustered with the strains of clusters A and B in 84 % of the bootstrap replicates in the ML nucleotide tree, with PP of 1 in the BI nucleotide tree and in 65 % of the bootstrap repeats in the ML amino acid tree.

All the MLSA trees computed for cluster C, (BI and ML nucleotide and amino acid sequence trees (**Figure 16**, **Appendix III** and **Appendix VI**) were congruent in their topologies except for the branch containing the *Azotobacter* species, which occupied different places in each tree, but always within the genus *Pseudomonas*. Trees constructed using the ML method were mostly congruent to the BI MLSA tree (**Figure 16**). Cluster C grouped with a clade containing the species *P. xanthomarina*, *P. balearica*, *P. stutzeri*, *P. azotifigens* and *P. urumqiensis* in all the trees computed, with confidence values of 62 and 87 % of bootstrap support in ML nucleotide and amino acid tree, respectively, and without confidence in the BI tree.

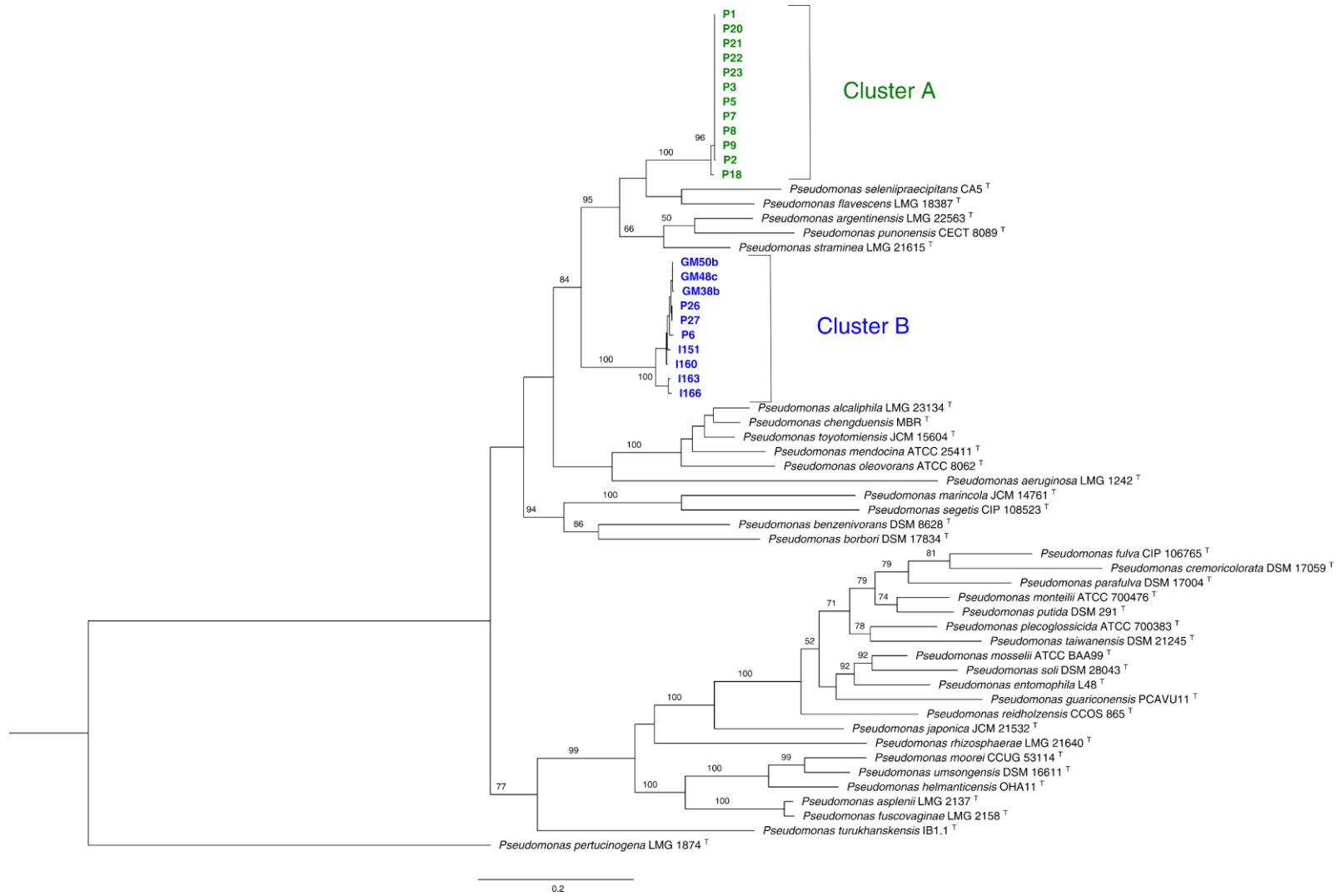


Figure 15: Maximum likelihood MLSA phylogenetic tree of the concatenated gene sequences *gyrB*, *rpoB* and *rpoD*, obtained from AOD-associated strains in clusters A and B, 35 closest phylogenetic neighbours and the outgroup *Pseudomonas pertucinogena*. Phylogenetic relationships amongst the strains were inferred from a dataset of partial concatenated *gyrB*, *rpoB* and *rpoD* nucleotide sequences (765, 750 and 657 bp long respectively), using the program PhyML. Bootstrap values were obtained from 1000 replicates and values below 50 % are considered low support and were removed from the branches. The scale bar indicates the nucleotide substitutions per site. Species names and strain numbers are shown next to the branches and accession numbers are available in **Appendix VII**. Clusters A and B in green and blue, respectively. ^T = type strain.

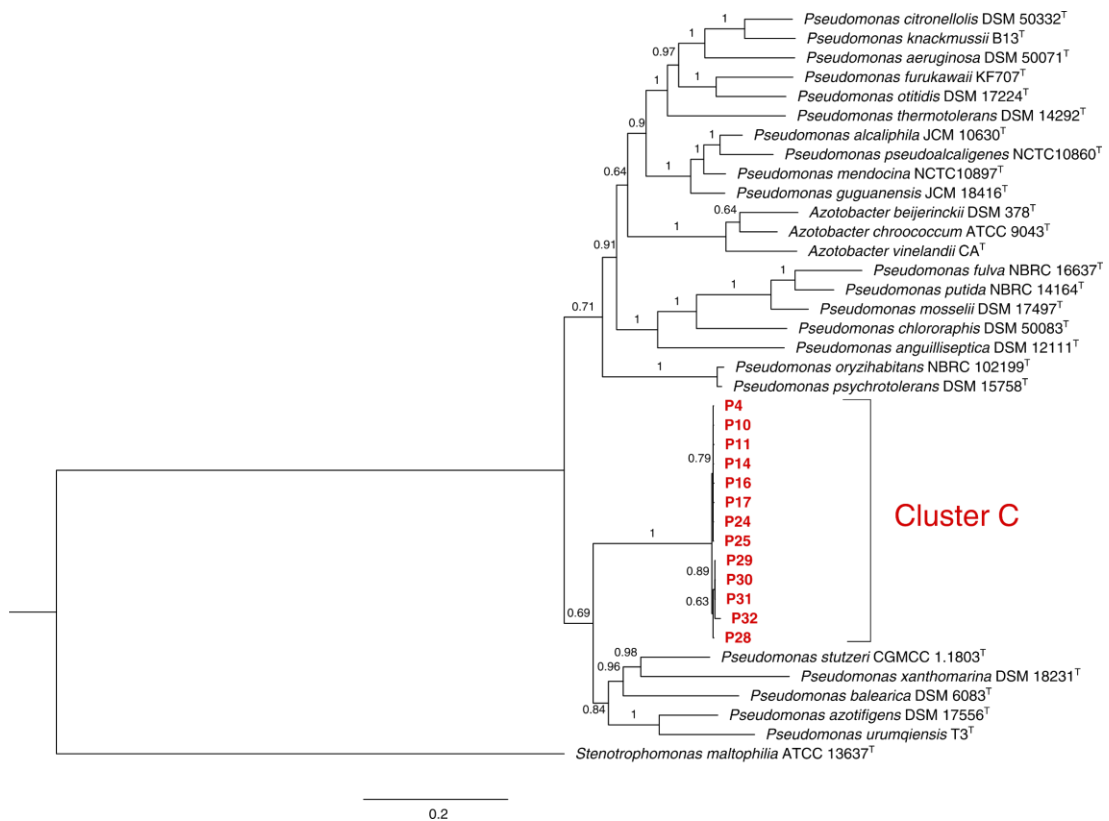


Figure 16: Bayesian MLSA phylogenetic tree of the concatenated gene sequences *gyrB*, *rpoB* and *rpoD*, obtained from the AOD-associated strains in cluster C, 25 closest phylogenetic neighbours and the outgroup *Stenotrophomonas maltophilia*. Phylogenetic relationships amongst the strains were inferred from a dataset of partial concatenated *gyrB*, *rpoB* and *rpoD* nucleotide sequences (771, 753 and 651 bp long respectively), using the program Mr Bayes. Posterior probabilities lower than 0.95 were considered low support. Values lower than 0.5 were removed from the branches. The scale bar indicates the nucleotide substitutions per site. Species names and strain numbers are shown next to the branches and accession numbers are available in **Appendix VII**. ^T = type strain.

3.2.1.3. DNA fingerprinting of AOD-associated *Pseudomonas*

DNA fingerprinting was used to assess the intra-cluster diversity (clonal identity) of the strains. To explore the infra-species level of genomic relatedness, three different DNA fingerprinting methods were used (BOX-PCR, ERIC-PCR and RAPD-PCR), from which the most discriminative ones are described in this section.

The DNA fingerprinting methods that provided most discriminative band patterns were RAPD-PCR for clusters A and B, and BOX-PCR for cluster C (**Figure 17** and **Figure 18**). Two

different DNA gel band patterns were observed within cluster A, four different patterns for cluster B, and three for cluster C. For the strains in cluster A, all collected in Bisham Woods, two DNA gel band patterns were observed. For the species in cluster B, one DNA gel band pattern was observed for the strains collected in Great Monk Woods, a different pattern was observed for the strains collected in Bisham Woods and two patterns were observed amongst the strains collected in Kew Gardens. Identical DNA gel band patterns suggested that the strains are clones. None of the closest neighbours displayed identical DNA gel band fingerprints to the AOD-associated strains.

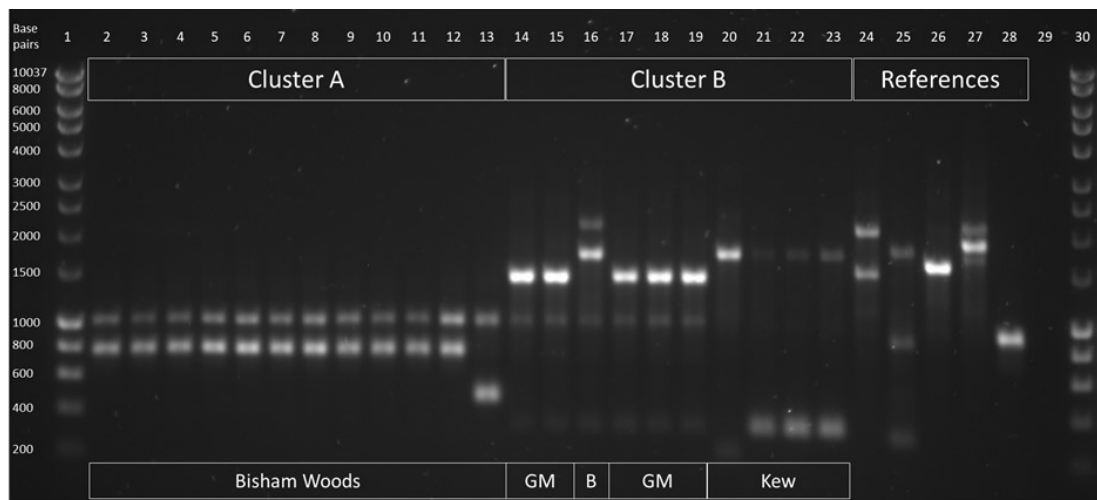


Figure 17: RAPD-PCR fingerprinting band patterns obtained with the primer OPA-04 from the AOD-associated strains included in clusters A and B, and the closest neighbours. Lanes: (1) Hyperladder 1kb, (2) P2, (3) P1, (4) P3, (5) P5, (6) P7, (7) P8, (8) P9, (9) P20, (10) P21, (11) P22, (12) P23, (13) P18, (14) P27, (15) P26, (16) P6, (17) GM38b, (18) GM48c, (19) GM50b, (20) I151, (21) I160, (22) I163, (23) I166, (24) *Pseudomonas flavescens* LMG 18387^T, (25) *Pseudomonas argentinensis* LMG 22563^T, (26) *Pseudomonas seleniipraecipitans* LMG 25475^T, (27) *Pseudomonas punonensis* LMG 26839^T, (28) *Pseudomonas straminea* LMG 21615^T, (29) non-template control, (30) Hyperladder 1kb. Sample collection sites are denoted below the gel lanes: GM = Great Monk Woods, Kew = Kew Gardens, B = Bisham Woods. ^T = type strain.



Figure 18: BOX-PCR fingerprinting band patterns obtained with the primer BOX-1AR from the AOD-associated strains included in cluster C, and the closest neighbours. Lanes: (1) Hyperladder 1kb, (2) P4, (3) P10, (4) P11, (5) P14, (6) P16, (7) P17, (8) P24, (9) P25, (10) P29, (11) P30, (12) P31, (13) P32, (14) P28, (15) *Pseudomonas azotifigens* LMG 23662^T, (16) *Pseudomonas balearica* LMG 18376^T, (17) *Pseudomonas stutzeri* LMG 11199^T, (18) *Pseudomonas xanthomarina* LMG 23572^T, (19) non-template control, (20) Hyperladder 1kb. Sample collection sites are denoted below the gel lanes: SB = Stratfield Brake, S = Send. ^T = type strain.

3.2.1.4. Whole genome sequencing

Following the phylogenetic study of the 16S rRNA gene and the MLSA of the AOD-associated *Pseudomonas*, the whole genomes of selected strains of clusters A, B, and C were sequenced. The quality of the *de novo* genome assemblies (assemblies without reference genome) was obtained using the assembly comparison software QUality assessment tool (QUAST) (Gurevich et al., 2013). QUAST evaluates genome assemblies by providing information on the genome and contigs length, quality statistics such as N50 and L50, the percentage of G + C on the genome and the number of contigs longer than 1kb; the accession numbers are also provided (**Table 8**). N50 is the length for which the collection of all contigs of that length or longer covers at least half the genome's size. L50 describes the smaller number of contigs whose length is N50 and higher. The average G + C content was 62.01 (± 0.02) mol % for the strains of cluster A, 64.96 (±0.02) mol % for the strains of cluster B and 63.67 (0.06) mol % for strains of cluster C.

Table 8: QUAST output of the genome assemblies obtained following the genome sequencing of the AOD-associated *Pseudomonas* and GenBank accession numbers.

Sample ID	N. contigs	N. contigs >=1kb	Total length (bp)	G + C (%)	N50	L50	Accession number
P2 (cluster A)	70	56	5408927	62.02	222841	9	QJUH00000000
P9 (cluster A)	58	52	5403278	62.02	225407	10	QJUI00000000
P18 (cluster A)	25	24	5570084	61.98	572561	4	QJUU00000000
P23 (cluster A)	68	58	5407537	62.02	221434	9	QJUK00000000
P27 (cluster B)	81	71	5730738	64.97	133269	15	QJUN00000000
P6 (cluster B)	119	105	5887770	64.94	104681	17	QJUL00000000
P26 (cluster B)	82	68	5735213	64.97	160737	13	QJUM00000000
P4 (cluster C)	84	74	4353263	63.72	103701	13	QJUU00000000
P17 (cluster C)	76	61	4357139	63.71	129538	11	QJUP00000000
P28 (cluster C)	79	68	4316885	63.58	104179	15	QJUQ00000000
P30 (cluster C)	54	46	4349767	63.67	206805	8	QJUR00000000

3.2.1.5. Average Nucleotide Identity studies based on BLAST (ANIb) and *in silico* DNA-DNA hybridisation (*isDDH*)

Average nucleotide identity studies based on BLAST were performed to determine the genomic similarity between two whole genomes. ANIb percentage of 95 % is considered the cut off value for species delimitation. ANI values of 98.3 – 100 % were obtained amongst strains contained in cluster A, 98.6 – 100 % amongst strains in cluster B, and 99.2 – 100 % amongst strains in cluster C. All the intra-cluster ANIb values were above 95 %, indicating that they belong to the same species, (**Table 9** and **Table 10**). The ANIb percentages obtained from the comparisons of the novel *Pseudomonas* and the closest neighbours are below species limit, *P. flavescens* being the closest to the threshold when comparing its genome with both cluster A (87 – 87.2 %) and cluster B (83.8 %). *P. stutzeri* obtained the highest ANIb percentage when compared to cluster C (77.6 – 77.7 %).

In silico DNA-DNA hybridisation studies (*is DDH*) were performed to evaluate the genetic distance between two genomes. A percentage of 70 % of *isDDH* is the threshold for species delimitation. *Is DDH* values obtained from the comparison of different strains of the novel *Pseudomonas* species are above the species delimitation threshold, 87.9 – 100 % for strains in cluster A, 92.5 – 100 % for strains in cluster B and 95.2 – 100 % for strains in cluster C,

(**Table 9** and **Table 10**). As for the ANIb results, the closest species to clusters A and B was *P. flavescens* (39.1 – 39.2 % and 33.7 – 33.8 %, respectively), and the closest species to cluster C was *P. stutzeri* (23.4 %). All the closest neighbours of clusters A, B and C displayed values of *isDDH* well below the species similarity value when the genomes were compared to AOD-associated strains.

Table 9: Heatmap of percentages of average nucleotide identity based on BLAST (ANi_b, below the black cells), and *in silico* DNA-DNA hybridisation (*is* DDH, above the black cells). Values of selected strains of AOD-associated *Pseudomonas* included in clusters A and B, and their closest phylogenetic neighbours. ANi_b values (in green) were obtained using the software JSpecies. Percentages > 95 % are above cut off value for species delimitation. *is*DDH values (in red) are percentages of genome-to-genome distance calculations, transformed to values equivalent to DDH %, by the distance calculator tool: GGDC 2.1, using a generalized linear model. Percentages > 70 % are above cut off value for species delimitation.

		<i>is</i> DDH%		Cluster / Species / (Strain)									
				Cluster A (P2)	Cluster A (P9)	Cluster A (P18)	Cluster A (P23)	Cluster B (P27)	Cluster B (P6)	Cluster B (P26)	<i>P. flavescens</i> (LMG 18387 ^T)	<i>P. argeninensis</i> (LMG 18387 ^T)	<i>P. punonensis</i> (CECT 8089 ^T)
ANiB%													
		Cluster A (P2)	Cluster A (P9)	Cluster A (P18)	Cluster A (P23)	Cluster B (P27)	Cluster B (P6)	Cluster B (P26)	<i>P. flavescens</i> (LMG 18387 ^T)	<i>P. argeninensis</i> (LMG 18387 ^T)	<i>P. punonensis</i> (CECT 8089 ^T)	<i>P. seleniipraecipitans</i> (LMG 25475 ^T)	<i>P. straminea</i> (JCM 2783 ^T)
Cluster / Species / (Strain)	Cluster A (P2)	*	100	87.9	100	31.5	31.7	31.5	39.2	34.6	33.8	35.8	33.9
	Cluster A (P9)	100	*	87.9	100	31.5	31.7	31.5	39.2	34.6	33.8	35.8	33.9
	Cluster A (P18)	98.3	98.3	*	87.9	31.5	31.5	31.4	39.1	34.7	33.9	35.8	33.9
	Cluster A (P23)	100	100	98.3	*	31.5	31.7	31.5	39.2	34.6	33.8	35.8	33.9
	Cluster B (P27)	85.1	85.1	84.9	85.1	*	92.5	100	33.8	32.5	31.2	31.8	32.2
	Cluster B (P6)	85	85	84.8	85	98.6	*	92.5	33.7	32.4	31.1	31.9	32.1
	Cluster B (P26)	85	85	84.8	85	100	98.8	*	33.8	32.5	31.1	31.8	32.2
	<i>P. flavescens</i> (LMG 18387 ^T)	87.2	87.2	87	87.2	83.8	83.8	83.8	*	35.2	34.6	35.4	34.5
	<i>P. argeninensis</i> (LMG 18387 ^T)	85	85	84.8	85	83.1	83.1	83.1	85.2	*	40	33.8	41.1
	<i>P. punonensis</i> (CECT 8089 ^T)	84.9	84.9	84.9	84.9	82.6	82.6	82.6	85	88.3	*	33.5	38.4
<i>P. seleniipraecipitans</i> (LMG 25475 ^T)	86	86	86	86	82.8	82.8	82.8	85.4	84.6	84.4	*	33.1	
<i>P. straminea</i> (JCM 2783 ^T)	84.7	84.7	84.6	84.7	83	83	83	84.7	88.7	87.7	83.9	*	

Accession numbers of genomes of AOD associated *Pseudomonas* in **Table 8**. Accession numbers of genomes of their closest phylogenetic neighbours: *Pseudomonas flavescens* LMG 18387^T, (FNDG00000000); *Pseudomonas argentinensis* LMG 22563^T, (FORC00000000); *Pseudomonas punonensis* CECT 8089^T, (FRBQ00000000); *Pseudomonas seleniipraecipitans* LMG 25475^T, (FNBM00000000) and *Pseudomonas straminea* JCM 2783^T, (FOMO00000000). ^T = type strain.

Table 10: Heatmap of percentages of average nucleotide identity based on BLAST (ANi_b, below the black cells), and *in silico* DNA-DNA hybridisation (*is* DDH, above the black cells). Values of selected strains of AOD-associated *Pseudomonas* included in cluster C, and their closest phylogenetic neighbours. ANi_b values (in green) were obtained using the software JSpecies. Percentages > 95 % are above cut off value for species delimitation. *is* DDH values (in red) are percentages of genome-to-genome distance calculations, transformed to values equivalent to DDH %, by the distance calculator tool: GGDC 2.1, using a generalized linear model. Percentages > 70 % are above cut off value for species delimitation.

		Cluster / Species / (Strain)												
		<i>is DDH%</i>				<i>ANiB%</i>								
		Cluster C (P4)	Cluster C (P17)	Cluster C (P28)	Cluster C (P30)	<i>P. stutzeri</i> (CGMCC 1.1803 ^T)	<i>P. azotifigens</i> (DSM 17556 ^T)	<i>P. balearica</i> (DSM 6083 ^T)	<i>P. xanthomarina</i> (DSM 18231 ^T)	<i>P. urumqiensis</i> (T3 ^T)	<i>P. thermotolerans</i> (DSM 14292 ^T)	<i>A. chroococcum</i> (ATCC 9043 ^T)	<i>A. beijerinckii</i> (DSM 378 ^T)	<i>A. vinelandii</i> (CA ^T)
Cluster / Species / (Strain)	Cluster C (P4)	*	100	95.2	96.1	23.4	23.2	23.2	21.9	21.8	22.5	22.6	22.7	23
	Cluster C (P17)	100	*	95.2	96.1	23.4	23.3	23.3	21.9	21.8	22.5	22.6	22.7	23
	Cluster C (P28)	99.2	99.2	*	95.6	23.4	23	23	21.9	21.7	22.5	22.6	22.7	23
	Cluster C (P30)	99.4	99.4	99.2	*	23.4	23.1	23.1	21.9	21.7	22.5	22.6	22.6	23
	<i>P. stutzeri</i> (CGMCC 1.1803 ^T)	77.6	77.6	77.7	77.6	*	23.1	23.1	22.1	21.5	22.6	22.6	22.8	23
	<i>P. azotifigens</i> (DSM 17556 ^T)	77.1	77.1	77	77	78.7	*	23.5	21.5	23.8	23.2	23.1	23.1	23
	<i>P. balearica</i> (DSM 6083 ^T)	77.2	77.2	77.2	77.2	81	78.8	*	21.4	21.6	22.2	22.1	22.5	22
	<i>P. xanthomarina</i> (DSM 18231 ^T)	75.6	75.6	75.6	75.6	78	76.5	76.8	*	20.5	20.4	20.9	21.1	21
	<i>P. urumqiensis</i> (T3 ^T)	75.5	75.6	75.5	75.5	77.2	80	76.9	75.4	*	21.2	21.4	21.4	21
	<i>P. thermotolerans</i> (DSM 14292 ^T)	77.3	77.3	77.2	77.3	77.6	78.7	77.2	74.9	76.3	*	23.7	24	23
<i>A. chroococcum</i> (ATCC 9043 ^T)	76.6	76.6	76.6	76.6	77.3	78.1	76.8	74.8	76.1	79	*	42	37	
<i>A. beijerinckii</i> (DSM 378 ^T)	76.6	76.6	76.6	76.6	77.2	77.7	76.8	74.6	75.8	78.9	89.8	*	34	
<i>A. vinelandii</i> (CA ^T)	76.2	76.2	76.1	76.1	76.5	77.2	76.1	74.4	75.5	77.9	87.4	86.1	*	

Accession numbers of genomes of AOD associated *Pseudomonas* in **Table 8**. Accession numbers of genomes their closest phylogenetic neighbours: *Pseudomonas stutzeri* CGMCC 1.1803^T, (CP002881); *Pseudomonas azotifigens* DSM 17556^T, (AUDU00000000); *Pseudomonas balearica* DSM 6083^T, (CP007511); *Pseudomonas xanthomarina* DSM 18231^T, (FQXA00000000); *Pseudomonas urumqiensis* T3^T, (RBZQ00000000); *Pseudomonas thermotolerans*

DSM 14292^T, (AQPA00000000); *Azotobacter chroococcum* ATCC 9043^T, (SJAA00000000); *Azotobacter beijerinckii* DSM 378^T, (FOFJ00000000) and *Azotobacter vinelandii* CA^T, (CP005094). ^T = type strain.

3.2.2. Cultural characteristics of AOD-associated *Pseudomonas*

Colonies of all *Pseudomonas* strains grown in KB agar were cream-coloured, circular, convex, smooth, and with entire margins. The diameter of the colonies of strains in cluster A and B was 2mm, and the diameter of strains in cluster C was 1 mm. All strains except for P1, P2, P3, P5, P7, P8, P9, P20, P21, P22 and P23 (cluster A) produced a pigment fluorescent under UV light.

3.2.3. Cell characteristics of AOD-associated *Pseudomonas*

All strains were Gram-negative, slightly curved short rods, and motile. Cells from each of strains P2, P7, P8, P18 and P22 (cluster A) were 1.7 μm x 0.4 μm in average length and width (n=5). Strains P6, P26 and P27 (cluster B) were in average 2.3 μm x 0.4 μm (n=5). Strains P4, P10C, P24, P29, P28, P31C and P32 (cluster C) were 1.5 μm x 0.4 μm in average (n=5).

TEM images of representative strains of each of the clusters A, B and C (P2, P27 and P4 respectively) showed that they possessed flagella. P2 and P27 had a single polar flagellum, and cells of P4 had amphitrichous flagella (**Figure 19**).

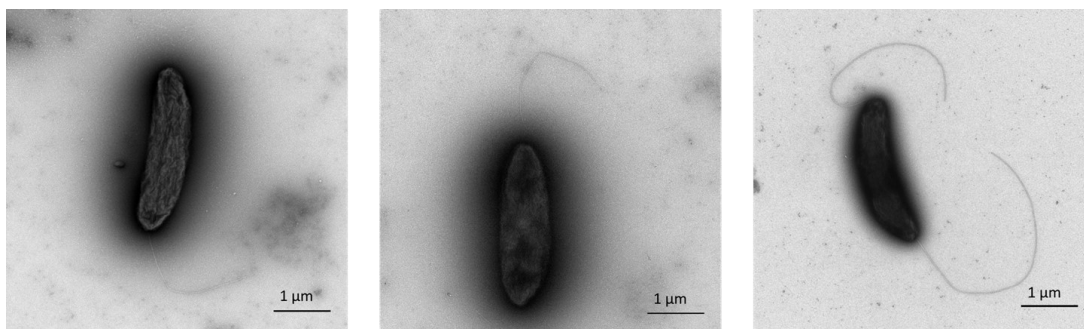


Figure 19: Transmission electron micrographs of cells of AOD-associated *Pseudomonas*. Representative strain of cluster A, P2 (left); representative strain of cluster B, P27 (centre); and representative strain of cluster C, P4 (right).

3.2.4. Phenotypic characterisation of the AOD-associated *Pseudomonas*

3.2.4.1. API 20NE and API 50 CH tests

No intra-cluster diversity was observed in the API 20NE result profiles. However, some intra-cluster diversity was observed in the biochemical profiles obtained with API 50 CH. Four percent of the API 50 CH carbon sources tested showed a different response for strains within cluster A; 4% for strains within cluster B, and 2 % of the tests showed a different result for strains within cluster C

Table 11 and **Table 12**). The complete API 20NE and API 50 CH profiles for all AOD-associated strains and the closest neighbours are in **Appendix VIII**.

Strains in cluster A responded differently than all the closest neighbours in 9 % of the API 20NE tests (nitrification and denitrification) and in 20 % of the API 50 CH tests (fermentation of glycerol, D-xylose, D-maltose, D-melibiose, D-saccharose, D-trehalose, gentiobiose, D-lyxose, D-fucose and D-arabitol). Strains in cluster B responded differently than all the closest neighbours in 14 % of the API 20NE tests (nitrification, denitrification and assimilation of L-arabinose), and in 24 % of the API 50 CH tests (fermentation of glycerol, L-arabinose, D-xylose, D-galactose, D-maltose, D-melibiose, D-saccharose, D-trehalose, gentiobiose, D-fucose and D-arabitol). Strains in cluster C responded differently than all the closest neighbours in 29 % of API 20NE tests (denitrification and assimilation of D-glucose, D-mannitol, potassium gluconate, caprate and citrate) and in 37 % of the API 50CH tests (fermentation of glycerol, L-arabinose, D-xylose, D-galactose, D-glucose, D-fructose, D-mannose, D-mannitol, D-maltose, D-lactose, D-melibiose, D-trehalose, amidon, glycogen, gentiobiose, D-fucose and D-arabitol). Strains in cluster A had identical API 20NE profiles as *P. flavescens*, *P. punonensis* and *P. straminea*. The inability to assimilate L-arabinose (API 20NE) was specific for strains in cluster B.

Cluster C and the neighbours were generally less reactive to the tests performed. *P. stutzeri* reacted positively to 7 API 20NE tests, *P. azotifigens*, *P. balearica* and *P. xanthomarina* reacted positively to 6 tests and only 2 positive API 20NE results were obtained from cluster C. *P. argentinensis* generated acid from 14 carbon sources, *P. flavescens* from 11, P18 (cluster A) was able to ferment 9 carbon sources, *P. seleniipraecipitans* 8, strains P2 and P9 from cluster A, *P. punonensis* and *P. straminea* fermented 7 carbon sources, and cluster B 5. *P. stutzeri* generated acid from 12 compounds, *P. xanthomarina* from 7, *P. balearica* from 6, P30 from cluster C was able to ferment 1 carbohydrate and P4, P28 (cluster C) and *P. azotifigens* were unable to ferment any carbohydrate.

3.2.4.2. Biolog GN2 microplates and catalase and oxidase activity

Intra-cluster diversity was observed in the profiles obtained from the AOD-associated species with the Biolog tests. For cluster A, 90 % of the carbon sources tested showed the same metabolic response in all the strains (

Table 11). The percentage of carbon sources for which the response was the same in all cluster B strains tested was 91 % and 95 % for cluster C (**Table 12**). The complete Biolog GN2 profiles for all AOD-associated strains and the closest neighbours are in **Appendix VIII**. Clusters A and B responded differently to the closest neighbours in 37 % and 38 % of the carbon sources, respectively. Strains in cluster C responded differently than the closest neighbours in 49 % of the Biolog tests. Strains in cluster A oxidised more carbon sources (an average of 40), followed by *P. flavescens* (38), *P. seleniipraecipitans* (35), *P. punonensis* (34), *P. straminea* (30), cluster B (26 in average), and *P. argentinensis* (25). The Biolog tests for cluster C and the closest related species showed that *P. stutzeri* was the species that oxidised more carbon sources (40), followed by *P. balearica* (36), *P. azotifigens* (31), cluster C (23 in average) and *P. xanthomarina*, which showed a positive result for only 2 carbon sources.

The tests in which clusters A and B showed a different oxidative response to one or more of the closest neighbours were: dextrin, glycogen (different result only in cluster B), D-arabitol, D-fructose, D-galactose (different result only in cluster A), α -D-glucose, D-mannose, sucrose, D-trehalose, succinic acid mono-methyl ester, acetic acid, formic acid, D-galacturonic acid, D-gluconic acid (different result only in cluster A), D-glucuronic acid, α -hydroxybutyric acid (different result only in cluster B), β -hydroxybutyric acid, γ -hydroxybutyric acid, malonic acid, propionic acid, quinic acid, D-saccharic acid, succinic acid, succinamic acid, glucuronamide, L-alaninamide, D-alanine, L-alanine, L-asparagine (different result only in cluster A), hydroxy-L-proline, L-pyroglytamic acid (different result only in cluster A), L-serine, L-threonine, D and L-carnitine (different result only in cluster B), urocanic acid, putrescine, 2-aminoethanol, glycerol and D and L α -glycerol phosphate (different result only in cluster B).

The carbon compounds that cluster C showed different oxidation response to one or more of the closest neighbours were: dextrin, glycogen, tween 40, tween 80, D-fructose, α -D-glucose, maltose, D-mannitol, turanose, pyruvic acid methyl ester, succinic acid mono-methyl ester, cis-aconitic acid, citrate, acetate, formic acid, D-gluconate, α -hydroxybutyric acid, β -hydroxybutyric acid, itaconic acid, α -ketobutyric acid, α -ketoglutaric acid, α -ketovaleric acid, D and L-lactic acid, malonate, propionate, D-saccharic acid, sebacic acid, succinic acid, bromosuccinic acid, succinamic acid, L-alaninamide, D-alanine, L-alanine, L-asparagine, L-aspartic acid, L-glutamic acid, L-leucine, L-proline, L-pyroglytamic acid, D-serine, L-serine, L-threonine, γ -aminobutyric acid, 2-aminoethanol, 2,3-butanediol, glycerol and D-glucose-6-phosphate. All AOD-associated *Pseudomonas* displayed catalase and cytochrome oxidase activity.

Table 11: Distinguishing phenotypic characteristics of the AOD-associated strains in cluster A, B and their closest neighbours, obtained with the tests API 20NE, API CH 50 and Biolog GN2. The tests in which clusters A and B showed a different oxidation response than one or more of the closest neighbours are displayed in this table and the complete phenotypic traits are available in **Appendix VIII**.

API 20 NE, characteristic:	Cluster A			Cluster B			<i>Pseudomonas flavescens</i>	<i>P. argentinensis</i>	<i>P. punonensis</i>	<i>P. seleniipraecipitans</i>	<i>P. straminea</i>
	P2	P9	P18	P27	P6	P26	LMG 18387 ^T	LMG 22563 ^T	LMG 26839 ^T	LMG 25475 ^T	LMG 21615 ^T
Nitrate reduction to nitrites (nitrification)	-	-	-	-	-	-	-	+	-	+	-
Nitrate reduction to nitrogen (denitrification)	-	-	-	-	-	-	-	-	-	+	-
Assimilation L-arabinose	+	+	+	-	-	-	+	+	+	+	+
API 50 CH, acid from:	Cluster A			Cluster B			<i>Pseudomonas flavescens</i>	<i>P. argentinensis</i>	<i>P. punonensis</i>	<i>P. seleniipraecipitans</i>	<i>P. straminea</i>
	P2	P9	P18	P27	P6	P26	LMG 18387 ^T	LMG 22563 ^T	LMG 26839 ^T	LMG 25475 ^T	LMG 21615 ^T
Glycerol	+	+	+	+	W+	+	+	+	-	+	W+
L-arabinose	+	+	+	-	-	-	+	+	+	+	+
D-xylose	-	-	-	-	-	-	-	+	-	-	-
D-galactose	+	+	+	-	-	-	+	+	+	+	+
D-maltose	-	-	-	-	-	-	+	+	-	-	-
D-melibiose	-	-	-	-	-	-	-	+	-	-	-

D-saccharose (sucrose)	-	-	-	-	-	-	+	-	-	-	-
D-trehalose	-	-	-	-	-	-	+	+	-	-	-
Gentiobiose	-	-	-	-	-	-	-	+	-	-	-
D-lyxose	w+	w+	+	w+	w+	w+	-	-	-	-	-
D-fucose	-	-	-	w+	+	w+	-	+	-	-	-
D-arabitol	w+	w+	+	w+	w+	w+	+	+	+	+	+
Biolog GN2, oxidation of:	Cluster A			Cluster B			<i>Pseudomonas flavescens</i>	<i>P. argentinensis</i>	<i>P. punonensis</i>	<i>P. seleniipraecipitans</i>	<i>P. straminea</i>
	P2	P9	P18	P27	P6	P26	LMG 18387 ^T	LMG 22563 ^T	LMG 26839 ^T	LMG 25475 ^T	LMG 21615 ^T
Dextrin	w+	w+	+	+	w+	+	w+	-	w+	w+	w+
Glycogen	w+	w+	+	-	w+	w+	w+	-	w+	w+	w+
D-arabitol	+	w+	+	+	+	+	+	w+	w+	+	+
D-fructose	+	+	+	w+	+	w+	+	-	w+	+	w+
D-galactose	+	+	+	-	-	-	+	+	+	+	+
α-D-glucose	+	+	+	+	+	+	+	+	+	w+	w+
D-mannose	+	+	+	w+	w+	+	+	-	-	+	w+
Sucrose	-	-	-	-	-	-	+	-	-	-	-
D-trehalose	-	-	-	-	-	-	+	+	-	-	-
Succinic acid mono-methyl ester	+	+	+	+	+	+	+	+	+	+	w+
Acetic acid	+	+	+	+	+	+	+	-	w+	+	-
Formic acid	+	w+	+	-	+	+	w+	-	w+	w+	w+
D-galacturonic acid	+	+	+	-	-	-	-	+	+	+	+

D-gluconic acid	+	+	+	-	-	-	+	+	+	+	+
D-glucuronic acid	+	+	+	-	-	-	-	+	+	+	+
α -hydroxybutyric acid	-	-	+	-	w+	w+	-	-	w+	w+	-
β -hydroxybutyric acid	+	+	-	-	+	w+	+	w+	+	+	+
γ -hydroxybutyric acid	+	+	+	+	+	+	+	w+	+	+	w+
Malonic acid	-	-	-	-	-	-	w+	-	+	-	-
Propionic acid	-	-	+	w+	+	w+	-	-	-	w+	-
Quinic acid	+	+	+	+	+	+	+	+	+	-	+
D-saccharic acid	+	-	+	-	-	-	+	-	+	+	-
Succinic acid	+	+	+	+	+	+	+	-	+	+	+
Succinamic acid	+	+	+	+	w+	w+	+	-	+	w+	+
Glucuronamide	+	+	+	-	-	-	-	-	+	+	+
L-alaninamide	w+	w+	w+	-	-	-	-	-	w+	w+	+
D-alanine	+	+	+	w+	w+	w+	-	-	w+	+	w+
L-alanine	+	+	+	w+	w+	w+	+	-	+	+	+
L-asparagine	+	+	+	-	+	w+	+	+	+	+	+
Hydroxy-L-proline	+	+	+	+	+	+	+	-	+	+	+
L-pyroglutamic acid	+	+	+	-	w+	w+	+	+	+	+	+
L-serine	+	+	+	w+	w+	+	+	-	+	+	+
L-threonine	-	-	-	-	-	-	-	-	w+	+	-
D,L-carnitine	+	-	w+	-	-	-	w+	w+	-	w+	w+
Urocanic acid	-	-	-	-	-	-	+	-	w+	-	+
Putrescine	-	-	w+	-	-	-	+	+	+	w+	w+
2-aminoethanol	+	+	+	-	-	w+	+	+	+	+	-

Glycerol	+	+	+	+	+	+	+	w+	w+	w+	w+
D,L α -glycerol phosphate	w+	w+	+	-	-	-	w+	-	w+	w+	w+

^T = type strain. +: 100 % of strains positive; -: 100 % of strains negative; w+: 100 % of strains weakly positive.

Table 12: Distinguishing phenotypic characteristics of the AOD-associated strains in cluster C, and their closest neighbours, obtained with the tests API 20NE, API CH 50 and Biolog GN2. The tests in which cluster C showed a different oxidation response than one or more of the closest neighbours are displayed in this table and the complete phenotypic traits are available in **Appendix VIII**.

API 20 NE, characteristic:	Cluster C			<i>Pseudomonas stutzeri</i>	<i>P. azotifigens</i>	<i>P. balearica</i>	<i>P. xanthomarina</i>
	P4	P28	P30	LMG 11199 ^T	LMG 23662 ^T	LMG 18376 ^T	LMG 23572 ^T
Nitrate reduction to nitrogen (denitrification)	-	-	-	+	-	+	+
Assimilation D-glucose	-	-	-	+	+	+	+
Assimilation D-mannitol	-	-	-	-	+	-	+
Assimilation potassium gluconate	-	-	-	+	+	+	+
Assimilation caprate	+	+	+	+	+	+	-
Assimilation citrate	-	-	-	+	+	-	-
API 50 CH, acid from:	Cluster C			<i>Pseudomonas stutzeri</i>	<i>P. azotifigens</i>	<i>P. balearica</i>	<i>P. xanthomarina</i>
	P4	P28	P30	LMG 11199 ^T	LMG 23662 ^T	LMG 18376 ^T	LMG 23572 ^T
Glycerol	-	-	-	+	-	+	+
L-arabinose	-	w+	-	+	-	-	-
D-xylose	-	-	-	+	-	-	-
D-galactose	-	w+	-	+	-	-	-
D-glucose	w+	-	-	+	w+	+	+

D-fructose	-	-	-	+	W+	+	+
D-mannose	-	-	-	+	-	-	-
D-mannitol	-	-	-	W+	W+	-	+
D-maltose	-	-	-	W+	-	+	+
D-lactose	-	-	+	-	-	-	-
D-melibiose	-	-	-	+	-	-	-
D-trehalose	-	-	-	W+	-	-	+
Amidon (starch)	-	-	-	+	-	+	-
Glycogen	-	-	-	+	-	+	-
Gentiobiose	-	-	-	+	-	-	-
D-fucose	-	-	-	+	-	W+	-
D-arabitol	-	-	-	-	W+	-	+
Potassium 5-ketogluconate	W+	W+	W+	-	-	-	-
Biolog GN2, oxidation of:	Cluster C			<i>Pseudomonas stutzeri</i>	<i>P. azotifigens</i>	<i>P. balearica</i>	<i>P. xanthomarina</i>
	P4	P28	P30	LMG 11199^T	LMG 23662^T	LMG 18376^T	LMG 23572^T
Dextrin	-	-	+	+	+	+	+
Glycogen	W+	-	+	+	+	+	-
Tween 40	-	+	+	+	+	+	-
Tween 80	+	+	+	+	+	+	-
D-fructose	-	-	-	+	-	W+	-
α-D-glucose	-	-	-	+	-	+	-
Maltose	-	-	-	+	-	+	-

D-mannitol	-	-	-	-	+	-	-
Turanose	-	-	-	+	-	-	-
Pyruvic acid methyl ester	+	+	+	+	+	+	-
Succinic acid mono-methyl ester	+	+	+	+	+	+	-
Acetic acid	+	+	+	+	+	+	-
<i>Cis</i> -aconitic acid	-	-	-	+	+	+	-
Citric acid	-	-	-	+	+	+	-
Formic acid	-	-	-	+	+	+	-
D-gluconic acid	-	-	-	+	+	+	-
α -hydroxybutyric acid	+	+	+	+	w+	+	-
β -hydroxybutyric acid	-	-	-	+	+	+	-
Itaconic acid	-	-	-	+	+	+	-
α -ketobutyric acid	+	+	+	+	+	+	-
α -ketoglutaric acid	+	+	+	+	+	+	-
α -ketovaleric acid	-	-	-	+	w+	+	-
D,L-lactic acid	+	+	+	+	+	+	-
Malonic acid	-	-	-	+	-	+	-
Propionic acid	+	+	+	+	+	+	-
D-saccharic acid	-	-	-	-	+	-	-
Sebacic acid	-	-	-	+	+	-	-
Succinic acid	+	+	+	+	+	+	-
Bromosuccinic acid	+	+	+	+	+	+	-
Succinamic acid	+	+	+	-	+	+	-
L-alaninamide	+	+	+	+	+	+	-

D-alanine	+	+	+	+	+	+	-
L-alanine	+	+	+	+	+	+	-
L-asparagine	+	+	+	+	+	+	-
L-aspartic acid	+	+	+	-	-	+	-
L-glutamic acid	+	+	+	+	+	+	-
L-leucine	-	-	-	+	-	+	-
L-proline	+	+	+	+	-	+	-
L-pyroglutamic acid	-	-	-	+	+	-	-
D-serine	-	-	+	-	-	-	-
L-serine	-	-	-	+	-	-	-
L-threonine	-	-	-	+	-	w+	-
γ-aminobutyric acid	-	-	+	-	+	-	-
2-aminoethanol	+	+	+	-	-	w+	-
2,3-butanediol	-	-	-	-	-	+	-
Glycerol	-	-	-	+	-	+	-
D-glucose-6-phosphate	-	-	-	+	-	-	-

^T = type strain. +: 100 % of strains positive; -: 100 % of strains negative; w+: 100 % of strains weakly positive.

3.2.4.3. Studies of pH, salt concentration and temperature tolerance ranges

Tolerance ranges of the AOD-associated bacteria were examined by growing them in supplemented media or at different temperatures. Colonies of clusters A, B and C were observed in the pH range 6.0 to 8.0. Strain P18 (cluster A) was observed growing at pH 9.0 after six days of incubation. All strains were able to grow in media supplemented with 3 % of salt or less, and P4 (cluster C) was also observed growing at 3.5 % salt supplemented media. Refrigeration temperatures (4 – 10 °C) were tolerated by strains belonging to clusters B and C, as well as strain P18 (cluster A) when grown in KB. All strains grew at 33 and 37 °C. Strains in cluster B and C formed colonies at 39 °C, whereas cluster A was unable to grow at this temperature. Only strains P28 and P30 (cluster C) were able to grow at 41 °C.

3.2.5. Chemotypic characterisation of the AOD-associated *Pseudomonas* by fatty acid methyl esters (FAMES) profiling

A selection of AOD-associated strains was sent for fatty acid profiling by Fera Science Ltd. and the results were compared to published FAMES profiles of the closest phylogenetic neighbours **Table 13** and **Table 14**. Summed features are sets of two or more fatty acids, which the Microbial Identification System (MIDI) did not manage to separate. The main fatty acids in clusters A and B were summed features 8 (34.5 and 39.7 %, respectively) and summed features 3 (22.2 and 17.9 %, respectively). The most abundant fatty acids in cluster C were summed features 8 (27.4 %), and C_{16:0} (24.0 %). Clusters A and B possessed 2.9 and 2.7 % of the fatty acid C_{17:0} cyclo, which had not been detected in any of their neighbours. The percentages of C_{17:0} cyclo found in cluster C (13.7 %) were considerably higher than those in the neighbours (0.4 - 4.0 %). The most abundant fatty acid in cluster C, summed feature 8 was not present in the neighbours: *P. stutzeri* and *P. xanthomarina*. The most abundant fatty acid in the closest neighbour to cluster C, *P. stutzeri* (41.3 % of C_{18:1}) was not detected at all in cluster C. All strains tested possessed the fatty acids characteristic of *Pseudomonas*, C_{10:0} 3OH and C_{12:0} 3OH (Palleroni, 2015), with the exceptions of: *P. stutzeri* and *P. xanthomarina*, which lacked C_{10:0} 3OH and presented only traces of C_{12:0} 3OH (Romanenko et al., 2005).

Traces (> 1 %) of the fatty acids C_{12:0} 2-OH, C_{10:0}, C_{14:0}, C_{17:0}, C_{18:0}, C_{17:1} ω8c and C_{19:0} cyclo ω8c were detected in cluster A. Traces of the fatty acids C_{10:0}, C_{14:0}, C_{18:0} and C_{17:0} iso were found in cluster B. And traces of C_{10:0} and C_{18:0} were detected in members of cluster C.

Table 13: Percentages of cell fatty acid methyl esters (FAMES) in representative AOD-associated strains of clusters A and B. Summed feature 3 is C_{16:1} ω6c and/or C_{16:1} ω7c and summed feature 8 is C_{18:1} ω7c and/or C_{18:1} ω6c. Data was generated in this study, except for the profiles of reference strains, which were obtained from Ramos *et al.* (2013). Values are displayed as average percentage per species investigated, with the standard deviation shown in parentheses. Cluster A displayed traces (< 1 %) of C_{12:0} 2-OH, C_{10:0}, C_{14:0}, C_{17:0}, C_{18:0}, C_{17:1} ω8c and C_{19:0} cyclo ω8c. Traces (< 1 %) of the fatty acids C_{10:0}, C_{14:0}, C_{18:0} and C_{17:0} iso were found in cluster B.

Fatty acid (%)	1	2	3	4	5	6
C _{10:0} 3-OH	3.3 (±0.2)	2.8 (±0.2)	3.7	2.4	4.8	3.9
C _{12:0} 3-OH	3.8 (±0.2)	3.1 (±0.5)	3.6	2.6	4.5	3.6
C _{12:0}	9.9 (±0.6)	9.3 (±0.5)	9.2	7.9	8.3	9.6
C _{16:0}	20.2 (±0.6)	22.0 (±0.4)	19.8	19.7	15.2	17.6
C _{17:0} cyclo	2.9 (±1.1)	2.7 (±0.4)	-	-	-	-
Summed feature 3	22.2 (±2.1)	17.9 (±0.6)	22.4	21.3	23.7	22.4
Summed feature 8	34.5 (±0.9)	39.7 (±0.3)	38.5	41.5	40.8	39.7

(1) Cluster A (average percentages amongst strains P2, P9, P18 and P23), (2) cluster B (average percentages amongst strains P27, P6, and P27), (3) *Pseudomonas flavescens* LMG 18387^T (4) *Pseudomonas argentinensis* LMG 22563^T (5) *Pseudomonas punonensis* LMT03^T (6) *Pseudomonas straminea* IAM 1598^T. - = not detected. ^T = type strain.

Table 14: Percentages of cell fatty acid methyl esters (FAMES) in representative AOD-associated strains of cluster C. Summed feature 3 is C_{16:1} ω6c and/or C_{16:1} ω7c and summed feature 8 is C_{18:1} ω7c and/or C_{18:1} ω6c. Data was generated in this study, except for the profiles of reference strains. FAMES data for *Pseudomonas stutzeri* and *Pseudomonas xanthomarina* was obtained from Romanenko *et al.* (2005). Data for *Pseudomonas azotifigens* and *Pseudomonas balearica* was collected from Anwar *et al.* (2017). Values are displayed as average percentage per species investigated, with the standard deviation shown in parentheses. Cluster C displayed traces (< 1 %) of C_{10:0} and C_{18:0}.

Fatty acid (%)	1	2	3	4	5
C _{10:0} 3-OH	2.9 (± 0.4)	-	3.4	3.4	-
C _{12:0}	8.4 (± 0.6)	6.8	10.0	9.6	7.8
C _{12:0} 3-OH	3.4 (± 0.3)	<1	2.8	3.4	<1
C _{16:0}	24.0 (± 0.8)	22.0	18.6	20.2	21.8
C _{16:1} ω9c	-	24.5	-	-	30.4
C _{17:0} cyclo	13.7 (± 4.0)	0.4	1.4	4.0	2.9
C _{18:1}	-	41.3	-	-	28.9
C _{19:0} cyclo ω8c	8.5 (± 3.0)	-	2.5	3.6	-
Summed feature 3	9.8 (± 3.9)	-	26.6	23.3	-
Summed feature 8	27.4 (± 2.3)	-	32.0	28.8	-

(1) Cluster C (average fatty acid percentages amongst strains P4, P17, P28 and P30), (2) *Pseudomonas stutzeri* CIP 103022^T (3) *Pseudomonas azotifigens* JCM 12708^T (4) *Pseudomonas balearica* DSM 6083^T (5) *Pseudomonas xanthomarina* CCUG 46543^T. - = not detected. ^T = type strain.

3.2.6. Phylogenetic study of the relationships amongst *Pseudomonas*, *Azomonas*, *Azotobacter* and *Azorhizophilus*

To examine the phylogenetic relationships of the genera *Pseudomonas*, *Azomonas*, *Azotobacter* and *Azorhizophilus*, analysis of the 16S rRNA gene and MLSA of the concatenated nucleotide sequences and translated amino acid sequences of the genes *gyrB*, *rpoB* and *rpoD* were performed. The phylogenies were inferred using genes or amino acid sequences from representatives of each of the 19 groups of *Pseudomonas* according to Gomila *et al.* (2015), and an extra species of each group (the groups are referred to in this section as Gomila's groups), as well as the *Pseudomonas* classified as outliers in the same study. In addition to these species, all available species of *Azomonas*, *Azotobacter* and *Azorhizophilus* were included in the present study. The phylogenetic inferences were performed using ML and BI methods. The nucleotide substitution model used for the 16S and the MLSA ML trees, was GTR + I + G. The best model for the 16S Bayesian tree was the transversional model with invariable sites and gamma distribution (TMV + I + G) (**Figure 20**). TIM1 + I + G was the fittest model for the Bayesian MLSA tree (**Figure 21**). LG + G + I + F was the model of amino acid substitution implemented in the MLSA of the amino acid sequences. ML trees constructed with the 16S gene and the concatenated nucleotide and translated amino acid sequences of the housekeeping genes are available in **Appendix IX**, **Appendix X** and **Appendix XI**.

A few characteristics were observed in all the trees. Both lineages stayed stable in all trees, the taxa remained in the same lineage in all analyses. Outliers occupied different positions within the trees, but generally, without jumping amongst lineages. The only exception was the outlier *P. caeni*, which appeared in the *P. aeruginosa* lineage in all trees except for the BI MLSA tree.

The number of Gomila's groups that remained paired (clustered together next to each other with or without confidence) in the phylogenetic analyses, out of a total of 19 groups was: 12 in the BI 16S tree, 13 in the ML 16S tree, 19 in the BI MLSA tree, 18 in the ML MLSA tree and 16 in the ML MLSA amino acid tree. The unpaired groups were normally disrupted by the change of position of an outlier. *Azomonas* and *Azotobacter* species did not cluster together in any of the phylogenies performed. *Azotobacter* and *Azorhizophilus* were located in the edge of the *P. aeruginosa* lineage on the 16S trees, rather than within the genus *Pseudomonas*, whereas the *Azomonas* and *Azotobacter* species disrupted the genus *Pseudomonas* in all MLSA phylogenetic trees performed. All *Azomonas*, *Azotobacter* and

Azorhizophilus species were in the *P. aeruginosa* lineage's side of the line, except for *Azomonas insignis*, which was positioned in the *P. fluorescens* lineage. MLSA data for *Azomonas insignis* was not available. *Azorhizophilus paspali*, clustered with confidence with *Azotobacter vinelandii* in the BI 16S tree and without confidence in the ML 16S tree, however MLSA data was not available for *Azorhizophilus paspali*.

The topologies of the 16S trees performed following the ML and the BI method were mostly congruent. The topologies of all MLSA trees (ML, BI, and ML amino acid) were also highly congruent with each other. MLSA data was unavailable for the species *Azomonas insignis*, *Azotobacter armeniacus*, *Azotobacter nigricans*, *Azotobacter salinestris* and *Azorhizophilus paspali* although they were included to the 16S phylogeny.

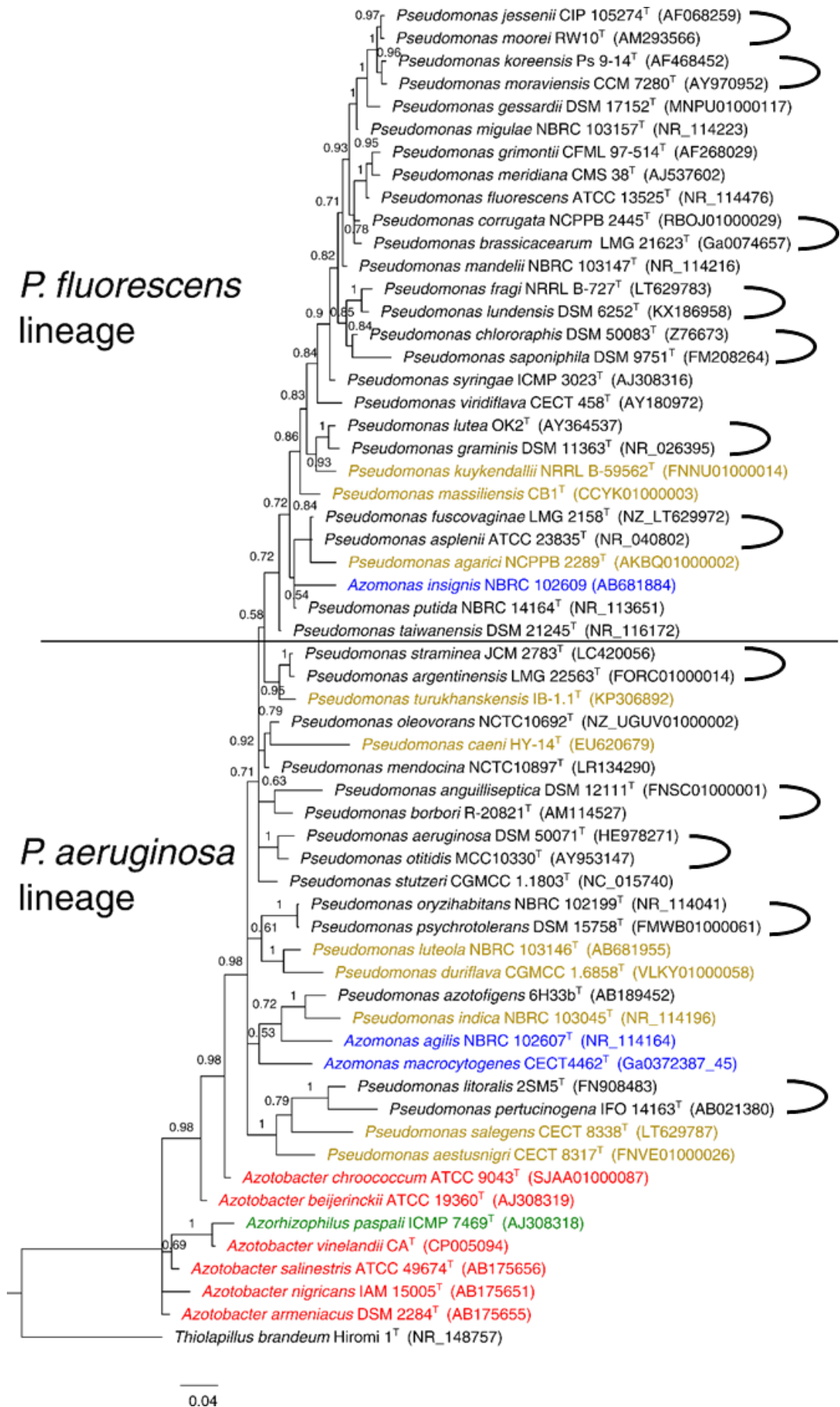


Figure 20: Bayesian 16S rRNA phylogenetic tree of selected *Pseudomonas* species, and all available members of *Azotobacter*, *Azomonas* and *Azorhizophilus*. The species included in this study were the representatives from each of the 19 *Pseudomonas* groups described in Gomila *et al.* (2015), an extra species per group, 10 *Pseudomonas* outliers of the genus (in brown), 6 *Azotobacter* species (in red), 3 *Azomonas* species (in blue), the *Azorhizophilus* species (in green), and the outgroup, *Thiolapillus brandeum*. Phylogenetic relationships amongst the 59 strains were inferred from a dataset of partial nucleotide sequences 1328 bp long using the program Mr Bayes. Posterior probabilities lower than 0.95 are considered low support. Values lower than 0.5 were removed from the branches. The scale bar indicates the nucleotide substitutions per site. Species names and strain numbers are shown next to the branches. \supset = pairs formed by the *Pseudomonas* species representative of each of Gomila's groups, and the extra species from the same group (Gomila *et al.*, 2015). $^{\text{T}}$ = type strain.

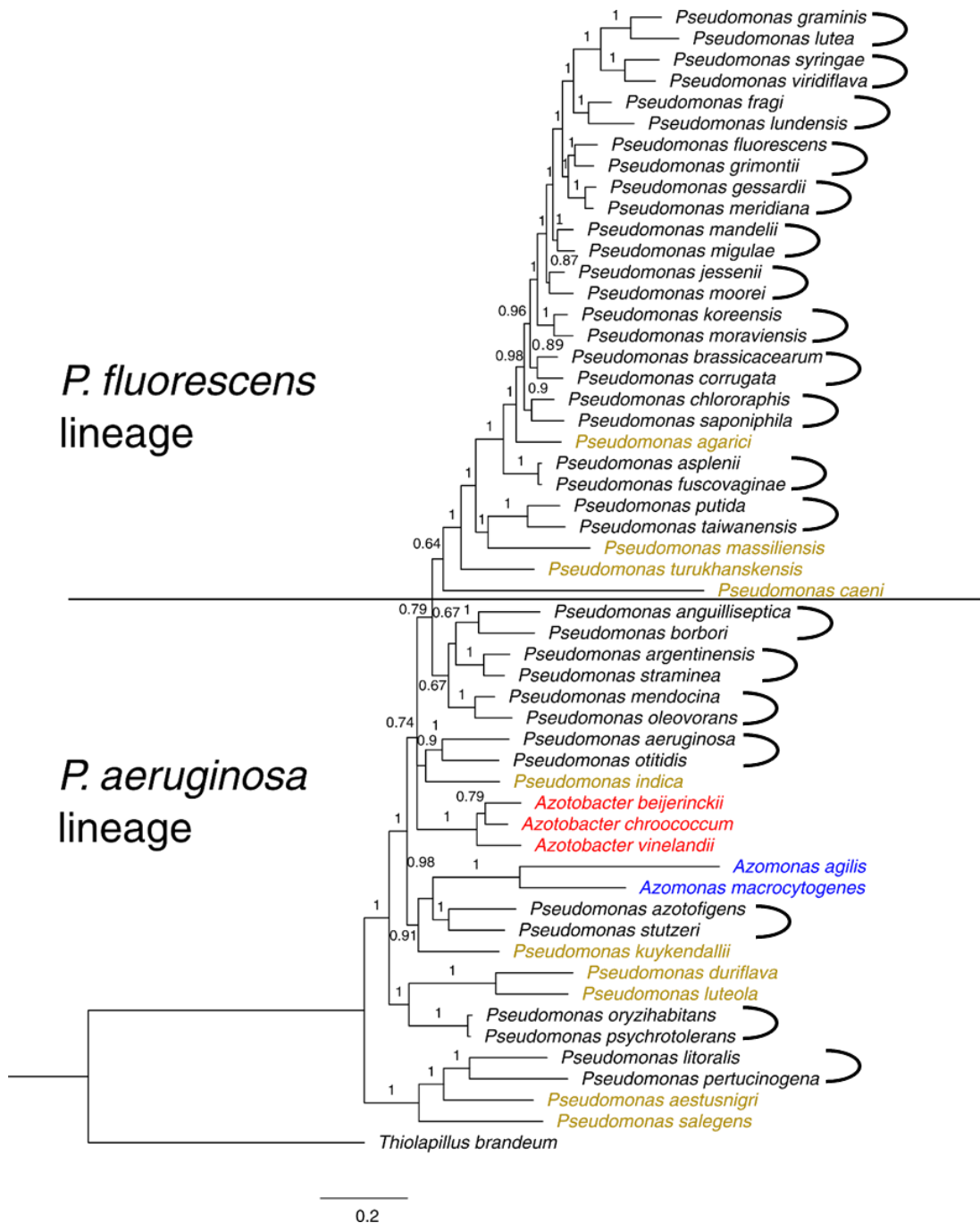


Figure 21: Bayesian MLSA phylogenetic tree of selected *Pseudomonas* species, and all available members of *Azotobacter*, *Azomonas* and *Azorhizophilus*. The species included in this study were the representatives from each of the 19 *Pseudomonas* groups described in Gomila *et al.* (2015), an extra species per group, the 10 *Pseudomonas* outliers of the genus (in brown), 3 *Azotobacter* species (in red), 2 *Azomonas* species (in blue), and the outgroup, *Thiopillius brandeum*. Phylogenetic relationships amongst the 54 strains were inferred from a dataset of partial concatenated *gyrB* – 807 bp, *rpoB* – 915 bp and *rpoD* – 759 bp genes, using the program Mr Bayes. Posterior probabilities lower than 0.95 are considered low

support. Values lower than 0.5 were removed from the branches. The scale bar indicates the nucleotide substitutions per site. Species names are shown next to the branches, strains and accession numbers are available in **Appendix XII**. \supset = pairs formed by the *Pseudomonas* species representative of each of Gomila's groups, and the extra species from the same group (Gomila et al., 2015). ^T = type strain.

3.3. Discussion

The biotic component of AOD is a combination of bacteria. Samples extracted from affected oaks mostly contain the species: *Gibbsiella quercinecans*, *Brenneria goodwinii* and *Rahnella victoriana* (Brady et al., 2010, 2014c; Denman et al., 2018, 2012), but *Pseudomonas* are also present (Denman et al., 2016b). It was crucial to find the taxonomic position of the unclassified *Pseudomonas*, before establishing their potential role in the disease, and, if shown to be pathogenic, to add them as targets to the diagnostic methods.

Thirty-five strains belonging to the family *Pseudomonadaceae* isolated from AOD symptomatic oaks were collected from AOD-affected sites in the South of England. The collection sites were Great Monk Wood, Bisham Woods, Send and Stratfield Brake and Kew Gardens. The strains were suspected to be novel *Pseudomonas* species and therefore they were subjected to a polyphasic study of bacterial classification to elucidate their taxonomic position. The polyphasic approach of bacterial classification consists in the phenotypic, genotypic and chemotypic characterisation of the bacterial strains in order to collect data that can be compared to the data obtained from the closest phylogenetic neighbours. The purpose was to detail the features of the strain that categorise it as member of a particular genus, and the features that make the novel strain unique, and distinguish it from its closest neighbours (Vandamme et al., 1996).

Phylogenetic analysis of the 16S rRNA of the 35 strains placed them into the genus *Pseudomonas*. The 16S analysis segregated the strains into three different clusters (A, B and C), two of them belonging to the *P. fluorescens* lineage (clusters A and B) and the third, within the *P. aeruginosa* lineage (cluster C). MLSA studies of the protein-encoding genes *gyrB*, *rpoB* and *rpoD*, and the corresponding translated amino acid sequences, placed clusters A and B in the *P. straminea* group and cluster C in the *P. stutzeri* group. Intra-cluster diversity was assessed by DNA fingerprinting. Several band patterns were observed for each of the clusters, indicating that each cluster was not formed exclusively by clones (clones were identified as strains displaying identical gel band patterns). However, generally, the strains collected in the same site were clones. The intra-cluster diversity is important because it is not convenient to describe a novel species from a single strain, or several strains that are clones amongst each other. Ideally, a novel species must be described from several strains that differ in features like the DNA fingerprints, the collection site or phenotypic features (Tindall et al., 2010).

Clusters A, B and C showed values of genome similarity (ANIb and *isDDH*) above the species threshold, suggesting that each cluster represented a distinct *Pseudomonas* species. The whole genome comparisons showed also that values of genome similarity well below the species threshold, were obtained when comparing the AOD-associated strains and the closest neighbours, suggesting that the AOD-associated strains do not belong to any of the closest species. The G + C DNA content of the AOD-associated strains were amongst the typical range for *Pseudomonas* (58 to 69 mol %), although that is not that discriminative, because the range is very wide (Palleroni, 2015).

The phenotypic and chemotypic characterisation of the strains supported the results obtained by the genotypic characterisation. The metabolic profiles obtained by the AOD-associated strains were different to those obtained by the closest neighbours, except for those obtained by cluster A and *P. flavescens*, *P. punonensis* and *P. straminea* in the API 20NE test. The strains in cluster C were generally less reactive in the phenotypic tests than the rest, possibly because of their inability to grow in acidic conditions, which is a characteristic trait of the genus, and was later confirmed in the pH tolerance tests. The AOD-associated bacteria are not halophilic, they are mesophilic and neutrophilic, although they can tolerate alkaline conditions (pH 8.0 - 9.0). The percentages of cell fatty acid methyl esters (FAMES) of the AOD-associated strains were typical for *Pseudomonas*, including in their composition the hydroxylated fatty acids C_{10:0} 3OH and C_{12:0} 3OH (Palleroni, 2015).

After the data collection and the comparative studies required for the polyphasic approach were performed, it was found that the AOD-associated *Pseudomonas* strains were distinctive enough from their closest neighbours. Therefore, on the basis of the polyphasic approach of bacterial classification, three novel species of *Pseudomonas* corresponding to clusters A, B and C were formally described. The proposed species name of cluster A was *Pseudomonas daroniae* sp. nov., cluster B was named *Pseudomonas dryadis* sp. nov., and cluster C was named *Pseudomonas kirkliae* sp. nov. (Bueno-Gonzalez et al., 2019, 2020). The type strains (T) chosen for each of the species, *P. daroniae* sp. nov., *P. dryadis* sp. nov., and *P. kirkliae* sp. nov. were the representative strains from each of the clusters: P2^T, P27^T and P4^T, respectively.

The etymologies of the specific epithets are as it follows: *Pseudomonas daroniae* sp. nov., da.ron.i'ae. N.L. fem. adj. daroniae from Daron, the Celtic goddess of oak; *Pseudomonas dryadis* sp. nov., dry.a'dis. L. gen. n. dryadis of a Dryad, of an oak tree nymph; and *Pseudomonas kirkliae* sp. nov., kirk.i'ae. N.L. fem. n. kirkliae, of Kirk, named after Susan Kirk

MBE for her technical contribution towards understanding the pathology of tree diseases in the United Kingdom between 1976 and 2015.

While exploring the taxonomic position of *Pseudomonas kirkieae* sp. nov., it was observed that species belonging to different genera were amongst its closest neighbours, those were *Azotobacter*, *Azomonas* and *Azorhizophilus*. To further investigate this, a simplified overview of the phylogenetic relationships amongst selected species within the genera included in the so called *Azotobacter* group (*Pseudomonas*, *Azotobacter*, *Azomonas* and *Azorhizophilus*) was performed. The phylogenetic study showed that *Azorhizophilus paspali* (Thompson and Skerman, 1979), whose basonym is *Azotobacter paspali* (Döbereiner, 1966), clustered with *Azotobacter vinelandii* in the 16S trees, suggesting that it belongs to the genus that it was first described as, although confirmation by MLSA was not performed due to the lack of genomic data. The lineages of *Pseudomonas* remained stable in all the phylogenetic trees performed, the BI MLSA tree being the most congruent with Gomila's classification (Gomila et al., 2015). Species of *Azomonas* and *Azotobacter* did not cluster together in any of the phylogenetic studies performed. Members of *Azomonas* and *Azotobacter* form well-supported clades on separate lineages suggesting that these two genera are not synonyms. The clades formed by *Azomonas* and *Azotobacter* species disrupt the genus *Pseudomonas*, appearing well-embedded on the genus in all MLSA analyses. These results suggested either that *Azomonas*, *Azotobacter* and *Pseudomonas* are the same genus, or that *Azotobacter* and *Azomonas* are separate genera, but *Pseudomonas* needs to be split due to the polyphyly of the genus. In the first case scenario, if *Azomonas* and *Azotobacter* would be added to the genus *Pseudomonas*, an important modification of the description of the genus would be mandatory to accommodate the characteristics of the new species. In the second case scenario, if the procedure would be to split *Pseudomonas*, the true *Pseudomonas* would be the ones in the *P. aeruginosa* lineage, because the type species of the genus is contained in it, although this lineage is the most heterogeneous. The first case scenario would support previous studies that establish a probable synonymy between *Azotobacter* and *Pseudomonas* (Özen and Ussery, 2012; Rediers, Vanderleyden and De Mot, 2004; Young and Park, 2007). However, according to the data obtained in this study and according to the predictions of several recent studies (Bueno-Gonzalez et al., 2020; Lalucat et al., 2020; Peix, Ramírez-Bahena and Velázquez, 2018), I do not believe the genus *Pseudomonas* can accommodate species from these genera. The description of the genus is already very heterogeneous and thus, I prefer to support the second case scenario in which *Pseudomonas* is divided into several novel genera. The effect of splitting *Pseudomonas* could be huge

because many species including those described in this study (*P. daroniae* sp. nov. and *P. dryadis* sp. nov., which belong to the *P. fluorescens* lineage, and perhaps even *P. kirkiae* sp. nov., which falls into the *P. aeruginosa* lineage, but behaves like an outlier) would move from *Pseudomonas* to a novel genus. Species contained in the *P. fluorescens* lineage and the *P. pertucinogena* lineage would have to be relocated to novel genera. The *P. fluorescens* lineage contains significant species such as the group of devastating plant pathogens represented by *P. syringae* or species involved in plant protection or bioremediation such as *P. fluorescens* and *P. putida*. A considerable research effort will be needed tackle this issue and to collect data for a polyphasic classification to help taxonomists to decide the most appropriate classification strategy for the bacteria in the *Azotobacter* group.

Taxonomists all over the world are constantly describing novel species of bacteria basing their research in the current concept of bacterial species, ourselves included. However, this chapter should not be finished without acknowledging that the concept of bacterial species is under debate (Caro-Quintero and Konstantinidis, 2012; Fraser et al., 2009). The evolution of bacteria cannot be compared to the evolution of any other organism whose genetic material is made up of the genetic material of the parent generation (vertical inheritance). Bacteria are able to obtain genetic material from completely different species through a process called horizontal gene transfer (HGT) (Bosi et al., 2017; Koonin and Wolf, 2008; Ros and Hurst, 2009). Bacterial genomes can contain a considerable proportion of horizontally transferred genes. The genes acquired by HGT do not have a relation of ancestry with the rest of the genes of a bacterium and they contribute to the huge genetic variation observed in bacteria, although there are authors that do not believe that HGT has a great impact in bacterial evolution (Kurland, Canback and Berg, 2003). HGT could be the reason why it is difficult to find the definitive phylogenetic position of some taxa.

A relevant example for this study is the case of *Azotobacter vinelandii*. The closest related genus to *Azotobacter* is *Pseudomonas*, however these two genera are quite different in terms of lifestyle. *Azotobacter* are able to fix nitrogen and to create dormant forms (cysts) that can last up to 10 years (Özen and Ussery, 2012; Setubal et al., 2009), whereas no dormant forms have ever been described in *Pseudomonas* and only *P. stutzeri* (of more than 220 species in the genus) is able to fix nitrogen. It is known that the genes encoding for the nitrogenase enzyme (responsible of the fixation of atmospheric nitrogen into ammonia) are present in the genome of *P. stutzeri* due to HGT (Yan et al., 2008; Young and Park, 2007). 16S rRNA and MLSA phylogenies performed in this study and others suggest that *Azotobacter*

species could belong to the genus *Pseudomonas* (Özen and Ussery, 2012; Rediers, Vanderleyden and De Mot, 2004; Young and Park, 2007), however whole genome comparisons place them in separate genera. There is evidence that the genome of *A. vinelandii* contains essential genes with different phylogenetic origins, 50 to 70% of the genome is similar to *Pseudomonas* but the rest could come from HGT. A study that examined the part of the genome of *A. vinelandii* that was not similar to *Pseudomonas*, found that it was not even similar to *Gammaproteobacteria* (the class that contains both *Azotobacter* and *Pseudomonas*), suggesting that this part of the genome (which encodes for essential biological functions) was acquired by HGT (González-Casanova et al., 2014). At least a third of the genome of *A. vinelandii* does not have a relation of ancestry with closely related bacteria and this is why it is believed that *A. vinelandii* is a chimera between the common ancestor of *Pseudomonas* and *Azotobacter* and many genes from various origins. Possibly, the uncertainty of taxonomists about the true “phylogenetic position” of *Azotobacter* species might be due to the fact that about half of its genome is not comparable with the tools that we currently use for estimation of evolutionary relationships. Other examples of polyphyletic origin of essential genes have been reported in *Fusobacterium nucleatum* (Mira et al., 2004) and the Themotogales (Zhaxybayeva et al., 2009).

Like the rest of the scientific fields, taxonomy resembles a puzzle from which we lack pieces. The evolving technologies for species identification and the fact that numerous novel bacterial species are described every year, help us to find the missing pieces and be closer to a more precise bacterial evolution history. The studies performed on the classification of the novel *Pseudomonas* associated with AOD and the findings that suggest that a taxonomical revision is needed within the *Azotobacter* group, shed more light into our knowledge about AOD lesion microbiome and into the “*Azotobacter* group” issue.

CHAPTER 4. Investigation of the
potential pathogenicity traits of the
AOD-associated *Pseudomonas*

4.1. Introduction

To protect themselves, plants possess several defences that can be structural such as waxy epidermal cuticles and cell walls as well as chemical such as toxins, enzymes and deliberate cell suicide. Plants trigger chemical defence responses that lead to specific defence signalling pathways (Garcia-Brugger et al., 2006). The activation of these defence pathways, commonly precede the secretion of substances that lead to hypersensitive response (HR) if the host is resistant, or disease if the host is susceptible. HR is the programmed death of the cells around the point of infection, this defensive mechanism is one of the most important ways to stop the progression of pathogens in plants (Gilchrist, 1998)

The compounds that are perceived by the plant and trigger chemical defence responses are known as elicitors (Nürnberg, 1999). Elicitors can be classified as general and race specific (Montesano, Brader and Palva, 2003). General elicitors are those capable of inducing a defence response in host and non-host plants, whereas race specific elicitors, also called effectors are produced by pathogens bearing avirulence (*avr*) genes, and they only trigger a defence response if the host contains the corresponding resistance gene (*R*) (Hammond-Kosack and Jones, 1996). This cultivar-specific resistance to phytopathogens is explained by the gene-for-gene theory, firstly described in *Melampsora lini*-flax interaction (Flor, 1942). The gene-for-gene theory describes a co-evolutionary relationship between the matching gene pairs for *R* in the host and *avr* in the pathogen. The mechanisms that phytopathogenic bacteria use to deliver effector proteins in the plant cells are called type III secretion systems (T3SS). T3SS are essential for HR induction in resistant hosts and disease production in compatible hosts (Alfano and Collmer, 1997; Lindsay, Lamb and Dixon, 1993).

Pseudomonas is one of main genera of phytopathogenic Gram-negative bacteria. A widely studied example for the gene-for-gene theory is the interaction between dwarf beans (*Phaseolus vulgaris*) and the plant pathogen *Pseudomonas syringae* pv. *phaseolicola* (*Pph*). Different bean cultivars possess specific *R* genes, matching the *avr* genes belonging to specific races of *Pph*. If a bean cultivar containing an *R* gene is inoculated with a race of *Pph* containing the corresponding *avr* gene, the interaction of the products of both genes activates signalling cascades that lead to resistance in the plant and HR developing. If there is no matching *avr* gene in the *Pph* race, the plant is susceptible to the halo-blight disease (Taylor et al., 1996). *Pph* race 4, strain 1302A, contains an avirulence gene known as *hopAR1*, therefore it triggers HR in bean cultivars with the specific *R* gene, such as Tendergreen

(Pitman et al., 2005), whereas *Pph* 1448A (race 6) does not include any known *avr* genes, causing disease on all bean cultivars (Mansfield et al., 1994).

Bacteria in the natural environment are normally sessile, attached to surfaces (soil, plants, etc.) and more rarely found in a planktonic state (Costerton, 1995; Scofield and Wu, 2019). The capacity of the microbe to form aggregates and attach to surfaces to form biofilms is key to phenomena such as the colonisation of roots and other plant structures and the establishment of a pathogen in its host. The ability of forming biofilms depends on factors such as the nature of the surface, which can condition the type of microbe that forms the biofilm (Hancock, Witsø and Klemm, 2011). The first step to biofilm formation is the attachment of the bacterial cells to the surface (followed by micro-colony formation and biofilm build up) (Klemm, Hancock and Schembri, 2010; Vasudevan, 2014).

Bacteria are able to enter, disseminate and persist in a host by means of extracellular molecules called virulence factors (VF). VFs are important for pathogenesis but they are also present in non-pathogenic bacterial strains. VFs in *Pseudomonas* are those related to adherence, antiphagocytosis, biosurfactant production, iron uptake, pigment production, protease production, quorum sensing, secretion systems and toxin production. Flagella, lipopolysaccharide (LPS), and type IV pili are the major VFs related to adherence in *Pseudomonas*. Flagella are involved in swimming motility and biofilm formation (Feldman et al., 1998; O'Toole and Kolter, 1998). The outer membrane of *Pseudomonas* (and the majority of the rest of gram-negative bacteria) is mostly formed by LPS (Henderson et al., 2016). LPS is an important VF that contributes to pathogenesis by being an endotoxin, facilitating biofilm formation, and conferring antibiotic resistance (Huszczynski, Lam and Khursigara, 2020). Type IV pili are a VF involved in twitching motility, which is a type of bacterial motility related to adherence, colonisation of host tissues and biofilm formation (Mattick, 2002; O'Toole and Kolter, 1998). Alginate production is the most common VF related to antiphagocytosis. Alginate is a mucoid exopolysaccharide that helps the persistence of bacteria creating a slime layer that makes their elimination difficult (Orgad et al., 2011). Rhamnolipid production is a VF related to biosurfactant activity. Biosurfactants are compounds produced by microbes, which lower the interfacial tension between a gas and a liquid, between two liquids and between a liquid and a solid. Rhamnolipids are glycolipidic biosurfactants that have diverse functions and roles (Abdel-Mawgoud, Lépine and Déziel, 2010). As VFs, rhamnolipids have been associated to the modulation of the immune response of the host, they present antimicrobial properties, and they help in swarming motility and

biofilm formation (Sierra, 1960; Kharazmi *et al.*, 1989; Abalos *et al.*, 2001; Caiazza, Shanks and O'Toole, 2005; Pamp and Tolker-Nielsen, 2007). The major VFs for iron uptake in *Pseudomonas* are siderophores: pyochelin and pyoverdine (Brandel *et al.*, 2012; Meyer, 2000). Siderophores are low-molecular weight molecules excreted by the cell to chelate iron from the extracellular medium (Boukhalfa and Crumbliss, 2002; Braun and Killmann, 1999; Hider and Kong, 2010). Pyoverdine is involved in the regulation of the production of extracellular VFs and it is also involved in the establishment of biofilms (Banin, Vasil and Greenberg, 2005; Cornelis, 2010; Glick *et al.*, 2010; Lamont *et al.*, 2002; Meyer *et al.*, 2008; Patriquin *et al.*, 2008; Rédly and Poole, 2003; Visca, Imperi and Lamont, 2007). Pyochelin has lower affinity for iron than pyoverdine, but it has also been associated with the modulation of host immune response (Lyczak, Cannon and Pier, 2002). One of the pigments secreted by *Pseudomonas*, pyocyanin, has been reported as critical for establishment of infection as it is a toxin that can kill by generating reactive oxygen species (Lau *et al.*, 2004; Ran, Hassett and Lau, 2003). Important VFs in *Pseudomonas* are also proteases such as alkaline protease, elastase A and elastase B. Proteases damage the tissues of the host and affect its defence mechanisms (Otdak and Trafny, 2005).

A major VF in *Pseudomonas* is the regulation through quorum sensing system. Bacterial cells maintain communication mechanisms in order to carry out joint actions that favour the development of the entire population. This mechanism is quorum sensing (QS) and it regulates the expression of genes according to cell density. The genes regulated by QS in *P. aeruginosa* are those linked to biofilm, swarming motility, exopolysaccharide production, virulence, and cell aggregation (Sauer *et al.*, 2002; Smith and Iglewski, 2003). In *Pseudomonas* there are VFs associated with secretion systems production, and toxins production. The major secretion systems in *Pseudomonas* are HSI-I, the already mentioned T3SS, and the xcp proteins, which are part of the type II secretion systems (Chapon-Hervé *et al.*, 1997; Mougous *et al.*, 2006; Pena *et al.*, 2019; Roy-Burman *et al.*, 2001).

The polymicrobial character of Acute Oak Decline (AOD) challenges Koch's postulates, which are four criteria enunciated by the physician Robert Hermann Koch in 1884. Koch's postulates relate one disease to one specific microbe, and this is not the case in AOD because it is caused by a consortia of microbes. Koch's postulates were enunciated at the beginning of the microbiology "era" and they have been modified and updated to accommodate plant polymicrobial diseases such as AOD (Denman *et al.*, 2018).

Plants can host a large number of species of bacteria in their surface (epiphytes), or in their interior (endophytes). All of the bacterial species have roles and they interact between each other and with their host. The nature of the relationships amongst the host and the bacteria can be beneficial, passive or detrimental (Hayat et al., 2010; Kube et al., 2010; Toth et al., 2003). In the field of phytopathology there are numerous examples of diseases caused by the collaboration of a group of bacteria, such as the bacterial dynamics in olive knot disease. In olive knot disease, harmless endophytes of the olive tree were shown to collaborate indirectly with the pathogen via quorum sensing signal sharing (*Pseudomonas savastanoi* pv. *savastanoi*), resulting in a better establishment and development of the disease (Buonaurio et al., 2015; da Silva et al., 2014).

Like olive knot disease, AOD is a complex poly-species disease produced by the collaboration of a group of bacteria. Denman *et al.* analysed the complete genomes of *Gibbsiella quercinecans* (Gq), *Brenneria goodwinii* (Bg), and *Rahnella victoriana* (Rvi), and did cultivation-based bacterial identifications as well as metagenomic, and metatranscriptomic analyses of the microbiome of healthy and diseased oaks. In addition, they performed bacterial inoculations on logs, some of them complemented with eggs of *Agrillus biguttatus* (Denman et al., 2018). As a result of this complete study, Bg and Gq were positioned as the key pathogens in AOD, but there were a few species like *Lonsdalea britannica* (Lb) and species of *Rahnella* that are also common in the lesion, and whose role in the disease is under study (Broberg et al., 2018; Denman et al., 2018). A later publication that compared the whole genomes of several members of the AOD pathobiome to the genomes of well-known plant pathogenic bacteria and non-pathogenic symbionts, found that Bg was the key pathogen in AOD, with Gq contributing to the necrosis (Doonan et al., 2019). Based on its genome, Lb showed the potential to become as virulent as Bg (Doonan et al., 2019). Regarding *Pseudomonadaceae*, members of this family have been consistently isolated from AOD affected trees (Denman et al., 2016b, 2018, 2014; Sapp et al., 2016). Metagenome analysis of the oak microbiome revealed that *Pseudomonas* were found in either AOD-affected or healthy trees (Denman et al., 2018). However, *Pseudomonas* is a large genus that contains species with very different ecological sources (i.e. soil, water, plants, animals) and, certain “*Pseudomonas fulva*-like” species were only found in AOD-affected trees (Denman et al., 2018). These “*P. fulva*-like” isolates could be associated with AOD and this is why they became the subject of further study. In **Chapter 3**, these “*P. fulva*-like” *Pseudomonads* were formally classified into three novel species: *Pseudomonas daroniae* sp. nov. (Pda), *Pseudomonas dryadis* sp. nov. (Pdr), and *Pseudomonas kirkieae* sp. nov. (Pki) (Bueno-Gonzalez

et al., 2019, 2020). After the formal classification of the AOD-associated *Pseudomonas*, the aim of the project and the focus of this chapter was to look for potential pathogenicity traits.

4.2. Results

4.2.1. Virulence factors in AOD-associated *Pseudomonas*

Whole genomes of AOD-associated *Pseudomonas* (Pda P2^T, Pdr P27^T, and Pki P4^T) were screened for VFs using the VFAnalyzer online platform. VFAnalyzer searches for hierarchical orthologous groups in the query genome and pre-analysed reference genomes from curated datasets of VFs. From the results of that search, it performs sequence similarity analyses to identify the VFs present in the query genome.

The VF profiles obtained were compared with those of seven *Pseudomonas* species (a total of 16 different strains and pathovars), available in the VFAnalyzer database (**Appendix XIII**). To evaluate if the VF profiles obtained from the AOD-associated *Pseudomonas* were particularly similar to the VF profiles of *Pseudomonas* species available in the VFAnalyzer database, an agglomerative hierarchical clustering (AHC) of the data was performed. According to the dendrogram obtained, there were four clusters within the similarity threshold selected automatically by XLSTAT (**Figure 22**). Cluster 1 contained the AOD-associated *Pseudomonas*. Cluster 2 contained the four different strains of *P. aeruginosa*. Cluster 3 contained *P. entomophila*, the three strains of *P. fluorescens*, *P. mendocina*, the three strains of *P. putida* and *P. stutzeri*. Cluster 4 contained the three strains of *P. syringae*. The AOD-associated *Pseudomonas* formed their own cluster and this cluster did not group close to any other species.

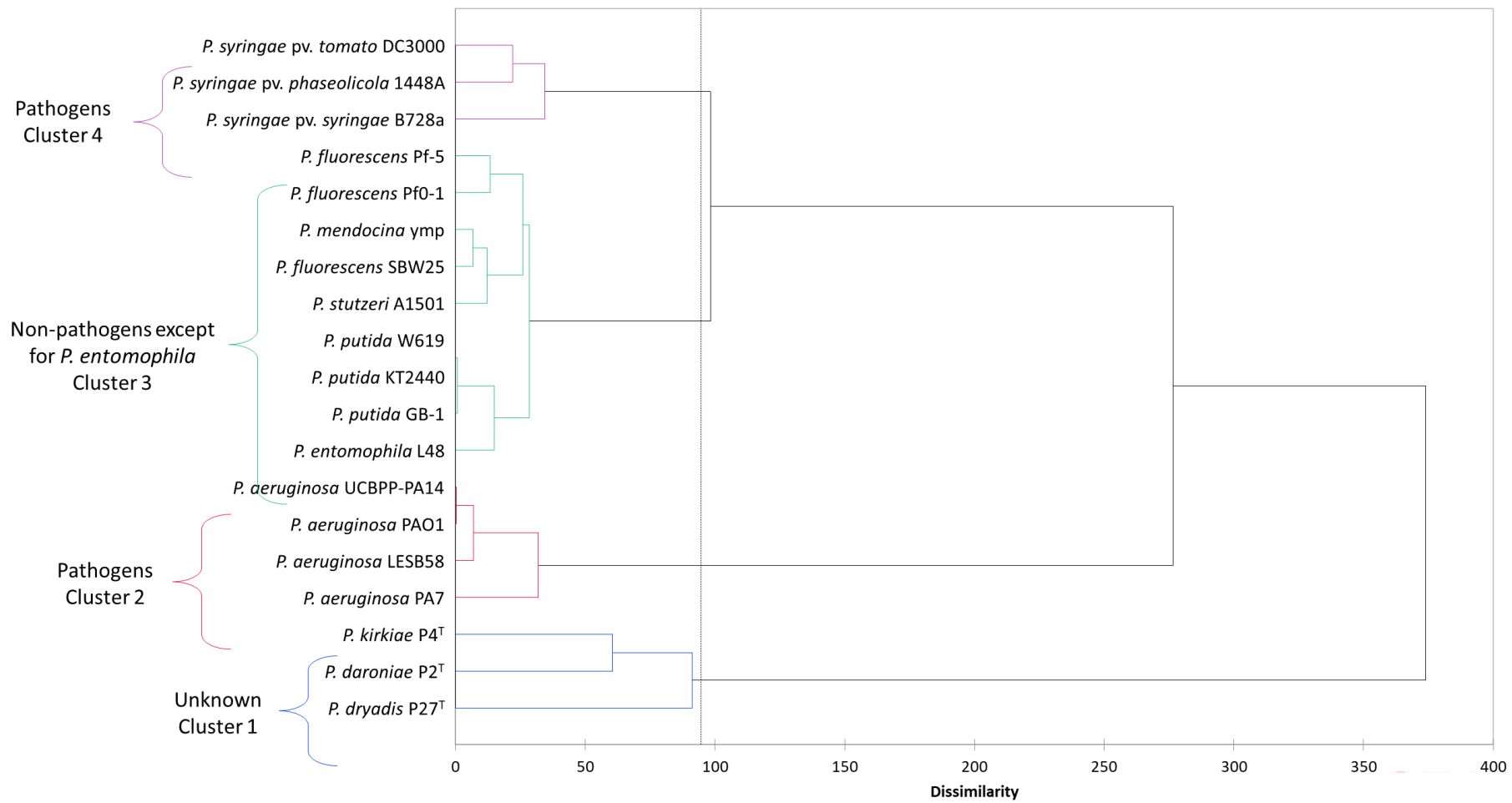


Figure 22: Agglomerative hierarchical clustering (AHC) of the profiles of virulence factors (VFs) obtained from the genomes of AOD-associated *Pseudomonas* and other *Pseudomonas* species. The AOD-associated *Pseudomonas* screened for VFs were *Pseudomonas daroniae* sp. nov. P2^T, *Pseudomonas dryadis* sp. nov. P27^T and *Pseudomonas kirkiiae* sp. nov. P4^T. The *Pseudomonas* species used for comparison were the strains LESB58, PA7, PAO1, and UCBPP-PA14 of *Pseudomonas aeruginosa*; *Pseudomonas entomophila* L48; strains Pf0-1, Pf-5, and SBW25 of *Pseudomonas fluorescens*; *Pseudomonas mendocina* ymp; strains GB-1, KT2440, and W619 of *Pseudomonas putida*; *Pseudomonas stutzeri* A1501; *Pseudomonas syringae* pv. *phaseolicola* 1448A, *Pseudomonas syringae* pv. *syringae* B728a and *Pseudomonas syringae* pv. *tomato* DC3000. VFs profiles available in **Appendix XIII**. ^T = type strain.

The VF profiles obtained from the AOD-associated *Pseudomonas* were compared with those in the non-plant pathogen *Pseudomonas fluorescens* SBW25, and the phytopathogen *Pph* 1448A (**Table 15**). All the species compared had genes encoding for type IV pili biosynthesis, type IV pili twitching motility related proteins, flagella, alginate biosynthesis and regulation, acyl homoserine lactone synthase, GacS/GacA two-component system, and Hcp secretion island-1 encoded type VI secretion system (H-T6SS). From the 16 related genes encoding for the pigment pyoverdine, only one was found in Pda (P2^T is a non-fluorescent strain), whereas 14 and 17 of the pyoverdine genes were present in the genome of Pdr and Pki, respectively (fluorescent strains). The genome of the pathogen (*Pph* 1448A) encoded for several virulence factors absent in the other four species, such as 10 genes related to the low affinity siderophore, pyochelin, and 27 genes related to T3SS typical for *P. syringae*. The non-plant pathogen genome contained genes for VFs such as rhamnolipid biosynthesis, involved in biofilm formation. VFs present only in Pda we not found, however, eight genes for VFs related to immune evasion (capsule formation) were found in Pdr; and a single gene for enterobactin siderophore was found in the Pki genome.

Table 15: Presence/absence chart of phytopathogenic virulence factors in the genomes of AOD-associated *Pseudomonas*: *P. daroniae* sp. nov., *P. dryadis* sp. nov. and *P. kirkiae* sp. nov., the non-plant pathogen *Pseudomonas fluorescens* SBW25, and the phytopathogen *Pseudomonas syringae* pv. *phaseolicola* 1448A. Data obtained from the VFAnalyzer in the Virulence Factors of Pathogenic Bacteria database (Liu et al., 2019).

Species, strain, (accession number)		<i>Pseudomonas daroniae</i> sp. nov. P2 ^T (QJUH00000000)	<i>P. dryadis</i> sp. nov. P27 ^T (QJUN00000000)	<i>P. kirkiae</i> sp. nov. P4 ^T (QJUN00000000)	<i>P. fluorescens</i> SBW25 (NC_012660)	<i>P. syringae</i> pv. <i>phaseolicola</i> 1448A (NC_005773)
Virulence factors	*Related genes					
Adherence						
Type IV pili biosynthesis	24	19	17	11	12	18
Type IV pili twitching motility related proteins	10	8	8	2	8	6
Lipopolysaccharide O-antigen	1**	2	6	0	0	0
Flagella	46	45	46	44	46	46
Flp type IV pili	4	0	4	4	0	0
Mannose-sensitive hemagglutinin (Msh) pilus, type IV pili	2	0	0	2	0	0
Polar flagella	1	1	1	1	0	0
Antiphagocytosis						
Alginate biosynthesis	13	3	3	4	13	13
Alginate regulation	12	10	10	8	9	10
Capsular polysaccharide	1	1	1	1	0	0
Capsule	5	5	0	5	0	0
Biosurfactant						

Rhamnolipid biosynthesis	3	0	0	0	1	0
Iron uptake						
Pyoverdine	16	1	14	17	0	0
Pyoverdine receptors	1	9	5	15	0	1
Pyochelin	10	0	0	0	0	10
Pyochelin receptor	1	0	0	1	14	12
Achromobactin biosynthesis and transport	8	9	9	0	8	8
Yersiniabactin	9	0	0	3	0	2
Enterobactin transport	1	1	1	0	0	0
Ferrous iron transport	1	1	1	1	0	0
Heme utilization	1	1	1	1	0	0
Iron/manganese transport	3	3	3	3	0	0
Iron acquisition						
Enterobactin siderophore	1	0	0	1	0	0
Protease						
Alkaline protease	1	0	0	0	1	0
Quorum sensing						
N-(3-oxo-dodecanoyl)-L-homoserine lactone QS system	2	0	0	0	1	0
N-(3-oxo-hexanoyl)-L-homoserine lactone QS system	2	0	0	0	0	2
Acylhomoserine lactone synthase	1	1	1	1	1	1
Regulation						
GacS/GacA two-component system	2	2	2	2	2	2
Secretion system						

Type III secretion system (T3SS)	1	1	1	0	0	0
<i>Pseudomonas aeruginosa</i> T3SS	36	2	2	0	0	0
<i>Pseudomonas syringae</i> T3SS	32	0	0	0	0	27
Harpins, pilus-associated proteins and other candidate T3SS helpers	6	0	0	0	0	4
<i>Pseudomonas syringae</i> T3SS effectors	81	2	2	2	0	30/3***
Hcp secretion island-1 encoded type VI secretion system (H-T6SS)	21	21	21	1	20	6
EPS type II secretion system	2	0	2	0	0	0
Type IV secretion system effectors	1	1	1	1	0	0
Toxin						
Phytotoxin coronatine	20	1	2	1	0	0
Phytotoxin syringopeptin	3	0	0	0	0	3
Exolysin	2	0	0	0	0	2
Alpha-hemolysin	1	0	1	1	0	0
Amino acid and purine metabolism						
Purine synthesis	1	1	1	1	0	0
Efflux pump						
AcrAB	1	1	1	1	0	0
Endotoxin						
Lipooligosaccharide	1	1	1	1	0	0
Stress adaptation						
Catalase	1	0	1	0	0	0
Catalase-peroxidase	1	1	1	1	0	0
Superoxide dismutase SodCI	1	1	1	1	0	0

Immune evasion						
Capsule	8	0	8	0	0	0
Others						
O-antigen (part of the surface lipopolysaccharide of Gram-negative bacteria)	2	2	2	2	0	0
Virulence-associated proteins	1	0	1	0	0	0

* Related genes: Number of related genes (by sequence similarity) with each virulence factor that have been found on the chromosome.

** In some cases, the number of related genes is lower than the number of genes present in the genome, this is due to the presence of multiple copies of the same gene.

*** 30/1: 30 related genes, and one related gene inactive.

 All related genes absent.

 All or some related genes present (number indicates how many related genes are present).

^T = type strain.

4.2.2. Hypersensitive response test of the AOD-associated *Pseudomonas* in bean pods

AOD-associated *Pseudomonas* were inoculated in detached green pods (dwarf French beans, *Phaseolus vulgaris*) to study their ability to trigger HR. The inoculum were single cultures of four different controls, and a selection of strains of Pda, Pdr and Pki, in triplicate. The controls added to each pod were the strain 1448A, race 6 of *Pph* (disease control); the strain 1302A, race 4 of *Pph* (hypersensitive response control); the strain SBW25 of *Pseudomonas fluorescens* (non-plant pathogenic control); and a sterile wound (non-inoculum control) (**Figure 23**). The AOD-associated *Pseudomonas* tested were Pda: strains P2^T, P1, P3, P5, P7, P8, P9, P18, P20, P21, P22, and P23; Pdr: strains P27^T, P6, and P26; and Pki: strains P4^T, P10, P11, P14, P16, P17, P24, P25, P28, P29, P30, P31, and P32.



Figure 23: Phenotype of the controls used in the hypersensitive response tests. The bacteria inoculated in these bean pods of *Phaseolus vulgaris* are: strain 1448A, race 6 of *Pseudomonas syringae* pv. *phaseolicola* (disease control); the strain 1302A, race 4 of *Pseudomonas syringae* pv. *phaseolicola* (hypersensitive response control); the strain SBW25 of *Pseudomonas fluorescens* (non-plant pathogenic control). One fresh colony was inoculated in each stabbing point. The non-inoculum control is a sterile wound. Image was taken after 48 hours of incubation at 25 °C.

Visually inspecting the bean pods, after 48 hours of incubation at 25 °C, it was concluded that the response generated by the strains of the three novel *Pseudomonas* species in the plant tissue was analogous to the response caused by the strain SBW25 of *Pseudomonas fluorescens* (Figure 24). SBW25 was inoculated as a non-plant pathogenic control, therefore the results suggested that the AOD-associated *Pseudomonas* by themselves do not trigger HR in bean pods.



Figure 24: Hypersensitive response test of the AOD-associated *Pseudomonas* in bean pods. The AOD-associated *Pseudomonas* tested were Pda: strains P2^T, P1, P3, P5, P7, P8, P9, P18, P20, P21, P22, and P23; Pdr: strains P27^T, P6, and P26; and Pki: strains P4^T, P10, P11, P14, P16, P17, P24, P25, P28, P29, P30, P31, and P32. The controls were placed at the stem end of each pod, in the stem end. D: strain 1448A, race 6 of *Pseudomonas syringae* pv. *phaseolicola* (disease control). HR: strain 1302A, race 4 of *Pseudomonas syringae* pv. *phaseolicola* (hypersensitive response control). NPP: strain SBW25 of *Pseudomonas fluorescens* (non-plant pathogenic control). NIC: non-inoculum control. The numbers in the pods refer to the inoculation in triplicates of the *Pseudomonas* associated with AOD. Each number corresponds to the code of the strain (for example: 6 = P6). One colony was inoculated in each stabbing point. Image was taken after 48 hours of incubation at 25 °C.

4.2.3. Hypersensitive response test of the AOD-associated *Pseudomonas* in tobacco leaves

AOD-associated *Pseudomonas* were inoculated in tobacco leaves (*Nicotiana benthamiana*) to study their ability to trigger HR. The AOD-associated *Pseudomonas* tested were the type strains of Pda, Pdr, and Pki (**Figure 25**). A positive HR control (strain 1302A, race 4 of *Pph*) and a sterile water control were also inoculated in the leaves for comparison. None of the AOD-associated *Pseudomonas* or the sterile water control triggered the HR response in the plant tissue.

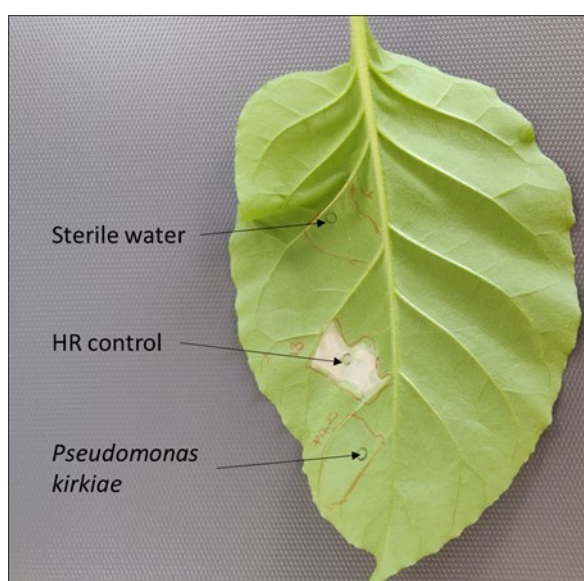


Figure 25: Hypersensitive response test of the AOD-associated *Pseudomonas* in tobacco leaves. The type strain of *Pseudomonas kirkiae* P4^T was inoculated in tobacco leaves along with an inoculation control (sterile water), and an HR control (strain 1302A, race 4 of *Pseudomonas syringae* pv. *phaseolicola*). ^T = type strain.

4.2.4. Cell attachment assays in AOD-associated *Pseudomonas*

Cell attachment assays were performed to study the ability of the AOD-associated *Pseudomonas* to attach themselves to abiotic surfaces. The cell attachment assays were performed using two different methods: in 6-well plates and in 50 mL Falcon tubes with glass coverslips inside. The attachment was measured in the three surfaces mentioned: the wells of the 6-well plates, the Falcon tubes and the glass coverslips. The 6-well plate assay was performed using TSB and the tube-coverslip assay was performed using TSB and also LB broth

(for Pki). *P. fulva* was added as positive control and a non-inoculum control was also added to all experiments. The corresponding phylogenetically closest neighbours of the AOD-associated *Pseudomonas* were included in the assays. All samples were analysed in triplicate. Attachment was measured by crystal violet staining. The results were compared visually and also spectrophotometer readings of the dyed attached cells, re-suspended in ethanol were taken at OD₅₉₀ **Appendix XIV: OPTICAL DENSITY VALUES OBTAINED AT 590 NM IN THE CELL ATTACHMENT ASSAYS.**

Appendix XIV. There are several results to report in this section:

4.2.4.1. Six-well plate assay of Pda, Pdr and Pki, performed in TSB

The six-well plate cell attachment assay was performed with strains of Pda, Pdr, and their phylogenetically closest neighbours (**Figure 26a, 26b**). Separately, the same assay was performed with strains of Pki, and their genetically closest neighbours (**Figure 26c, 26d**). Bacteria were incubated statically, at 25 °C, for six days, in TSB. None of the AOD-associated strains demonstrated the ability of attachment to the surface of the wells. The OD₅₉₀ values obtained after detaching and diluting the stained attached AOD-associated *Pseudomonas* cells were lower than the values obtained by the positive control (*P. fulva*). OD₅₉₀ values of Pki strains were especially low. Inconsistencies were observed in the results obtained for the positive control, *P. fulva*, between the study carried out for Pda / Pdr and the study carried out for Pki. According to the OD₅₉₀ values and visual inspection, some of the closest neighbours had similar or more cell numbers attached to the well than the positive control, *P. fulva*. These were *P. punonensis*, *P. straminea*, and *P. azotifigens*. The strain P18 of Pda had the highest OD₅₉₀ values of all the AOD-associated *Pseudomonas*.

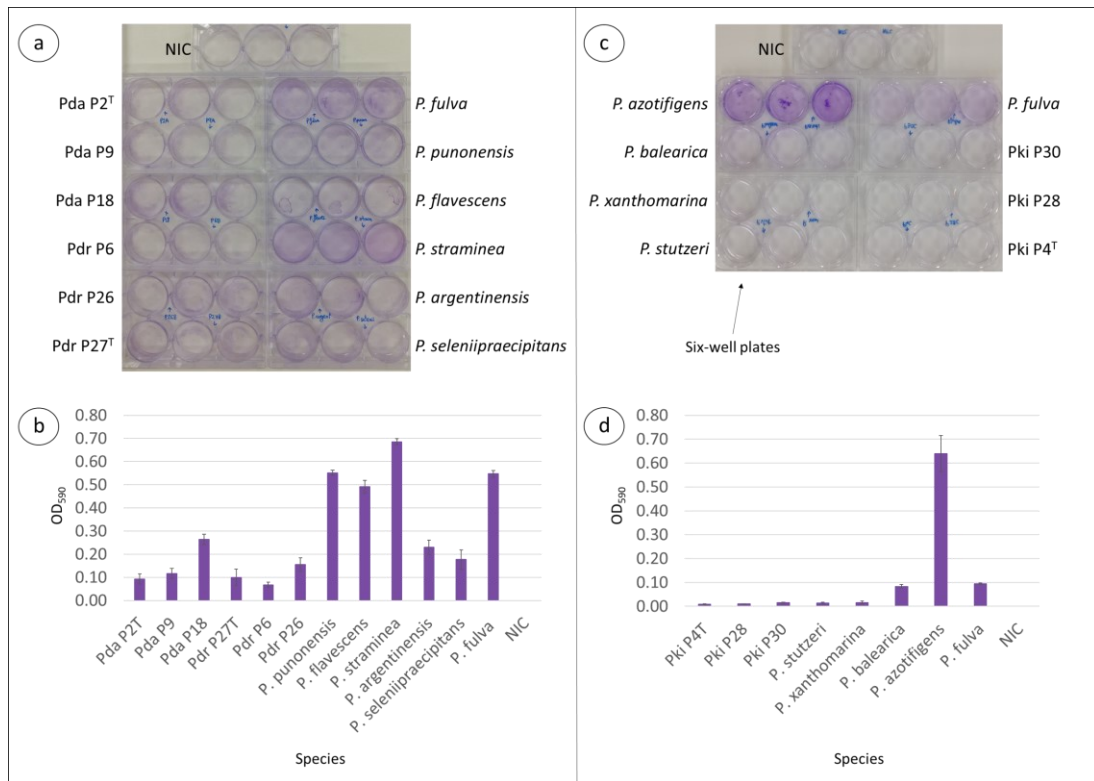


Figure 26: Six-well plate assay of the AOD-associated *Pseudomonas*, performed in TSB. Cell attachment to six-well plates was measured by crystal violet staining (optical density at 590 nm, OD₅₉₀). AOD-associated *Pseudomonas* and their phylogenetically closest neighbours were studied as well as the positive control *Pseudomonas fulva* LMG 11722^T and a non-inoculum control (NIC). Figures **a** and **c** are the stained six-well plates. The incubation medium was discarded and the cells attached to the walls of the wells were stained with crystal violet. Figures **b** and **d**: spectrophotometer readings of the dyed attached cells, re-suspended in ethanol, taken at OD₅₉₀. Each bar represents the average (mean; n=9) of OD₅₉₀ ± standard error.

Figures **a** and **b**: assay performed for the AOD-associated *Pseudomonas*: Pda: *Pseudomonas daroniae* sp. nov. (strains P2^T, P9, and P18), and Pdr: *Pseudomonas dryadis* sp. nov. (strains P27^T, P6, and P26); and their phylogenetically closest neighbours: *Pseudomonas flavescens* LMG 18387^T, *Pseudomonas argentinensis* LMG 22563^T, *Pseudomonas punonensis* LMG 26839^T, *Pseudomonas seleniipraecipitans* LMG 25475^T, and *Pseudomonas straminea* LMG 21615^T.

Figures **c** and **d**: assay performed for the AOD-associated *Pseudomonas*: Pki: *Pseudomonas kirkiae* sp. nov. (strains P4^T, P28, and P30); and their phylogenetically closest neighbours:

Pseudomonas stutzeri LMG 11199^T, *Pseudomonas azotifigens* LMG 23662^T, *Pseudomonas balearica* LMG 18376^T, and *Pseudomonas xanthomarina* LMG 23572^T. ^T = type strain.

4.2.4.2. Tube-coverslip assay of Pda, Pdr and Pki, performed in LB: cell attachment in Falcon tubes

In addition to 6-well plates, the ability of bacteria to adhere to abiotic surfaces was studied with an experiment involving 50 mL Falcon tubes with glass coverslips inside. The tube-coverslip assay was performed on strains of Pda, Pdr and their closest neighbours (**Figure 27a**). Separately, the same test was performed on Pki strains and their closest neighbours (**Figure 27b**). *P. fulva* was introduced as a positive control because it is a known biofilm producer. The bacteria were incubated statically, at 25 °C, for six days, in LB. Cultures could be differentiated by cells that adhered to Falcon tubes, cells that adhered to glass coverslips, and cells that adhered to both surfaces. In the case of cell adhesion in Falcon tubes, the results were obtained by crystal violet staining. The cells adhered to the tubes were stained, re-suspended in ethanol and spectrophotometric readings were taken at optical density at 590 nm (OD₅₉₀) **Appendix XIV**. In the case of the cells adhered to the glass coverslips, the comparison was made visually.

Pda and Pdr did not adhere to the tube, however two of the three tested strains of Pki did. OD₅₉₀ values obtained from the tube inoculated with P30 were high compared to the rest, but did not reach the value of the positive control. However, the type strain, P4^T, showed statistically higher OD values than those obtained by the positive control, *P. fulva*. *P. fulva* cells adhered to all surfaces tested in all the media tested.

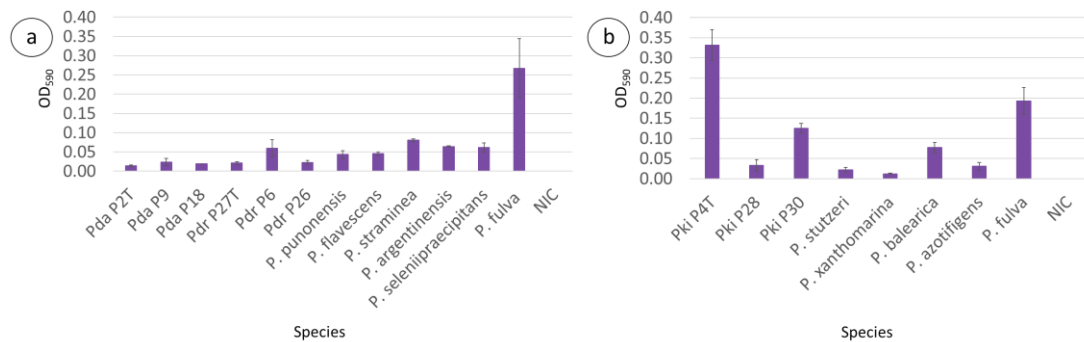


Figure 27: Tube-coverslip assay of the AOD-associated *Pseudomonas*, performed in LB: cell attachment in Falcon tubes. Cell attachment to Falcon tubes was measured by crystal violet staining (optical density at 590 nm, OD₅₉₀). Spectrophotometer readings of the dyed attached cells, re-suspended in ethanol were taken at OD₅₉₀. AOD-associated *Pseudomonas* and their phylogenetically closest neighbours were studied as well as the positive control *Pseudomonas fulva* LMG 11722^T and a non-inoculum control (NIC). Each bar represents the average (mean; n=9) of OD₅₉₀ ± standard error.

(a): OD₅₉₀ values obtained by the AOD-associated *Pseudomonas*: Pda: *Pseudomonas daroniae* sp. nov. (strains P2^T, P9, and P18), and Pdr: *Pseudomonas dryadis* sp. nov. (strains P27^T, P6, and P26); and their phylogenetically closest neighbours: *Pseudomonas flavescens* LMG 18387^T, *Pseudomonas argentinensis* LMG 22563^T, *Pseudomonas punonensis* LMG 26839^T, *Pseudomonas seleniipraecipitans* LMG 25475^T, and *Pseudomonas straminea* LMG 21615^T.

(b): OD₅₉₀ values obtained by the AOD-associated *Pseudomonas*: Pki: *Pseudomonas kirkieae* sp. nov. (strains P4^T, P28, and P30); and their phylogenetically closest neighbours: *Pseudomonas stutzeri* LMG 11199^T, *Pseudomonas azotifigens* LMG 23662^T, *Pseudomonas balearica* LMG 18376^T, and *Pseudomonas xanthomarina* LMG 23572^T. ^T = type strain.

4.2.4.3. Tube-coverslip assay of Pda, Pdr and Pki, performed in LB: cell attachment in glass coverslips

The glass coverslips of the tube-coverslip assay were inspected visually to determine the ability of bacteria to adhere to a glass surface (**Figure 28**). The positive control, *P. fulva*, adhered more effectively to the glass, by far than any other strain. None of the AOD-

associated *Pseudomonas* showed the ability to adhere to glass, as the colour of the coverslip was much lighter than that of any other strain.

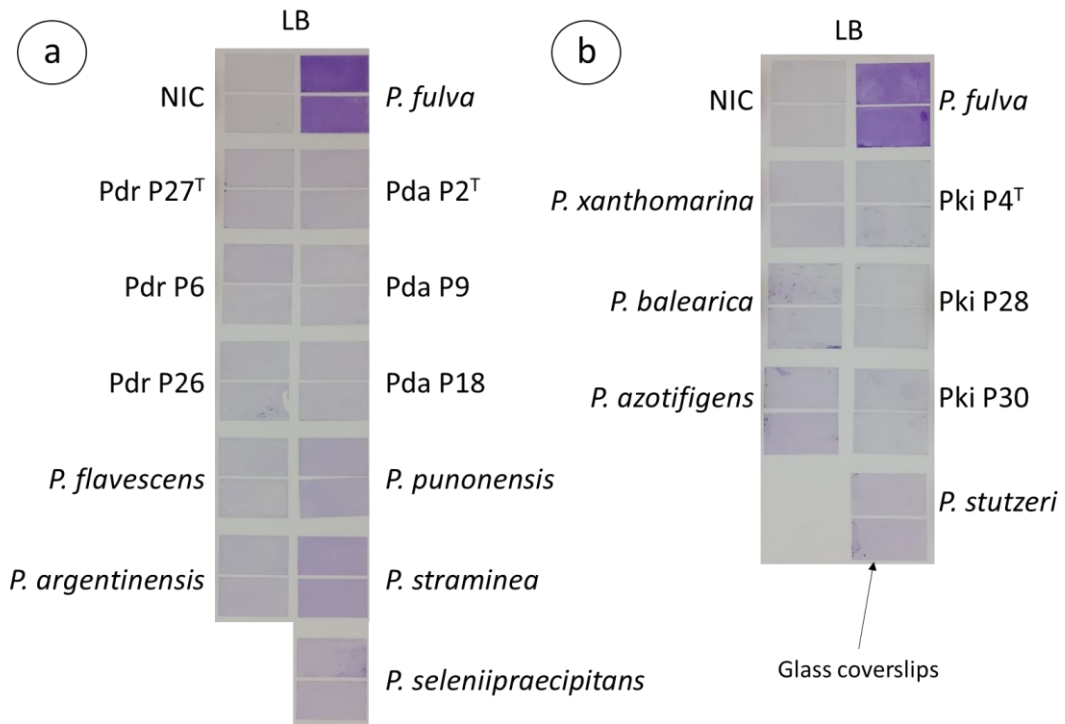


Figure 28: Tube-coverslip assay of the AOD-associated *Pseudomonas*, performed in LB: cell attachment in glass coverslips. Cell attachment to the glass coverslips was measured visually after crystal violet staining of the cells attached to the glass. AOD-associated *Pseudomonas* and their phylogenetically closest neighbours were added to this study as well as the positive control, *Pseudomonas fulva* LMG 11722^T and a non-inoculum control (NIC).

(a): glass coverslips from the assay including the AOD-associated *Pseudomonas*: Pda: *Pseudomonas daroniae* sp. nov. (strains P2^T, P9, and P18), and Pdr: *Pseudomonas dryadis* sp. nov. (strains P27^T, P6, and P26); and their phylogenetically closest neighbours: *Pseudomonas flavescens* LMG 18387^T, *Pseudomonas argentinensis* LMG 22563^T, *Pseudomonas punonensis* LMG 26839^T, *Pseudomonas seleniipraecipitans* LMG 25475^T, and *Pseudomonas straminea* LMG 21615^T.

(b): glass coverslips from the assay including the AOD-associated *Pseudomonas*: Pki: *Pseudomonas kirkiae* sp. nov. (strains P4^T, P28, and P30); and their phylogenetically closest neighbours: *Pseudomonas stutzeri* LMG 11199^T, *Pseudomonas azotifigens* LMG 23662^T,

Pseudomonas balearica LMG 18376^T, and *Pseudomonas xanthomarina* LMG 23572^T. ^T = type strain.

4.2.4.4. Tube-coverslip assay of Pki, performed in LB and TSB: cell attachment in Falcon tubes and glass coverslips

To determine if the choice of inoculation media made a difference in cell attachment, the tube-coverslip assay for Pki was performed using two different media, TSB and LB (**Figure 29** and **Figure 30**). A selection of strains, including P4^T, P28 and P30 of Pki, their genetically closest neighbours, and *P. fulva* were tested. Bacteria were incubated statically, at 25 °C, for six days. The OD₅₉₀ values obtained from the cells attached to the interior of the tubes were higher for all strains when the bacteria were incubated in LB compared to TSB. This happened in all the species tested except for *P. xanthomarina* (although the OD₅₉₀ of *P. xanthomarina* was lower than 0.05 in both media).

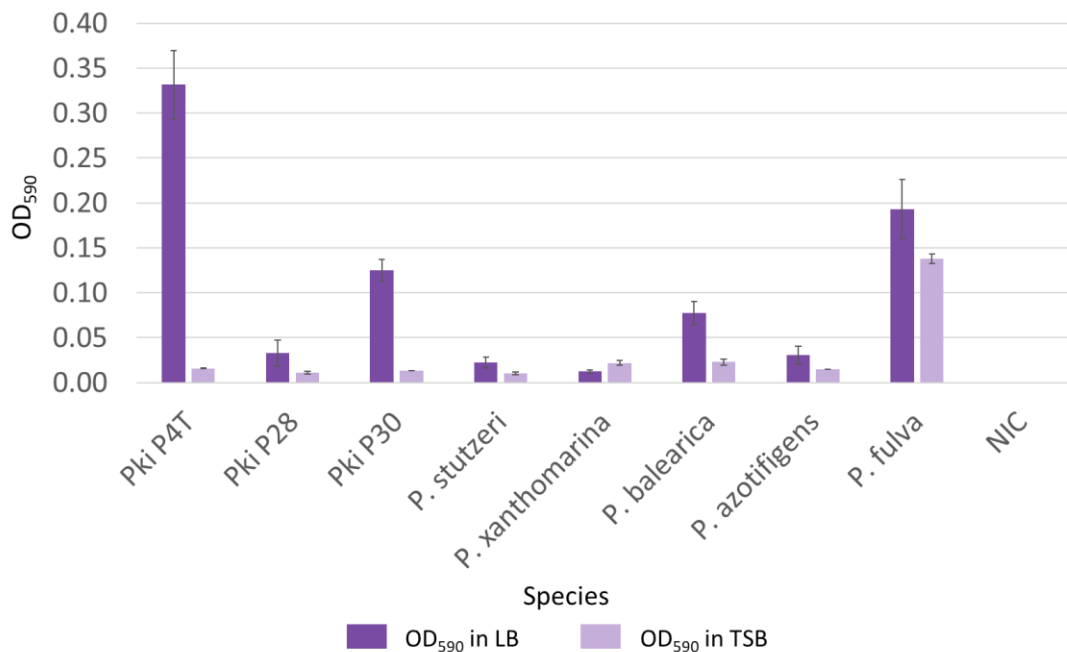


Figure 29: Tube-coverslip assay of the AOD-associated *Pseudomonas*, performed in LB and TSB: cell attachment in Falcon tubes. Cell attachment to the Falcon tubes was measured after crystal violet staining (optical density at 590 nm, OD₅₉₀) of the cells attached to the tube. Spectrophotometer readings of the dyed attached cells, re-suspended in ethanol were taken at OD₅₉₀. OD₅₉₀ values obtained by the AOD-associated *Pseudomonas* and their phylogenetically closest neighbours were compared as well as the positive control

Pseudomonas fulva LMG 11722^T and a non-inoculum control (NIC). Each bar represents the average (mean; n=9) of OD₅₉₀ ± standard error. Each bar represents the average (mean; n=9) of OD₅₉₀ ± standard error. The AOD-associated *Pseudomonas* was: Pki: *Pseudomonas kirkiiae* sp. nov. (strains P4^T, P28, and P30). The neighbours were, *Pseudomonas stutzeri* LMG 11199^T, *Pseudomonas azotifigens* LMG 23662^T, *Pseudomonas balearica* LMG 18376^T, and *Pseudomonas xanthomarina* LMG 23572^T. ^T = type strain.

The glass coverslips of the tube-coverslip assay were inspected visually to compare the cell attachment abilities of the bacteria inoculated (**Figure 30**). The strain with the highest attachment ability was *P. fulva* in both LB and TSB. In the case of *P. fulva*, (as seen in the Falcon tubes), more cells remained attached to the glass coverslips when incubated in LB compared to TSB. However, for the rest of the strains the adhesion was too low to be comparable. None of the Pki strains showed the ability to adhere to glass. The results of cellular adhesion to the interior of the Falcon tube and to the glass coverslip did not always correlate. P4^T and P30 adhered strongly to the tube but not to the coverslip (**Figure 30a**).

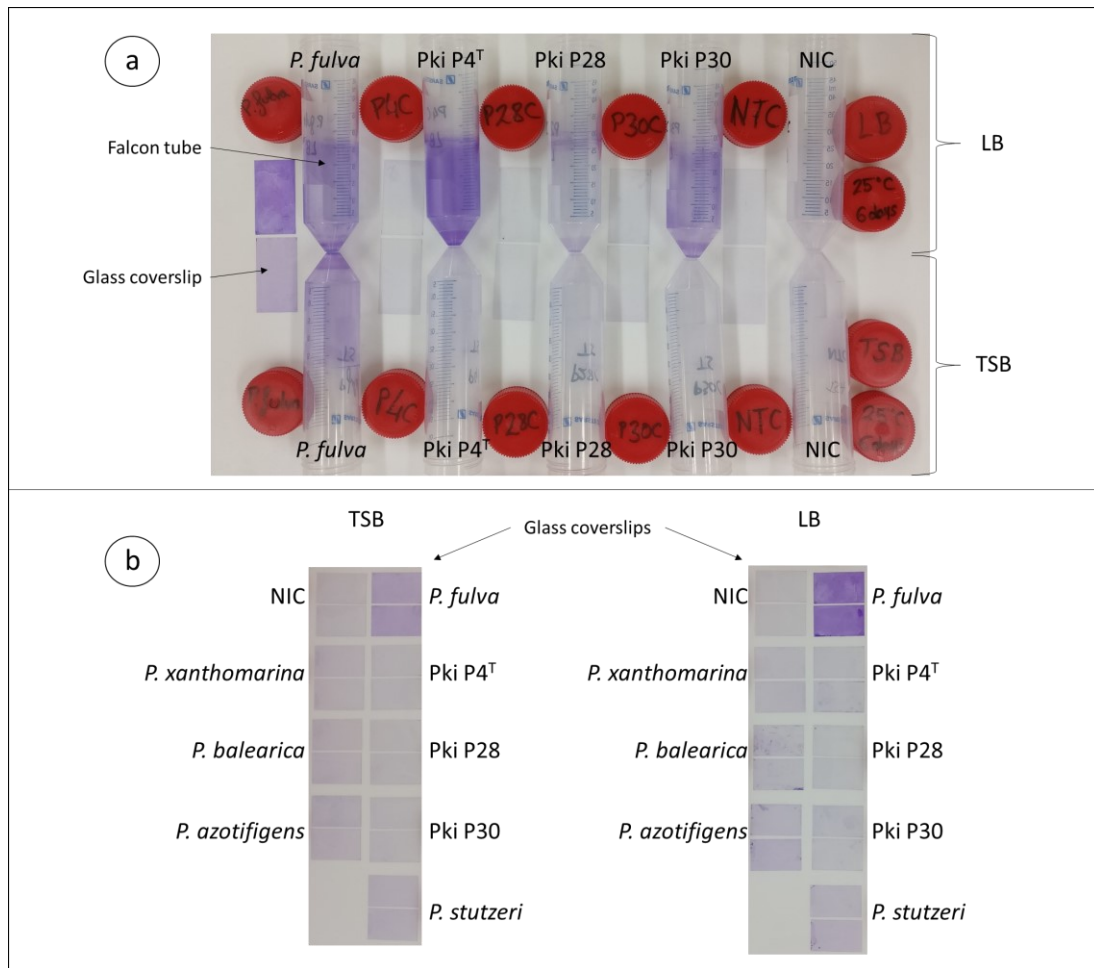


Figure 30: Tube-coverslip assay of the AOD-associated *Pseudomonas*, performed in LB and TSB: cell attachment in Falcon tubes and glass coverslips. Cell attachment was compared after crystal violet staining of the cells attached to the coverslips and the tubes. Figure **a**: Falcon tubes and glass coverslips. Figure **b**: glass coverslips. The incubation medium was discarded and the cells attached to the walls of the tubes and to the coverslips were stained with crystal violet. AOD-associated *Pseudomonas* and their phylogenetically closest neighbours were added to this study as well as the positive control, *Pseudomonas fulva* LMG 11722^T and a non-inoculum control (NIC). The AOD-associated *Pseudomonas* were: Pki: *Pseudomonas kirkiae* sp. nov. The neighbours were *Pseudomonas stutzeri* LMG 11199^T, *Pseudomonas azotifigens* LMG 23662^T, *Pseudomonas balearica* LMG 18376^T, and *Pseudomonas xanthomarina* LMG 23572^T. ^T = type strain.

4.3. Discussion

The aim of this chapter was to study the potential pathogenicity traits of the AOD-associated *Pseudomonas* species that were formally described in **Chapter 3**. To study if a particular bacterium causes disease symptoms in its host, a pathogenicity test is required. The pathogenicity test consists of the artificial inoculation of a pure culture of bacteria, suspected to cause disease, in the same cultivar of the host or a related one, or in another susceptible species, in order to reproduce the same symptoms of the disease. The bacteria must be re-isolated and compared to the pure inoculated culture. This strategy can be time consuming, especially if the host is woody, such as oak. However, there are faster and less destructive ways for the plant to study whether a bacterium exhibits potentially pathogenic traits. Putative virulence factors (VFs) were searched for in the genomes of the AOD-associated *Pseudomonas*, to study their ability to trigger hypersensitive response (HR) in plant tissue, and to study their ability to adhere to surfaces.

Although there is no an exact profile of VFs typical of a pathogen or a non-pathogen, the comparison of the profile of the pathogenic *Pseudomonas syringae* pv. *phaseolicola* 1448A with that of non-pathogenic *Pseudomonas fluorescens* SBW25 could establish the parameters to characterize the VF profile of a pathogenic *Pseudomonas* and differentiate it from a non-pathogenic *Pseudomonas*. It seems that the VF profiles of 1448A and SBW25 are very similar to each other; particularly those VFs related to adherence, antiphagocytosis, amino acid and purine metabolism, efflux pump, endotoxin, stress adaptation and immune response evasion. The specific differences between pathogenic (1448A) and non-pathogenic (SBW25) strains are that the non-pathogenic lacks several of what could be categorized as "attacking VFs". "Attacking VFs", for example those that encode the production of toxins or some of the secretion systems, are absent in the genome of the non-pathogen and present in the genome of the pathogen. However, the genome of the non-pathogenic *Pseudomonas* seem to contain more VFs that could be categorised as "defence VFs", such as those related to biofilm formation (that helps bacterial establishment within the plant) and alkaline protease (whose role seems to have to do with avoiding recognition by the plant immune system (Figaj et al., 2019)), absent in the pathogenic *Pseudomonas*.

According to VFAnalyzer, the AOD-associated *Pseudomonas* possess several VFs that pathogen 1448A and non-pathogen SBW25 did not have in their genomes. All the VF profiles studied contained VFs related to having flagella but only AOD-associated *Pseudomonas* contained VFs specifically related to polar flagella, which were, in fact, seen through

transmission electron microscopy (**Figure 19**). The VFs exclusive to AOD-associated *Pseudomonas* were mainly related to iron uptake, more pyoverdine than pyochelin-related, which could represent a selective advantage for the AOD-associated *Pseudomonas* in the nutrient deficient plant environment. One of the strains of Pda, all the strains of Pdr and all the strains of Pki studied in **Chapter 3** are fluorescent under UV light, therefore it makes sense that they have genes that encode for the synthesis of fluorescent pigment production such as pyoverdine. AOD-associated *Pseudomonas* were also found to be genetically capable of synthesizing purines, believed to help stressed plants by providing them with a source of nitrogen (Izaguirre-Mayoral, Lazarovits and Baral, 2018). Additionally, AOD-associated *Pseudomonas* have VFs related to antibiotic resistance (efflux pumps) and stress adaptation (Blanco et al., 2016). In conclusion, it seems that the VFs profiles of the AOD-associated *Pseudomonas* contain more “defence VFs” than “attack VFs”. This may indicate that they are endophytes, although the VF profiles of the AOD-associated *Pseudomonas* also contain some “attack VFs” encoding for the production of toxins and some types of secretion systems, therefore a definitive conclusion on the potential pathogenicity traits cannot be extracted from the study of the VFs in the genome alone. Additionally, a genetic potential to become a pathogen does not imply that the bacterium will express the genes that encode for the VFs (Barbosa et al., 2014; Loman and Pallen, 2015; Vinatzer, Monteil and Clarke, 2014; Xu et al., 2011).

As a remark on the VFAnalyzer tool: pyoverdine is the main siderophore in 1448A (Owen and Ackerley, 2011), however, none of the 16 related genes encoding for pyoverdine were found by VFAnalyzer in the genome of 1448A. This contradiction suggests that it would be convenient to contrast the VF profiles obtained with the VFAnalyzer tool with those obtained by other different tools. As the creators of the platform themselves state, VFAnalyzer has some limitations (Liu et al., 2019). One of the limitations is that the database of genomes with which the query genomes are compared contains only 32 genera of common bacterial pathogens. Another limitation is that the platform requires almost complete or complete genomes to function properly, and thus a highly fragmented genome can lead to unreliable results.

To group different species of *Pseudomonas* into clusters of similar VF profiles, AHC of the VF profiles was performed. It was intended to see if the AOD-*Pseudomonas* clustered with any other *Pseudomonas* species. Methods for exploring data such as PCA or AHC allow to

formulate hypotheses without necessarily having a precise question. The virulence factor profiles obtained for the AOD-associated *Pseudomonas* did not cluster with any other species in the AHC, which does not necessarily mean that they are not pathogenic. The relationship between the presence of functional virulence genes and the pathogenic activity has been studied, but presenting genes that encode for virulence factors in the genome does not necessarily mean that the bacterium will express them, therefore pathogenicity tests *in planta* are always necessary (Barbosa et al., 2014; Loman and Pallen, 2015; Vinatzer, Monteil and Clarke, 2014; Xu et al., 2011). Most plant pathogens are capable of inducing HR in non-host plant species or indicator plants (Klement and Goodman, 1967), and this is the reason why the HR tests in tobacco leaves and bean pods were performed.

AOD-associated *Pseudomonas* were inoculated in bean pods. The narrow brown ring that can be observed around the stabbing point inoculated with the AOD-associated *Pseudomonas* is probably not HR, but the response of the plant to the inoculation of a large amount of bacteria. This conclusion was reached because the response of the plant to the inoculation of the AOD-associated *Pseudomonas* is comparable to the response of the plant to the inoculation of the non-plant pathogen control, which also caused a narrow brown ring around the point where it was inoculated. In the case of HR tests, when the bacterium causes HR, it is possible to draw conclusions about its pathogenicity. If AOD-associated *Pseudomonas* caused HR in the pods, it could mean that they are able to trigger T3SS-mediated virulence processes, which are a crucial in many plant and animal pathogens (Toth, Pritchard and Birch, 2006). The fact that the AOD-associated *Pseudomonas* did not trigger HR in the pods or the tobacco leaves does not mean that they are not pathogenic, but if they would have caused HR, some suppositions could have been made about the potential pathogenicity traits of the AOD-associated *Pseudomonas*.

The ability to form biofilms is a useful weapon for the colonization of hostile spaces, and is a common (not exclusive) feature in pathogens. The first step to form biofilms is the adhesion of cells to a surface (Klemm, Hancock and Schembri, 2010), and in order to collect more information on the potential pathogenicity of the AOD-associated *Pseudomonas*, cell attachment studies were carried out.

P. fulva has been characterised as a strong biofilm producer (Jałowiecki et al., 2018). Assuming that the biofilm formation ability would probably mean good cell attachment ability, *P. fulva* was added to the cell attachment assays as a positive control. The phylogenetically closest neighbours of the AOD-associated *Pseudomonas* were also added to

the study, and even though that was probably not necessary for the study, they provided some contrast in the results. It was observed that the OD₅₉₀ of *P. fulva* was lower in the assay performed for Pki (**Figure 26d**) than for the assay performed for Pda and Pdr (**Figure 26b**). This could be due to a more vigorous rinsing of the wells, meaning that the results within the study for Pki are comparable to each other, but they are not comparable to the results obtained for Pda/Pdr. The variation from experiment to experiment can be due to conditions such as the personal handling of the experiment or differences in the material of the microtiter plates from batch to batch (Bordeleau et al., 2018; Skogman, Vuorela and Fallarero, 2012). The poor reproducibility of this assay has been previously reported, leading to a range of different cell attachment assays being performed in this project (Kragh et al., 2018).

Except for some strains of Pki, the cell attachment assays suggested that the AOD-associated *Pseudomonas* generally have poor cell attachment abilities when it comes to the surfaces tested. This does not mean that they cannot adhere to another surfaces, but this result adds to the other results obtained in the other experiments in this chapter. Some strains of Pki are able to attach themselves to the Falcon tubes but not to the glass coverslips. In the rest of the surfaces tested there was no significant cellular attachment. In contrast, several genes encoding for VFs associated to adherence (type IV pili and flagella) were found in the genomes of all Pda, Pdr and Pki strains. The ability to adhere to surfaces depends, among other things, on the type of surface (Hancock, Witsø and Klemm, 2011). Surface dependant cell attachment was observed in the tube-coverslip assays. In these, the same strain was incubated simultaneously in contact with the interior of a Falcon tube and a glass coverslip, and it was observed that some strains of Pki adhered to the plastic of the tube, but not to the glass inside the tube.

Another result was that the cell attachment of bacteria incubated in LB was greater than the levels of attachment of the same bacteria incubated in TSB. In the routine laboratory work, it was observed that, although TSB and LB are both rich nutrient media, the species used in this study, generally grow better in TSB than in LB. Therefore, it is possible that the cell attachment abilities are triggered under hostile environmental conditions such as nutrient deficiency. This is not surprising as growth media has been reported previously as influential for biofilm formation (Hancock, Witsø and Klemm, 2011; Ueda and Saneoka, 2015). It would be interesting to repeat the experiment using minimal media (M9). Since M9 is a very low nutrient medium, it is more challenging for bacterial growth. Having seen that cell

attachment abilities increase when the medium is suboptimal, the hypothesis would be that growing in M9 would trigger bacterial adhesion to a greater extent than when the bacteria are incubated in LB broth.

The VF profiles of the AOD-associated *Pseudomonas* did not cluster with any *Pseudomonas* pathogen available in VFAnalyzer database; the strains did not trigger HR in bean pods or tobacco leaves; and they did not show particularly good cell attachment skills under the conditions tested (except for some strains of Pki). The studies described in this chapter (VFs, HR and cell attachment) were performed to obtain information on the potential pathogenicity traits of AOD-associated *Pseudomonas*. The results are not conclusive on their own, but when all the results are put together and analysed together, the balance seems to tip towards suggesting that the three novel *Pseudomonas* species are not pathogens. If the AOD-associated *Pseudomonas* could cause HR, had numerous "typically pathogenic VFs" in their genomes, and if they were able to successfully adhere to surfaces, this would have led us to think that they are more likely to be pathogenic. Even if the results obtained in this chapter suggest that the novel AOD-associated *Pseudomonas* species are not pathogenic, non-pathogenic bacteria could still benefit the activity of pathogenic species in several ways. They could exchange secondary metabolic products, release substances that facilitate the creation of biofilms, or produce compounds that suppress the defence responses of the plant (Harwood and Parales, 1996). Some concepts to continue this research path could be those related to the study of the possible effects that the presence of Pda, Pdr and Pki have on the performance of AOD pathogens such as Bg.

**CHAPTER 5. Development of HRM-
based tools for the identification and
detection of AOD-associated bacteria**

5.1. Introduction

Acute Oak Decline (AOD) is caused by the interaction of several bacterial species. The lesion microbiome shows a significantly similar composition pattern, where *Brenneria goodwinii* (Bg) and *Gibbsiella quercinecans* (Gq) are the most abundant bacterial species. Bg and Gq are responsible for the tissue necrosis, and *Rahnella victoriana* (Rvi), *Lonsdalea britannica* (Lb), other members of *Brenneria*, *Rahnella*, *Lonsdalea*, *Erwinia* and *Ewingella* are also associated with the lesion microbiome, although their role in the disease is still unclear (Broberg et al., 2018; Denman et al., 2018, 2014; Doonan et al., 2019). Novel species belonging to the *Pseudomonadaceae* are also routinely isolated in AOD sites, and three of these, *Pseudomonas daroniae* sp. nov. (Pda), *Pseudomonas dryadis* sp. nov. (Pdr) and *Pseudomonas kirkiae* sp. nov. (Pki), have been formally described in **Chapter 3**, and their role in AOD is studied in **Chapter 4** (Bueno-Gonzalez et al., 2019, 2020).

As a result of the increasing amount of cases of AOD, many field samples need to be processed on a daily basis, therefore a quick and cost-effective detection and identification method is needed, and this is the aim of this part of the project. The tool chosen for this purpose is high resolution melt analysis (HRM). HRM analysis is a real-time PCR-based technique in which single nucleotide polymorphisms (SNP) can be identified in amplicons, without gels or DNA sequencing. PCR amplification followed by HRM analysis is an innovative technology, widely used for the identification of genetic variation in DNA amplicons (Gundry et al., 2003; Wittwer et al., 2003).

Due to the high level of genomic and phenotypic similarity of some of the species associated with AOD, day-to-day identification of strains can be difficult and time consuming, as typically, PCR amplification and sequencing of the *gyrB* gene was used. While this identification method is reliable, the sequencing of the *gyrB* may not provide sufficient resolution for accurate bacterial species identification and it is a labour-intensive and time-consuming procedure. In 2016, a rapid identification technique based on SNP detection by HRM analysis of the *atpD* gene was developed for the most frequently isolated species from AOD (Brady et al., 2016). Recently, a fluorogenic DNA probe-based PCR assay, which uses target-specific primers and a *TaqMan* probe was developed at Forest Research and is now being used for the routine screening of Gq, Bg, Rvi, and Lb from field samples (personal communication). While *TaqMan* assays are more sensitive and specific than HRM assays, HRM assays based on intercalating dyes are substantially cheaper and easy to use. This is because intercalating dyes are not sequence-specific, they emit fluorescence in the presence

of double stranded DNA regardless of the nucleic acid sequence (VanGuilder, Vrana and Freeman, 2008). Another advantage of HRM technology is that using an intercalating dye, it is possible to generate a DNA melting curve, after the amplification reaction. The melt analysis is essential to differentiate amongst amplicons, and also to differentiate amongst amplicons and undesired PCR artefacts such as primer-dimers or non-specific amplified sequences. Therefore, like *TaqMan*-based assays, HRM is able to track the presence of a target by tracking the increase in fluorescence, but it is also able to provide additional validation of the result thanks to the melt curve analysis, (the dissociation kinetics of the amplified products) which corroborates the nature of the amplicon (VanGuilder, Vrana and Freeman, 2008).

In the HRM analysis, the fluorescence data points collected during the melt analysis are plotted against the temperature (**Figure 31a**). Normalisation of the data is performed by equalising the highest fluorescence value to 100% and the lowest to zero, in order to compare the samples using the same scale (**Figure 31b**). The data can also be plotted so the melting temperature (T_m : the temperature at which half of the DNA products of the sample are denatured or melted, and the other half are still double-stranded) corresponds to the peak of the derivative curve (**Figure 31c**). Melting temperature (T_m) is specific to each DNA product, and it depends on factors such as the length of the sequence or the G+C content. The difference between HRM and other DNA melt analysis methods is that HRM is able to collect more fluorescence data points, at finer temperature steps, to differentiate amongst two amplicons that only differ in one SNP.

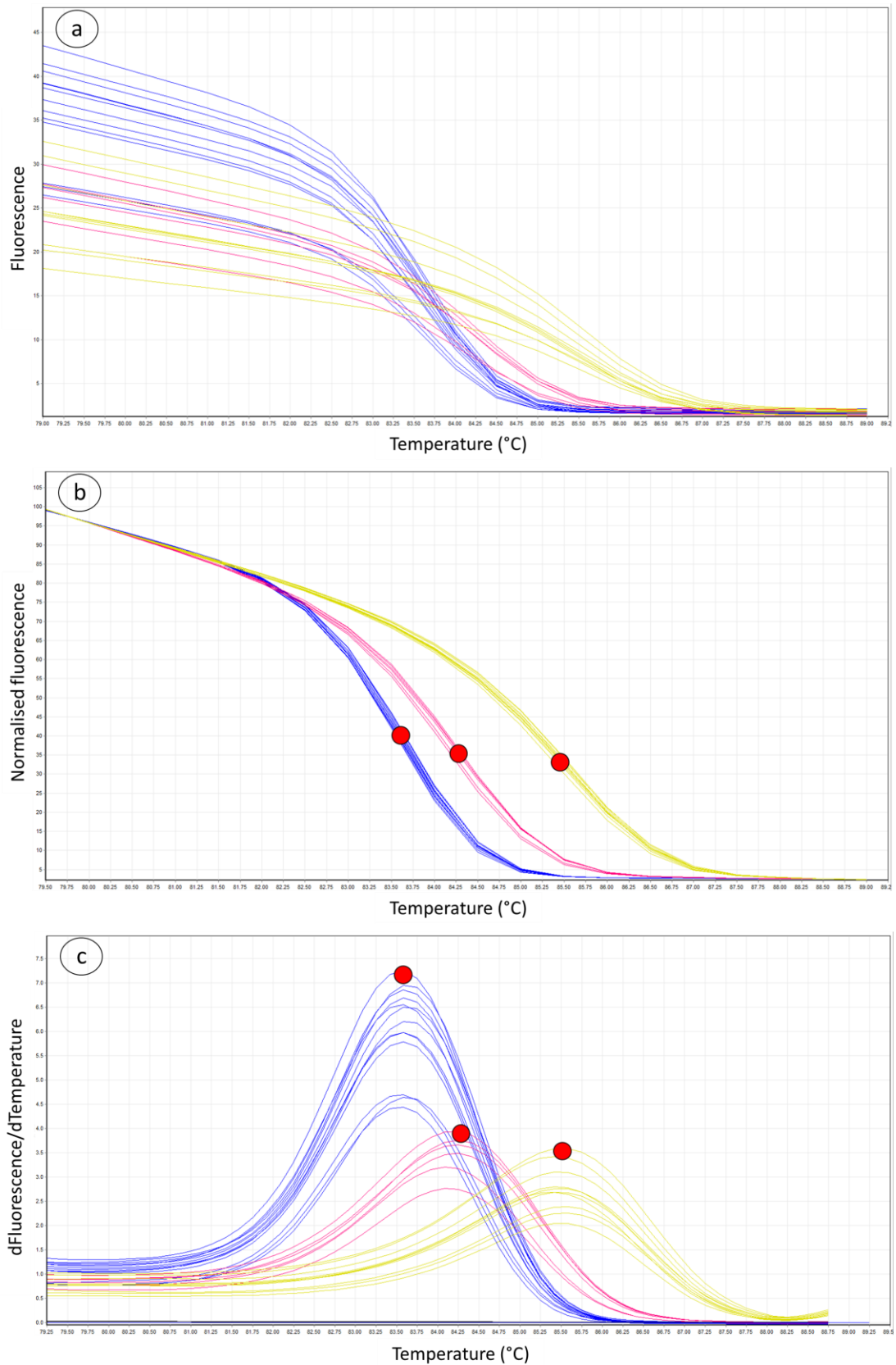


Figure 31: Example of a single nucleotide polymorphism-based high resolution melting analysis of three different bacterial species. A: fluorescence graph, B: normalised

fluorescence graph, C: derivative fluorescence graph. The red dots represent the melting temperature of each of the amplicons.

The statistical analysis of the HRM data collected with the RotorGene is performed with the specific Rotor-Gene ScreenClust HRM Software (Reja et al., 2010). ScreenClust analyses the raw HRM data following four steps: normalisation, generation of a residual plot, principal component analysis (PCA) (Pearson, 1901) and clustering of the data, (**Figure 32**). Following normalisation of the data (performed as for HRM analysis), a residual plot is generated by subtracting all the differentiated curves from the composite median of all curves. The individual sample characteristics are then extracted by PCA from the residual plot, and the software clusters the data according to the variation among the samples. The software analyses the probability that a sample belongs to a particular cluster and how well it belongs in the cluster (typicality). The analysis of the HRM data can be performed in two modes, supervised and unsupervised. In the supervised mode, known samples are added as controls and in the unsupervised mode all samples are unknown, and the clustering is performed by the software. The unsupervised mode is aimed at finding *de novo* data groups without a prior knowledge on the number and kind of genotypes present in the data set, and supervised mode is useful for methods such as SNP genotyping, where the genotypes are known, (Rotor-Gene® ScreenClust HRM® Software User Guide).

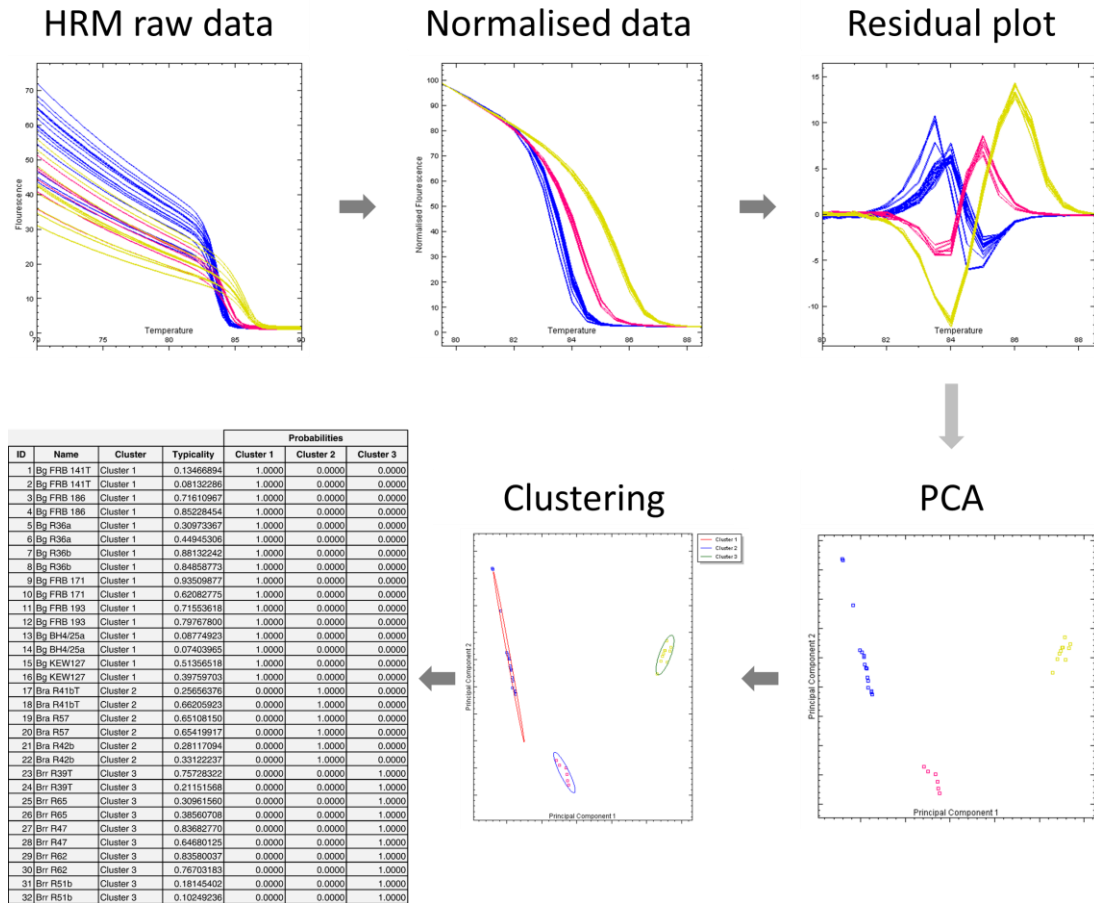


Figure 32: Workflow followed by the Rotor-Gene ScreenClust HRM software. The software analyses statistically the raw data generated by high resolution melting. PCA = principal component analysis.

HRM is a highly sensitive tool that can be used for many purposes, in this project, several HRM-based assays were developed to allow detection and identification of AOD-associated bacteria from swabs taken from trees, as well as directly from plant material. In addition, multiplex HRM including several diagnostic loci was investigated.

5.2. Results

5.2.1. HRM of the *atpD* gene

Original samples (a single colony in 750 μ L of water) of the type strains of Bg, Gq, and Rvi that were previously used in the study by Brady *et al.* (2016), as well as freshly prepared samples of the type strains of the same three species were analysed using HRM. The assay targeted a 119 bp region of the *atpD* gene (**section 2.6.2**). The conditions used were as described in Brady *et al.*, (2016). Both original and freshly prepared samples of the same species showed identical curve profiles. T_m s obtained were very similar amongst the old and fresh samples of the same species. The T_m of Bg samples was 85.8 $^{\circ}$ C (\pm 0.07 $^{\circ}$ C), the T_m of Gq samples was 86.72 $^{\circ}$ C (\pm 0.04 $^{\circ}$ C) and the T_m of Rvi samples was 85.1 $^{\circ}$ C (\pm 0.04 $^{\circ}$ C).

ScreenClust software grouped the samples in three clusters, one for all the samples containing Gq, another one for all the samples containing Bg and another one for the samples containing Rvi. The software did not discriminate between old and freshly prepared samples of the same species.

5.2.1.1. HRM of the *atpD* gene: different sample preparation methods

Pure cultures of type strains of Bg, Gq, and Rvi were prepared by three different methods (a single colony in water, 15 μ g of purified DNA from a single colony, and a single colony grown in LB broth and diluted to an OD_{600} of 0.1, as described in **section 2.6.2.1**). Samples were analysed using HRM of the 119 bp fragment of the *atpD* gene. The objective was to see if the melting temperature of the amplicon varied depending on the preparation method and to find out if any of the preparation methods was less suitable for HRM. Statistical differences were observed amongst the T_m of each of the methods for each of the species (**Figure 33**), following a two-factor ANOVA test without replication (p-value = 0.001). For all species tested, the lowest T_m observed was for the pure DNA sample, the next lowest T_m was of samples suspended in water and the highest T_m for all species was for the samples grown in LB broth. None of the preparation methods were inappropriate for their use in HRM. The difference in T_m between one species and another remained similar across the different preparation methods, which indicated that the sample preparation did not affect the difference in T_m between one species and another.

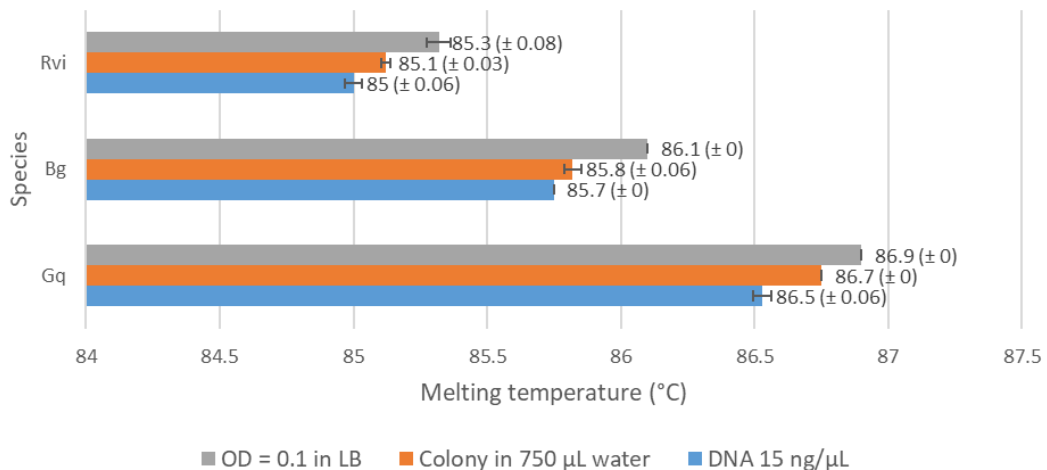


Figure 33: Melting temperatures of the amplicons obtained from the HRM assay of the *atpD* gene (119 bp) of the bacterial species *Gibbsiella quercinecans* (Gq), *Brenneria goodwinii* (Bg) and *Rahnella victoriana* (Rvi), prepared following three different methods. Sample preparation methods were: 15 µg of purified DNA from a single colony, a single colony in 750 µL of water, and a single colony that had been grown in LB broth and diluted to an OD₆₀₀ of 0.1. The primers used in this HRM assay were Gq6bF and Gq6bR. Error bars represent the standard errors. Labels next to each bar represent the average (mean; n=3) of T_m (°C) ± standard deviation.

5.2.1.2. HRM of the *atpD* gene: combined species test

The HRM assay of the *atpD* gene using the primers Gq6bF and Gq6bR had previously been designed to work with pure bacterial cultures (Brady et al., 2016). Before developing novel assays that are able to identify several species simultaneously, the HRM assay of the 119 bp fragment of the *atpD* gene was performed following the method of (Brady et al., 2016) with the modification that mixed cultures (combinations of two species in different ratios) were used instead of pure cultures (**section 2.6.2.2**). Combinations of type strains of species Gq, Bg and Rvi were used in this experiment.

Combinations of bacterial species that included Gq had a T_m similar to the control, 100 % Gq, except for the combination 75 % Bg - 25 % Gq in which the T_m was lower (**Figure 34**). In other combinations, such as those that contained Bg and Rvi, the T_m was between the T_m observed for the controls of the respective bacterial species which suggests that amplicons for both species were generated in the assay.

Cluster analysis of the raw HRM data was performed using the tool ScreenClust, with the unsupervised mode (**Figure 35**). The samples containing Gq, Rvi and the combinations of both grouped in two clusters, one with only samples of 100 % of Rvi, and another one with samples of 100 % Gq and the percentage combinations, (**Figure 35a**). The samples containing Bg, Rvi and the percentage combinations of both grouped in two different clusters, one with 100 % Rvi and another one with the rest of the samples, (**Figure 35a**). The samples containing Gq, Bg and the combinations of both, grouped in three clusters, one containing the sample 100 % Bg, another cluster containing the sample 75 % Bg - 25 % Gq and the other cluster containing the rest of the samples, (**Figure 35b**). The results showed that the presence of Gq masked the other species, and in the combinations without Gq (Bg – Rvi), the presence of Bg masked the presence of Rvi. This suggested that the analysis of the 119 bp fragment of the *atpD* gene fails to discriminate amongst different species in mixed cultures, and therefore it is not valid for testing field samples.

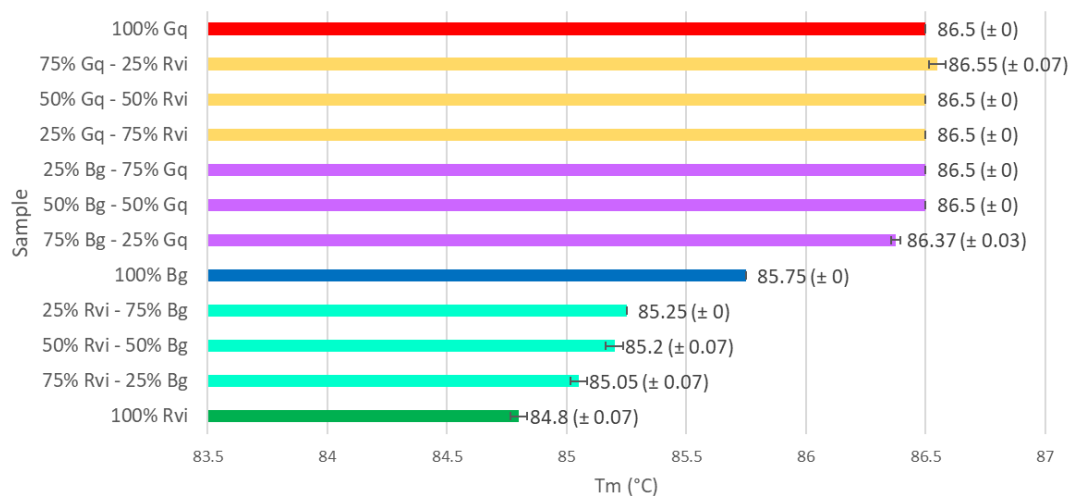


Figure 34: Melting temperatures of the amplicons obtained from the HRM assay of the *atpD* gene (119 bp) of the bacterial species *Gibbsiella quercinecans* (Gq), *Brenneria goodwinii* (Bg) and *Rahnella victoriana* (Rvi), for the combined species test. Samples were prepared by combining cell suspensions of two bacterial species at different proportions. Controls of pure cultures of each of the species tested were included (100% Gq, 100% Bg and 100% Rvi). The primers used in this HRM assay were Gq6bF and Gq6bR. Error bars represent the standard errors. Labels next to each bar represent the average (mean; n=3) of T_m (°C) ± standard deviation.

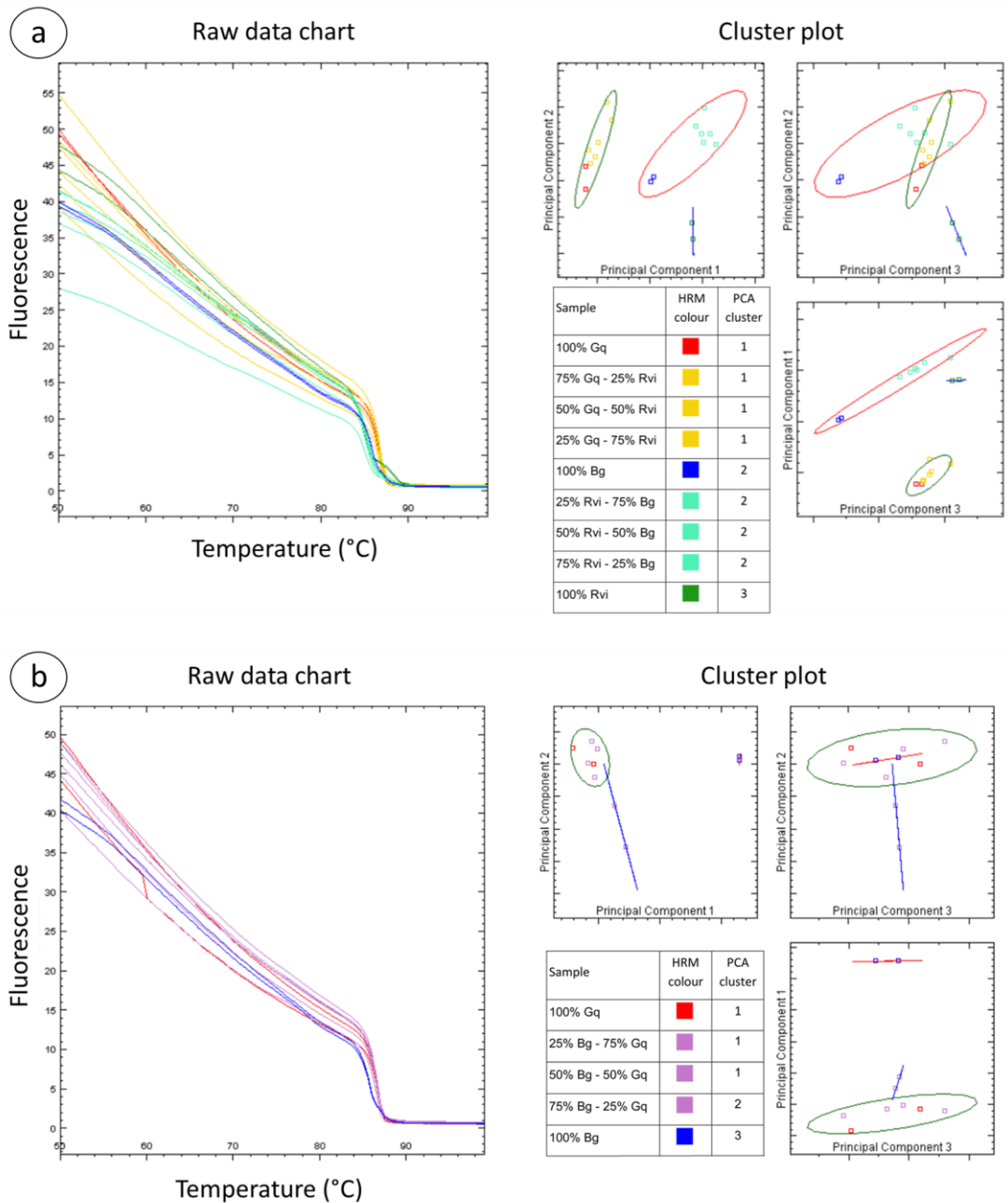


Figure 35: Unsupervised ScreenClust cluster analysis of the data set obtained in the HRM assay of the *atpD* gene (119 bp) of the bacterial species *Gibbsiella quercinecans* (Gq), *Brenneria goodwinii* (Bg) and *Rahnella victoriana* (Rvi), for the combined species test. ScreenClust tool was used for the statistical interrogation of the raw HRM data obtained from the Rotor-Gene cycler (raw data chart), allowing the software to choose the most appropriate cluster number and principal component number (unsupervised mode). Samples contain combinations of cell suspensions of two bacterial species at different proportions. Controls of pure cultures of each of the species tested were included (100% Gq, 100% Bg and 100% Rvi). A: ScreenClust cluster analysis of the data set obtained in the HRM

assay of the *atpD* gene (119 bp) of the combination of Gq, Rvi and Bg. B: ScreenClust cluster analysis of the data set obtained in the HRM assay of the *atpD* gene (119 bp) of the combination of Gq and Bg. The number of clusters and principal components selected by default were 3 and 3, respectively in both analyses. The 3 clusters are highlighted by ellipses in the cluster plots.

5.2.2. HRM of the *atpD* gene: HRM combined with agarose gel fingerprinting for the identification of AOD-associated bacteria including *Pseudomonas*

A novel assay to identify pure cultures of AOD associated bacteria including pseudomonads using the primers Gq6bF-AOD1R was developed. The assay targeted a bigger region of the *atpD* gene than the assay used in the previous sections, 320 bp long (**section 2.6.3**). HRM analysis of the derivative melt profiles of type strains (^T) of Bg, Brr, Gq, Rvi, Rva, Lb, Pda (strains P2^T and P18), Pdr (strains P27^T and P6) and Pki (strains P4^T and P28) was performed. The derivative melt plot suggested that both strains of Pda contained non-specific amplicons. This was indicated by the presence of more than one peak in the derivative curve (**Figure 36a**). The HRM assay failed to discriminate between Gq and Lb as the melting temperatures of these two species were identical. Moreover, the assay also struggled to discriminate amongst Rvi and Rva. Both strains of Pda displayed identical melt profiles and strains of Pki did not show amplification.

The gel analysis of the PCR products showed that non-specific amplicons were present in all of the samples, even when there was only one peak in the derivative HRM curve. The gel band patterns obtained were unique for each of the species analysed. Both strains of Pda showed identical band patterns; however strains of Pdr showed different band patterns between each other, suggesting some intra-species diversity. Strains of Pki displayed very faint, nearly imperceptible, band patterns that seemed to differ amongst each other, although the only deduction that can be made is that there was little to no amplification (**Figure 36b**). By separating HRM-amplified DNA products using agarose gel electrophoresis, it was possible to discriminate individual species, even amongst samples that the HRM was not able to differentiate, like Gq and Lb. The 320 bp specific PCR target was present in samples Bg, Brr, Gq, Rvi, Rva, Lb, and absent in *Pseudomonas* which displayed several bands of other sizes (non-specific amplification and primer-dimers). In Bg, Brr, Gq, Rvi, Rva, Lb there was also some non-specific amplification and primer-dimers.

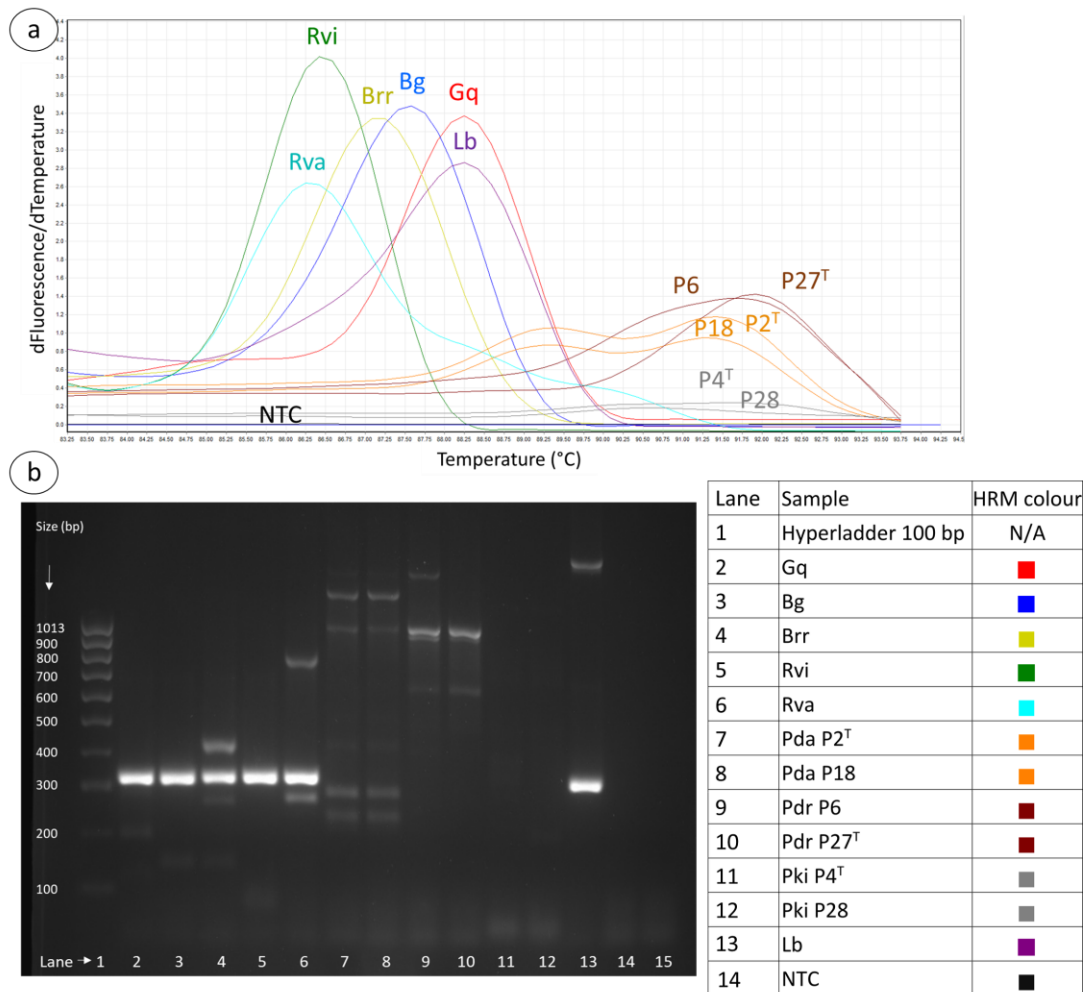


Figure 36: Derivative melt plot of the HRM of the 320 bp fragment of the *atpD* gene (a), and agarose gel electrophoresis of the DNA fragments amplified in the HRM assay of the 320 bp fragment of the *atpD* gene (b). Derivative melt profiles are of type strains of *Gibbsiella quercinecans* (Gq), *Brenneria goodwinii* (Bg), *Brenneria roseae* ssp. *roseae* (Brr), *Rahnella victoriana* (Rvi), *Rahnella variigena* (Rva), *Lonsdalea britannica* (Lb), as well as *Pseudomonas daroniae* sp. nov. (Pda, strains P2^T and P18), *Pseudomonas dryadis* sp. nov. (Pdr, strains P27^T and P6), and *Pseudomonas kirkiiae* sp. nov. (Pki, strains P4^T and P28). The primers used in this HRM assay were Gq6bF and AOD1R. The gel electrophoresis bands of 320 bp represent the target of the primers used in this assay. Molecular weight marker, HyperLadder 100 bp. NTC = non-template control. ^T = type strain.

5.2.3. Duplex-HRM assay of genes *atpD* and *rpoD* for the identification of AOD-associated bacteria including AOD-associated *Pseudomonas*

The assay in the previous section was modified to eliminate the need to perform a separate analysis by agarose gel electrophoresis. The PCR conditions were adjusted, and the concentration of the primers Gq6bF and AOD1R was halved (**section 2.6.3.1**). The HRM of the 320 bp fragment of the *atpD* gene was performed in pure cultures of the type strains of the species Bg, Brr, Gq, Rvi, Rva, Lb, Pda, Pdr and Pki. As a result of the changes, the non-specific amplification and the primer-dimers observed in **Figure 36** disappeared. Being the non-specific amplification and the primer-dimers any other band that was not 320 bp in size, which was the size of the target fragment of the *atpD* gene. Due to the lack of non-specific amplification, the *Pseudomonas* no longer amplified. Separation of DNA products by agarose gel electrophoresis confirmed that the target amplicon (320 bp fragment of the *atpD* gene) was present in Bg, Brr, Gq, Rvi, Rva, and Lb and absent in *Pseudomonas*: Pda, Pdr and Pki. The agarose gel electrophoresis band present in the samples Bg, Brr, Gq, Rvi, Rva, and Lb was 320 bp of size and no gel bands were observed for samples Pda, Pdr, and Pki.

To be able to detect and differentiate also AOD-associated *Pseudomonas* with this assay, a couple of different primers were tested. The primers PsEG30F and PsEG790R targeted a portion of 746 bp of the *rpoD* gene. PsEG30F and PsEG790R were genus specific for *Pseudomonas* (Mulet et al., 2009), and they amplified their target in *Pseudomonas* but no amplification was observed in Bg, Brr, Gq, Rvi, Rva, and Lb. The amplicons generated by PsEG30F and PsEG790R were resolved by agarose gel electrophoresis. A gel band of approximately 750 bp was observed for the samples Pda, Pdr, and Pki, and no bands were observed in Bg, Brr, Gq, Rvi, Rva, and Lb.

When the four primers (Gq6bF, AOD1R, PsEG30F and PsEG790R) were used in combination, distinguishable melting profiles were observed for all samples, except for Rvi and Rva which generated indistinguishable melting profiles (**Figure 37**). In addition, as observed in the fluorescence plots, the 320 bp fragment of the *atpD* and the 746 bp fragment of the *rpoD* gene were clearly discernible by their melting temperatures (**Figure 37**). The substantial differences in the melting temperatures between the *atpD* and the *rpoD* genes were due to factors such as the differences in amplicon size, G + C mol %, etc. Samples were grouped into eight clusters using the tool ScreenClust. Each cluster represented a different species with the exception of the samples Rvi and Rva which shared the same cluster, indicated by red arrows in (**Figure 38**).

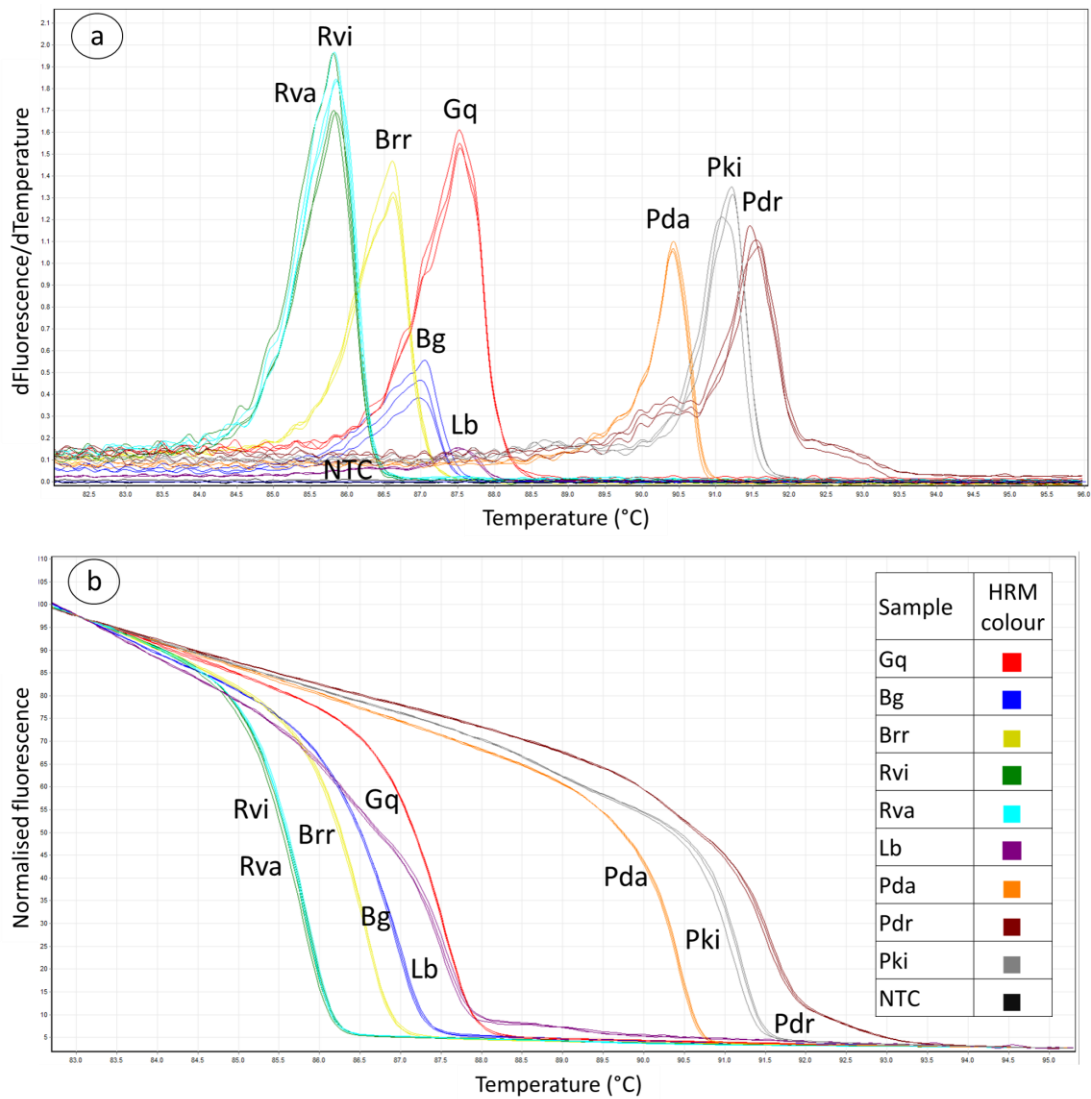


Figure 37: Derivative (a) and normalised (b) fluorescence plots of the duplex-HRM assay of genes *atpD* and *rpoD* for the identification of AOD-associated bacteria including *Pseudomonas*. The samples analysed by duplex-HRM were the type strains of the AOD-associated bacteria: *Gibbsiella quercinecans* (Gq), *Brenneria goodwinii* (Bg), *Brenneria roseae* ssp. *roseae* (Brr), *Rahnella victoriana* (Rvi), *Rahnella variigena* (Rva), *Lonsdalea britannica* (Lb), *Pseudomonas daroniae* sp. nov. (Pda), *Pseudomonas dryadis* sp. nov. (Pdr), and *Pseudomonas kirkiiae* sp. nov. (Pki). The primers used in this HRM assay were Gq6bF, AOD1R, PsEG30F and PsEG790R. NTC = non-template control.

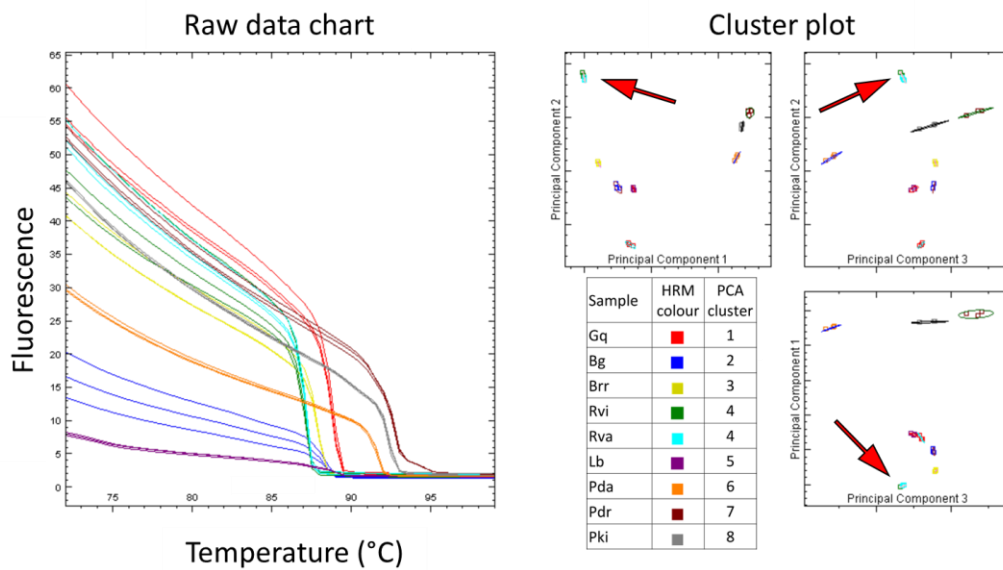


Figure 38: Unsupervised ScreenClust cluster analysis of the data set obtained in the duplex-HRM assay of genes *atpD* and *rpoD* for the identification of AOD-associated bacteria including *Pseudomonas*. ScreenClust tool was used for the statistical interrogation of the raw HRM data obtained from the Rotor-Gene cycler (raw data chart), allowing the software to choose the most appropriate cluster number and principal component number (unsupervised mode). The HRM data was obtained by duplex-HRM of the type strains of the AOD-associated bacteria: *Gibbsiella quercinecans* (Gq), *Brenneria goodwinii* (Bg), *Brenneria roseae ssp. roseae* (Brr), *Rahnella victoriana* (Rvi), *Rahnella variigena* (Rva), *Lonsdalea britannica* (Lb), *Pseudomonas daroniae* sp. nov. (Pda), *Pseudomonas dryadis* sp. nov. (Pdr), and *Pseudomonas kirkiae* sp. nov. (Pki). The number of clusters and principal components selected by default were 3 and 8, respectively. The 8 clusters are highlighted by ellipses in the cluster plot. The red arrows point at the cluster that contains Rvi and Rva.

5.2.4. Multiplex-HRM assay for the detection and identification of Bg, Gq, Rvi, and Lb

Up to this point, tools had been designed for use with pure samples (a single bacterial species). However, a diagnostic tool able to detect and identify AOD-associated bacteria from environmental samples (several, mixed bacterial species) was also needed and so a multiplex-HRM assay was designed to meet this demand (**section 2.6.4.**). The targets chosen were the species Bg, Gq, Rvi and Lb. A pair of primers was created for specific fragments of each of the target's genomes of the targeted species, Bg, Gq, Rvi and Lb (**Table 5**). The specificity of each of the primer pairs was assessed by testing them in singleplex-HRM reactions. It was observed that the primers did not bind to any non-targets (i.e. primers Bgi2F and Bgi2R, designed to amplify only Bg, did not amplify Gq, Rvi or Lb). Once the specificity of the primers within the 4 bacterial targets was confirmed, all the primers were combined and used in further reactions.

Pure samples of Bg, Gq, Rvi and Lb were tested in the same multiplex-HRM assay to compare the T_m of the amplicons generated. The T_m of amplicons generated by the primers Bgi2F, Bgi2R, Gqi3F, Gqi3R, Rvii1F, Rvii1R, Lbi2F, and Lbi2R did not overlap, in fact they differed from each other by more than 2.5 °C, resulting in the derivative melting profiles easily distinguishable for each of the four targets (**Figure 39**).

The derivative fluorescence peak for Bg, Gq and Rvi were similar in height (derivate of the fluorescence / derivate of the temperature) this was expected because although the efficiency of a PCR does not only depend on that, the targeted amplicons were present in their genomes the same amount of times (in this case all the targets are embedded in single copy genes). However, the derivative fluorescence peak for Lb was greater than the rest because the target sequence is contained in a double copy gene; this feature was intended, the aim was to ensure the detection of LB, which is the least common isolated target of the four (**Figure 39**).

Samples were grouped using the tool ScreenClust. Technical replicates for the same species were grouped into the same cluster and different species were grouped into separate clusters (**Figure 40**).

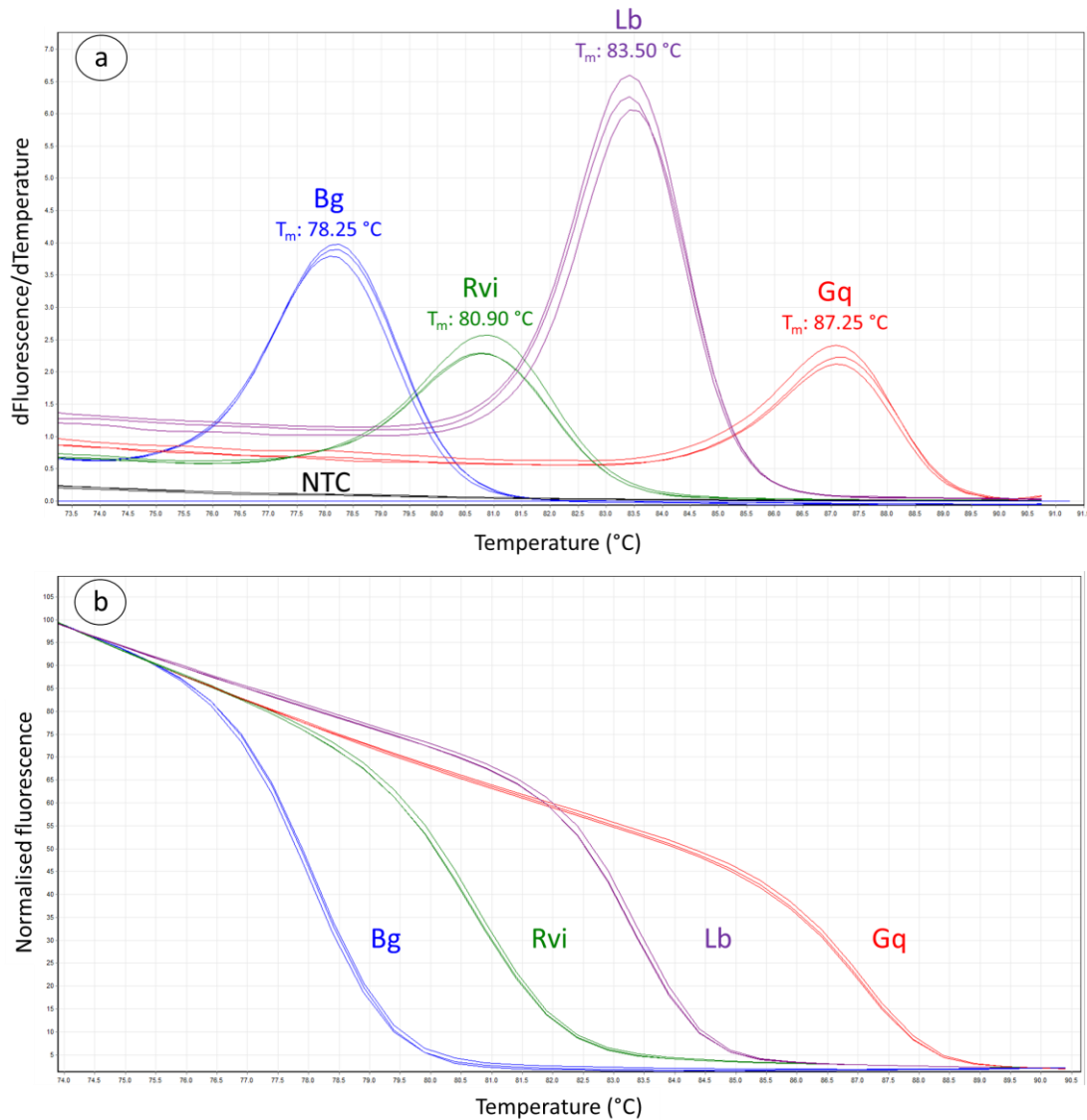


Figure 39: Derivative (a) and normalised (b) fluorescence plots of the multiplex-HRM assay for the detection and identification of AOD-associated bacteria *Brenneria goodwinii* (Bg), *Gibbsiella quercinecans* (Gq), *Rahnella victoriana* (Rvi) and *Lonsdalea britannica* (Lb). Melting points (T_m) and curve profiles for all samples are distinguishable and melting points are a minimum of 2.5 °C different from each other. The primers used in this HRM assay were Bgi2F, Bgi2R, Gqi3F, Gqi3R, Rvii1F, Rvii1R, Lbi2F, and Lbi2R. NTC = non-template control.

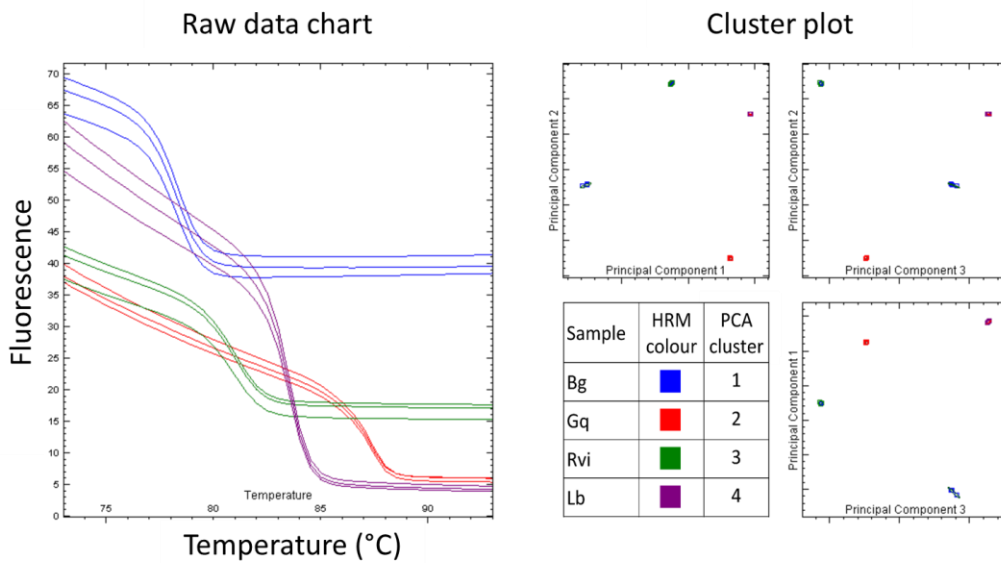


Figure 40: Unsupervised ScreenClust cluster analysis of the data set obtained in the multiplex-HRM assay for the detection and identification of AOD-associated bacteria *Brenneria goodwinii* (Bg), *Gibbsiella quercinecans* (Gq), *Rahnella victoriana* (Rvi) and *Lonsdalea britannica* (Lb). ScreenClust tool was used for the statistical interrogation of the raw HRM data obtained from the Rotor-Gene cyler (raw data chart), allowing the software to choose the most appropriate cluster number and principal component number (unsupervised mode). The number of clusters and principal components selected by default were 3 and 4, respectively. The 4 clusters are highlighted by ellipses in the cluster plot.

5.2.4.1. Multiplex-HRM assay specificity test

The multiplex-HRM assay was able to detect and identify AOD-associated bacteria from cultured pure samples using primers intended to be species-specific. Here, the species-specificity of the primers was tested against several partially identified isolates collected from AOD sites, which are phylogenetically similar to the targets of the multiplex-HRM (**section 2.6.4.1**). These are referred to as “Other species” in the figures below: *Erwinia billingiae* (strains 119, 157, R-45), *Pantoea* sp. (strains 120, 121, 124, DI 19b and DI 7a), *Enterobacter* sp. (strain 123), *Serratia proteamaculans* (strain 126.2), *Ewingella americana* (strains LMG 7869^T and FOD 24/3b), and *Erwinia rhapontici* (strains A3 P19 and Outwood 149) (**Figure 41**). Positive controls Bg, Gq, Rvi and Lb were added to the test. The strains of the “Other species” group did not generate any false positives.

As well as testing the specificity of the multiplex-HRM method against AOD-associated isolates, phylogenetically similar to the targets, the specificity was tested also against other species from the genera *Brenneria*, *Gibbsiella*, *Rahnella* and *Lonsdalea*. These included type strains of: *Brenneria roseae* subsp. *americana*, *Brenneria roseae* subsp. *roseae*, *Brenneria alni*, *Brenneria salicis*, *Brenneria nigrifluens*, *Brenneria rubrifaciens*, *Gibbsiella dentisursi*, *Gibbsiella greigii*, *Rahnella bruchi*, *Rahnella variigena*, *Rahnella woolbedingensis*, *Rahnella inusitata*, *Rahnella aquatilis*, *Lonsdalea iberica* and *Lonsdalea quercina*. The multiplex-HRM assay testing the species contained in the genera *Brenneria*, *Gibbsiella*, *Rahnella* and *Lonsdalea* was species-specific for Bg, Rvi, and Lb, and genus-specific in the case of *Gibbsiella*. All species tested except those belonging to *Gibbsiella*, showed a completely flat derivative profile, as for the NTC. In the case of the members of *Gibbsiella*, a derivative peak was observed at 87.25 °C in the three species and a second peak was also observed in *Gibbsiella dentisursi* at 81.75 °C (**Figure 42**).

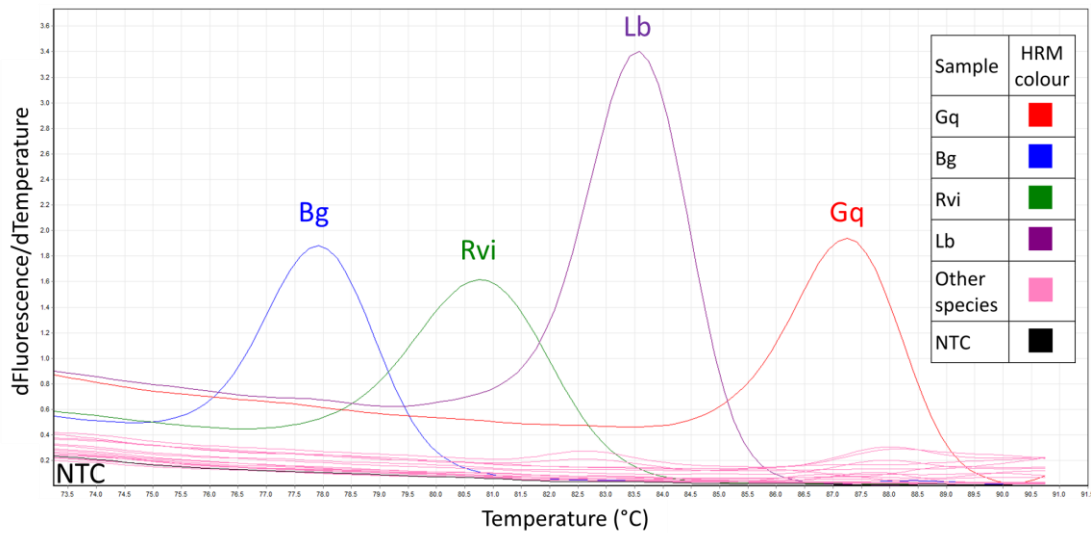


Figure 41: Derivative fluorescence plot of the multiplex-HRM assay for the detection and identification of AOD-associated bacteria *Brenneria goodwinii* (Bg), *Gibbsiella quercinecans* (Gq), *Rahnella victoriana* (Rvi) and *Lonsdalea britannica* (Lb). The samples contained in the “Other species” group were isolates commonly found in AOD sites and phylogenetically close to the targets of the multiplex-HRM assay: *Erwinia billingiae* (strains 119, 157, R-45), *Pantoea* sp. (strains 120, 121, 124, DI 19b and DI 7a), *Enterobacter* sp. (strain 123), *Serratia proteamaculans* (strain 126.2), *Ewingella americana* (strains LMG 7869^T and FOD 24/3b), and *Erwinia rhapontici* (strains A3 P19 and Outwood 149). The primers used in this HRM assay were Bgi2F, Bgi2R, Gqi3F, Gqi3R, Rvii1F, Rvii1R, Lbi2F, and Lbi2R. NTC = non-template control.

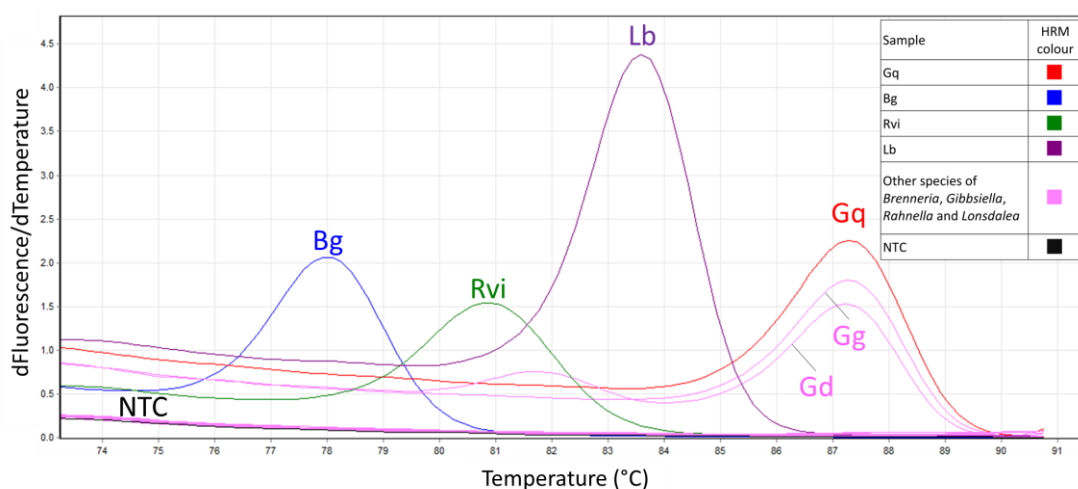


Figure 42: Derivative fluorescence plot of the multiplex-HRM assay for the detection and identification of AOD-associated bacteria *Brenneria goodwinii* (Bg), *Gibbsiella quercinecans* (Gq), *Rahnella victoriana* (Rvi) and *Lonsdalea britannica* (Lb). The species tested (in pink) were those belonging to the genera *Brenneria*, *Gibbsiella*, *Rahnella* and *Lonsdalea*. These included type strains of: *Brenneria roseae* subsp. *americana*, *Brenneria roseae* subsp. *roseae*, *Brenneria alni*, *Brenneria salicis*, *Brenneria nigrifluens*, *Brenneria rubrifaciens*, *Gibbsiella dentisursi* (Gd), *Gibbsiella greigii* (Gg), *Rahnella bruchi*, *Rahnella variigena*, *Rahnella woolbedingensis*, *Rahnella inusitata*, *Rahnella aquatilis*, *Lonsdalea iberica* and *Lonsdalea quercina*. The primers used in this HRM assay were Bgi2F, Bgi2R, Gqi3F, Gqi3R, Rvii1F, Rvii1R, Lbi2F, and Lbi2R. NTC = non-template control.

5.2.4.2. Multiplex-HRM assay sensitivity test

The multiplex-HRM assay was found to be specific for the bacterial species tested (**section 2.6.4.2**). Here, the sensitivity of the assay was tested by performing the multiplex-HRM assay on serial dilutions of species of interest (Bg, Gq, Rvi and Lb). The minimum number of CFU that the multiplex-HRM assay was able to detect was 16,000 CFU of Bg (dilution factor 10^{-2}), 284 CFU of Gq (dilution factor 10^{-4}), 2,480 CFU of Rvi (dilution factor 10^{-3}), and 296 CFU of Lb (dilution factor 10^{-4}) (**Figure 43**).

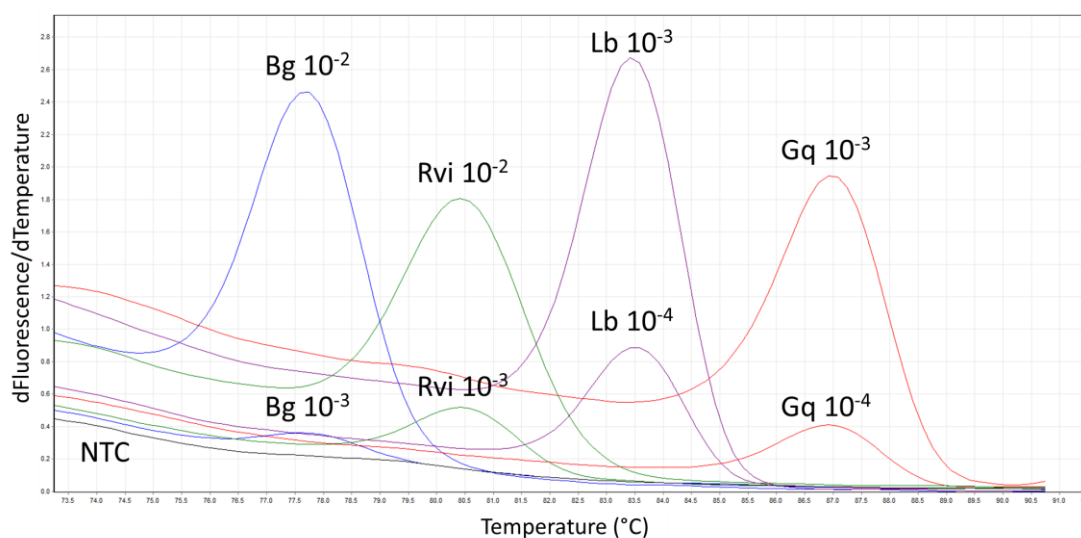


Figure 43: Derivative fluorescence plot of the sensitivity study of the multiplex-HRM assay for the detection and identification of AOD-associated bacteria *Brenneria goodwinii* (Bg), *Gibbsiella quercinecans* (Gq), *Rahnella victoriana* (Rvi) and *Lonsdalea britannica* (Lb). The lower limit of detection of the multiple-HRM method was tested by analysing serial dilutions of cell suspensions of each of the targets (Bg, Gq, Rvi and Lb). The primers used in this HRM assay were Bgi2F, Bgi2R, Gqi3F, Gqi3R, Rvii1F, Rvii1R, Lbi2F, and Lbi2R. NTC = non-template control.

5.2.5. SNP-based HRM assay for the differentiation of species and subspecies of the genus *Brenneria*

To differentiate between the species and subspecies of a particular isolate known to belong to the genus *Brenneria*, a SNP-based HRM assay was developed (**section 2.6.5**). The SNP-based HRM assay used primers Bgi3F and Bgi3R (**Table 5**). All available type strains of species and subspecies of *Brenneria* were added to this study: *Brenneria goodwinii* (Bg), *Brenneria roseae* ssp. *roseae* (Brr), *Brenneria roseae* ssp. *americana* (Bra), *Brenneria alni* (Ba), *Brenneria nigrifluens* (Bn), *Brenneria salicis* (Bsa) and *Brenneria rubrifaciens* (Bru). Species *Brenneria corticis* and *Brenneria populi* were not tested in vitro because they were unavailable in the Korean and Chinese culture collections, where they were deposited, due to restrictions on the Korean plant protection law, and a technical problem in the Chinese website. Whole genome sequence data from *Brenneria corticis* was available, but the species was not

available in any culture collection, therefore, although melt curve predictions were generated for *B. corticis*, results are not shown because the species was not tested *in vitro*.

Amplification was observed for all samples by cycle 19 with the exception of samples Bsa and Bru. Samples Bru and Ba amplified about 8 PCR cycles later than the rest of the samples and also had a lower derivative fluorescence, but they were still visually distinguishable from the rest of the samples. Low late amplification after cycle 33 was observed in the NTC and it was attributed to the formation of primer dimers (**Figure 44**). All species tested were distinguishable by comparing T_m and derivative fluorescence for each species. The individual melting curves for each of the species and subspecies of *Brenneria* differed by a temperature shift or curve shape, according to the presence of single nucleotide polymorphisms of the DNA sequence amplified by the primers (**Figure 44**). HRM results were analysed in the tool ScreenClust; the technical replicates for each species clustered together and in separate clusters from the other species (**Figure 45**). This assay was designed for its use with pure cultures.

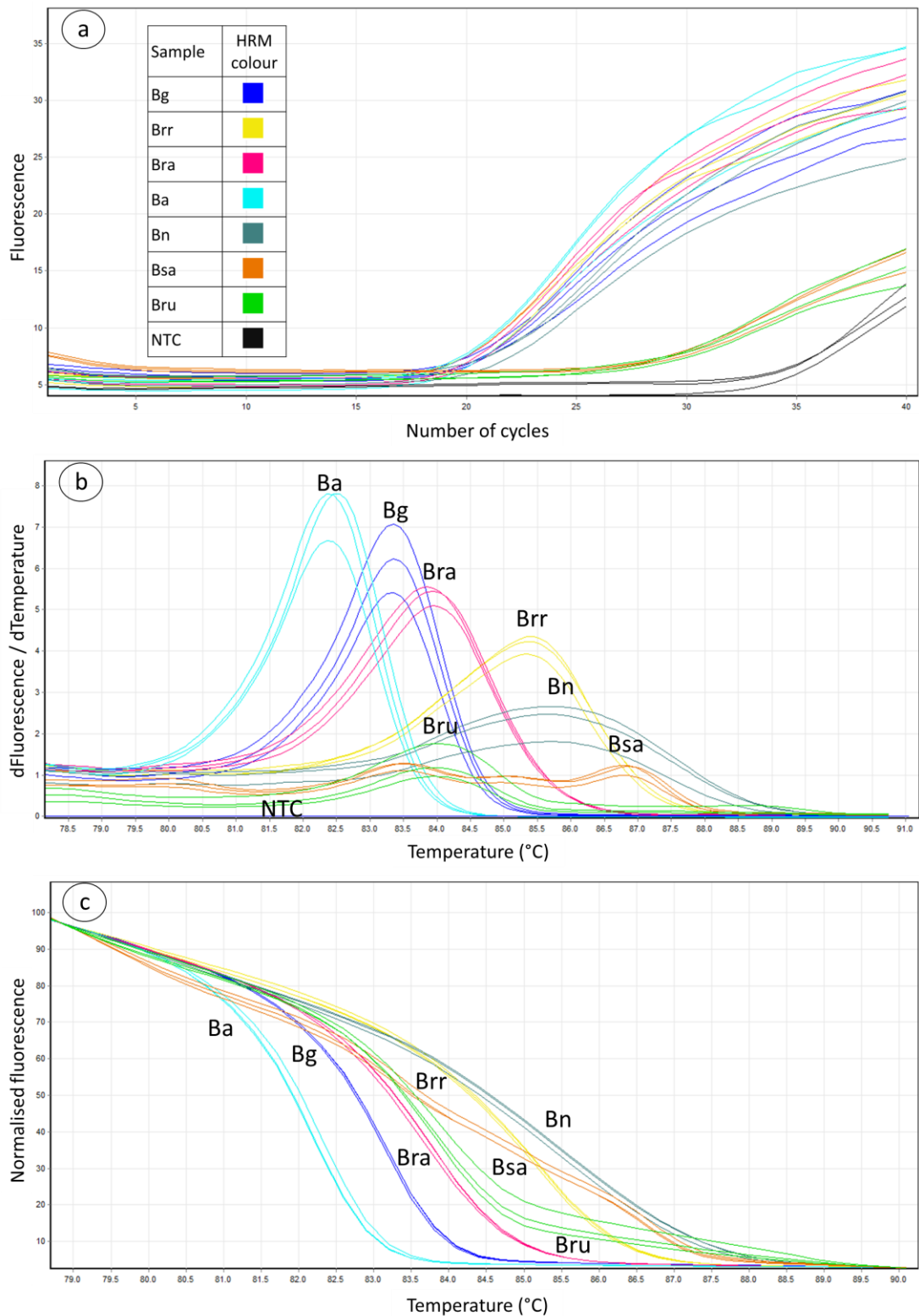


Figure 44: Amplification (a), derivative (b) and normalised (c) fluorescence plots of the single nucleotide polymorphism (SNP)-based HRM assay for the differentiation of species and subspecies of the genus *Brenneria*. Samples included in the assay were type strains of *Brenneria goodwinii* (Bg), *Brenneria roseae* ssp. *roseae* (Brr), *Brenneria roseae* ssp. *americana*

(Bra), *Brenneria alni* (Ba), *Brenneria nigrifluens* (Bn), *Brenneria salicis* (Bsa) and *Brenneria rubrifaciens* (Bru). The primers used in this HRM assay were Bgi3F and Bgi3R. NTC = non-template control.

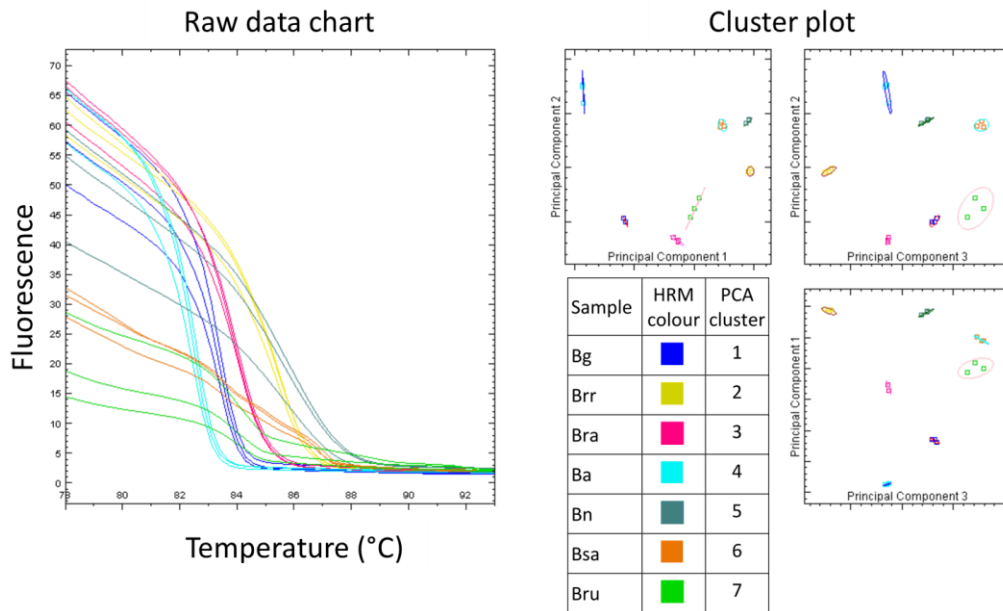


Figure 45: Unsupervised ScreenClust cluster analysis of the data set obtained in the single nucleotide polymorphism (SNP)-based HRM assay for the differentiation of species and subspecies of the genus *Brenneria*. Samples included in the assay were the type strains of *Brenneria goodwinii* (Bg), *Brenneria roseae* ssp. *roseae* (Brr), *Brenneria roseae* ssp. *americana* (Bra), *Brenneria alni* (Ba), *Brenneria nigrifluens* (Bn), *Brenneria salicis* (Bsa) and *Brenneria rubrifaciens* (Bru). ScreenClust tool was used for the statistical interrogation of the raw HRM data obtained from the Rotor-Gene cycler (raw data chart), allowing the software to choose the most appropriate cluster number and principal component number (unsupervised mode). The number of clusters and principal components selected by default were 3 and 7, respectively. The 7 clusters are highlighted by ellipses in the cluster plot.

5.2.6. SNP-based HRM assay for the differentiation of species of the genus *Rahnella*

To elucidate the species of a particular isolate known to belong to the genus *Rahnella*, a SNP-based HRM assay was developed (**section 2.6.5.1**). The SNP-based HRM assay used primers specific for *Rahnella*, Rvii1F and Rvii1R. The species included in the assay were the type strains of *Rahnella victoriana* (Rvi), *Rahnella variigena* (Rva), *Rahnella bruchi* (Rbru), *Rahnella woolbedingensis* (Rwo), *Rahnella aquatilis* (Raq), and *Rahnella inusitata* (Rinu). The individual melting curves for each of the species and subspecies of *Rahnella* differed by a temperature shift or curve shape, according to the presence of SNPs of the DNA sequence amplified by the primers (**Figure 46**). Rvi's T_m , $81.1 (\pm 0.09)$, was more than 4 °C different than the rest of the species tested, whose T_m s were within the region $88.35 (\pm 0.09)$ °C to $89.42 (\pm 0.08)$ °C, suggesting that primers only bind to the target in Rvi. More than one peak was observed in samples Rva, Rwo, Raq and Rinu, indicating non-specific amplification, which helps in the discrimination amongst these samples. Screenclust clustered technical replicates for each of the species in the same cluster, and different species were grouped in different clusters (**Figure 47**). This assay was designed for its use with pure cultures.

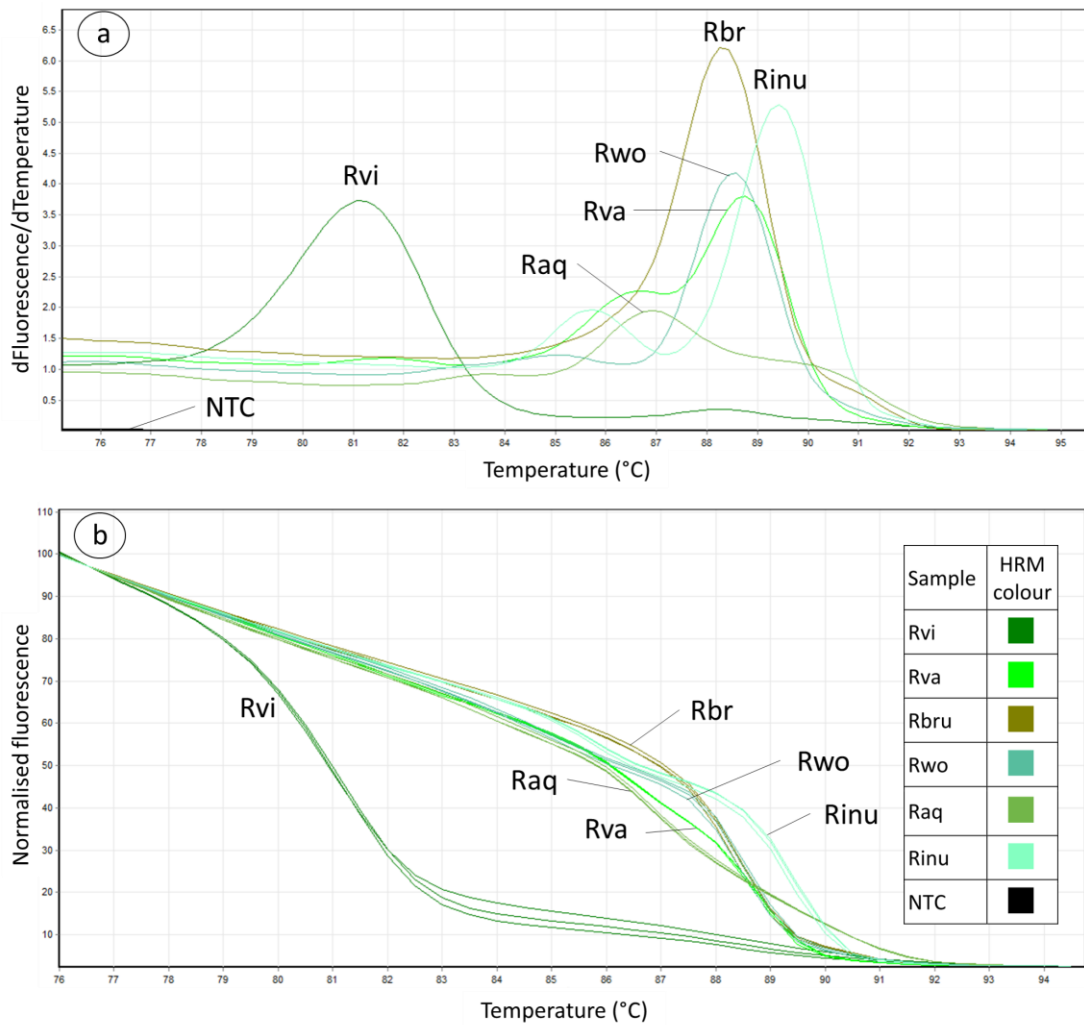


Figure 46: Derivative (a) and normalised (b) fluorescence plots of the single nucleotide polymorphism (SNP)-based HRM assay for the differentiation of species of the genus *Rahnella*. Samples included in the assay were the type species of *Rahnella victoriana* (Rvi), *Rahnella variigena* (Rva), *Rahnella bruchi* (Rbru), *Rahnella woolbedingensis* (Rwo), *Rahnella aquatilis* (Raq), and *Rahnella inusitata* (Rinu). The HRM primers used were Rvii1F and Rvii1R. NTC = non-template control.

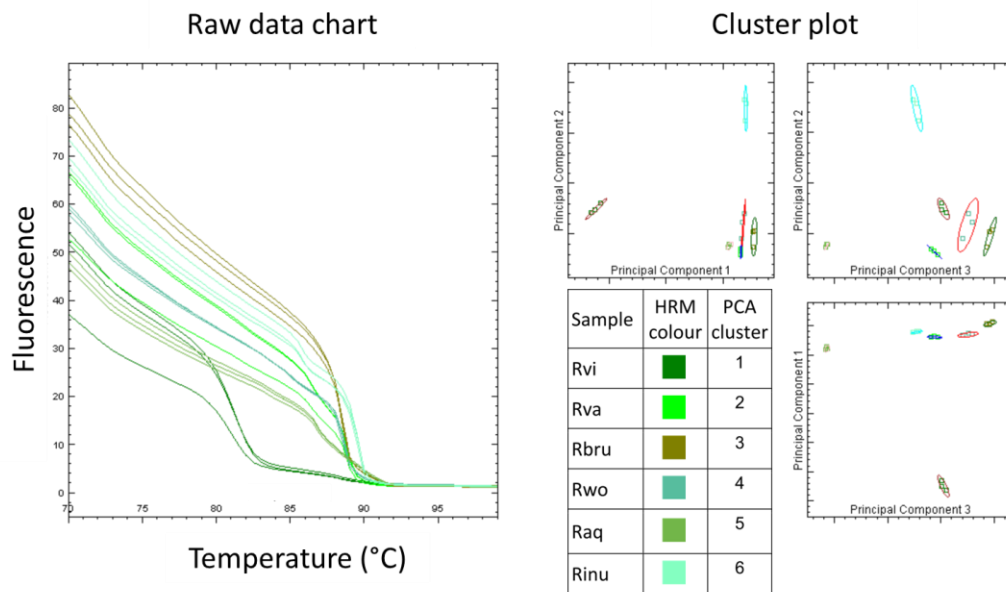


Figure 47: Unsupervised ScreenClust cluster analysis of the data set obtained in the single nucleotide polymorphism (SNP)-based HRM assay for the differentiation of species of the genus *Rahnella*. Samples included in the assay were the type strains of *Rahnella victoriana* (Rvi), *Rahnella variigena* (Rva), *Rahnella bruchi* (Rbru), *Rahnella woolbedingensis* (Rwo), *Rahnella aquatilis* (Raq), and *Rahnella inusitata* (Rinu). ScreenClust tool was used for the statistical interrogation of the raw HRM data obtained from the Rotor-Gene cycler (raw data chart), allowing the software to choose the most appropriate cluster number and principal component number (unsupervised mode). The number of clusters and principal components selected by default were 3 and 6 respectively. The 6 clusters are highlighted by ellipses in the cluster plot.

5.2.7. SNP-based HRM assay for the differentiation of species of the genus *Gibbsiella*

To elucidate the species of a particular isolate known to belong to the genus *Gibbsiella*, a SNP-based HRM assay was developed (**section 2.6.5.2**). The SNP-based HRM assay used primers specific for species of *Gibbsiella*, Gqi4F and Gqi4R. The species included in the assay were strains FRB 97^T, BH 1/65b, AT 18b, BH 1/86 and Kew 224 of *Gibbsiella quercinecans*; strains FRB 224^T, USA 42, R 52b, R 54a and R66a of *Gibbsiella greigii*; and the synonyms, strain DSM 23818^T of *Gibbsiella dentisursi* and strain JCM 18389^T of *Gibbsiella papilionis*. The individual melting curves for each of the species and subspecies of *Gibbsiella* differed by a temperature shift or curve shape, according to the presence of SNPs of the DNA sequence amplified by the primers. Amplification was observed for Gq strains before the cycle 23, whereas for the other two species amplification was not observed until the cycle 29 (**Figure 48a**). In addition to these differences, the derivative melting profile of Gg was clearly distinguishable from the rest because its melt profile was similar to the NTC probably due to the primers missing the target (**Figure 48b**). The differences amongst Gq and Gd were more subtle, amplicons generated by both Gq and Gd had similar T_m . However Gd amplified approximately 7 cycles later than Gq and therefore its derivative peak was visually lower. Normalised curves were visually distinguishable, (**Figure 48c**), and ScreenClust clustered each species in a separate cluster (**Figure 49**). This assay was designed for its use with pure cultures.

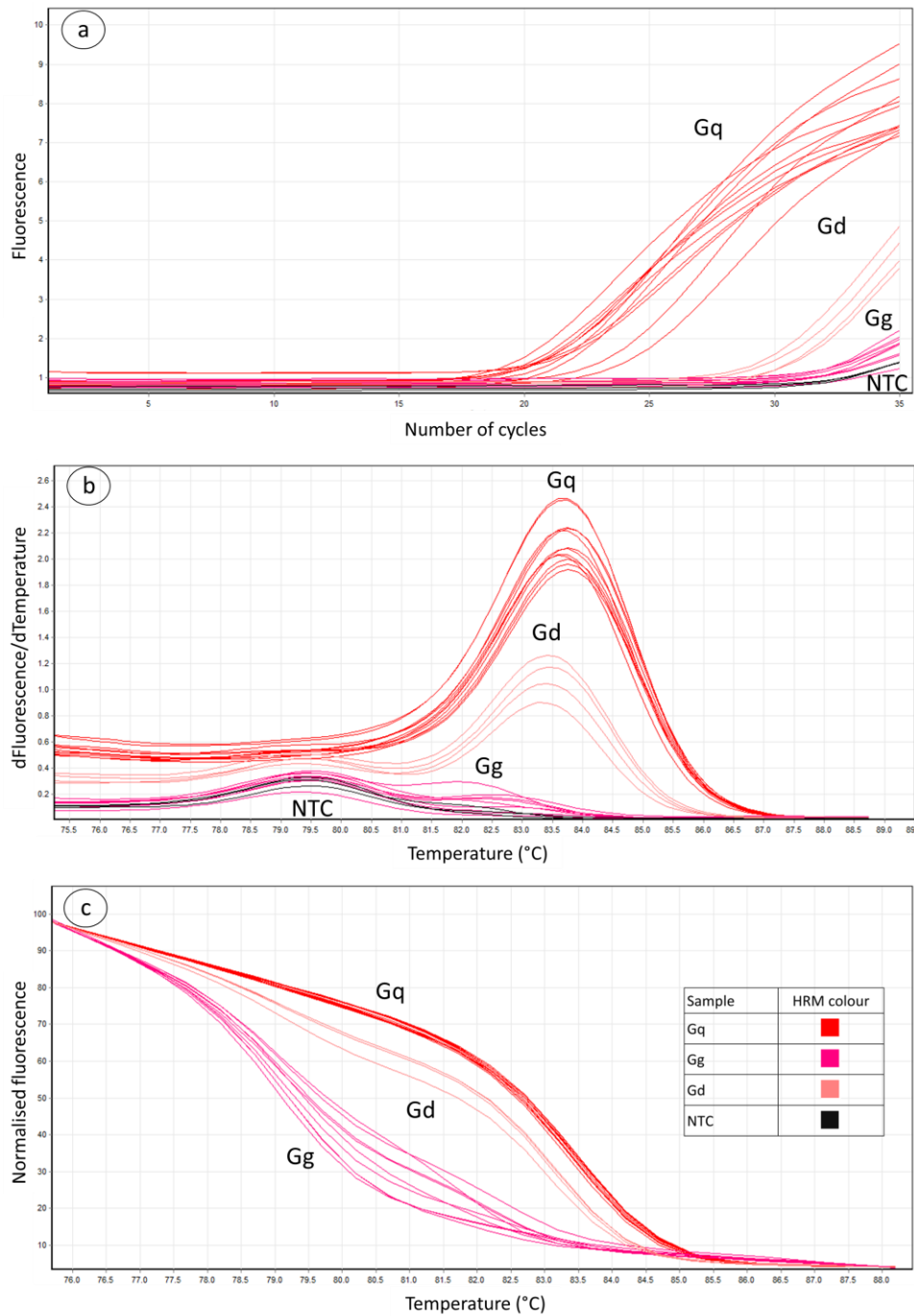


Figure 48: Amplification (a), derivative (b) and normalised (c) fluorescence plots of the single nucleotide polymorphism (SNP)-based HRM assay for the differentiation of species of the genus *Gibbsiella*. Samples included in the assay were strains FRB 97^T, BH 1/65b, AT 18b, BH 1/86 and Kew 224 of *Gibbsiella quercinecans*; strains FRB 224^T, USA 42, R 52b, R 54a and R66a of *Gibbsiella gregii*; and the synonyms, strain DSM 23818^T of *Gibbsiella dentisursi* and strain JCM 18389^T of *Gibbsiella papilionis*. The HRM primers used were Gqi4F and Gqi4R. NTC = non-template control.

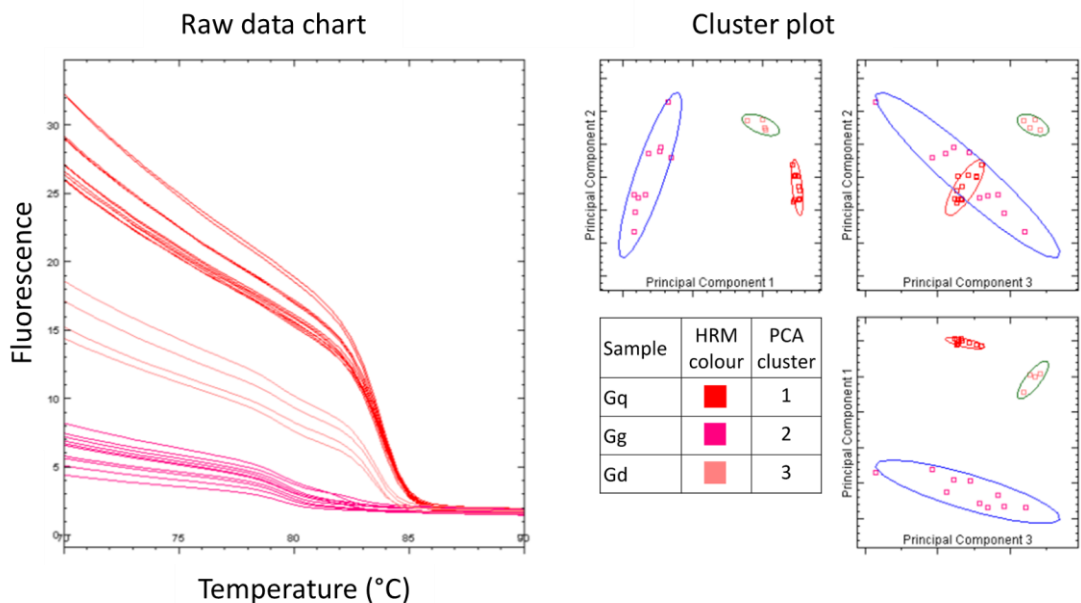


Figure 49: Unsupervised ScreenClust cluster analysis of the data set obtained in the single nucleotide polymorphism (SNP)-based HRM assay for the differentiation of species of the genus *Gibbsiella*. Samples included in the assay were the species included in the assay were strains FRB 97^T, BH 1/65b, AT 18b, BH 1/86 and Kew 224 of *Gibbsiella quercinecans*; strains FRB 224^T, USA 42, R 52b, R 54a and R 66a of *Gibbsiella greigii*; and the synonyms, strain DSM 23818^T of *Gibbsiella dentisursi* and strain JCM 18389^T of *Gibbsiella papilionis*. ScreenClust tool was used for the statistical interrogation of the raw HRM data obtained from the Rotor-Gene cycler (raw data chart), allowing the software to choose the most appropriate cluster number and principal component number (unsupervised mode). The number of clusters and principal components selected by default were 3 in both cases. The 3 clusters are highlighted by ellipses in the cluster plot.

5.3. Discussion

This chapter reports the development of several HRM-based assays to work with pure and mixed samples of AOD-associated bacteria. One duplex-HRM assay, one multiplex-HRM assay and three SNP-based HRM assays. The targets for each of the assays are very different. The duplex-HRM assay is aimed at the differentiation of pure cultures of AOD-associated bacteria, including pathogens, and frequently isolated bacteria of unknown role in the disease. The targets of the SNP-based HRM assays are pure samples of one of the three genera *Brenneria*, *Gibbsiella* or *Rahnella*. And the multiplex-HRM is aimed at the diagnosis of the four most suitable AOD indicators from mixed (field) samples.

Typically, samples analysed by HRM are processed prior to the assay. The DNA of the sample is usually extracted, purified and the concentration is standardised prior to HRM analysis. To remove this time consuming step and its associated cost, and with the aim to develop a rapid diagnostic tool, different sample preparation methods were compared and their suitability for HRM testing was assessed, concluding that cell suspensions in water and LB broths were suitable for direct HRM testing (**Figure 33**). The amplicons generated from cells in water melted at lesser temperatures than amplicons generated from cells suspended in LB broth. The difference between the samples in water and in broth is the liquid in which the cells are suspended in, suggesting that the LB broth challenges the dissociation of the DNA strands, requiring a higher temperature for their denaturation.

Before designing new diagnostic tools, training in HRM technique was acquired by replicating the work in (Brady et al., 2016), and by testing the limits of this assay. The HRM of the *atpD* gene (119 bp) proved unsuitable for mixed samples because whenever certain species like Gq were present in the mixture, the presence of other species was concealed **Figure 34**. A new primer (AOD1R) was then designed to work in combination with the forward primer from the study mentioned above (Gq6bF). This method targeted a bigger region of the same gene, and complemented with gel electrophoresis, discriminated effectively amongst all the AOD associated bacteria, including species difficult to differentiate, like those belonging to the genus *Rahnella* (**Figure 36**). The HRM of the *atpD* gene combined with agarose gel fingerprinting can be applied exclusively to pure cultures and it takes approximately two hours extra in comparison to HRM only assays, because of the gel. In conclusion this technique is suitable for confirmation but not for routine screening of samples. This method could complement other identification assays or serve as confirmation method for any dubious bacterial identification.

To dispense with the gel electrophoresis, the HRM assay of the 320 bp fragment of the *atpD* gene was adjusted to eliminate non-specific amplification artefacts. After adjusting primer concentrations and PCR conditions, the primers Gq6bF and AOD1R were unable to anneal to *Pseudomonas*. To make the assay also able to detect also *Pseudomonas*, the primers Gq6bF and AOD1R were complemented with an extra pair of primers: PsEG30F and PsEG790R, which targeted a fragment of the *rpoD* gene. PsEG30F and PsEG790R are specific for *Pseudomonas* (Mulet et al., 2009). The duplex-HRM assay based on the combination of primers Gq6bF, AOD1R, PsEG30F and PsEG790R was an effective and rapid method for species identification from pure cultures, with the caveat of being specific only at genus level in the case of *Rahnella* (**Figure 37**). The duplex-HRM assay could be implemented as routine screening method for identification of pure samples of bacteria associated with AOD. Although in **Chapter 4**, a series of results suggested that the AOD-associated *Pseudomonas* are not pathogenic, the duplex-HRM assay of *atpD* and *rpoD* for the identification of AOD-associated bacteria including AOD-associated *Pseudomonas* could be very useful. This is because there is an increasing amount of projects related to AOD that focus in bacterial species interactions and bacterial community dynamics.

The HRM assays for the identification of pure cultures will hopefully be useful for many research projects in the interdisciplinary group studying AOD, and have already proven useful in this project. However, in addition to these, a tool for the diagnostic of AOD-affected environmental samples (mixture of bacteria) was still needed. To develop the diagnostic assay for environmental samples (multiplex-HRM), it was essential to have a clear list of targets and non-targets for the method. The ideal target for the diagnostic method of a microbial disease is a microbe that it is present in 100% of the diseased samples and absent from disease-free samples.

The targets chosen for the multiplex-HRM assay were the species *Brenneria goodwinii*, *Gibbsiella quercinecans*, *Rahnella victoriana* and *Lonsdalea britannica*. Why are those four species good targets? The microbiome associated with AOD lesions has been carefully studied although the roles of some of the bacterial species are still under study. Metabarcoding studies performed in 2016 did not find a shift of microbiome in AOD affected sites, but in AOD lesions there was clear dominance of a particular member of the family *Enterobacteraceae*, (called operational taxonomic unit 5035 in the study), that could possibly be Bg, which changed from *Enterobacteraceae* to *Pectobacteriaceae* later the same year (Adeolu et al., 2016; Sapp et al., 2016). In contrast, a study performed two years after, found

that there was a shift in the microbiome composition of healthy and diseased samples (Denman et al., 2018) (**Table 16**). According to that study, when the microbiome was characterised by traditional isolation techniques, Gq was found in 100 % of the diseased samples and Bg was isolated in 65 %. Gq and Bg were very rarely isolated from healthy samples, and very likely to be isolated from diseased samples (**Table 16**). The fact that Gq and Bg appeared in very low numbers in healthy trees might mean that these bacteria are hemibiotrophic pathogens or pathobionts, (Broberg *et al*, 2018). Pathobionts or hemibiotrophic pathogens are microorganisms that live in symbiosis with the host, but are able to become pathogenic when the conditions of the host change (van Overbeek and Saikkonen, 2016). According to Denman and colleagues, Rvi and Lb were less likely to appear in diseased samples than Gq and Bg (39 and 17 %, respectively), but they were never isolated from healthy samples (Denman et al., 2018) (**Table 16**). Metagenomic analysis of the lesion microbiome using the same samples, showed that, in fact, Bg was the most abundant bacteria, followed by Rvi, and Gq in the fourth place; Lb was very rarely found (Denman et al., 2018). Recently, a genomic study in the pathobiome of the lesion found that Bg and Lb are the primary pathogens, causing the tissue necrosis, and that the rest of the species in the pathobiome, including Gq and Rvi and *Rahnella variigena* (Rva) amongst others, could be collaborating in the maceration of the tissues as secondary phytopathogens by releasing necrotizing enzymes (Doonan et al., 2019). By comparing the whole genomes of the key members of the pathobiome with the genomes of known phytopathogens and endosymbionts, Doonan and his colleagues observed that Bg's genome contains pathogenic traits such as a type three secretion system. The secondary pathogens presented less pathogenicity traits in their genomes, and they could be enhancing the symptoms caused by Bg and Lb, like it happens in other polypathogen diseases such as the olive knot disease. In the olive knot disease, *Pantoea agglomerans* and species of the genome *Erwinia*, act as endosymbionts in the tree until the pathogen, *Pseudomonas savastanoi* pv. *savastanoi* triggers the disease, point in which the mentioned species act as disease enhancers (Buonauro et al., 2015).

Table 16: Isolation frequency of Gq, Bg, Rvi and Lb in sites and trees with different health status. Samples were collected and traditionally isolated from 38 AOD-diseased oaks from

23 sites, 13 healthy oaks in 11 of these sites, and 15 healthy oaks from five sites with no history of AOD. Data obtained from Denman *et al.*, 2018.

Taxon	Percentage of sites where each species was isolated		Percentage of trees where each species was isolated	
	Healthy tissue	Symptomatic tissue	Healthy trees*	Symptomatic trees
Gq	6.2	100	3.6	81.6
Bg	12.5	65.2	7.1	60.5
Rvi	0	39.1	0	36.8
Lb	0	17.4	0	13.1

* Total of 28 healthy trees: 13 from 11 AOD sites and 15 from no AOD sites. Gq: *Gibbsiella quercinecans*. Bg: *Brenneria goodwinii*. Rvi: *Rahnella victoriana*. Lb: *Lonsdalea britannica*.

Considering the compendium of AOD pathobiome studies Bg and Gq are the optimal targets for the diagnosis AOD. Rvi and Lb are less likely to be present in the sample or be detected depending on the sample preparation prior to HRM, but also seem to be good targets for the diagnosis of AOD. Once established the targets for the assay, a multiplex-HRM assay was developed for the detection and identification of Bg, Gq, Rvi and LB from field samples. This rapid assay (35 minutes long) is capable of detecting up to four targets in the same tube, and it is easy to set up, as the assay is based on PCR (**Figure 39**). The method, based on the amplification of target-specific amplicons with non-overlapping melting temperatures was inspired by a study that described a multiplex-HRM assay able to identify several gene variations involved in inflammatory pathways on preterm human birth (Pereyra *et al.*, 2012). Pereyra and her colleagues created a multiplex-HRM assay with four targets that were sequences containing particular SNPs in four different genes. The multiplex-HRM assay that I developed is different than Pereyra's assay because it is not based on SNP genotyping, but in the amplification of DNA sequences present in one target and absent from the rest. The differences between amplicons generated from the targets are in this case not SNPs but the complete nucleotide sequence, being the dissimilarities so tangible that the T_{ms} of the amplicons generated by the four targets differs by more than 2.5 °C. The T_{ms} of the amplicons generated four targets are so distinguishable that the primers of the multiplex HRM assay could work perfectly well with amplicon melting technologies less sensitive than HRM.

The multiplex-HRM method is specific for Bg, Rvi, Lb and the genus *Gibbsiella* (*Gibbsiella dentisursi* and *Gibbsiella greigii* have a curve profile identical to Gq) (**Figure 41**). The sensitivity of the test ranged from 284 to 16,000 CFU (**Figure 42** and **Figure 43**). HRM is not extremely sensitive, but the number of CFU is not a limiting factor when testing pure cultures, as plenty of cells should be available, and in the case of field samples, enrichment steps can be implemented to increase the number of CFU (**Chapter 6**).

Additional SNP-based HRM tools to differentiate pure cultures of species of *Brenneria*, *Rahnella* and *Gibbsiella* have also been developed and they are rapid and cost-effective ways to confirm species ID of a sample of a known genus (**Figure 44**, **Figure 46** and **Figure 48**). The individual melting curves observed for each of the samples differed by a temperature shift or curve shape, according to the presence of SNPs on the amplicons generated. Studies of specificity and sensitivity are still to be performed for these assays.

The multiplex-HRM assay is specific only at genus level in the case of *Gibbsiella*. However, the multiplex-HRM tool for the detection and identification of Bg, Gq, Rvi and Lb could be made species-specific for Gq if one of the targets, Lb, is eliminated from the assay. A multiplex-HRM assay, species-specific for Bg, Gq and Rvi could be achieved by simply swapping the primer pair Gqi3F - Gqi3R for those used in the SNP-based assay for discrimination of *Gibbsiella* species, Gqi4F - Gqi4R. The amplicons generated from Gq and Gd with Gqi4F-Gqi4R melt at 83.65 °C and 83.40 °C, respectively, which are too similar to 83.50 °C, the T_m of the amplicon generated by Lb in the original multiplex-HRM assay. The amplicons generated in the multiplex-HRM must melt at non-overlapping temperatures to be discernible in the fluorescence graphs. In this case, Gq, Gd and Lb cannot be distinguished from each other by their melting temperature. To compromise, four targets were chosen over three in the diagnostic method instead of having species-specificity for Gq. Even if the multiplex-HRM assay does not differentiate between species of *Gibbsiella*, a SNP-based HRM assay was developed for this purpose. The lack of species-specificity for the primers that target *Gibbsiella* in the multiplex-HRM assay, should not be a problem because the other species of the genus other than Gq, have never been isolated in AOD lesions so far. In conclusion, the multiplex-HRM tool can be adapted to the needs of the researcher. For a complete species-specificity when it comes to the detection of Bg, Gq and Lb, the combination of primers: Bgi2F, Bgi2R, Gqi4F, Gqi4R, Rvii1F, and Rvii1R is likely to work well because all primers have similar T_{ms} and the amplicons generated do not have overlapping

T_{ms} . However, this combination needs to be tested, and the detection of Lb would be no longer possible with this assay.

The molecular tools described in this chapter are intended to facilitate research related to AOD bacteria. Most of the HRM tools can complement each other to identify with accuracy the targets and confirm doubtful results. The HRM technique does not require any post-run manipulations such as electrophoresis gels or sequencing of amplicons, reducing drastically the risk of contamination. The estimated price of analysing one sample by HRM is £ 1. All the HRM assays described take less than an hour to set up and the setup is simple (like preparing for a PCR).

In conclusion, field samples collected from AOD lesions, containing a mixture of bacterial species can potentially be diagnosed using the multiplex-HRM assay for the detection and identification of Bg, Gq, Rvi, and Lb. The duplex-HRM assay of genes *atpD* and *rpoD* for the identification of AOD-associated bacteria including AOD-associated *Pseudomonas* could be helpful to differentiate between AOD-associated *Pseudomonas* and the rest of the most commonly isolated AOD-associated bacteria. Pure samples of *Brenneria* can be identified up to subspecies level using the SNP-HRM assay of the section 5.2.5. Pure samples of *Rahnella* and *Gibbsiella* can be identified up to species level using the SNP-HRM assays described in sections 5.2.6 and 5.2.7, respectively.

**CHAPTER 6. Optimisation of pre-HRM
field sample processing, and validation
of multiplex-HRM assay**

6.1. Introduction

The rapid and accurate detection and identification of microbial pathogens is a common challenge in public health and environment protection. The technology and approach chosen for the microbial diagnosis depends on the characteristics of the microbe and the type of sample under study. Normally, the target of a diagnostic method is a single microbial species, which causes the disease. In the case of AOD, the putative bacterial pathogens are several species of bacteria instead of only one.

In diagnostic microbiology, an environmental microbial sample can be diagnosed directly (i.e. mediated by electron or fluorescent microscopy); after culture and physiological examination (i.e. incubating the sample in selective media or different oxygen availability conditions); through culture-independent analysis of the microbiome by metagenomics, metatranscriptomics, metaproteomics and metabolomics, and by target-specific technologies based on antibody or DNA detection and microarray based methods. In the majority of the diagnostic methods that are based on PCR, the samples need some type of pre-assay preparation. This project focussed on the development of a diagnostic method using HRM technology. HRM is based on qPCR (quantitative PCR, real time PCR), (Higuchi et al., 1992, 1993; Wittwer et al., 1997), and as for the development of diagnostic methods based on real time PCR, there are a number of points to have in consideration during the design, optimization, and validation of an HRM assay. There are guidelines to find a consensus in the essential and desirable criteria to consider in order to improve experimental practice and interpretation of the data obtained by qPCR-based and HRM assays (Bustin et al., 2009; Van Der Stoep et al., 2009; Taylor et al., 2011). Firstly it is crucial to understand the type of environmental sample that will be diagnosed. One of the symptoms of AOD are vertical lesions in the stem from which dark fluid emanates (**Figure 50**). Generally, the samples collected from symptomatic oak are these dark exudates, although the diagnosis can also be performed from different types of plant material. It is necessary to consider the potential inhibitors contained in the sample, the amount of bacteria present in it, and the method for sample collection, handling and storage conditions. Once in the lab, it is sometimes necessary to add a pre-assay sample preparation step that might include the purification or enrichment of the sample. In the majority of cases the extraction and purification of the DNA is required. When designing the assay there are many factors to consider, such as the quality of the primers and master mix, the optimal amount of starting DNA template, the amplicon sequence, length, its localisation within the genome and

amplicon yield after PCR. Special attention to the thermocycler settings is also important, as well as a careful protocol design, validation and the evaluation of the HRM parameters (specificity and sensitivity tests of the assay), data analysis, results for the non-template controls, intra-assay variation studies (repeatability), inter-assay variation studies (reproducibility) (Bustin et al., 2009).

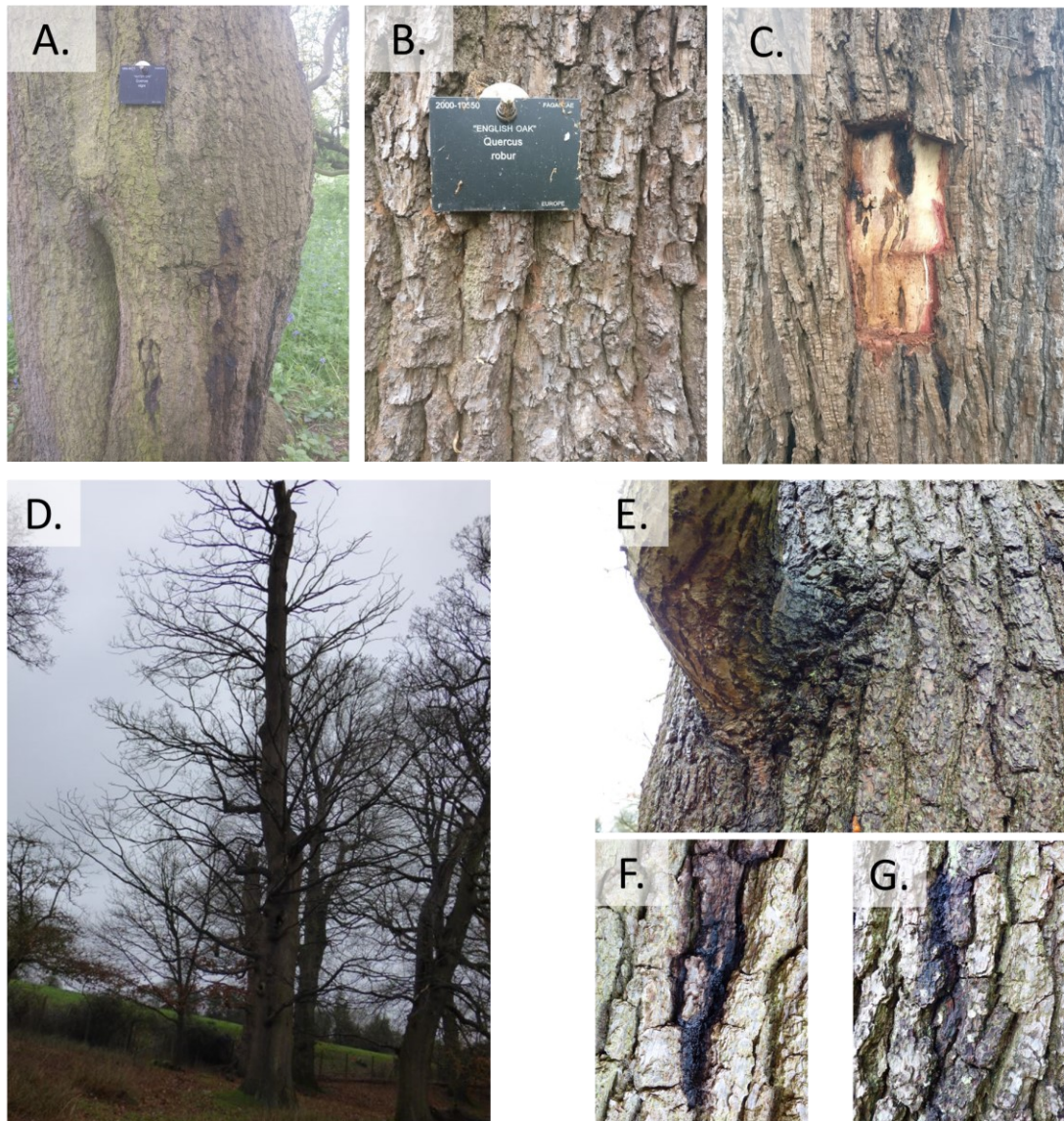


Figure 50: Trees sampled in Kew Gardens and Knole Park. A. *Quercus nigra* in Kew, reference number 16775. B. *Quercus robur* in Kew, reference number 10550. C. *Quercus robur* in Kew, reference number 19017. D., E., F., and G. *Quercus robur* in Knole Park, reference number 901.

To diagnose the samples from AOD-affected trees, the method followed by Forest Research for pre-assay sample processing is as follows:

1. The head of the swab used to collect the sample, was soaked in sterile distilled water (SDW). The cell suspension is taken into a 1mL syringe and filtered with constant pressure into a 1.5ml PCR tube using a 5µm pore hydrophilic syringe filter (Sartorius Stedim Biotech).
2. One mL of SDW is used to wash the sample through the filter and into the PCR tube.
3. The filtered sample is centrifuged at ≤ 13000 rpm for 4 minutes.
4. Supernatant is carefully discarded using a sterile pipette making sure not to dislodge the pellet.
5. One mL of SDW is added and then sample vortexed for 2 minutes at high speed or pipetted violently 30 times to mix.
6. Wash step is repeated centrifuging at ≤ 13000 rpm for 3 minutes.
7. The supernatant is discarded.
8. 100µL of SDW are added.
9. The suspension is vortexed.
10. Sample is then used in a qPCR or stored at -20 °C.
11. The details of the qPCR assay have recently been published (Crampton et al., 2020).

The aim of this chapter is to optimise the pre-HRM processing of the field samples obtained from stem AOD lesion or another plant material, and also to validate the multiplex-HRM assay described in **Chapter 5** by testing field samples.

6.2. Results

6.2.1. Field sample processing optimisation studies

In **Chapter 5** a series of techniques based on HRM were developed and tested under laboratory conditions. One of the HRM-based techniques - the multiplex-HRM assay for the detection and identification of Bg, Gq, Rvi, and Lb - was designed for the analysis of environmental samples (swabs from stem exudates). This chapter describes the field sample processing optimization studies performed to make the multiplex HRM assay work with field samples. As a measure of quality control, a selection of the amplicons generated by the HRM assays described in the following sections were sequenced. The sequencing of the PCR products was to confirm that the amplicon was the expected product and not a false positive result. HRM results were also validated by traditional isolation of the bacteria present in each sample and identification by partial 16S rRNA sequencing. The studies of optimisation of pre-HRM sample processing and the identification of the bacteria present in the samples were performed in parallel. The sections dedicated to the description of the optimisation of the pre-HRM sample processing, contain references to the results of the bacterial isolations, described later in the chapter.

The field sample processing optimisation studies described in the following sections were performed using a simplified version of the multiplex-HRM assay that targeted only two species instead of four. The duplex-HRM targeted Bg and Gq, with the primers Bgi3F-Bgi3R-Gqi1F-Gqi1R (**Table 5**). Samples from oak stem were sterile swabs soaked or rubbed into the lesion exudates between the bark plates and from stem layers underneath the lesion.

ScreenClust was used for the statistical interrogation of the raw HRM data obtained in all the assays described in this chapter, allowing the software to choose the most appropriate cluster number and principal component number (unsupervised mode), to group the samples in clusters. The results of the HRM analyses correlated in all cases with the clustering results obtained by ScreenClust.

6.2.1.1. Duplex-HRM assay for the detection and identification of Bg and Gq in initial stem suspensions

The duplex-HRM assay was performed directly using as DNA template the initial stem suspensions (the head of each swab cut into a 1.5 mL tube with 750 µL of sterile ¼ Ringers solution), obtained from all the samples from Kew Gardens (Kew 1, Kew 2, Kew 3, Kew 4, Kew 5, Kew 6, Kew 7, Kew 8, Kew 9, Kew 10 and Kew 11) (**section 2.8.1**). The results were negative for all the samples tested, even though, the symptoms displayed by some of the trees sampled in Kew Gardens were very indicative of AOD. Due to this and because Bg and Gq were isolated from some of the samples, the results of the duplex-HRM assay of the initial stem suspensions were considered false negatives.

6.2.1.2. Duplex-HRM assay for the detection and identification of Bg and Gq in overnight LB broths

To promote detection of the targets, an enrichment step of the sample was introduced. The enrichment step was meant to increase the amount of target (in this case, cells of Bg and Gq), and to reduce the proportion of PCR inhibitors in the sample. The first attempt to enrich the samples was to incubate the glycerol stocks saved from the initial stem suspensions at 25 °C, in a shaking incubator, in LB broths, overnight (**section 2.8.2**). The derivative profiles of the samples enriched this way were obtained by duplex-HRM assay and compared (**Figure 51**). The results of the duplex-HRM assay did not correlate in all cases with the results of the traditional isolation and identification of the bacteria present in the samples, meaning that this sample processing method is not optimal (

). The results of the isolation and the duplex-HRM correlated for samples Kew 1, Kew 2, Kew 4, and Kew 8. Samples Kew 3, Kew 5, Kew 6 and Kew 11 contained Bg but this target was

missed by the duplex HRM. Members of the genera *Brenneria* or *Gibbsiella* were not isolated from Kew 7, but the duplex-HRM detected Bg. Kew 9 and Kew 10 contained Bg and *Gibbsiella* sp. according to the isolations but only Gq was detected by the duplex-HRM. Kew 2 presented a similar derivative melt profile to the control “Bg + Gq”. The derivative melt profiles for Kew 2 and the control Bg + Gq presented two peaks, one at the same T_m as Gq and another one at Bg’s T_m , suggesting the presence of both targets.

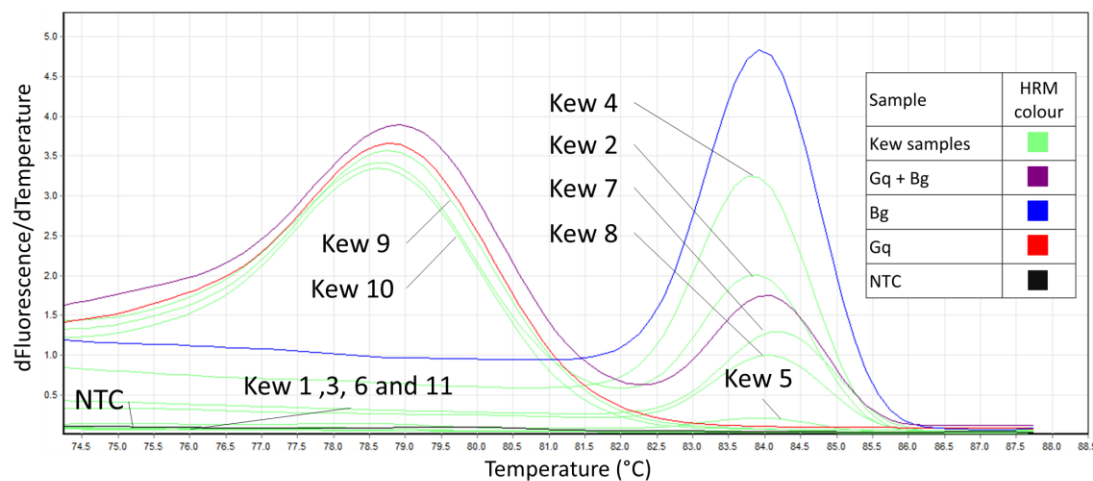


Figure 51: Derivative fluorescence plot of the duplex-HRM assay for the detection and identification of AOD-associated bacteria *Brenneria goodwinii* (Bg) and *Gibbsiella quercinecans* (Gq), in overnight LB broths. The samples included in this assay were overnight LB broths inoculated with the samples collected from Kew Gardens (in green), the positive controls, Bg (in blue) and Gq (in red), and a third positive control inoculated with both Bg and Gq (in purple). All the samples were tested in triplicates but data for replicates is not shown. The primers used in this HRM assay were Bgi3F, Bgi3R, Gqi1F, and Gqi1R. NTC = non-template control.

Table 17: Isolates from samples collected in Kew Gardens, and results of the duplex-HRM assay for the detection and identification of AOD-associated bacteria *Brenneria goodwinii* (Bg) and *Gibbsiella quercinecans* (Gq), in overnight LB broths.

Sample	<i>Brenneria</i> sp. or <i>Gibbsiella</i> sp. isolated aerobically?	<i>Brenneria</i> sp. or <i>Gibbsiella</i> sp. isolated anaerobically?	Duplex-HRM result
Kew 1	None	None	None
Kew 2	Gq	Bg and Gq	Bg and <i>Gibbsiella</i> sp.
Kew 3	Bg	Not performed	None
Kew 4	Bg	Not performed	Bg
Kew 5	Bg	Not performed	None
Kew 6	None	Bg	None
Kew 7	None	Not performed	Bg
Kew 8	None	Bg	Bg
Kew 9	Bg and <i>Gibbsiella</i> sp.	Not performed	<i>Gibbsiella</i> sp.
Kew 10	Bg and <i>Gibbsiella</i> sp.	Not performed	<i>Gibbsiella</i> sp.
Kew 11	Bg	Not performed	None

6.2.1.3. Duplex-HRM assay for the detection and identification of Bg and Gq in Kew 2: optimal temperature and atmosphere test

To increase the fitness of Bg during incubation, and to reduce competition amongst Bg and other bacterial species, different incubation conditions were compared with the duplex-HRM assay (**section 2.8.3**). To find the best incubation conditions, the same sample (Kew 2) was incubated in several ways, and the derivative melt profiles obtained by each of the samples were compared using the duplex-HRM assay.

To investigate the temperature of incubation that increases the fitness of Bg without avoiding the growth of Gq, the glycerol stock saved from sample Kew 2 was streaked out on LB plates. The plates were incubated aerobically at 25, 35 and 41 °C and anaerobically at 35 °C. The temperature that allowed for a clear detection and identification of Bg without affecting the detection of Gq was 35 °C. Therefore the detection of Bg and Gq was optimal when the sample was incubated at 35 °C and on solid media. Gq was hardly detected by the

duplex-HRM assay, in the samples incubated at 25 and 41 °C (**Figure 52**). Similar derivative melt profiles were observed for the samples incubated on plates at 35 °C in aerobic and anaerobic conditions. The derivative melt profiles of Kew 2 incubated on LB plates at 35 °C, anaerobically and aerobically were also similar to each other.

Glycerol stocks of Rvi and Lb were also plated out in LB and incubated anaerobically at 35 °C to ensure that they form colonies in this conditions.

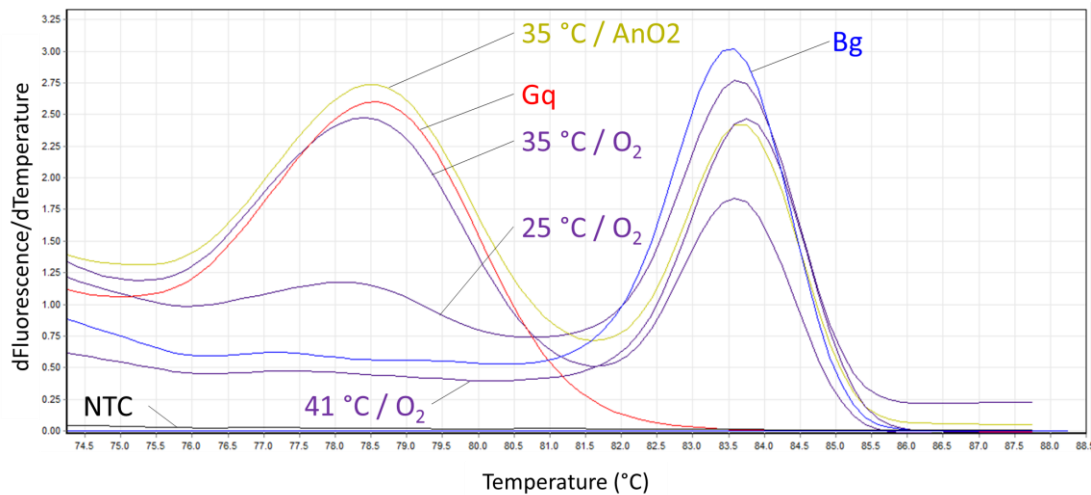


Figure 52: Derivative fluorescence plot of the duplex-HRM assay for the detection and identification of AOD-associated bacteria *Brenneria goodwinii* (Bg) and *Gibbsiella quercinecans* (Gq), in sample Kew 2: optimal temperature and atmosphere test. The sample included in this assay was Kew 2 incubated on LB plates, at different temperatures and aerobically (in purple), and anaerobically (in yellow). Positive controls Bg (in blue) and Gq (in red) were also added to the assay. All the samples were tested in triplicates but data for replicates is not shown. The primers used in this HRM assay were Bgi3F, Bgi3R, Gqi1F, and Gqi1R. NTC = non-template control.

6.2.1.4. Duplex-HRM assay for the detection and identification of Bg and Gq in Kew 2: optimal media and atmosphere test

According to the results obtained in the previous section, the detection of Bg and Gq was optimal when the sample was incubated on solid media at 35 °C. A duplex-HRM assay was performed using Kew 2 incubated in different media and atmosphere conditions, to confirm the results obtained in the previous section (**section 2.8.4**). Kew 2 was inoculated in LB broths and on LB plates. All the broths were incubated statically and at 35 °C to see if this was better

than the results obtained shaking the broths. The broths were incubated aerobically, anaerobically and in microaerophilic conditions (with a layer of sterile mineral oil covering the liquid-air interface), and the plates were incubated anaerobically. The samples were tested by duplex-HRM (**Figure 53**). The results of the duplex-HRM confirmed that the best detection of Bg and Gq was obtained in the sample that had been incubated anaerobically, on solid media at 35 °C. The derivative peaks that indicated the presence of Bg and Gq were similar in height (derivative fluorescence), in the samples incubated using the optimal conditions (LB plates, 35 °C and anaerobic conditions).

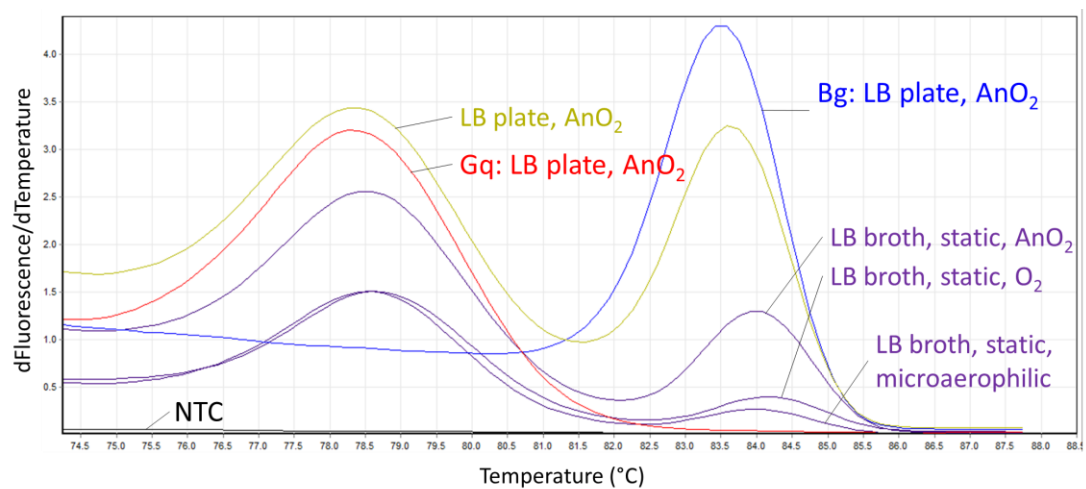


Figure 53: Derivative fluorescence plot of the duplex-HRM assay for the detection and identification of AOD-associated bacteria *Brenneria goodwinii* (Bg) and *Gibbsiella quercinecans* (Gq), in sample Kew 2: optimal media and atmosphere test. Sample Kew 2 was incubated in different ways. The sample was incubated at 35 °C, in LB broths, aerobically, and in microaerophilic conditions (in purple), and anaerobically in LB plates (in yellow). Positive controls Bg (in blue) and Gq (in red) were added to the assay. All the samples were tested in triplicates but data for replicates is not shown. The primers used in this HRM assay were Bgi3F, Bgi3R, Gqi1F, and Gqi1R. NTC = non-template control.

6.2.1.5. Duplex-HRM assay for the detection and identification of Bg and Gq in Kew 1, Kew 2, Kew 3, Kew 6 and Kew 11: optimal media and atmosphere test

To find out if the incubation conditions chosen as optimal for sample Kew 2 were optimal as well for other field samples, glycerol stocks from Kew 1, Kew 2, Kew 3, Kew 6 and Kew 11 were incubated at different temperatures, using different types of media and in the presence or absence of atmospheric oxygen during the incubation. Then, the derivative melt profiles obtained by each of the samples were compared using the duplex-HRM assay (**section 2.8.5**). The results obtained in this section supported the results observed for sample Kew 2. The derivative melt profiles obtained by the samples Kew 1, Kew 3, Kew 6 and Kew 11 matched the results of the traditional bacterial isolation, exclusively when the samples were incubated on LB agar plates, anaerobically and at 35 °C. The differences between incubating a sample aerobically and anaerobically can be easily observed comparing the results of the duplex-HRM assay of the samples incubated on solid media at 35 °C, aerobically and anaerobically (**Table 18**). The results of the aerobic incubation indicate non-specific amplification in samples Kew 1, Kew 2 and Kew 11, this is suggested by the presence of a low derivative peak at temperatures that do not correspond to any of the targets (peak at 79.4 °C and 74.2 °C) or to a late amplification. The non-specific amplification events did not appear in the samples incubated anaerobically, suggesting that the noise produced by the microbes interfering with the assay was eliminated by the anaerobic incubation step.

Table 18: Isolates from samples collected in Kew Gardens, and results of the duplex-HRM assay for the detection and identification of AOD-associated bacteria *Brenneria goodwinii* (Bg) and *Gibbsiella quercinecans* (Gq), in optimal media and atmosphere test.

		Duplex-HRM results						AOD-associated bacteria isolated
Sample	Enrichment conditions ↳	LBb, shaking O ₂ 25 °C	LBb, shaking O ₂ 35 °C	LBp, 25 °C O ₂	LBp, 35 °C, O ₂	LBp, 41 °C, O ₂	LBp, 35 °C, AnO ₂	
	Kew 1	Peak at 79.4 °C	X	X	Peak at 79.4 °C	X	X	None
	Kew 2	Bg, Gq	Bg, Gq	Bg, Gq and peak at 74.2 °C	Bg, Gq and peak at 74.2 °C	Bg	Bg and Gq	Bg and Gq
	Kew 3	X	X	Bg	Bg	Bg	Bg	Bg
	Kew 6	X	X	Bg	Bg	Bg	Bg	Bg
	Kew 11	X	X	Bg	Bg and peak at 79.4 °C	Bg	Bg	Bg

X: negative result. LBb: LB broth. LBp: LB plate. O₂: aerobic incubation. AnO₂: anaerobic incubation.

6.2.1.6. Multiplex-HRM assay for the detection and identification of Bg, Gq, Rvi and Lb in KP 1, KP 2 and KP 3: optimal atmosphere test

In the previous section it was concluded that the anaerobic incubation of the field samples on solid media at 35 °C was the optimal enrichment step, prior to duplex-HRM, in the samples from Kew. To investigate if this could also be the case using the multiplex-HRM instead of the duplex-HRM, and with a different set of samples, samples from Knole Park were prepared aerobically and anaerobically and analysed by multiplex-HRM. Glycerol stocks from KP 1, KP 2 and KP 3 were plated out on LB and incubated aerobically and anaerobically at 35 °C. The derivative melt profiles obtained from testing Knole Park samples by multiplex-HRM, after

aerobic and anaerobic enrichment were compared (**Figure 54**). Supporting previous results, the samples incubated in the anaerobic chamber permitted a clearer detection of the targets, and the derivative peaks were similar in derivative fluorescence. The results of the HRM of the sample KP 3 incubated aerobically failed to detect the presence of Gq that otherwise was clearly observed in the profile of KP 3 incubated anaerobically.

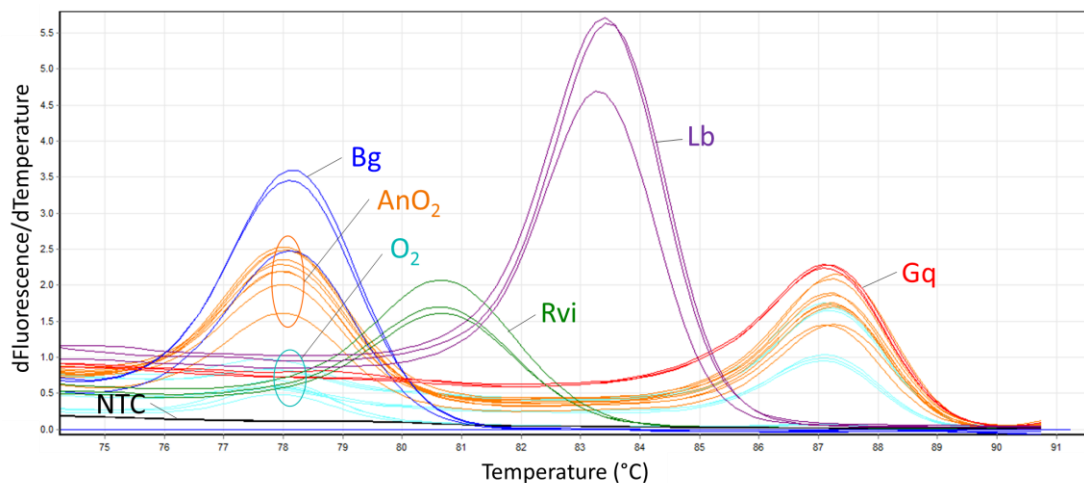


Figure 54: Derivative fluorescence plot of the multiplex-HRM assay for the detection and identification of AOD-associated bacteria *Brenneria goodwinii* (Bg), *Gibbsiella quercinecans* (Gq), *Rahnella victoriana* (Rvi) and *Lonsdalea britannica* (Lb) in samples from Knoke Park: optimal atmosphere test. The samples included in this assay were KP 1, KP 2 and KP 3. Samples were incubated in LB plates aerobically (in light blue), and anaerobically (in orange). Controls added were Bg (in dark blue), Gq (in red), Rvi (in green) and Lb (in purple). All the samples were tested in triplicates. The primers used in this HRM assay were Bgi2F, Bgi2R, Gqi3F, Gqi3R, Rvii1F, Rvii1R, Lbi2F, and Lbi2R. NTC = non-template control.

6.2.2. Validation of the multiplex-HRM assay for the detection and identification of Bg, Gq, Rvi and Lb. Isolation, purification and identification of bacteria from oak stem

Once the optimal sample processing method prior to HRM was established, the validation of the multiplex-HRM assay was performed. The assay was validated by processing field samples in the optimal manner and analysing them to detect and identify the presence of the four targets using the multiplex-HRM assay. After multiplex-HRM assay the amplicons

generated were sequenced to verify the presence of the target. The bacteria present in each sample was isolated, purified and identified by partial 16S rRNA gene sequencing. Samples were taken from external bleeds in all cases except from the tree 19017 from Kew, from which the bark was removed and samples were taken from the different layers exposed. Isolation, purification and identification of bacteria from the samples was performed aerobically in the samples from Kew Gardens and anaerobically in a selection of samples from Kew and the rest of the oak stem samples.

- **Kew Gardens:** Bacteria contained in samples from Kew Gardens were isolated, purified and identified by 16S rRNA sequencing (**Table 19**). AOD-associated bacteria were not isolated from the water oak in Kew (*Quercus nigra*), whereas Bg was present in most of the rest of the swabs collected from oaks displaying symptoms of AOD.

To compare the bacterial species obtained from the same sample after aerobic and anaerobic incubation, glycerol stocks from samples Kew 2, Kew 6 and Kew 8 were plated out on LB and incubated aerobically and anaerobically. After incubation, the colonies were purified and identified by sequencing of the partial 16S rRNA gene. As expected, only facultative anaerobes were isolated from the samples incubated anaerobically, whereas the number of bacterial species isolated from samples incubated aerobically was considerably larger. During the identification of the bacterial isolates contained in Kew 2 and Kew 6, incubated aerobically, the presence of Bg was missed; whereas Bg was isolated from the samples incubated anaerobically. Kew 2, incubated aerobically, contained eight species of bacteria; whereas the same sample contained only three species when incubated anaerobically, from which two of them were targets for the assay. Kew 6, incubated aerobically, contained seven bacterial species; whereas only two were isolated anaerobically, being one of them a target for the assay. Kew 8, incubated aerobically, contained five bacterial isolates; whereas only three were isolated from the same sample incubated anaerobically, being one of them a target for the assay. The results suggested that it would be better for the detection and identification of Bg, Gq, Rvi and Lb to incubate the samples anaerobically, therefore that is how the following isolations were performed.

Table 19: Bacterial isolates from Kew Gardens and results of the multiplex-HRM assay for the detection and identification of AOD-associated bacteria *Brenneria goodwinii* (Bg), *Gibbsiella quercinecans* (Gq), *Rahnella victoriana* (Rvi) and *Lonsdalea britannica* (Lb). The isolates were

purified and identified by partial 16S rRNA gene sequencing. The genes were identified by comparison against the EzBioCloud database. The bacterial isolation was performed after aerobic incubation in all the samples (in black), and also after anaerobic isolation for samples Kew 2, Kew 6 and Kew 8 (in red). Members of the genera *Brenneria*, *Gibbsiella*, *Rahnella* and *Lonsdalea* are in bold.

Sample	M-HR M	Isolates	16S rRNA amplicon size (bp)	O ₂ /AnO ₂	EzBioCloud ID	% EzBio Cloud
Kew 1	Neg.	111	922	O ₂	<i>Microbacterium oxydans</i>	100
		112	953	O ₂	<i>Pseudomonas punonensis</i>	98.6
		114	980	O ₂	<i>Brevibacterium aurantiacum</i>	97.5
		115	815	O ₂	<i>Isoptericola nanjingensis</i>	99.1
		116	927	O ₂	<i>Isoptericola nanjingensis</i>	99.1
		117	968	O ₂	<i>Staphylococcus warneri</i>	99.4
Kew 2	Bg & Gq	118	967	O ₂	<i>Pseudacidovorax intermedius</i>	95.9
		119	994	O ₂	<i>Erwinia billingiae</i>	99.4
		120	913	O ₂	<i>Pantoea cedenensis</i>	99.5
		121	989	O ₂	<i>Pantoea dispersa</i>	98.8
		122	967	O ₂	Gq	99.5
		124	859	O ₂	<i>Erwinia sp.</i>	99.4
		125	888	O ₂	<i>Pseudomonas constantinii</i>	99.3
		126	949	O ₂	Gq	99.1
		126.2	948	O ₂	<i>Rouxiiella chamberiensis</i>	99.2
		126.3	904	O ₂	<i>Xanthomonas sp.</i>	98.2
		222	960	AnO ₂	Bg	99.4
		223	963	AnO ₂	<i>Mangrovibacter phragmitis</i>	94.4
		224	809	AnO ₂	Gq	99.2
		225	894	AnO ₂	Bg	99.7
226	851	AnO ₂	<i>Mangrovibacter phragmitis</i>	94.2		
Kew 3	Bg	127	953	O ₂	Bg	99.2
		133	831	O ₂	Bg	99.5
		183	883	O ₂	Bg	99.7
		185	893	O ₂	Bg	99.3
		188	901	O ₂	<i>Streptomyces setonii</i>	99.8
Kew 4	-	134	517	O ₂	<i>Xanthomonas maliensis</i>	97.5
		135	851	O ₂	Bg	98.5

		136	908	O ₂	<i>Microbacterium populi</i>	98.4
		137	999	O ₂	<i>Microbacterium populi</i>	98.6
		138	950	O ₂	<i>Aureimonas populi</i>	97.0
		139	988	O ₂	<i>Pseudomonas dryadis</i>	99.0
		140	1006	O ₂	<i>Pseudoclavibacter terrae</i>	99.5
		141	954	O ₂	Bg	99.3
		142	962	O ₂	<i>Arenivirga flava</i>	97.9
Kew 5	Bg	143	955	O ₂	Bg	99.5
		144	919	O ₂	<i>Arenivirga flava</i>	97.6
		145	1039	O ₂	<i>Sinirhodobacter sp.</i>	98.1
		146	999	O ₂	<i>Arenivirga flava</i>	98.1
Kew 6	Bg	147	997	O ₂	<i>Pseudoclavibacter terrae</i>	99.6
		148	916	O ₂	<i>Arenivirga flava</i>	97.9
		149	1461	O ₂	<i>Rahnella bruchi</i>	99.9
		150	938	O ₂	<i>Rhodococcus erythropolis</i>	99.9
		151	1431	O ₂	<i>Pseudomonas dryadis</i>	99.9
		152	969	O ₂	<i>Arenivirga flava</i>	98.0
		153	841	O ₂	<i>Bacillus licheniformis</i>	99.1
		154	950	O ₂	<i>Achromobacter sp.</i>	97.7
		186	918	O ₂	<i>Arenivirga flava</i>	98.2
		227	892	AnO ₂	Bg	99.5
		228	886	AnO ₂	<i>Rahnella bruchi</i>	99.6
Kew 7	-	155	887	O ₂	<i>Pseudomonas</i>	99.2
		157	851	O ₂	<i>Erwinia billingiae</i>	99.7
		160	1433	O ₂	<i>Pseudomonas dryadis</i>	99.4
		161	895	O ₂	<i>Raoultella ornithinolytica</i>	99.3
Kew 8	Bg	162	942	O ₂	<i>Raoultella ornithinolytica</i>	99.6
		163	1433	O ₂	<i>Pseudomonas dryadis</i>	99.3
		164	731	O ₂	<i>Stenotrophomonas rhizophila</i>	99.7
		165	578	O ₂	Bg	99.8
		166	1433	O ₂	<i>Pseudomonas dryadis</i>	99.6
		167	819	O ₂	<i>Cellulomonas terrae</i>	97.7
		229	717	AnO ₂	Bg	99.2
		230	667	AnO ₂	<i>Rahnella woolbedingensis</i>	99.9
		231	606	AnO ₂	<i>Raoultella terrigena</i>	98.5
Kew 9	-	168	853	O ₂	<i>Gibbsiella greigii</i>	99.6
		169	886	O ₂	Bg	99.3
		170	888	O ₂	Bg	99.9
Kew 10	-	172	900	O ₂	Bg	99.8
		173	892	O ₂	<i>Raoultella ornithinolytica</i>	99.4
		174	887	O ₂	Bg	99.9

		175	892	O ₂	<i>Erwinia billingiae</i>	99.3
Kew 11	Bg	176	889	O ₂	Bg	99.3
		177	889	O ₂	<i>Xanthomonas cucurbitae</i>	98.2
		178	885	O ₂	Bg	99.9
		179	887	O ₂	Bg	99.3
		187	637	O ₂	<i>Xanthomonas sacchari</i>	98.4

M-HRM: multiplex-HRM results. -: Not tested by multiplex-HRM. O₂/AnO₂: Aerobic or anaerobic incubation. EzBioCloud ID: result of the identification of the isolate using EzBioCloud. % EzBioCloud: percentage of sequence similarity according to the EzBioCloud database. Bp: base pairs. Neg.: negative result.

Derivative melting profiles obtained from the samples Kew 1, Kew 2, Kew 3, Kew 6 and Kew 11 were generated and compared by multiplex-HRM. Derivative peaks indicating the presence of Bg and Gq were observed in Kew 2, and the peak for Bg and the peak for Gq were similar in height (derivative fluorescence) (**Figure 55**). Bg was detected in samples Kew 3, Kew 6 and Kew 11. The result of the assay for Kew 1 was negative. The results of the multiplex-HRM assay agree with the results obtained from the isolation and identification of bacteria from the samples through 16S rRNA gene sequencing. *Lonsdalea* sp. were not isolated or detected by multiplex-HRM. *Rahnella bruchi* was isolated from Kew 6 and *Rahnella woolbedingensis* was isolated from Kew 8, but these species did not interfere in the assay because the multiplex-HRM is intentionally blind to them. The results of the sequencing of the amplicons generated, corresponded to the results of the HRM.

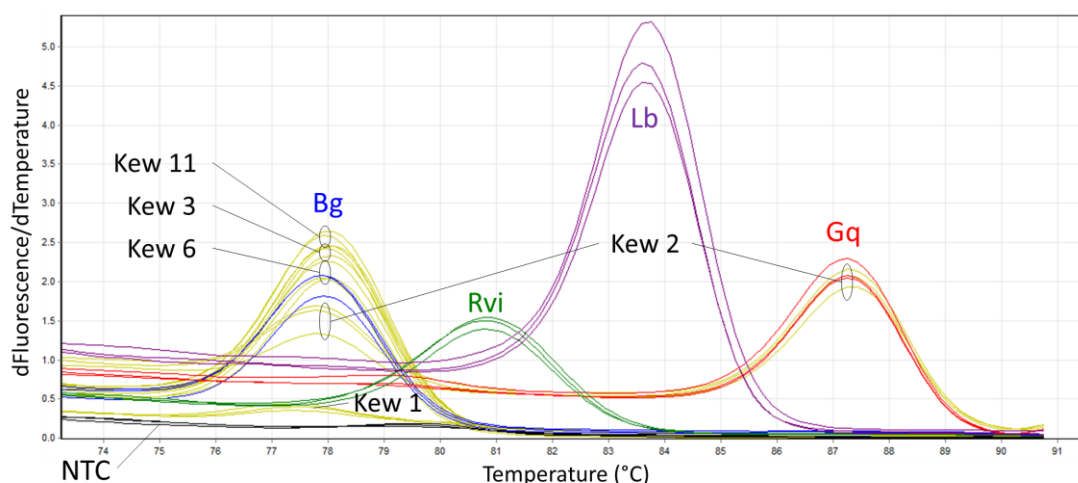


Figure 55: Derivative fluorescence plot of the multiplex-HRM assay for the detection and identification of AOD-associated bacteria *Brenneria goodwinii* (Bg), *Gibbsiella quercinecans* (Gq), *Rahnella victoriana* (Rvi) and *Lonsdalea britannica* (Lb) in samples from Kew Gardens. The samples analysed in this assay were Kew 1, Kew 2, Kew 3, Kew 6 and Kew 11 (in yellow). Controls added were Bg (in blue), Gq (in red), Rvi (in green) and Lb (in purple). All the samples were tested in triplicates. The primers used in this HRM assay were Bgi2F, Bgi2R, Gqi3F, Gqi3R, Rvii1F, Rvii1R, Lbi2F, and Lbi2R. NTC = non-template control.

- **Knole Park:** Bacteria contained in samples from Knole Park were isolated, purified and identified by 16S rRNA sequencing (**Table 20**). The samples KP 1, KP 2, KP 3 and KP 4 were incubated anaerobically as a consequence of the results obtained from samples from Kew. The bacterial species isolated from the samples were almost exclusively the intended targets for the multiplex-HRM. Only one additional species was also isolated from KP 1, *Raoultella terrigena*.

In parallel, derivative melting profiles obtained by multiplex-HRM from the samples KP 1, KP 2, KP 3 and KP 4 were generated and analysed (**Figure 56**). All of the samples from KP contained Bg and Gq according to the multiplex-HRM assay performed. Bg and Gq were also isolated from these samples. *Rahnella* sp. or *Lonsdalea* sp. were not isolated or detected by multiplex-HRM. The results of the sequencing of the amplicons generated, corresponded to the results of the HRM.

Table 20: Bacterial isolates from Knole Park and results of the multiplex-HRM assay for the detection and identification of AOD-associated bacteria *Brenneria goodwinii* (Bg), *Gibbsiella quercinecans* (Gq), *Rahnella victoriana* (Rvi) and *Lonsdalea britannica* (Lb). The isolates were purified and identified by partial 16S rRNA gene sequencing. The genes were identified by comparison against the EzBioCloud database. The bacterial isolation was performed after anaerobic incubation. Members of the genera *Brenneria*, *Gibbsiella*, *Rahnella* and *Lonsdalea* are in bold.

Sample	M-HRM	Isolate	EzBioCloud ID	% EzBioCloud	Bp
KP 1	Bg & Gq	457a	<i>Raoultella terrigena</i>	99.4	1433
		457b	Gq	99.9	1322
		457c	Bg	100	1321
		457d	Bg	100	1393
		457e	Bg	100	1432
KP 2	Bg & Gq	458a	Bg	99.6	1329
		458b	Bg	99.8	1322
		458c	Gq	99.6	1298
		458d	Bg	99.7	1394
KP 3	Bg & Gq	459a	Bg	99.6	1379
		459b	Bg	99.7	1391
		459c	Bg	99.6	1399
		459d	Gq	99.7	1394
KP 4	Bg & Gq	460a	Bg	99.9	1434
		460b	Gq	99.4	1275
		460c	Bg	99.4	1444

M-HRM: multiplex-HRM results. EzBioCloud ID: result of the identification of the isolate using EzBioCloud. % EzBioCloud: percentage of sequence similarity according to the EzBioCloud database. Bp: base pairs, 16S rRNA amplicon size.

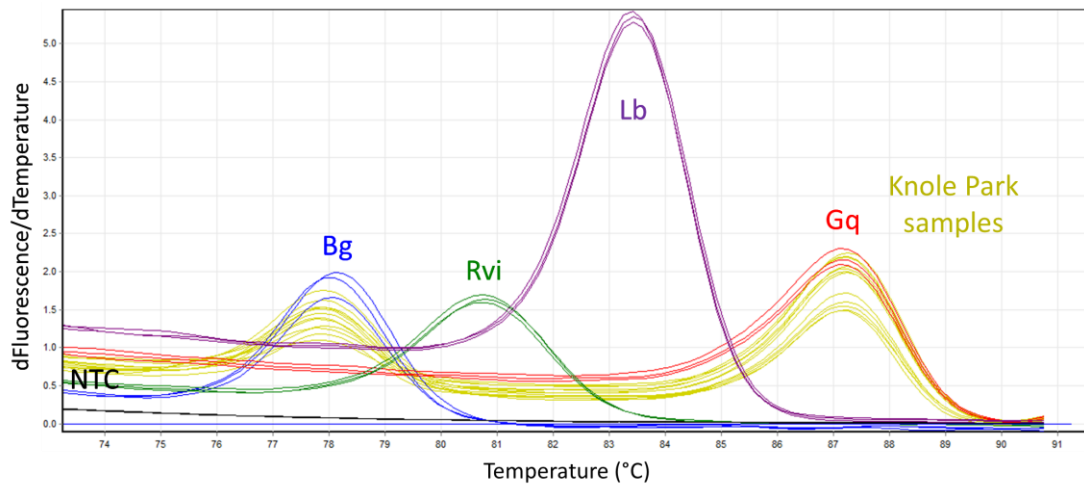


Figure 56: Derivative fluorescence plot of the multiplex-HRM assay for the detection and identification of AOD-associated bacteria *Brenneria goodwinii* (Bg), *Gibbsiella quercinecans* (Gq), *Rahnella victoriana* (Rvi) and *Lonsdalea britannica* (Lb) in samples from Knole Park. The samples analysed in this assay were KP 1, K2 2, KP 3, and KP 4 (in yellow). Controls added were Bg (in blue), Gq (in red) Rvi (in green) and Lb (in purple). All the samples were tested in triplicates. The primers used in this HRM assay were Bgi2F, Bgi2R, Gqi3F, Gqi3R, Rvii1F, Rvii1R, Lbi2F, and Lbi2R. NTC = non-template control.

- Log tests:** 98 samples from the log tests were processed in the optimal manner. Twenty-three of the 98 samples were not tested by multiplex-HRM. This is because when the glycerol stocks were plated out on eosin methylene blue (EMB) and incubated anaerobically, no colonies appeared on the plates, and therefore there was no sample to test. The lack of anaerobic bacterial growth was interpreted as an absence of Bg, Gq, Rvi or Lb in the sample (negative result). The rest of the samples were analysed by multiplex-HRM, and the amplicons generated were sequenced (**Table 21**). Derivative melting profiles obtained from the 75 samples were generated and analysed by multiplex-HRM. Forty-five samples contained Bg, negative results were obtained in 25 samples. The presence of Rvi was detected in five of the samples. The results of the sequencing of the 50 amplicons generated, corresponded to the results of the HRM.

Table 21: Multiplex-HRM assay for the detection and identification of AOD-associated bacteria *Brenneria goodwinii* (Bg), *Gibbsiella quercinecans* (Gq), *Rahnella victoriana* (Rvi) and *Lonsdalea britannica* (Lb) in samples from the log tests. The samples not tested due to the lack of anaerobic growth on the plates (X), were considered negative for the presence of Bg, Gq, Rvi or Lb.

Sample	M-HRM	Sample	M-HRM	Sample	M-HRM	Sample	M-HRM
Log 1	Bg	Log 26	X	Log 51	X	Log 76	Bg
Log 2	Bg	Log 27	Negative	Log 52	X	Log 77	Bg
Log 3	Bg	Log 28	Negative	Log 53	Negative	Log 78	X
Log 4	Bg	Log 29	Rvi	Log 54	X	Log 79	X
Log 5	Negative	Log 30	X	Log 55	Negative	Log 80	Rvi
Log 6	Bg	Log 31	Negative	Log 56	Negative	Log 81	Negative
Log 7	X	Log 32	Negative	Log 57	X	Log 82	X
Log 8	Bg	Log 33	Negative	Log 58	Bg	Log 83	Bg
Log 9	Bg	Log 34	Bg	Log 59	Bg	Log 84	X
Log 10	X	Log 35	X	Log 60	Bg	Log 85	Bg
Log 11	X	Log 36	Negative	Log 61	Bg	Log 86	Bg
Log 12	X	Log 37	Bg	Log 62	Bg	Log 87	Bg
Log 13	X	Log 38	Negative	Log 63	Bg	Log 88	Bg
Log 14	X	Log 39	X	Log 64	Bg	Log 89	Negative
Log 15	Bg	Log 40	Bg	Log 65	Bg	Log 90	Bg
Log 16	Negative	Log 41	Bg	Log 66	X	Log 91	Bg
Log 17	Negative	Log 42	Bg	Log 67	Negative	Log 92	Bg
Log 18	X	Log 43	Bg	Log 68	Negative	Log 93	Bg
Log 19	Negative	Log 44	Bg	Log 69	Rvi	Log 94	Bg
Log 20	X	Log 45	Bg	Log 70	Bg	Log 95	Bg
Log 21	Negative	Log 46	Bg	Log 71	Negative	Log 96	X
Log 22	Rvi	Log 47	Bg	Log 72	X	Log 97	Bg
Log 23	Rvi	Log 48	Bg	Log 73	Negative	Log 98	Bg
Log 24	Bg	Log 49	Negative	Log 74	Negative		
Log 25	Negative	Log 50	Bg	Log 75	Negative		

M-HRM: multiplex-HRM results.

The samples between Log 1 and Log 38, which were analysed by multiplex-HRM, were studied further. Isolation, purification and identification by partial 16S sequencing of the bacteria present in the samples was performed. The results of the multiplex-HRM correlated

with the bacteria identified in most of the samples tested (**Table 22**). However some results of the multiplex-HRM were different to the results of the bacterial isolations. These were: Log 4, Log 25 and Log 27. The conflicts were false negatives (Log 25 and Log 27), and false positives in Log 4. There was also some late amplification in Log 5.

Table 22: Bacterial isolates from the log tests and results of the multiplex-HRM assay for the detection and identification of AOD-associated bacteria *Brenneria goodwinii* (**Bg**), *Gibbsiella quercinecans* (**Gq**), *Rahnella victoriana* (**Rvi**) and *Lonsdalea britannica* (**Lb**). The isolates were purified and identified by partial 16S rRNA gene sequencing. The genes were identified by comparison against the EzBioCloud database. The bacterial isolation was performed after anaerobic incubation. Members of the genera *Brenneria*, *Gibbsiella*, *Rahnella* and *Lonsdalea* are in bold.

Sample	M-HRM	Isolate	EzBioCloud ID	% EzBioCloud	Bp
Log 1	Bg	358a	Bg	99.5	1445
		358b	Bg	99.7	1432
		358c	Bg	99.5	1437
Log 2	Bg	359a	Bg	100	457
Log 3	Bg	360a	Bg	99.7	1381
Log 4	Bg	361a	<i>Citrobacter bitternis</i>	98.8	444
		361b	<i>Citrobacter bitternis</i>	99.9	861
Log 5	Neg.	362a	<i>Citrobacter bitternis</i>	99.6	1446
		362b	<i>Citrobacter bitternis</i>	98.9	1423
Log 8	Bg	365a	Bg	100	404
Log 9	Bg	366a	Bg	99.3	1437
Log 15	Bg	372a	Bg	99.5	1435
		372b	Bg	99.8	1391
Log 16	Neg.	373a	<i>Enterococcus faecalis</i>	99.7	1446
		373b	<i>Enterococcus faecalis</i>	99.7	1420
		373c	<i>Enterococcus faecalis</i>	99.9	1447
Log 17	Neg.	374a	<i>Klebsiella variicola</i>	99.2	757
		374b	<i>Klebsiella quasivariicola</i>	99.5	1203
Log 22	Rvi	379a	Rvi	99.6	1404
		379b	Rvi	99.7	1273
Log 23	Rvi	380a	Rvi	99.7	1261
Log 24	Bg	381a	Bg	99.7	603
		381b	Bg	99.7	653
Log 25	Neg.	382a	Rvi	99.1	1025

Log 26	Rvi	383a	Rvi	99.7	1427
Log 27	Neg.	384a	Rvi	99.6	1415
Log 28	Neg.	385a	<i>Rahnella woolbedingensis</i>	99.2	495
Log 29	Rvi	386a	Rvi	99.6	1420
Log 31	Neg.	388a	<i>Pseudomonas helmanticensis</i>	99.3	1348
Log 32	Neg.	389a	<i>Rahnella woolbedingensis</i>	99.7	1434
Log 33	Neg.	390a	Not identified	Not identified	15
Log 34	Bg	391a	Bg	99.6	1250
		391b	Bg	99.5	602
Log 36	Neg.	393a	Not identified	Not identified	67
		393b	<i>Citrobacter bitternis</i>	99.8	1281
Log 37	Bg	394a	Bg	99.0	872
		394b	Bg	99.7	1426
Log 38	Neg.	395a	<i>Citrobacter bitternis</i>	99.9	903
		395b	<i>Citrobacter bitternis</i>	98.5	265

M-HRM: multiplex-HRM results. EzBioCloud ID: result of the identification of the isolate using EzBioCloud. % EzBioCloud: percentage of sequence similarity according to the EzBioCloud database. Bp: base pairs. Neg.: Negative result.

6.2.3. SNP-based HRM assay for the differentiation of species of the genus *Rahnella*

From the strains isolated in the Log tests, nine were identified as belonging to the genus *Rahnella* (according to EzBioCloud). These samples were analysed using the multiplex-HRM assay for the detection and identification of Bg, Gq, Rvi and Lb (**section 2.6.4**), and afterwards, with the SNP-based HRM assay for the differentiation of species of the genus *Rahnella* (**section 2.6.5.1**). From the nine *Rahnella* strains, five were negative in the multiplex-HRM, and the other four were positive for Rvi (**Table 23**). The results of the SNP-HRM assay agreed with multiplex-HRM assay in the positive result in Rvi for five of the strains, and identified the other four as Rva (**Figure 57**). Note: Identification of isolates by partial 16S rRNA sequencing is not always reliable at the species level. Therefore, the results of sequence comparison with databases such as BLAST or EzBioCloud are taken as a guide, but not strictly.

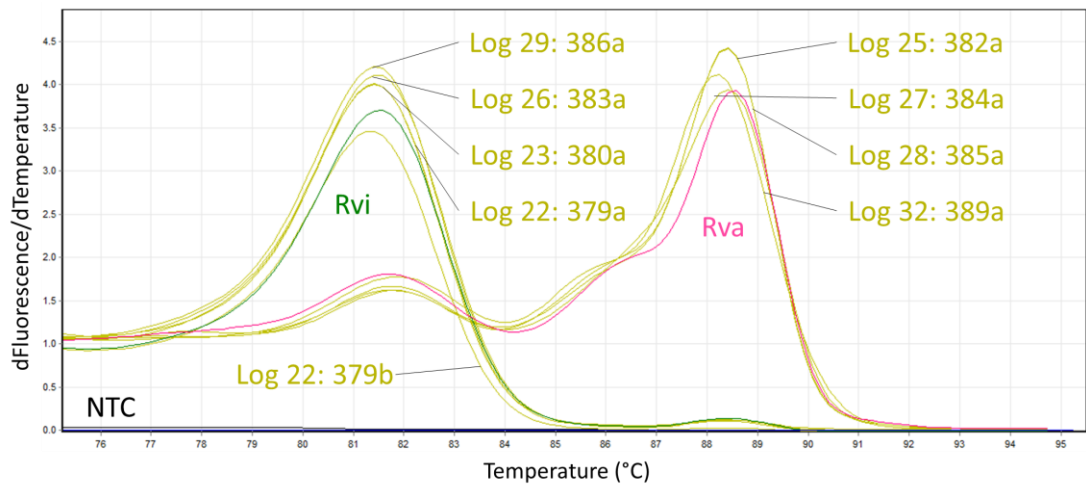


Figure 57: Derivative fluorescence plot of the single nucleotide polymorphism (SNP)-based HRM assay for the differentiation of species of the genus *Rahnella*. Samples included in the assay were the strains belonging to the genus *Rahnella*, isolated from the samples collected from the log tests (in yellow). The controls added to the assay were *Rahnella victoriana* (Rvi, in green) and *Rahnella variigena* (Rva, in pink). Control data for samples *Rahnella bruchi*, *Rahnella woolbedingensis*, *Rahnella aquatilis*, and *Rahnella inusitata* not shown. All the samples were tested in triplicates but data for replicates is not shown. The HRM primers used were Rvii1F and Rvii1R. NTC = non-template control.

Table 23: Multiplex-HRM assay for the detection and identification of AOD-associated bacteria *Brenneria goodwinii* (Bg), *Gibbsiella quercinecans* (Gq), *Rahnella victoriana* (Rvi) and *Lonsdalea britannica* (Lb), and single nucleotide polymorphism (SNP)-based HRM assay for the differentiation of species of the genus *Rahnella* of the isolates belonging to the genus *Rahnella* from the log tests. The isolates were purified and identified by partial 16S rRNA gene sequencing. The genes were identified by comparison against the EzBioCloud database and also the GenBank BLAST database.

Sample	M-HRM	Isolate	SNP-HRM	EzBioCloud ID	% Ez.	BLAST ID	% BLAST
Log 22	Rvi	379a	Rvi	Rvi	99.6	Uncultured <i>Rahnella</i> sp.	99.6
		379b	Rvi	Rvi	99.7	<i>Rahnella</i> sp.	99.4
Log 23	Rvi	380a	Rvi	Rvi	99.7	<i>Rahnella</i> sp.	99.9
Log 25	Neg.	382a	Rva	Rvi	99.1	<i>Rahnella</i> sp.	99.6
Log 26	Rvi	383a	Rvi	Rvi	99.7	Uncultured <i>Rahnella</i> sp.	99.8
Log 27	Neg.	384a	Rva	Rvi	99.6	Uncultured <i>Rahnella</i> sp.	99.9
Log 28	Neg.	385a	Rva	Rwo	99.2	Uncultured <i>Rahnella</i> sp.	99
Log 29	Rvi	386a	Rvi	Rvi	99.6	Uncultured <i>Rahnella</i> sp.	99.4
Log 32	Neg.	389a	Rva	Rwo	99.7	Rva	100

EzBioCloud ID: result of the identification of the isolate using EzBioCloud. % EzBioCloud: percentage of sequence similarity according to the EzBioCloud database. BLAST ID: result of the identification of the isolate using BLAST. BLAST %: percentage of sequence similarity according to the BLAST database. Rva: *Rahnella variigena*. Rwo: *Rahnella woolbedingensis*.

6.2.4. Isolation, purification and identification of endophytic and epiphytic bacteria from oak leaves and multiplex-HRM test

Endophytic and epiphytic bacteria from oak leaves were studied to find out if leaves could be a reservoir for AOD-associated bacteria in trees not displaying symptoms of AOD. Leaves were collected from a *Q. robur* sapling and a mature *Q. robur*. Half of the leaves from the sapling and half of the leaves from the mature oak were surface sterilised. These leaves should contain only the endophytic bacteria. The leaves that did not go through the surface sterilisation contained endophytic and epiphytic bacteria. The samples were prepared as described in **section 2.7.2**. The bacteria from each sample was isolated, purified and identified by 16S rRNA gene sequencing (**Figure 58**). Samples L1, L2, L3, L4, L5, L6, L7, L8, R1,

R2, R3, R4, R5, R6, R7, R8, Bg, Gq, Rvi and Lb were prepared following the optimal enrichment method and analysed using the multiplex-HRM assay. All the samples were negative for the presence of Bg, Gq, Rvi or Lb, according to the multiplex-HRM assay. Matching results (absence of Bg, Gq, Rvi and Lb) were obtained by the traditional bacterial isolation, no AOD-associated bacteria were found in the samples. The composition of culturable bacteria from sapling and mature tree leaves was similar to each other, except for the fact that the sampling contained no culturable endophytes.

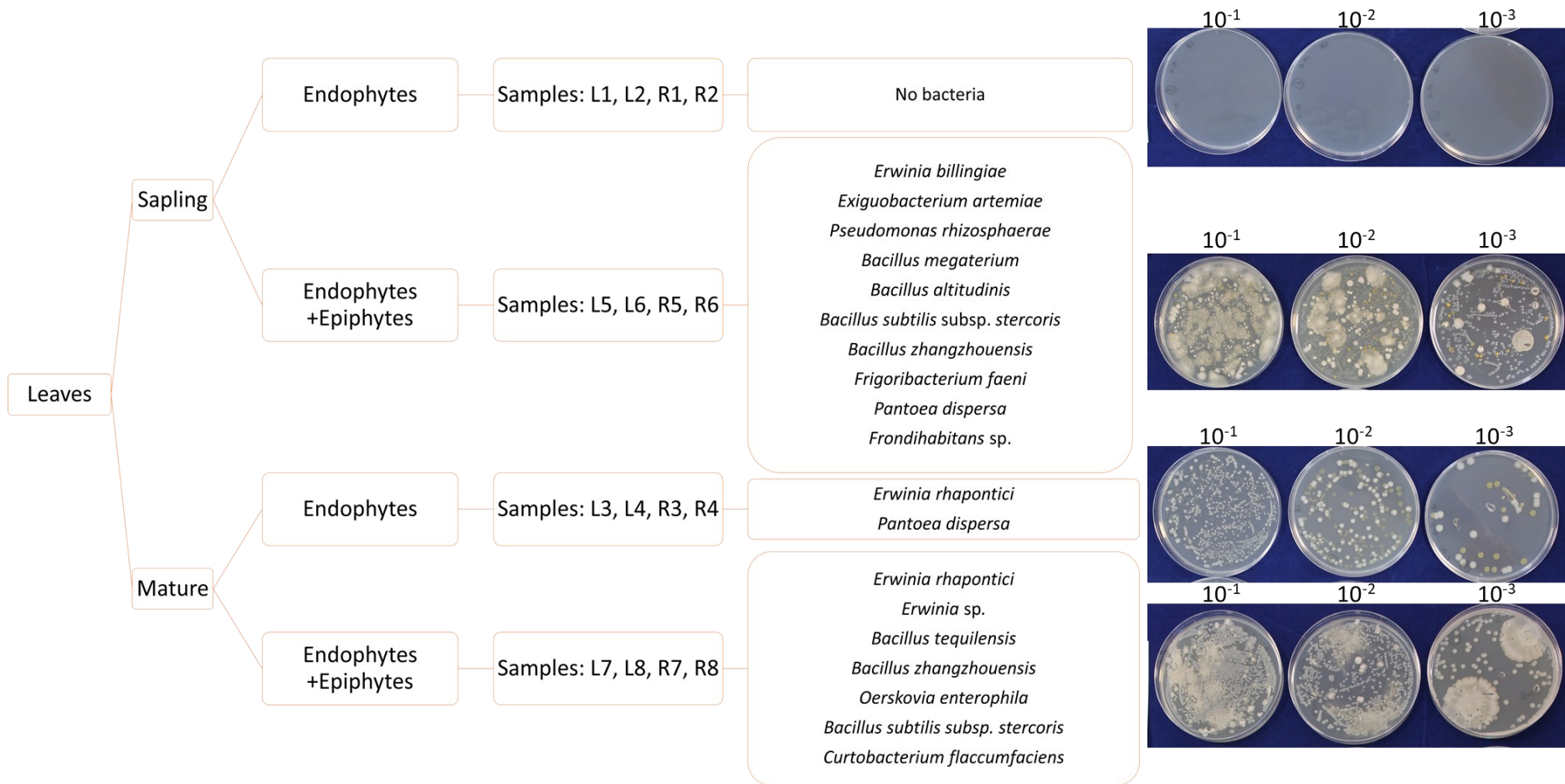


Figure 58: Bacterial endophytes and epiphytes isolated from leaves of sapling and mature *Quercus robur*. The isolates were purified and identified by partial 16S rRNA gene sequencing. The genes were identified by comparison against the EzBioCloud database. In the Petri dishes the epiphytes and endophytes microbes associated with oak leaves. Leaves surface sterilised or not surface sterilised were crushed in 2 mL of Ringers. 100 µL of this liquid was grown overnight in LB broths (25 °C, shaking conditions). 20 µL of LB broth were plated out in LB plates and incubated for 4 days at 25 °C.

6.3. Discussion

The aim of this part of the project was to optimise the field sample processing prior to HRM analysis. Several HRM-based techniques were described in **Chapter 5**, but only one was designed for the detection and identification of the targets directly from field samples, the multiplex-HRM assay for the detection and identification of Bg, Gq, Rvi and Lb. The sensitivity and the specificity of the multiplex-HRM assay were tested and described in **Chapter 5**, and the optimisation of pre-HRM field sample processing, and the validation of the multiplex-HRM assay are described in the present chapter.

The first change introduced in contrast with the method used for sample processing at Forest Research (**section 6.1**) was to use Ringer's solution instead of SDW to suspend the bacterial cells of the swab. This change was introduced to avoid the osmotic shock that most of the bacteria suffer when they are suspended in SDW. The viability of the cells is not important for the HRM assay (HRM is unable to differentiate alive or dead cells), but it is necessary to keep the bacteria alive as much as possible if the next step is an enrichment of the sample. The filtration, centrifugation and vortexing steps were also removed from the sample preparation method, because these steps also compromise the viability of the bacteria, and increase the risk of losing the target (debris could easily block the pores of the filters and avoid the filtering of the bacteria of interest).

As expected, negative results were observed when swabs from Kew Gardens soaked in Ringers (initial stem suspension) were tested using the duplex-HRM assay. However, AOD-associated bacteria were present in some of the swabs, according to the 16S rRNA gene sequencing of the isolates. The negative results observed were expected because when the swabs were submerged in Ringers, the suspension was visibly impure, with a brown colour and floating debris on them (**Figure 59**). There are several reasons why the amplification did not take place. Up to 30 % of the bark of a tree is formed by xylan. The reason of the negative PCR results could be the presence in the sample of substances that inhibit the PCR like xylan, debris, polyphenols, polysaccharides, or resins (Demeke and Adams, 1992; Henson and French, 1993; John, 1992; Malvick and Grunden, 2005; Wilson, 1997). In addition, the amplification might have failed due to a low starting amount of DNA template. The low amount of starting DNA template could be due to a low number of bacterial cells in the sample because, at this point, the samples had not been incubated or enriched in any way. Logically, another reason for a negative result could be the complete absence of the target in the sample, however, the symptoms in some of the trees were highly indicative of AOD.



Figure 59: Initial stem suspension. Samples collected from stem bleeds in Acute Oak Decline-affected oaks, submerged in Ringers solution.

To solve the lack of amplification, an enrichment step was added to the processing of the field samples prior to HRM. Incubating the samples would allow for multiplication of the bacteria present in the sample. Knowing that Bg and Gq are normally the predominant bacteria in AOD samples, a duplex-HRM assay was used instead of the multiplex-HRM assay for the studies on the optimisation of the sample processing. A duplex-HRM was used instead of the multiplex-HRM as the optimisation required many HRM runs and reducing the amount of primers and targets meant less pre-assay preparation time and less chances of false positives and other errors. In addition, the primers for the duplex-HRM were not those used for Gq and Bg in the final multiplex-HRM assay because the study of the best conditions for sample incubation and the study of the best HRM method were running in parallel, and by the time the sample processing studies were completed, the best multiplex-HRM method had not been selected yet.

Incubating the samples in LB broths, for 20 hours at 25 °C, in shaking conditions, was not the optimal method to detect Bg and Gq, because the duplex-HRM assay failed to detect the target in most of the samples. There are several factors that can affect the detection of AOD-associated bacteria in samples known to contain the target. The media, the temperature of incubation, the atmospheric conditions (level of O₂), or other factors could be sub-optimal for the enrichment of the samples. In addition to this, field samples contain a mixture of bacterial species, meaning that there could be competition for the resources amongst them and the bacterial community pre-incubation could be very different to the community post-

incubation. The microbial composition of a field sample can vary from its original state (before collection) to the moment that it is going to be used for the diagnosis. Bacterial species in the lesion microbiome are in equilibrium with each other, with their host and with the environment. Once collected, the microbiome of a sample might vary due to a change of conditions such as the level of humidity or oxygen. Once the sample is in the lab, the microbiome can continue changing. These changes depend on details like the conditions of sample storage or the type of enrichment conditions applied to the sample, if any, as not all the species of bacteria need the same conditions to thrive. It may happen that a particular bacterial species that was very abundant in the freshly collected sample ends up disappearing from the sample with the time, or being masked by another bacterial species present in the original sample in lower numbers, but fitter under the new conditions. And this might be happening in AOD samples.

A relevant study to this project looked into this further by comparing the microbial profiles obtained by traditional isolation and by metagenomic analysis. The study used samples collected from 38 AOD-diseased oaks from 23 sites, 13 healthy oaks in 11 of these sites, and 15 healthy oaks from five sites with no history of AOD (Denman et al., 2018). In the study by Denman *et al.*, Gq was isolated from all the 23 diseased sites sampled, whereas Bg was isolated from 15, Rvi was isolated from 9 and Lb from only 4. Gq was isolated from 83 % of diseased trees and 4 % of the healthy trees. Bg was more difficult to isolate being found only in 16 % of diseased trees and <0.1 % of the healthy trees. Rvi and Lb were only isolated from diseased trees. This could lead researchers to think that Gq is the main pathogen in the disease, but the analysis of the AOD lesion metagenome showed that Bg, Gq and Rvi were present in all the diseased trees, but Bg was the most abundant species, followed by Rvi and in fourth place, Gq. This suggests that the microbial profile obtained from the same sample can be very different depending on the type of microbiome analysis performed (traditional isolation vs. metagenomic study). Gq was clearly overrepresented in the isolation studies, which could be due to this species being very fit under enrichment conditions. However, Bg was the most abundant species in the lesion, according to the metagenomic studies, and it was underrepresented in the isolation studies, probably due to its low fitness under enrichment conditions (Denman et al., 2018). It is probable that the main AOD pathogen, Bg, is able to thrive under the hard conditions that the host imposes, however, whenever Bg is grown in nutrient-rich media, the same traits that make the microbe an excellent warrior in the tree, take a genetic toll and make it less fit when there is no war. Denman *et al.*'s study, and the evidence that Bg grows substantially slower in the laboratory than Gq inspired the

tailoring of the sample processing prior to the diagnostic of AOD-associated bacteria from mixed samples (multiplex HRM), described in this chapter, (Denman et al., 2018). Considering that Gq and Rvi are fitter in the lab, than Bg and Lb, it is reasonable to expect that, in mixed field samples enriched in the lab, Bg could be underrepresented due to its lower fitness, and that Lb could also be underrepresented due to being less fit in the lab and being found only sporadically in the field. To counteract this, the primers for Lb in the multiplex HRM target a gene that it is present twice in its genome, ideally making Lb more detectable.

The sample processing prior to HRM was optimised until the detection of Bg was as effective as the detection of Gq from field samples. More variables factor into this, but generally, it can be considered that the height of a derivative peak can correlate to the amount of DNA amplified, and the amount of DNA amplified can correlate to the number of bacterial cells in the sample. Having this in consideration, the ideal derivative melting profile obtained by a sample containing Bg and Gq, tested by duplex-HRM, is a curve with two recognisable and distinguishable peaks.

Incubation on solid media was better for the detection of Bg and Gq, probably because the level of competition between both species is reduced drastically. In liquid media, cells are planktonic and they are normally able to move and interact with each other, whereas in solid media, wherever the cell lands, it forms a colony, and normally, the interaction amongst species is reduced. There can be segregation of antibiotic substances by one species to inhibit the growth of others, but in this case it did not appear to happen. Having chosen solid media over liquid media, the best temperature of incubation was also investigated, 35 °C being the most suitable one. In addition, it was noticed that, having the choice, it was best to incubate the plates in anaerobic conditions. This is evident looking at the differences between the bacterial species isolated from the same sample, when the isolation is aerobic or anaerobic. When the isolation is aerobic many more species are isolated and the presence of Bg is frequently missed (sometimes the presence of Gq is also missed). The AOD-associated bacteria, Bg, Gq, Rvi and Lb are facultative anaerobes, meaning that they are able to survive in anaerobic conditions if needed. When the incubation of the samples is performed anaerobically, only facultative anaerobes form colonies. This is because strict aerobes do not grow in these conditions, and strict anaerobes do not even survive the sample collection. This is also an excellent way to prevent potential false positives because the less bacterial

species grow in the sample, the less possibilities there are for one to interfere with the HRM diagnosis.

Not forgetting about the rest of the targets of the assay, Rvi and Lb, were incubated anaerobically in LB and EMB plates to test their fitness at 35 °C in the anaerobic chamber. Rvi and Lb formed colonies of similar size as those formed by Bg and Gq after the same type of enrichment.

Once the optimal sample processing method prior to HRM was selected, the multiplex-HRM was validated. The validation was performed testing field samples from several oak trees and the log tests performed at Forest Research. The results of the multiplex-HRM of field samples generally corresponded to the results of the isolation and sequencing, but there were four exceptions. Four dubious results from a total of 84 environmental samples tested (five from Kew, four from Knole Park and 75 from the log tests) means a 95.2 % of successful sample diagnosis, although it would be convenient to test a larger number of field samples to know better the level of accuracy of the test.

The four dubious results were the following: Log 5 presented low late amplification that yielded a derivative melting profile with a low derivative fluorescence peak at 80.5 °C. This was interpreted as a negative result because it was due to late amplification, but the T_m was very similar to the T_m of Rvi and it is important to consider that if the multiplex-HRM is run for more than 30 cycles, false positive results can happen. Only *Citrobacter bitternis* was isolated from Log 5 and it could be the responsible of the late amplification, but the same species has also been isolated from other samples and it did not cause the same problem. Log 4 contained Bg according to the multiplex-HRM assay, however, this species was not isolated from Log 4. This could be due to a human error during the isolations, or it could also be due to the HRM result being a false positive due to a fail in the assay or crossed contamination. The opposite situation happened in Log 25 and Log 27, which tested negative in the HRM assay, but Rvi was isolated. This could be a false negative or it could be due to a poor identification. *Rahnella* sp. are challenging to identify accurately even having the 16S rRNA gene nucleotide sequence, this is probably due to the high level of sequence conservation of the 16S ribosomal gene. This is why the samples containing *Rahnella* sp. were also tested with the SNP-based HRM assay for the differentiation of species of the genus *Rahnella*. The results of the SNP-based HRM assay agreed with the results of the multiplex-HRM in all the samples tested, and the samples that came back negative in the multiplex-HRM, were Rva, according to the SNP-based assay.

The multiplex-HRM method is effective when the sample tested is a pure culture, but when the sample is environmental, the risk of errors increases considerably. For this reason an optimisation of the sample preparation method prior to HRM was needed. As concluding remarks, the best way to incubate the field samples from AOD-affected oaks is to plate them out on LB or EMB media and incubate the plates for 72 hours, anaerobically. After incubation, some of the bacterial growth is suspended in water and tested directly by multiplex-HRM (Figure 60).

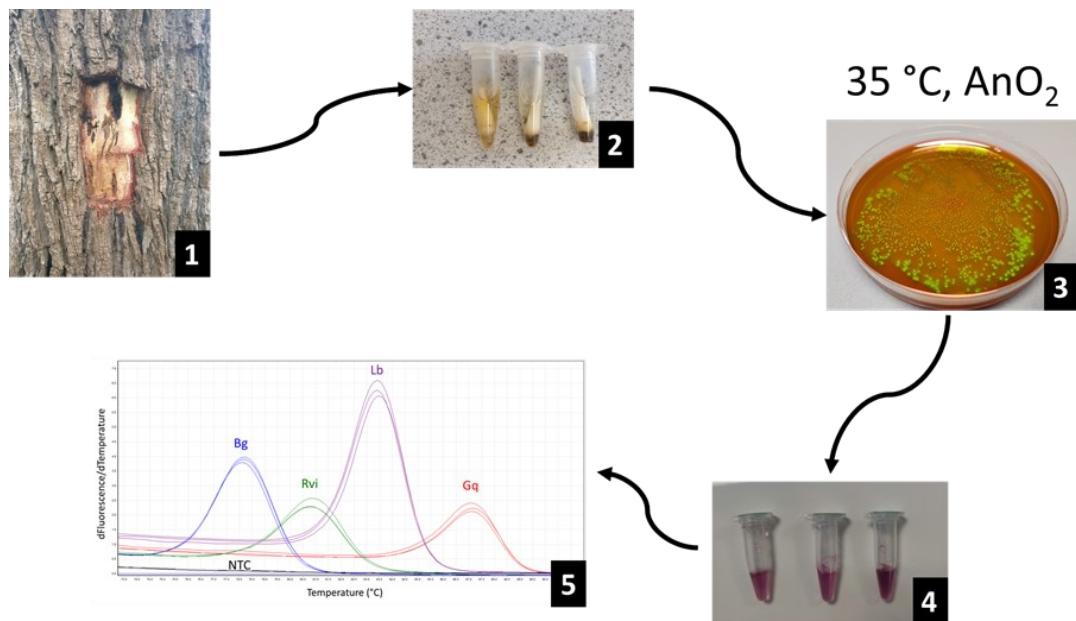


Figure 60: Optimal pre-HRM assay sample processing. The optimal method to process field samples collected from Acute Oak Decline stem lesion (1) or another type of plant material is to submerge the swabs in Ringer’s solution to make what it is called “initial stem suspension (2). From the initial stem suspension, glycerol stocks can be saved to be analysed in the future. For enrichment, initial stem suspension or glycerol stocks obtained from field samples are plated out on LB or EMB media, and incubated anaerobically at 35 °C for 2 to 3 days (3). One μ L of a suspension created by dissolving in water a loopful of bacterial growth collected from the plate (4), is directly used as DNA template for the HRM assay (5).

Future work: before the results described in **Chapters 5 and 6** can be published, there are a number of aspects to consider. It would be necessary to validate and to test the specificity and sensitivity of the SNP-based HRM methods for the differentiation of *Brenneria* sp., *Rahnella* sp., and *Gibbsiella* sp. In addition, it would be good to validate the multiplex-HRM assay by testing more field samples. As mentioned in the discussion of Chapter 5, it would also be interesting to test the combination of primers: Bgi2F, Bgi2R, Gqi4F, Gqi4R, Rvii1F, and Rvii1R in a triplex-HRM assay. The triplex-HRM assay is likely to be species-specific for all the targets (as opposed to the multiplex-HRM assay, which is specific only to genus level in the case of *Gibbsiella* sp.), however the detection of Lb would no longer be possible. But as Lb has not been isolated from any of the samples studied in this thesis, it may be an acceptable compromise.

Looking back at the project with perspective, it would have been interesting as well to explore other sample processing methods apart from the enrichment. For example, magnetic bead-based DNA isolation (Azimi et al., 2011). AOD affected tissue samples contain contaminant particles and substances that inhibit the detection of the DNA in the sample, such as resins and tannins. Filtrating the liquid sample to clean off the contaminants can compromise the amount of bacteria left in it, making the detection more difficult, and risking obtaining false negative results. Magnetic bead-based DNA isolation attracts the DNA present in a sample using magnetic beads. The DNA is captured by the beads, which in turn, can be extracted from the tube, using magnetic bars, and leaving the debris and contamination behind. To release the DNA of the bacteria would be as simple as heating the sample for a few minutes at 95°C as this breaks the bacterial membranes, and releases their DNA into the liquid, and this happens in the denaturation step of the PCR. This change in the sample processing protocol could mean saving a substantial amount of time (2 to 3 days), because the enrichment step (plating out the sample in agar plates, and incubating them anaerobically) could be eliminated. However, the importance of the enrichment step must be taken into consideration, because it not only allows the target species to multiply and be more detectable, but it also clears the sample from all the species of bacteria that are unable to grow without oxygen, resulting in a very pure sample. The magnetic bead-based DNA isolation could be applied in heavily infected samples, because they have a high number of bacterial pathogen targets already, and other species of bacteria are not that numerous.

CHAPTER 7. Final discussion

7.1. Introduction

British forests are invaluable and iconic for the United Kingdom. Woodland areas are central to the conservation efforts as they are essential for the biodiversity (supporting wildlife and the ecosystem), the economy (timber production), and the society (recreation areas). Endemic oak trees *Quercus robur* and *Q. petraea* (English or pedunculate oak and sessile oak) are threatened by a disease known as Acute Oak Decline (AOD). AOD is a polymicrobial syndrome that affects mostly mature oaks in the middle and South of the UK, as well as in several other countries. AOD has the potential to devastate oak populations as it can kill the tree in approximately five years. AOD is caused by a consortia of bacterial pathogens, and associated with the disease there is a buprestid beetle (*Agrilus biguttatus*) whose role in the disease is under investigation. The bacteria associated with AOD produce necrotic patches in the inner bark and the main symptom of AOD are vertical cracks between the bark plates of the stem from which dark fluids ooze out (Denman et al., 2014). More than 200 samples from oaks suspected to have AOD were processed and diagnosed by Forest Research in 2020. A huge effort has been made the last decade to characterise the pathobiome of the disease, defining novel genera and species to accommodate the undescribed bacterial pathogens, however, a few species commonly isolated from the lesion remained undescribed.

The objectives of this project were to formally classify the undescribed “*fulva*-like” *Pseudomonas*, commonly present in AOD lesions (Broberg et al., 2018; Denman et al., 2018, 2016b; Sapp et al., 2016), and to evaluate their possible role in the disease; to develop and validate a rapid diagnostic method for the AOD-associated bacteria *Brenneria goodwinii* (Bg), *Gibbsiella quercinecans* (Gq), *Rahnella victoriana* (Rvi), and *Lonsdalea britannica* (Lb); and last of all, to develop diagnostic methods for other species belonging to the AOD-associated genera *Brenneria*, *Gibbsiella*, *Rahnella* and *Lonsdalea*. The diagnostic methods were designed using a real-time PCR-based technique known as high resolution melting (HRM).

7.2. General overview

In response to the consistent isolation of unknown “*fulva*-like” *Pseudomonas* in AOD lesions, 35 isolates were collected and subjected to a polyphasic approach of bacterial classification. This was to determine their taxonomic position and to confirm that they belonged to novel taxa. Once all the specific features of the bacteria were collected, comparative studies were carried out to evaluate whether the differences between the bacteria under study and their closest formally described neighbours, were significant enough to classify them as new taxa. The isolates were found to belong to three novel species: *Pseudomonas daroniae* sp. nov. (Pda), *Pseudomonas dryadis* sp. nov. (Pdr), and *Pseudomonas kirikiae* sp. nov. (Pki) (Bueno-Gonzalez *et al.*, 2019, 2020).

While studying the phylogenetic relationships of the AOD-associated *Pseudomonas*, it was observed that, depending on the method used for the inference, Pki shared clade with species from four genera: *Pseudomonas*, *Azomonas*, *Azotobacter* and *Azorhizophilus*. The grouping inconsistencies, suggested that Pki is on the taxonomic edge of the genus *Pseudomonas* and led us to perform further phylogenetic studies of the relationships amongst the four genera. The boundaries between these four genera, collectively known as the “*Azotobacter* group”, have been a matter of controversy amongst taxonomists for some time. For instance, some authors claim that the genus *Pseudomonas* should be divided into several novel genera (Lalucat *et al.*, 2020; Peix, Ramírez-Bahena and Velázquez, 2018). Others believe that *Azomonas* and *Azotobacter* should be included in *Pseudomonas* (Özen and Ussery, 2012; Rediers, Vanderleyden and De Mot, 2004; Young and Park, 2007), whereas later studies suggested that *Azotobacter* is an independent genus (Parks *et al.*, 2018; Qin *et al.*, 2014).

After phylogenetic analysis of 16S rRNA gene sequences and MLSA of a selection of species of the four genera in the “*Azotobacter* group” it was concluded that that *Azomonas* and *Azotobacter* are two separate genera, and that *Pseudomonas* should be divided into several novel genera, agreeing with Peix, Lalucat, and their colleagues (Lalucat *et al.*, 2020; Peix, Ramírez-Bahena and Velázquez, 2018). 16S rRNA

phylogenies suggested that *Azorhizophilus paspasli* belongs to *Azotobacter*, although confirmation was not possible due to the lack of *Azorhizophilus* genes for the MLSA in the databases. The suggested taxonomic rearrangement has important consequences, including that the true *Pseudomonas* will be only those included in the lineage of the type species, *P. aeruginosa*, and that would exclude many other *Pseudomonas* from the genus, including Pda, Pdr, and Pki.

Following the formal description of the novel AOD-associated *Pseudomonas* (Bueno-Gonzalez *et al.*, 2019, 2020), studies were carried out to see if the strains have potential plant-pathogenicity traits. The steps followed were to screen their whole genomes for virulence factors (VFs); hypersensitive response (HR) tests in bean pods, and tobacco leaves; and cell attachment assays. Although non-pathogenic bacteria may also possess pathogenicity traits, if AOD-associated *Pseudomonas* had many potential pathogenicity traits, this could suggest that they have a role in AOD., either as a pathogen or as an assistant to the pathogen. If the AOD-associated *Pseudomonas* are an indicator of disease they could also have been considered as targets for the diagnostic methods developed in this project.

However, genetic potential does not mean genetic expression, it seems that the AOD-associated *Pseudomonas* genomes do not have VFs commonly present in pathogenic *Pseudomonas*, such as those that encode type III secretion systems. This being the case, the profiles of VFs of the AOD-associated *Pseudomonas* were not especially similar to those of the endophyte *Pseudomonas fluorescens* SBW25 either. It was observed that in the agglomerative hierarchical clustering (AHC) of the profiles of VFs, Pki grouped with the other two species of AOD-associated *Pseudomonas*: Pda and Pdr instead of grouping with species genetically closer such as *P. stutzeri*. It may be that the VF profile is more influenced by what the AOD-associated *Pseudomonas* have in common, which is, among other things, inhabiting an oak that is suffering from AOD, than by taxonomic proximity.

The AOD-associated *Pseudomonas* did not elicit HR in bean pods and tobacco leaves. Negative HR does not mean that the strains are not pathogenic, but a positive HR would have mean that they could be pathogenic. Lastly, a typical but not exclusive

feature of pathogens, the ability to create biofilms, was studied in the AOD-associated *Pseudomonas*. The ability of the cells to adhere to three different surfaces was tested: well plates, Falcon tubes and glass coverslips. Of the three AOD-associated *Pseudomonas* species studied, only Pki strains P4^T and P30 showed adherence abilities to one of the surfaces, the Falcon tubes. However, an important note must be made here: the Pki cell attachment was only observed when the incubation medium was LB broth. In routine laboratory work it was seen that AOD-associated *Pseudomonas* grow poorly on LB broth, particularly Pki. It may be that a hostile environment such as a suboptimal culture medium is causing the expression of the genes that contribute to cell attachment. As previously reported, the environment in which a bacterium is incubated has an impact on the cell attachment abilities of the inoculated species (Hancock, Witsø and Klemm, 2011; Ueda and Saneoka, 2015).

The presence in their genomes of typical VFs of a pathogen, a positive HR in plant tissue, or strong cell attachment abilities would have suggested that the AOD-associated *Pseudomonas* could potentially be pathogenic, but the results of the tests were generally negative. Acknowledging that a negative response does not mean that they are not potential pathogens, it was decided that the AOD-associated *Pseudomonas* do not present a typical phytopathogenic features, and they were not included as targets for the diagnostic methods developed for bacteria associated with AOD.

Once the AOD-associated *Pseudomonas* were formally described, and their potential pathogenicity traits were studied, the focus of the project was the development of a rapid diagnostic method for bacteria associated with AOD and to expand the bacteria that can be identified to include other species of the genera commonly found in symptomatic oaks. Several diagnostic methods were developed: a multiplex-HRM for the detection and identification of Bg, Gq, Rvi and Lb from field samples, and several tools designed to work with pure cultures, including: a duplex-HRM assay of the genes *atpD* and *rpoD* for the identification of AOD-associated bacteria including Pda, Pdr and Pki; and three SNP-based HRM assays for the differentiation of species and subspecies of the AOD-associated genera *Gibbsiella*, *Brenneria* and *Rahnella*.

To design a simple diagnostic method, the first thing studied was the possibility of removing the DNA extraction step in order to save time and resources during sample processing. Melting temperatures (T_{ms}), and derivative fluorescence curves of the same sample prepared in different formats were analysed. That is, the same sample was analysed by HRM both after its DNA was extracted and in crude form (without DNA extraction). The result showed that as long as all the samples are prepared in the same way, the difference in T_m between one sample and another remained stable, allowing one sample to be differentiated from another. It was concluded that DNA extraction can be optional and from that point on, cells in suspension were used for HRM analyses instead of purified DNA, with the consequent saving of time and reagents.

The original HRM analysis of the *atpD* gene (Brady et al., 2016) was not valid for samples containing more than one species of bacteria. Therefore a new assay was designed based on this one, but targeting a longer fragment of the same gene. Being a larger fragment, the number of SNPs was also greater, and therefore the discriminatory power of the assay increased. With the HRM assay of the longer *atpD* fragment, all strains tested could be clearly differentiated, when the HRM analysis was complemented by gel electrophoresis analysis of the amplicons generated (**Figure 36**). However, it is not practical to have to combine the HRM assay with a subsequent analysis by gel electrophoresis, so the assay continued to be adjusted in order to dispense with the gel. The concentration of primers and the conditions of the PCR were adjusted, until PCR artefacts like primer-dimers and non-specific amplification were eliminated, and as a result, the AOD-associated *Pseudomonas* no longer amplified with this assay. In order to amplify the *Pseudomonas*, the HRM assay of the long fragment of the *atpD* gene was combined with the HRM assay of a portion of the *rpoD* gene, which used specific primers for *Pseudomonas* (Mulet et al., 2009). The result of this addition was a duplex-HRM assay of the genes *atpD* and *rpoD*. The duplex-HRM assay was able to clearly identify all strains tested except for Rvi and Rva, which had indistinguishable melting profiles (**Figure 37**). The samples included in this assay were pure cultures of Gq, Bg, *Brenneria roseae* ssp. *roseae* (Brr), Rvi, *Rahnella variigena* (Rva), Lb, Pda, Pdr, and Pki.

The duplex-HRM assay is intended for identification of AOD-associated bacteria from pure cultures and it can be very useful in routine laboratory work, but samples from the environment rarely contain only one species of microbe, and more commonly can contain up to hundreds. Therefore, it was important to design a diagnostic method capable of detecting and identifying AOD-associated bacteria in mixed samples. For this purpose, a multiplex-HRM assay for the detection and identification of Bg, Gq, Rvi, and Lb was developed. The assay worked satisfactorily, both in *in silico* predictions, and in tests carried out with artificial cocktails of AOD-associated bacteria (**Figure 39**). However, in the validation of the method with environmental samples it was observed that directly testing field samples did not work, there was no amplification. Direct testing meant dipping and squeezing the head of each swab taken from an AOD lesion into a 1.5 mL tube with Ringers solution, and testing that suspension. A likely explanation is that the suspension contained too much debris and PCR inhibitors such as xylan, polyphenols, or resins (Demeke and Adams, 1992; Henson and French, 1993; John, 1992; Malvick and Grunden, 2005; Wilson, 1997) coming from the trunk of the tree, and therefore the result was a false negative. It was known that it was a false negative because the trees showed clear symptoms of AOD, and several of the target species had been isolated from the swabs by culturing.

Apart from the contaminants, the field samples presented another challenge: as in any environmental sample, hundreds of species of microbes can be present in the swab. The non-targeted microbes present in the sample posed three problems: background noise, potential false positives, and potential masking of the targeted species (false negatives). The way in which these three problems were overcome was by turning to the biology of the targeted species. All targeted bacteria are facultative anaerobes, this trait allowed the introduction of an anaerobic incubation step. Through the anaerobic incubation step, the sample is enriched in facultative anaerobes, leaving the strict aerobes precluded. This was verified with both multiplex-HRM and traditional isolation of bacteria from samples grown with and without oxygen (**section 6.2.1**). Another problem that had to be overcome was that the presence of Bg is masked by other members of the AOD-pathobiome such as Gq, which grows very well under laboratory conditions. In studies including metagenomic

and traditional isolation of the same AOD samples, Bg was found to be the most abundant microbe in metagenomic studies, but was nevertheless underrepresented in the isolation (Denman et al., 2018). To avoid this interaction between species that makes some of them undetectable, the microbes of the sample were incubated on solid medium. Where the cell lands, it forms its colony, so in theory no representation of any species capable of growing in that environment and conditions is lost. Apart from the type of medium, the optimal incubation temperature was found to be 35 °C. In conclusion, detection and identification of Bg, Gq, Rvi and Lb was optimal when processing the sample: dipping and squeezing the head of each swab in 750 µL of Ringers solution, incubating 10 µL of the suspension in LB or EMB media for 48-72 hours, anaerobically at 35 °C. After incubation, some of the bacterial growth is suspended in water and one µL of this suspension is tested directly by multiplex-HRM.

Once the optimal method to process the samples prior to HRM analysis was established, the method was validated with environmental samples from several AOD-affected locations. While this project was being executed, a research paper was published describing a multiplex Taqman qPCR assay for the detection and identification for Bg, Gq, Rvi, and Lb (Crampton et al., 2020). This is currently the tool used for the routine diagnosis of the field samples from trees suspected to suffer from AOD. Both TaqMan-based and multiplex-HRM assays to diagnose AOD-associated bacteria are non-destructive, which is fundamental, given the environmental importance of mature oak trees.

The TaqMan-based assay is considerably more sensitive than the multiplex-HRM assay, being able to detect a minimum of 14 cells of Gq, 76 of Bg, 75 fo Lb, and 25 of Rvi. The multiplex-HRM assay presented higher detection thresholds (16,000 CFU of Bg, 284 CFU of Gq, 2,480 CFU of Rvi and 296 CFU of Lb), although number of cells should not be a limiting factor for diagnosis if the pre-HRM field sample processing is carried out as suggested.

In terms of specificity, the TaqMan-based assay lacks specificity to species-level in three of its targets (Gq, Rvi and Lb), whereas the multiplex-HRM assay is species-

specific for three of its four targets (Bg, Rvi, and Lb). Neither of the methods are species-specific for Gq, but it seems that the species of this genus are genetically very close. Ongoing research points to an incorrect positioning of *Gibbsiella* species (personal communication from Dr Carrie Brady). Multiplex-HRM is cheaper, the cost of an HRM assay is approximately £1 whereas each TaqMan-based sample analysis has been calculated to cost £6 (personal communication from Dr Dr Bridget Crampton). An advantage of multiplex-HRM over TaqMan-based assays is the possibility to melt the amplification product and double-check that the melting temperature of the product is as expected. This is a robust way to make sure the amplification is specific and HRM technology can do so in a very precise manner, as it is able to distinguish between amplicon products melting at temperatures different only a fraction of a degree.

The SNP-based HRM assay for the differentiation of species and subspecies of the genus *Brenneria* was effective in the discrimination of pure cultures of strains of Bg, *Brenneria roseae* ssp. *roseae* (Brr), *Brenneria roseae* ssp. *americana* (Bra), *Brenneria alni* (Ba), *Brenneria nigrifluens* (Bn), *Brenneria salicis* (Bsa) and *Brenneria rubrifaciens* (Bru) (**Figure 44**).

The SNP-based HRM assay for the differentiation of species of the genus *Rahnella* was effective as well in the discrimination of pure cultures of the strains tested (Rvi, *Rahnella variigena* (Rva), *Rahnella bruchi* (Rbru), *Rahnella woolbedingensis* (Rwo), *Rahnella aquatilis* (Raq), and *Rahnella inusitata* (Rinu); **Figure 46**). When the study of bacterial isolation of the field samples was made, it was seen that some isolates were *Rahnella* sp. The identification was made by sequencing the 16S rRNA partial gene, and this type of identification can sometimes only be reliable up to the genus level. So the opportunity was taken to test the SNP-based HRM assay for the differentiation of species of the genus *Rahnella*. Of the nine isolates tested, five were Rvi and four were Rva. This result fits with expectations, since these two species are commonly isolated in AOD sites.

The SNP-based HRM assay for the differentiation of species of the genus *Gibbsiella* was also effective for the discrimination of pure cultures of the species tested (*Gq*, *Gibbsiella gregii* and *Gibbsiella dentisursi* = *Gibbsiella papilionis*) (**Figure 48**).

Lastly, to investigate if leaves of oaks not displaying AOD symptoms could be a reservoir for AOD-associated bacteria, isolation, purification and identification by partial 16S rRNA gene sequencing of endophytic and epiphytic bacteria from oak leaves was performed (**Figure 58**). Bg, Gq, Rvi and Lb were also screened for in the samples collected from the leaves using multiplex-HRM assay. None of the AOD-associated bacterial strains were found between the endophytes and epiphytes of leaves of sapling and mature *Quercus robur*.

7.3. Conclusion

In conclusion, three novel AOD-associated *Pseudomonas* were formally described and several HRM-based tools, intended to be useful for AOD diagnosis and research were developed. A multiplex-HRM assay was developed and validated for the detection and identification of Bg, Gq, Rvi and Lb in field samples. A duplex HRM assay was developed for the identification of pure cultures of several AOD-associated strains, including Pda, Pdr, and Pki, and also, three HRM assays based on SNP detection for the differentiation of pure cultures of different species and subspecies of the genera *Brenneria*, *Gibbsiella* and *Lonsdalea*, were also developed (**Figure 61**).

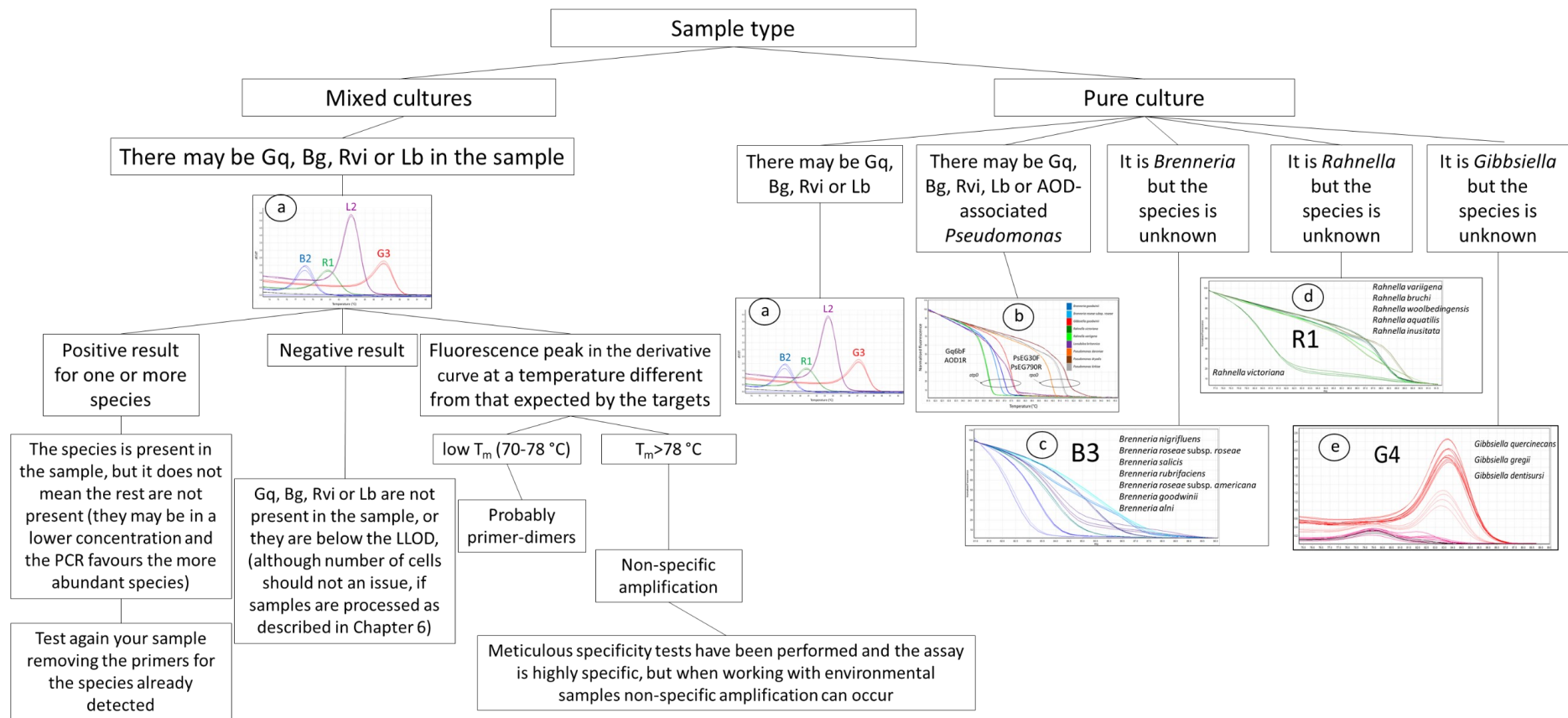


Figure 61: Flowchart of the optimized Acute Oak Decline molecular diagnostic workflow protocol according to the sample type. Figure a: Multiplex-HRM assay for the detection and identification of Bg, Gq, Rvi, and Lb. Figure b: Duplex-HRM assay of genes *atpD* and *rpoD* for the identification of AOD-associated bacteria including AOD-associated *Pseudomonas*. Figure c: SNP-based HRM assay for the differentiation of species and subspecies of the genus *Brenneria*.

Figure d: SNP-based HRM assay for the differentiation of species of the genus *Rahnella*. Figure e: SNP-based HRM assay for the differentiation of species of the genus *Gibbsiella*. B2, R1, L2, G3, B3, and G4 are primers Bgi2F- Bgi2R, Rvii1F-Rvii1R, Lbi2F-Lbi2R, Gqi3F- Gqi3R, Bgi3F- Bgi3R, and Gqi4F- Gqi4R, respectively.

7.4. Future work

From the work performed in the description of the novel AOD-associated *Pseudomonas* it was concluded that a reclassification of the bacteria included in the *Azotobacter* group is needed. The reclassification proposed for *Pseudomonas* and the rest of the genera included in the *Azotobacter* group will be a large and laborious task, which should be based on a polyphasic approach and the sequencing and analysis of the complete genomes of the species that do not already have them available.

In terms of the potential pathogenicity traits of the AOD-associated *Pseudomonas*, although for now it was decided that AOD-associated *Pseudomonas* do not present a typical pathogenic genotypic and phenotypic profile, it remains to be seen whether they help the establishment and progression of AOD putative pathogens. That may be an interesting line for future studies. Experiments that could be performed to test if there are positive or negative synergies between the novel AOD-associated *Pseudomonas* species and the AOD pathogens would be to compare the growth curves of combinations of two species of bacteria (AOD pathogen + AOD-associated *Pseudomonas*) to those obtained for pure cultures of the same species. In addition, this study can be done using different media to see if this has any effect on the synergy. Regarding the cell attachment assays, it may be that a hostile environment such as a suboptimal culture medium is causing the expression of the genes that contribute to cell attachment. Therefore, it would be interesting to repeat the cell attachment experiments with an even more challenging medium for AOD-associated *Pseudomonas* than LB. If the bacterium is in an optimal environment, it has no reason to waste its energy on survival strategies. If the cell attachment assays were repeated using minimal media (M9), the expression of the genes that collaborate in the cell attachment would possibly be triggered even further than when they were incubated in LB, resulting in higher cell attachment levels. It was observed that when studying bacterial survival strategies, it is convenient to push the bacterium to its limit to see what it is really capable of.

Regarding the HRM diagnostic tools, studies of specificity and sensitivity are still to be performed for the three SNP-based HRM tools to differentiate pure cultures of species and subspecies of *Brenneria*, *Rahnella* and *Gibbsiella*. Additionally, the multiplex-HRM assay is specific only at genus level for *Gibbsiella*. This means that the assay is susceptible to false positives for Gq if another species of the genus are present in the sample. Although it is not a serious problem because the other two species of the genus have never been isolated in AOD-affected trees, it can be solved in the following way. During the design of the multiplex-HRM assay, several primers pairs that specifically targeted Gq were designed. The primers used for the SNP-based HRM assay for the differentiation of species of the genus *Gibbsiella* can be used in the multiplex-HRM, and those are species-specific. Therefore, a future line of work could be to experiment with a different combination of primers that includes species-specific by Gq, in this case the proposed combination of primers is Bgi2F, Bgi2R, Gqi4F, Gqi4R, Rvii1F, and Rvii1R. Finally, an improvement that could be added to all the assays described in this section could be the absolute quantification of the bacteria present in the samples, through the introduction of standard curves of serial dilutions of cell suspensions of each of the targets.

Although the multiplex-HRM assay is robust when the field samples are processed in the optimum way, it is necessary to continue validating the method with a greater number of field samples. Another type of pre-HRM sample processing could also be tried, such as magnetic bead-based DNA isolation (Azimi et al., 2011), although the importance of the anaerobic incubation step should not be underestimated, since it cleans the sample from practically any species of bacteria other than the ones we are interested in detecting.

Comparison studies of the diagnostic capacity of the multiplex-HRM assay and the TaqMan-based assay should be performed (Crampton et al., 2020). It would also be interesting to test the analysis based on TaqMan probes with anaerobically processed samples to see if it improves its specificity in the same way that it improved that of the multiplex-HRM assay.

REFERENCES

- Abalos, A. et al. (2001) Physicochemical and antimicrobial properties of new rhamnolipids produced by *Pseudomonas aeruginosa* AT10 from soybean oil refinery wastes. *Langmuir*. 17, (5), pp. 1367–1371.
- Abdel-Mawgoud, A.M., Lépine, F. and Déziel, E. (2010) Rhamnolipids: Diversity of structures, microbial origins and roles. *Applied Microbiology and Biotechnology*. 86 (5), pp. 1323-1336.
- Adékambi, T., Drancourt, M. and Raoult, D. (2009) The *rpoB* gene as a tool for clinical microbiologists. *Trends in Microbiology*. 17 (1), pp. 37-45.
- Adeolu, M. et al. (2016) Genome-based phylogeny and taxonomy of the ‘*Enterobacteriales*’: proposal for *Enterobacterales* ord. nov. divided into the families *Enterobacteriaceae*, *Erwiniaceae* fam. nov., *Pectobacteriaceae* fam. nov., *Yersiniaceae* fam. nov., *Hafniaceae* fam. nov., Morgane. *International Journal of Systematic and Evolutionary Microbiology*. 66 (12), pp. 5575–5599.
- Ait Tayeb, L. et al. (2005) Molecular phylogeny of the genus *Pseudomonas* based on *rpoB* sequences and application for the identification of isolates. *Research in Microbiology*. 156 (5–6), pp. 763–773.
- Alarcon, B. et al. (1990) Differentiation of *Erwinia carotovora* ssp. *carotovora* and *Erwinia carotovora* ssp. *atroseptica* isolated from potato by western blot and subsequent indirect elisa. *Journal of Applied Bacteriology*. 69 (1), pp. 17–24.
- Alfano, J.R. and Collmer, A. (1997) The type III (Hrp) secretion pathway of plant pathogenic bacteria: Trafficking harpins, Avr proteins, and death. *Journal of Bacteriology*. 179 (18), pp. 5655–5662.
- Anwar, N. et al. (2017) *Pseudomonas tarimensis* sp. nov., an endophytic bacteria isolated from *Populus euphratica*. *International Journal of Systematic and Evolutionary Microbiology*. 67 (11), pp. 4372–4378.
- Anzai, Y. et al. (2000) Phylogenetic affiliation of the pseudomonads based on 16S rRNA sequence. *International Journal of Systematic and Evolutionary Microbiology*. 50 (4), pp. 1563–1589.
- Apel, K. and Hirt, H. (2004) Reactive oxygen species: metabolism, oxidative stress, and signal

transduction. *Annual Review of Plant Biology*. 55 (1), pp. 373-399.

Auch, A.F. et al. (2010) Digital DNA-DNA hybridization for microbial species delineation by means of genome-to-genome sequence comparison. *Standards in Genomic Sciences*. 2 (1), pp. 117-134.

Auch, A.F., Klenk, H.P. and Göker, M. (2010) Standard operating procedure for calculating genome-to-genome distances based on high-scoring segment pairs. *Standards in Genomic Sciences*. 2 (1), pp. 142-148.

Azimi, S.M. et al. (2011) A magnetic bead-based DNA extraction and purification microfluidic device. *Microfluidics and Nanofluidics*. 11 (2), pp. 157-165.

Aziz, R.K. et al. (2008) The RAST Server: Rapid annotations using subsystems technology. *BMC Genomics*. 9 (1), p. 75.

Banin, E., Vasil, M.L. and Greenberg, E.P. (2005) Iron and *Pseudomonas aeruginosa* biofilm formation. *Proceedings of the National Academy of Sciences of the United States of America*. 102 (31), pp. 11076-11081.

Barbosa, E. et al. (2014) On the limits of computational functional genomics for bacterial lifestyle prediction. *Briefings in Functional Genomics*. 13 (5), pp. 398-408.

Bass, D. et al. (2019) The Pathobiome in Animal and Plant Diseases. *Trends in Ecology and Evolution*. 34 (11), pp. 996-1008.

Beiki, F. et al. (2016) New *Pseudomonas* spp. are pathogenic to citrus. *PLoS ONE*. 11 (2), pp. 1–16.

Beye, M. et al. (2018) Careful use of 16S rRNA gene sequence similarity values for the identification of *Mycobacterium* species. *New Microbes and New Infections*. 22, pp. 24-29.

Bhattacharya, S. et al. (2007) BioMEMS and nanotechnology-based approaches for rapid detection of biological entities. *Journal of Rapid Methods and Automation in Microbiology*. 15 (1), pp. 1-32.

Biosca, E.G. et al. (2003) Isolation and characterization of *Brenneria quercina*, causal agent for bark canker and drippy nut of *Quercus* spp. in Spain. *Phytopathology*. 93 (4), pp. 485–492.

Blanco, P. et al. (2016) Bacterial multidrug efflux pumps: much more than antibiotic resistance determinants. *Microorganisms*. 4 (1), p. 14.

- Bolger, A.M., Lohse, M. and Usadel, B. (2014) Trimmomatic: A flexible trimmer for Illumina sequence data. *Bioinformatics*. 30 (15), pp. 2114–2120.
- Boonham, N. et al. (2003) Detection of potato viruses using microarray technology: Towards a generic method for plant viral disease diagnosis. *Journal of Virological Methods*. 108 (2), pp. 181–187.
- Bordeleau, E. et al. (2018) Abrasive treatment of microtiter plates improves the reproducibility of bacterial biofilm assays. *RSC Advances*. 8 (57), pp. 32434–32439.
- Bosi, E. et al. (2017) The pangenome of (Antarctic) *Pseudoalteromonas* bacteria: evolutionary and functional insights. *BMC Genomics*. 18 (1), p. 93.
- Boukhalfa, H. and Crumbliss, A.L. (2002) Chemical aspects of siderophore mediated iron transport. *BioMetals*. 15, pp. 325–339.
- Brady, C. et al. (2014a) Description of *Brenneria roseae* sp. nov. and two subspecies, *Brenneria roseae* subspecies *roseae* ssp. nov and *Brenneria roseae* subspecies *americana* ssp. nov. isolated from symptomatic oak. *Systematic and Applied Microbiology*. 37, pp. 396–401.
- Brady, C. et al. (2010) Description of *Gibbsiella quercinecans* gen. nov., sp. nov., associated with Acute Oak Decline. *Systematic and Applied Microbiology*. 33, pp. 444–450.
- Brady, C. et al. (2014b) *Gibbsiella greigii* sp. nov., a novel species associated with oak decline in the USA. *Systematic and Applied Microbiology*. 37 (6), pp. 417–422.
- Brady, C. et al. (2015) *Gibbsiella papilionis* Kim et al. 2013 is a later heterotypic synonym of *Gibbsiella dentisursi* Saito et al. 2013. *International Journal of Systematic and Evolutionary Microbiology*. 65 (12), pp. 4788–4791.
- Brady, C. et al. (2012) Proposal to reclassify *Brenneria quercina* (Hildebrand and Schroth 1967) Hauben et al. 1999 into a new genus, *Lonsdalea* gen. nov., as *Lonsdalea quercina* comb. nov., descriptions of *Lonsdalea quercina* subsp. *quercina* comb. nov., *Lonsdalea quercina* subsp. *ib.* *International journal of systematic and evolutionary microbiology*. 62 (7), England, pp. 1592–1602.
- Brady, C. et al. (2014c) *Rahnella victoriana* sp. nov., *Rahnella bruchi* sp. nov., *Rahnella woolbedingensis* sp. nov., classification of *Rahnella* genomospecies 2 and 3 as *Rahnella variigena* sp. nov. and *Rahnella inusitata* sp. nov., respectively and emended description of the genus *Rahnella*. *Systematic and Applied Microbiology*. 37 (8), pp.545–552.

Brady, C. et al. (2016) Rapid identification of bacteria associated with Acute Oak Decline by high-resolution melt analysis. *Letters in Applied Microbiology*. 63 (2), pp. 89-95.

Brady, C. et al. (2017) Taxonomy and identification of bacteria associated with acute oak decline. *World Journal of Microbiology and Biotechnology*. 33 (7), p. 143.

Brandel, J. et al. (2012) Pyochelin, a siderophore of *Pseudomonas aeruginosa*: Physicochemical characterization of the iron(iii), copper(ii) and zinc(ii) complexes. *Dalton Transactions*. 41 (9), p. 2820.

Braun, V. and Killmann, H. (1999) Bacterial solutions to the iron-supply problem. *Trends in Biochemical Sciences*. 24 (3), pp. 104-109.

Brettin, T. et al. (2015) RASTtk: A modular and extensible implementation of the RAST algorithm for building custom annotation pipelines and annotating batches of genomes. *Scientific Reports*. 5 (1), 8365.

Broberg, M. et al. (2018) Integrated multi-omic analysis of hostmicrobiota interactions in acute oak decline. *Microbiome*. 6 (1), p. 21.

Broome, A. et al. (2019) Responding to ash dieback (*Hymenoscyphus fraxineus*) in the UK: Woodland composition and replacement tree species. *Forestry: An International Journal of Forest Research*. 92 (1), pp. 108-119.

Brown, N. et al. (2015) A review of *Agrilus biguttatus* in UK forests and its relationship with acute oak decline. *Forestry*. 88 (1), pp. 53–63.

Brown, N. et al. (2017) Acute oak decline and *Agrilus biguttatus*: the co-occurrence of stem bleeding and D-shaped emergence holes in Great Britain. *Forests*. 8 (3), p. 87.

Brown, N. et al. (2018) Predisposition of forests to biotic disturbance: predicting the distribution of Acute Oak Decline using environmental factors. *Forest Ecology and Management*. 407, pp. 145-154.

Brown, N. et al. (2016) Spatial and temporal patterns in symptom expression within eight woodlands affected by Acute Oak Decline. *Forest Ecology and Management*. 360, pp. 97–109.

Bueno-Gonzalez, V. et al. (2019) *Pseudomonas daroniae* sp. nov. and *Pseudomonas dryadis* sp. nov., isolated from pedunculate oak affected by acute oak decline in the UK. *International*

Journal of Systematic and Evolutionary Microbiology. 69 (11), pp. 3368-3376.

Bueno-Gonzalez, V. et al. (2020) *Pseudomonas kirkiiae* sp. nov., a novel species isolated from oak in the United Kingdom, and phylogenetic considerations of the genera *Pseudomonas*, *Azotobacter* and *Azomonas*. *International Journal of Systematic and Evolutionary Microbiology*. 70 (4), pp. 2426-2434.

Buonaurio, R. et al. (2015) The olive knot disease as a model to study the role of interspecies bacterial communities in plant disease. *Frontiers in Plant Science*. 6, p. 434.

Bustin, S.A. et al. (2009) The MIQE guidelines: minimum information for publication of quantitative real-time PCR experiments. *Clinical Chemistry*. 55 (4), pp. 611-22.

Caiazza, N.C., Shanks, R.M.Q. and O'Toole, G.A. (2005) Rhamnolipids modulate swarming motility patterns of *Pseudomonas aeruginosa*. *Journal of Bacteriology*. 187 (21), pp. 7351-7361.

Caro-Quintero, A. and Konstantinidis, K.T. (2012) Bacterial species may exist, metagenomics reveal. *Environmental Microbiology*. 14 (2), pp. 347-355.

Caruso, P. et al. (2002) Enrichment double-antibody sandwich indirect enzyme-linked immunosorbent assay that uses a specific monoclonal antibody for sensitive detection of *Ralstonia solanacearum* in asymptomatic potato tubers. *Applied and Environmental Microbiology*. 68 (7), pp. 3634–3638.

Chalupowicz, L. et al. (2019) Diagnosis of plant diseases using the Nanopore sequencing platform. *Plant Pathology*. 68 (2), pp. 229-238.

Chapon-Hervé, V. et al. (1997) Regulation of the *xcp* secretion pathway by multiple quorum-sensing modulons in *Pseudomonas aeruginosa*. *Molecular Microbiology*. 24 (6), pp. 1169-1172.

Clerc, a, Manceau, C. and Nesme, X. (1998) Comparison of randomly amplified polymorphic DNA with amplified fragment length polymorphism to assess genetic diversity and genetic relatedness within genospecies III of *Pseudomonas syringae*. *Applied and environmental microbiology*. 64 (4), pp. 1180–1187.

Coker, T.L.R. et al. (2019) Estimating mortality rates of European ash (*Fraxinus excelsior*) under the ash dieback (*Hymenoscyphus fraxineus*) epidemic. *PLANTS, PEOPLE, PLANET*. 1 (1), pp. 48-58.

- Colwell, R.R. (1970) Polyphasic taxonomy of the genus *Vibrio*: numerical taxonomy of *Vibrio cholerae*, *Vibrio parahaemolyticus*, and related *Vibrio* species. *Journal of Bacteriology*. 104 (1), pp. 410–433.
- Compant, S., Clément, C. and Sessitsch, A. (2010) Plant growth-promoting bacteria in the rhizo- and endosphere of plants: their role, colonization, mechanisms involved and prospects for utilization. *Soil Biology and Biochemistry*. 42 (5), pp. 669-678.
- Compton, J. (1991) Nucleic-Acid Sequence-Based Amplification. *Nature*. 350 (6313), pp. 91–92.
- Cornelis, P. (2010) Iron uptake and metabolism in pseudomonads. *Applied Microbiology and Biotechnology*. 86 (6), pp. 1637-1645.
- Costerton, J.W. (1995) Overview of microbial biofilms. *Journal of Industrial Microbiology*.
- Cotta, M.A. et al. (2009) *Robinsoniella peoriensis* gen. nov., sp. nov., isolated from a swine-manure storage pit and a human clinical source. *International Journal of Systematic and Evolutionary Microbiology*. 59 (1), pp. 150-155.
- Crampton, B.G. et al. (2020) A multiplex real-time PCR assay enables simultaneous rapid detection and quantification of bacteria associated with Acute Oak Decline. *Plant Pathology*. 69 (7), pp. 1301-1310.
- Dahllöf, I., Baillie, H. and Kjelleberg, S. (2000) *rpoB*-based microbial community analysis avoids limitations inherent in 16S rRNA gene intraspecies heterogeneity. *Applied and Environmental Microbiology*. 66 (8), pp. 3376–3380.
- Darling, A.C.E. et al. (2004) Mauve: Multiple alignment of conserved genomic sequence with rearrangements. *Genome Research*. 14 (7), pp. 1394-1403.
- Darriba, D. et al. (2012) jModelTest2: more models, new heuristics and parallel computing. *Nature Methods*. 9 (8), p. 772.
- Demeke, T. and Adams, R.P. (1992) The effects of plant polysaccharides and buffer additives on PCR. *BioTechniques*. 12 (3), pp. 332-4.
- Denman et al. (2013) Acute Oak Decline in Britain. *Biosecurity in natural forests and plantations, genomics and biotechnology for biosecurity in forestry, 2013*. Bruno and Cerna Hora, Czech Republic: IUFRO, 128, pp. 20–25.

- Denman, S. et al. (2014) A description of the symptoms of Acute Oak Decline in Britain and a comparative review on causes of similar disorders on oak in Europe. *Forestry*. 87 (4), pp. 535–551.
- Denman, S. et al. (2012) *Brenneria goodwinii* sp. nov., associated with acute oak decline in the UK. *International Journal of Systematic and Evolutionary Microbiology*. 62 (10), pp. 2451–2456.
- Denman, S. et al. (2017) Identification of *Armillaria* species on declined oak in Britain: Implications for oak health. *Forestry*. 90 (1), pp. 148–161.
- Denman, S. et al. (2016a) Isolation studies reveal a shift in the cultivable microbiome of oak affected with Acute Oak Decline. *Systematic and Applied Microbiology*. 39 (7), pp. 484–490.
- Denman, S. et al. (2016b) Isolation studies reveal a shift in the cultivable microbiome of oak affected with Acute Oak Decline. *Systematic and Applied Microbiology*. 39 (7), pp. 484–490.
- Denman, S. et al. (2018) Microbiome and infectivity studies reveal complex polyspecies tree disease in Acute Oak Decline. *ISME Journal*. 12 (2), pp. 386–399.
- Denman, S., Kirk, S. and Webber, J. (2010) Managing acute oak decline. *Practice Note - Forestry Commission*. (15), p.6 pp.
- Denman, S. and Webber, J. (2009) Oak declines: new definitions and new episodes in Britain. *Quarterly Journal of Forestry*. 103 (4), pp. 285–290.
- Dôbereiner, J. (1966) *Azotobacter paspali* sp. n., uma bactéria fixadora de nitrogênio na rizosfera de *Paspalum*. *Pesquisa Agropecuária Brasileira*. 1 (1), pp. 357–365.
- Doetsch, R.N. (1981) Determinative Methods of Light Microscopy. *Manual of Methods for General Bacteriology*. pp.21–33.
- Doonan, J. et al. (2019) Genomic analysis of bacteria in the Acute Oak Decline pathobiome. *Microbial Genomics*. 5 (1).
- Doonan, J.M. et al. (2020) Host-microbiota-insect interactions drive emergent virulence in a complex tree disease. *Proceedings. Biological sciences*. 287 (1933).
- Dwight, Z., Palais, R. and Wittwer, C.T. (2011) uMELT: Prediction of high-resolution melting curves and dynamic melting profiles of PCR products in a rich web application. *Bioinformatics*. 27 (7), pp. 1019–1020.

- Edwards, U. et al. (1989) Isolation and direct complete nucleotide determination of entire genes. Characterization of a gene coding for 16S ribosomal RNA. *Nucleic Acids Research*. 17 (19), pp. 7843–7853.
- Feau, N. and Hamelin, R.C. (2017) Say hello to my little friends: how microbiota can modulate tree health. *New Phytologist*. 215 (2), pp. 508-510.
- Feldman, M. et al. (1998) Role of flagella in pathogenesis of *Pseudomonas aeruginosa* pulmonary infection. *Infection and Immunity*. 66 (1), pp. 43-51.
- Felsenstein, J. (1985) Confidence limits on phylogenies: an approach using the bootstrap. *Evolution*. 39 (4), pp. 783–791.
- Fernandes, A. and Marcelo, M. (2002) A possible synergistic effect of *Erwinia* sp. on the development of Olive knot symptoms caused by *Pseudomonas syringae* pv. *savastanoi* in *Olea europaea*. *Acta Horticulturae*. 586, pp. 729–731.
- Fierer, N. (2017) Embracing the unknown: disentangling the complexities of the soil microbiome. *Nature Reviews Microbiology*. 15 (10), pp. 579-590.
- Figaj, D. et al. (2019) The role of proteases in the virulence of plant pathogenic bacteria. *International Journal of Molecular Sciences*. 20 (3), p. 672.
- Flor, H.H. (1942) Inheritance of pathogenicity in *Melampsora lini*. *Phytopathology*. 32, pp. 653–669.
- Frankowski, J. et al. (2001) Purification and properties of two chitinolytic enzymes of *Serratia plymuthica* HRO-C48. *Archives of Microbiology*. 176 (6), pp. 421-426.
- Fraser, C. et al. (2009) The bacterial species challenge: making sense of genetic and ecological diversity. *Science*. 323 (5915), pp. 741-746.
- Gallego, F.J., Perez De Algaba, A. and Fernandez-Escobar, R. (1999) Etiology of oak decline in Spain. *European Journal of Forest Pathology*. 29 (1), pp. 17-27.
- Garcia-Brugger, A. et al. (2006) Early signaling events induced by elicitors of plant defenses. *Mol Plant Microbe Interact*. 19 (7), pp. 711–724.
- García-Valdés, E. and Lalucat, J. (2016) *Pseudomonas: molecular and applied biology*. Kahlon, R.S. (ed.) Cham, Springer International Publishing. pp. 1-518.

- Garrido-Sanz, D. et al. (2016) Genomic and genetic diversity within the *Pseudomonas fluorescens* complex. *PLoS ONE*. 11 (2).
- Giannakis et al. (2019) Diagnosing Acute Oak Decline Using Ground Penetrating Radar. *Proceedings*. 24.
- Gilchrist, D.G. (1998) Programmed cell death in plant disease: the purpose and promise of cellular suicide. *Annual Review of Phytopathology*. 36 (1), pp. 393–414.
- Glick, B.R. (2004) Bacterial ACC deaminase and the alleviation of plant stress. *Advances in Applied Microbiology*. 56, pp. 291-312.
- Glick, B.R. (2012) Plant growth-promoting bacteria: mechanisms and applications. *Scientifica*. 2012, pp. 1–15.
- Glick, R. et al. (2010) Increase in rhamnolipid synthesis under iron-limiting conditions influences surface motility and biofilm formation in *Pseudomonas aeruginosa*. *Journal of Bacteriology*. 192 (12), pp. 2973-2980.
- Gomila, M. et al. (2017) Clarification of taxonomic status within the *Pseudomonas syringae* species group based on a phylogenomic analysis. *Frontiers in Microbiology*. 8.
- Gomila, M. et al. (2005) Identification of culturable bacteria present in haemodialysis water and fluid. *FEMS Microbiology Ecology*. 52 (1), pp. 101–114.
- Gomila, M. et al. (2015) Phylogenomics and systematics in *Pseudomonas*. *Frontiers in Microbiology*. 6.
- González-Casanova, A. et al. (2014) Strong seed-bank effects in bacterial evolution. *Journal of Theoretical Biology*. 356, pp. 62-70.
- González, A.J. and Ciordia, M. (2020) *Brenneria goodwinii* and *Gibbsiella quercinecans* isolated from weeping cankers on *Quercus robur* L. in Spain. *European Journal of Plant Pathology*. 156 (3), pp. 965-969.
- Gori, A., Cerboneschi, M. and Tegli, S. (2012) High-resolution melting analysis as a powerful tool to discriminate and genotype *Pseudomonas savastanoi* pathovars and strains. Zhang, Z. (ed.) *PLoS ONE*. 7 (1), p.e30199.
- Goris, J. et al. (2007) DNA-DNA hybridization values and their relationship to whole-genome sequence similarities. *International Journal of Systematic and Evolutionary Microbiology*. 57

(1), pp. 81–91.

Guindon, S. et al. (2010) New algorithms and methods to estimate maximum-likelihood phylogenies: assessing the performance of PhyML 3.0. *Systematic Biology*. 59 (3), pp. 307–321.

Gundry, C.N. et al. (2003) Amplicon melting analysis with labeled primers: a closed-tube method for differentiating homozygotes and heterozygotes. *Clinical Chemistry*. 49 (3), pp. 396-406.

Gurevich, A. et al. (2013) QUAST: Quality assessment tool for genome assemblies. *Bioinformatics*. 29 (8), pp. 1072–1075.

Haas, D. and Défago, G. (2005) Biological control of soil-borne pathogens by fluorescent pseudomonads. *Nature Reviews Microbiology*. 3 (4), pp. 307-319.

Hall, T.A. (1999) BioEdit: a user-friendly biological sequence alignment editor and analysis program for Windows 95/98/NT. *Nucleic acids symposium series*. 41 (41), 95–98.

Hammond-Kosack, K.E. and Jones, J.D.G. (1996) Resistance gene-dependent plant defense responses. *The Plant Cell*. 8 (10), p. 1773.

Hancock, V., Witsø, I.L. and Klemm, P. (2011) Biofilm formation as a function of adhesin, growth medium, substratum and strain type. *International Journal of Medical Microbiology*. 301 (7), pp. 570-576.

Hardoim, P.R. et al. (2012) Dynamics of seed-borne rice endophytes on early plant growth stages. *PLoS ONE*. 7 (2), e30438.

Hardoim, P.R. et al. (2015) The hidden world within plants: ecological and evolutionary considerations for defining functioning of microbial endophytes. *Microbiology and Molecular Biology Reviews*. 79 (3), 293-320.

Hartmann, G. and Blank, R. (1992) Winterfrost, Kahlfrass und Prachtkäferbefall als Faktoren im Ursachenkomplex des Eichensterbens in Norddeutschland. *Forst und Holz*. 47 (15), pp. 443–452.

Harwood, C.S. and Parales, R.E. (1996) The β -ketoacid pathway and the biology of self-identity. *Annual Review of Microbiology*. 50 (1), pp.553–590.

Hayat, R. et al. (2010) Soil beneficial bacteria and their role in plant growth promotion: A

review. *Annals of Microbiology*. 60 (4), pp. 579-598.

Henderson, J.C. et al. (2016) The power of asymmetry: architecture and assembly of the gram-negative outer membrane lipid bilayer. *Annual Review of Microbiology*. 70 (1), 255-278.

Henson, J.M. and French, R. (1993) The polymerase chain reaction and plant disease diagnosis. *Annual Review of Phytopathology*. 31 (1), pp. 81-109.

Hider, R.C. and Kong, X. (2010) Chemistry and biology of siderophores. *Natural Product Reports*. 27 (5), p. 637.

Higuchi, R. et al. (1993) Kinetic PCR analysis: real-time monitoring of DNA amplification reactions. *Bio/Technology*. 11 (9), pp. 1026-1030.

Higuchi, R. et al. (1992) Simultaneous amplification and detection of specific DNA sequences. *Bio/Technology*. 10 (4), pp. 413-417.

Hilario, E., Buckley, T.R. and Young, J.M. (2004) Improved resolution on the phylogenetic relationships among *Pseudomonas* by the combined analysis of *atpD*, *carA*, *recA* and 16S rDNA. *Antonie van Leeuwenhoek, International Journal of General and Molecular Microbiology*. 86 (1), pp. 51-64.

Hill, L. et al. (2019) The £15 billion cost of ash dieback in Britain. *Current Biology*. 29 (9), pp. R315-R316.

Huelsenbeck, J.P. and Ronquist, F. (2001) MRBAYES: bayesian inference of phylogenetic trees. *Bioinformatics*. 17 (8), pp. 754–755.

Hulton, C.S.J., Higgins, C.F. and Sharp, P.M. (1991) ERIC sequences: a novel family of repetitive elements in the genomes of *Escherichia coli*, *Salmonella typhimurium* and other enterobacteria. *Molecular Microbiology*. 5 (4), pp. 825–834.

Huszczynski, S.M., Lam, J.S. and Khursigara, C.M. (2020) The role of *Pseudomonas aeruginosa* lipopolysaccharide in bacterial pathogenesis and physiology. *Pathogens*. 9 (1), p. 6.

Innerebner, G., Knief, C. and Vorholt, J.A. (2011) Protection of *Arabidopsis thaliana* against leaf-pathogenic *Pseudomonas syringae* by *Sphingomonas* strains in a controlled model system. *Applied and Environmental Microbiology*. 77 (10), pp. 3202-3210.

Izaguirre-Mayoral, M.L., Lazarovits, G. and Baral, B. (2018) Ureide metabolism in plant-

associated bacteria: purine plant-bacteria interactive scenarios under nitrogen deficiency. *Plant and Soil*. 428 (1–2), pp. 1-34.

Jacquot, C. and others (1950) The cause of woody tumours found on oaks attacked by *A. biguttatus*. *Compte Rendu Hebdomadaire des Seances de l'Academie des Sciences*. 231, pp. 1552–1554.

Jałowicki, Ł. et al. (2018) Properties of antibiotic-resistant bacteria isolated from onsite wastewater treatment plant in relation to biofilm formation. *Current Microbiology*. 75 (5), pp. 639-649.

Janse, J.D. and Obradovic, A. (2010) *Xylella fastidiosa*: Its biology, diagnosis, control and risks. *Journal of Plant Pathology*. 92 (1), pp. 35-148.

Jeffreys, A.J., Wilson, V. and Thein, S.L. (1985) Individual-specific 'fingerprints' of human DNA. *Nature*. 316 (6023), pp.76–79.

John, M.E. (1992) An efficient method for isolation of RNA and DNA from plants containing polyphenolics. *Nucleic Acids Research*. 20 (9), p. 2381.

Kharazmi, A. et al. (1989) Effect of *Pseudomonas aeruginosa* rhamnolipid on human neutrophil and monocyte function. *APMIS*. 97 (7-12), pp. 1068-1072.

Klement, Z. and Goodman, R.N. (1967) The hypersensitive reaction to infection by bacterial plant pathogens. *Annual Review of Phytopathology*. 5 (1), pp. 17-44.

Klemm, P., Hancock, V. and Schembri, M.A. (2010) Fimbrial adhesins from extraintestinal *Escherichia coli*. *Environmental Microbiology Reports*. 2 (5), pp. 628-640.

Konstantinidis, K.T. and Tiedje, J.M. (2005) Genomic insights that advance the species definition for prokaryotes. *Proceedings of the National Academy of Sciences*. 102 (7), pp. 2567–2572.

Koonin, E. V. and Wolf, Y.I. (2008) Genomics of bacteria and archaea: the emerging dynamic view of the prokaryotic world. *Nucleic Acids Research*. 36 (21), pp. 6688-6719.

Kragh, K.N. et al. (2018) The inoculation method could impact the outcome of microbiological experiments. *Applied and Environmental Microbiology*. 84 (5).

Kube, M. et al. (2010) Genome comparison of the epiphytic bacteria *Erwinia billingiae* and *E. tasmaniensis* with the pear pathogen *E. pyrifoliae*. *BMC Genomics*. 11 (1), p. 393.

- Kurland, C.G., Canback, B. and Berg, O.G. (2003) Horizontal gene transfer: A critical view. *Proceedings of the National Academy of Sciences of the United States of America*. 100 (17), pp. 9658-9662.
- Kushalappa, A.C. et al. (2002) Volatile fingerprinting (SPME-GC-FID) to detect and discriminate diseases of potato tubers. *Plant Disease*. 86 (2), pp. 131–137.
- Lalucat et al. (2020) Genomics in bacterial taxonomy: impact on the genus *Pseudomonas*. *Genes*. 11 (2), p. 139.
- Lamichhane, J.R. and Venturi, V. (2015) Synergisms between microbial pathogens in plant disease complexes: a growing trend. *Frontiers in Plant Science*. 6, p. 385.
- Lamont, I.L. et al. (2002) Siderophore-mediated signaling regulates virulence factor production in *Pseudomonas aeruginosa*. *Proceedings of the National Academy of Sciences of the United States of America*. 99 (10), pp. 7072-7077.
- Lan, Y., Rosen, G. and Hershberg, R. (2016) Marker genes that are less conserved in their sequences are useful for predicting genome-wide similarity levels between closely related prokaryotic strains. *Microbiome*. 4 (1), p. 18.
- Lane, D.J. (1991) 16S/23S rRNA sequencing. Stackebrandt E., Goodfellow M. (ed), *Nucleic acid techniques in bacterial systematics*. John Wiley and Sons, New York, NY. pp. 115–175.
- Laothawornkitkul, J. et al. (2008) Discrimination of plant volatile signatures by an electronic nose: a potential technology for plant pest and disease monitoring. *Environmental Science and Technology*. 42 (22), pp. 8433–8439.
- Larkin, M.A. et al. (2007) Clustal W and Clustal X version 2.0. *Bioinformatics*. 23 (21), pp. 2947–2948.
- Lau, G.W. et al. (2004) *Pseudomonas aeruginosa* pyocyanin is critical for lung infection in mice. *Infection and Immunity*. 72 (7), pp. 4275-4278.
- Le, S.Q. and Gascuel, O. (2008) An Improved general amino acid replacement matrix. *Molecular Biology and Evolution*. 25 (7), pp. 1307–1320.
- Lefort, V., Longueville, J.E. and Gascuel, O. (2017) SMS: Smart Model Selection in PhyML. *Molecular biology and evolution*. 34 (9), pp. 2422–2424.
- Lezhava, A. et al. (2010) Exciton primer-mediated SNP detection in SmartAmp2 reactions.

Human Mutation. 31 (2), pp. 208–217.

Li, H. et al. (2009) The Sequence Alignment/Map format and SAMtools. *Bioinformatics*. 25 (16), pp. 2078–2079.

Li, H. and Durbin, R. (2010) Fast and accurate long-read alignment with Burrows-Wheeler transform. *Bioinformatics*. 26 (5), pp. 589–595.

Li, Z. et al. (2020) Agricultural nanodiagnosics for plant diseases: recent advances and challenges. *Nanoscale Advances*. 2 (8), pp. 3083-3094.

Lindsay, W.P., Lamb, C.J. and Dixon, R.A. (1993) Microbial recognition and activation of plant defense systems. *Trends in Microbiology*. 1 (5), pp. 181–187.

Liu, B. et al. (2019) VFDB 2019: A comparative pathogenomic platform with an interactive web interface. *Nucleic Acids Research*. 47 (1), pp. 687-692.

Liu, H. et al. (2017) Inner plant values: Diversity, colonization and benefits from endophytic bacteria. *Frontiers in Microbiology*. 8.

Loman, N.J. and Pallen, M.J. (2015) Twenty years of bacterial genome sequencing. *Nature Reviews Microbiology*. 13 (12), pp. 787-794.

Lonsdale, D. (2015) Review of oak mildew, with particular reference to mature and veteran trees in Britain. *Arboricultural Journal*. 37 (2), 61-84.

López, M.M. et al. (2009) Are molecular tools solving the challenges posed by detection of plant pathogenic bacteria and viruses? *Current issues in molecular biology*. 11 (1), pp. 13–46.

Lyczak, J.B., Cannon, C.L. and Pier, G.B. (2002) Lung infections associated with cystic fibrosis. *Clinical Microbiology Reviews*. 15 (2), pp. 194-222.

Maiden, M.C.J. et al. (1998) Multilocus sequence typing: a portable approach to the identification of clones within populations of pathogenic microorganisms. *Proceedings of the National Academy of Sciences of the United States of America*. 95 (6), pp. 3140-3145.

Malvick, D.K. and Grunden, E. (2005) Isolation of fungal DNA from plant tissues and removal of DNA amplification inhibitors. *Molecular Ecology Notes*. 5 (4), pp. 958-960.

Manion, P.D. (1981) Tree disease concepts. Pearson Education Australia.

Mansfield, J. et al. (1994) Characterization of *avrPphE*, a gene for cultivar-specific avirulence

from *Pseudomonas syringae* pv. *phaseolicola* which is physically linked to *hrpY*, a new *hrp* gene identified in the halo-blight bacterium. *Mol. Plant-Mic. interactions*. 7 (6), p.726.

Marchi, G. et al. (2006) Interaction between *Pseudomonas savastanoi* pv. *savastanoi* and *Pantoea agglomerans* in olive knots. *Plant Pathology*. 55 (5), pp. 614–624.

Marqués, S. and Ramos, J.L. (1993) Transcriptional control of the *Pseudomonas putida* TOL plasmid catabolic pathways. *Molecular Microbiology*. 9 (5), pp. 923-929.

Martin, B. et al. (1992) A highly conserved repeated DNA element located in the chromosome of *Streptococcus pneumoniae*. *Nucleic Acids Research*. 20 (13), pp. 3479–3483.

Martínez-Carranza, E. et al. (2019) Evolution of bacteria seen through their essential genes: The case of *Pseudomonas aeruginosa* and *Azotobacter vinelandii*. *Microbiology*. 165 (9), 976-984.

Mattick, J.S. (2002) Type IV pili and twitching motility. *Annual Review of Microbiology*. 56 (1), pp. 289-314.

Meier-Kolthoff, J.P. et al. (2013) Genome sequence-based species delimitation with confidence intervals and improved distance functions. *BMC Bioinformatics*. 14 (1), p. 60.

Meier-Kolthoff, J.P., Klenk, H.P. and Göker, M. (2014) Taxonomic use of DNA G+C content and DNA-DNA hybridization in the genomic age. *International Journal of Systematic and Evolutionary Microbiology*. 64 (2), pp. 352-356.

Merritt, J.H., Kadouri, D.E. and O’Toole, G.A. (2011) Growing and analyzing static biofilms. *Current Protocols in Microbiology*. 00 (1). pp. 1-17.

Messing, J. (1983) New M13 vectors for cloning. *Methods in Enzymology*. 101, pp. 20-78.

Meyer, J.M. (2000) Pyoverdines: Pigments, siderophores and potential taxonomic markers of fluorescent *Pseudomonas* species. *Archives of Microbiology*. 174 (3), pp. 135-142.

Meyer, J.M. et al. (2008) Siderotyping of fluorescent *Pseudomonas*: molecular mass determination by mass spectrometry as a powerful pyoverdine siderotyping method. *BioMetals*. 21 (3), pp. 259-271.

Mignard, S. and Flandrois, J.P. (2006) 16S rRNA sequencing in routine bacterial identification: A 30-month experiment. *Journal of Microbiological Methods*. 67 (3), pp. 574–581.

- Mira, A. et al. (2004) Evolutionary relationships of *Fusobacterium nucleatum* based on phylogenetic analysis and comparative genomics. *BMC Evolutionary Biology*. 4 (1), p. 50.
- Mitchell, R.J. et al. (2019) Collapsing foundations: the ecology of the British oak, implications of its decline and mitigation options. *Biological Conservation*. 233, pp. 316-327.
- Montesano, M., Brader, G. and Palva, E.T. (2003) Pathogen derived elicitors: Searching for receptors in plants. *Molecular Plant Pathology*. 4 (1), pp. 73–79.
- Moore, E.R.B. et al. (1996) The determination and comparison of the 16S rRNA gene sequences of species of the genus *Pseudomonas* (sensu stricto and estimation of the natural intrageneric relationships. *Systematic and Applied Microbiology*. 19 (4), pp. 478–492.
- Moore, W.E.C. et al. (1987) Report of the *ad hoc* committee on reconciliation of approaches to bacterial systematics. *International Journal of Systematic and Evolutionary Microbiology*. 37 (4), pp. 463-464.
- Moraal, L.G., Achterberg, C. van and van Achterberg, C. (2001) *Spathius curvicaudis* (Hymenoptera: Braconidae) new for The Netherlands; a parasitoid of the oak buprestid beetle, *Agrilus biguttatus* (Coleoptera: Buprestidae). *Entomologische Berichten*. 61 (11), pp. 165-168.
- Moraal, L.G. and Hilszczanski, J. (2000) The oak buprestid beetle (*Agrilus biguttatus*) (F.) (Col., *buprestidae*), a recent factor in oak decline in Europe. *Journal of Pest Science*. 73, pp. 134–138.
- Moradi-Amirabad, Y. et al. (2019) *Brenneria* spp. and *Rahnella victoriana* associated with acute oak decline symptoms on oak and hornbeam in Iran. *Forest Pathology*. 49 (4), p. e12535.
- Morgulis, A. et al. (2008) Database indexing for production MegaBLAST searches. *Bioinformatics*. 24 (16), pp. 1757–1764.
- Mori, Y. et al. (2001) Detection of loop-mediated isothermal amplification reaction by turbidity derived from magnesium pyrophosphate formation. *Biochemical and Biophysical Research Communications*. 289 (1), pp. 150–154.
- Mougous, J.D. et al. (2006) A virulence locus of *Pseudomonas aeruginosa* encodes a protein secretion apparatus. *Science*. 312 (5779), pp. 1526-1530.

- Mulet, M. et al. (2009) An *rpoD*-based PCR procedure for the identification of *Pseudomonas* species and for their detection in environmental samples. *Molecular and Cellular Probes*. 23 (3–4), pp. 140–147.
- Mulet, M. et al. (2012) Concordance between whole-cell matrix-assisted laser-desorption/ionization time-of-flight mass spectrometry and multilocus sequence analysis approaches in species discrimination within the genus *Pseudomonas*. *Systematic and Applied Microbiology*. 35 (7), pp. 455–464.
- Mulet, M., Lalucat, J. and García-Valdés, E. (2010) DNA sequence-based analysis of the *Pseudomonas* species. *Environmental Microbiology*. 12 (6), pp. 1513–1530.
- Niemann, S. et al. (1997) Evaluation of the resolving power of three different DNA fingerprinting methods to discriminate among isolates of a natural *Rhizobium meliloti* population. *Journal of Applied Microbiology*. 82 (4), pp. 477–484.
- Nürnbergger, T. (1999) Signal perception in plant pathogen defense. *Cellular and Molecular Life Sciences*. 55 (2), pp. 167–182.
- O'Mahony, M.M. et al. (2006) The use of ozone in the remediation of polycyclic aromatic hydrocarbon contaminated soil. *Chemosphere*. 63 (2), pp. 307-314.
- O'Sullivan, D.J. and O'Gara, F. (1992) Traits of fluorescent *Pseudomonas* spp. involved in suppression of plant root pathogens. *Microbiological Reviews*. 56 (4), pp. 662-676.
- O'Toole, G.A. and Kolter, R. (1998) Flagellar and twitching motility are necessary for *Pseudomonas aeruginosa* biofilm development. *Molecular Microbiology*. 30 (2), pp. 295-304.
- Okamoto, H. et al. (2009) Unified hyperspectral imaging methodology for agricultural sensing using software framework. *Acta Horticulturae*. 824, pp. 49–56.
- Ołdak, E. and Trafny, E.A. (2005) Secretion of proteases by *Pseudomonas aeruginosa* biofilms exposed to ciprofloxacin. *Antimicrobial Agents and Chemotherapy*. 49 (8), pp. 3281-3288.
- Oleksyn, J. and Przybyl, K. (1987) Oak decline in the Soviet Union - scale and hypotheses. *European Journal of Forest Pathology*. 17 (6), pp. 321-336.
- Orgad, O. et al. (2011) The role of alginate in *Pseudomonas aeruginosa* EPS adherence, viscoelastic properties and cell attachment. *Biofouling*. 27 (7), pp. 787-798.
- van Overbeek, L.S. and Saikkonen, K. (2016) Impact of bacterial-fungal interactions on the

colonization of the endosphere. *Trends in Plant Science*. 21 (3), pp. 230-242.

Overbeek, R. et al. (2014) The SEED and the rapid annotation of microbial genomes using subsystems technology (RAST). *Nucleic Acids Research*. 42 (1) pp. 206-214.

Owen, J.G. and Ackerley, D.F. (2011) Characterization of pyoverdine and achromobactin in *Pseudomonas syringae* pv. *phaseolicola* 1448a. *BMC Microbiology*. 11 (1), p. 218.

Özen, A.I. and Ussery, D.W. (2012) Defining the *Pseudomonas* genus: where do we draw the line with *Azotobacter*? *Microbial Ecology*. 63 (2), pp. 239–248.

Palleroni, N.J. et al. (1973) Nucleic acid homologies in the genus *Pseudomonas*. *International Journal of Systematic Bacteriology*. 23 (4), 333-339.

Palleroni, N.J. (2015) *Pseudomonas*. *Bergey's Manual of Systematics of Archaea and Bacteria*. pp. 58–69.

Pamp, S.J. and Tolker-Nielsen, T. (2007) Multiple roles of biosurfactants in structural biofilm development by *Pseudomonas aeruginosa*. *Journal of Bacteriology*. 189 (6), pp. 2531-2539.

Paran, I. and Michelmore, R.W. (1993) Development of reliable PCR-based markers linked to downy mildew resistance genes in lettuce. *Theoretical and Applied Genetics*. 85 (8), pp. 985–993.

Parks, D.H. et al. (2018) A standardized bacterial taxonomy based on genome phylogeny substantially revises the tree of life. *Nature Biotechnology*. 36 (10), pp. 996-1004.

Patriquin, G.M. et al. (2008) Influence of quorum sensing and iron on twitching motility and biofilm formation in *Pseudomonas aeruginosa*. *Journal of Bacteriology*. 190 (2), pp. 662-671.

Paul, R. et al. (2019) Extraction of plant DNA by microneedle patch for rapid detection of plant diseases. *ACS Nano*. 13 (6), pp. 6540-6549.

Pearson, K. (1901) LIII. On lines and planes of closest fit to systems of points in space. *The London, Edinburgh, and Dublin Philosophical Magazine and Journal of Science*. 2 (11), pp. 559-572.

Peix, A., Ramírez-Bahena, M.-H. and Velázquez, E. (2018) The current status on the taxonomy of *Pseudomonas* revisited: an update. *Infection, Genetics and Evolution*. 57, pp. 106–116.

Peix, A., Ramírez-Bahena, M.H. and Velázquez, E. (2009) Historical evolution and current

status of the taxonomy of genus *Pseudomonas* infection. *Genetics and Evolution*. 9 (6), pp. 1132-1147.

Pena, R.T. et al. (2019) Relationship between quorum sensing and secretion systems. *Frontiers in Microbiology*. 10 (JUN).

Pereyra, S. et al. (2012) Rapid multiplex high resolution melting method to analyze inflammatory related SNPs in preterm birth. *BMC Research Notes*. 5 (1), p. 69.

Petr, M. et al. (2014) A spatial and temporal drought risk assessment of three major tree species in Britain using probabilistic climate change projections. *Climatic Change*. 124 (4), pp. 791-803.

Petri, L. (1907) Untersuchungen über die Identität des Rotzbacillus des Oelbaumes. *Zentrallblatt für Bakteriologie, Parasitenkunde, Infektionskrankheiten und Hygiene XIX*. pp. 531–538.

Pettifor, B.J. et al. (2020) Survival of *Brenneria goodwinii* and *Gibbsiella quercinecans*, associated with acute oak decline, in rainwater and forest soil. *Systematic and Applied Microbiology*. 43 (2).

Piepenburg, O. et al. (2006) DNA detection using recombination proteins. *PLoS Biology*. 4 (7), pp. 1115–1121.

Pitman, A.R. et al. (2005) Exposure to host resistance mechanisms drives evolution of bacterial virulence in plants. *Current Biology*. 15 (24), pp. 2230–2235.

Prakash, O. et al. (2007) Polyphasic approach of bacterial classification - an overview of recent advances. *Indian Journal of Microbiology*. 47 (2), pp. 98-108.

Qin, Q.L. et al. (2014) A proposed genus boundary for the prokaryotes based on genomic insights. *Journal of Bacteriology*. 196 (12), pp. 2210-2215.

Quinlan, A.R. and Hall, I.M. (2010) BEDTools: A flexible suite of utilities for comparing genomic features. *Bioinformatics*. 26 (6), pp. 841–842.

Ragazzi, A., Fedi, I.D. and Mesturino, L. (1989) The oak decline: a new problem in Italy. *European Journal of Forest Pathology*. 19 (2), pp. 105-110.

Ramos, E. et al. (2013) *Pseudomonas punonensis* sp. nov., isolated from straw. *International journal of Systematic and Evolutionary Microbiology*. 63 (Pt 5), pp. 1834–1839.

- Ran, H., Hassett, D.J. and Lau, G.W. (2003) Human targets of *Pseudomonas aeruginosa* pyocyanin. *Proceedings of the National Academy of Sciences of the United States of America*. 100 (24), pp. 14315-14320.
- Rediers, H., Vanderleyden, J. and De Mot, R. (2004) *Azotobacter vinelandii*: a *Pseudomonas* in disguise? *Microbiology*. 150 (5), pp. 1117–1119.
- Rédly, G.A. and Poole, K. (2003) Pyoverdine-mediated regulation of *FpvA* synthesis in *Pseudomonas aeruginosa*: Involvement of a probable extracytoplasmic-function sigma factor, Fpvl. *Journal of Bacteriology*. 185 (4), pp. 1261-1265.
- Reed, K. et al. (2020) Novel dendrochronological modelling demonstrates that decades of reduced stem growth predispose trees to Acute Oak Decline. *Forest Ecology and Management*. 476, p. 118441.
- Reed, K. et al. (2018) The lifecycle of *Agrilus biguttatus*: the role of temperature in its development and distribution, and implications for Acute Oak Decline. *Agricultural and Forest Entomology*. 20 (3), pp. 334-346.
- Reinhold-Hurek, B. et al. (2015) Roots shaping their microbiome: global hotspots for microbial activity. *Annual Review of Phytopathology*. 53 (1), pp. 403-424.
- Reja, V. et al. (2010) ScreenClust: Advanced statistical software for supervised and unsupervised high resolution melting (HRM) analysis. *Methods*. 50 (4), pp. 10-14.
- Reller, L.B., Weinstein, M.P. and Petti, C.A. (2007) Detection and identification of microorganisms by gene amplification and sequencing. *Clinical Infectious Diseases*. 44 (8), pp. 1108–1114.
- Richter, M. et al. (2015) JSpeciesWS: A web server for prokaryotic species circumscription based on pairwise genome comparison. *Bioinformatics*. 32 (6), pp. 929–931.
- Richter, M. and Rosselló-Móra, R. (2009) Shifting the genomic gold standard for the prokaryotic species definition. *Proceedings of the National Academy of Sciences of the United States of America*. 106 (45), pp. 19126-19131.
- Robson, A.D., Yeates, J.S. and Porter, W.M. (1989) Soil acidity and plant growth. *Soil acidity and plant growth*.
- Romanenko, L.A. et al. (2005) *Pseudomonas xanthomarina* sp. nov., a novel bacterium

isolated from marine ascidian. *The Journal of General and Applied Microbiology*. 51 (2), pp. 65–71.

Ros, V.I.D. and Hurst, G.D.D. (2009) Lateral gene transfer between prokaryotes and multicellular eukaryotes: ongoing and significant? *BMC Biology*. 7 (1), p. 20.

Rosselló-Móra, R. and Amann, R. (2015) Past and future species definitions for Bacteria and Archaea. *Systematic and Applied Microbiology*. 38 (4), pp. 209-216.

Roy-Burman, A. et al. (2001) Type III protein secretion is associated with death in lower respiratory and systemic *Pseudomonas aeruginosa* infections. *The Journal of Infectious Diseases*. 183 (12), pp. 1767-1774.

Ruffner, B. et al. (2020) First report of acute oak decline disease of native and non-native oaks in Switzerland. *New Disease Reports*. 41 (1), p. 18.

Al Rwahnih, M. et al. (2015) Comparison of next generation sequencing vs. biological indexing for the optimal detection of viral pathogens in grapevine. *Phytopathology*. 105 (6), pp. 758-763.

Sankaran, S. et al. (2010) Review: a review of advanced techniques for detecting plant diseases. *Computers and Electronics in Agriculture*. 72 (1), pp. 1–13.

Santos, S.R. and Ochman, H. (2004) Identification and phylogenetic sorting of bacterial lineages with universally conserved genes and proteins. *Environmental Microbiology*. 6 (7), pp. 754–759.

Sapp, M. et al. (2016) Metabarcoding of bacteria associated with the Acute Oak Decline Syndrome in England. *Forests*. 7 (12), p. 95.

Sauer, K. et al. (2002) *Pseudomonas aeruginosa* displays multiple phenotypes during development as a biofilm. *Journal of Bacteriology*. 184 (4), pp. 1140-1154.

Savastano, L. (1886) Les maladies de l'olivier, et la tuberculose en particulier. *C. R. Séance*. 103, p. 1144.

Schroeter, J. (1872) *Beitrage zur Biologie der Pflanzen*.

Scofield, J. and Wu, H. (2019) Microbial biofilms. *Encyclopedia of Microbiology*. Chapter 1, p. 114.

Scuderi, G. et al. (2010) Development of a simplified NASBA protocol for detecting viable cells of the citrus pathogen *Xanthomonas citri* subsp. *citri* under different treatments. *Plant Pathology*. 59 (4), pp. 764–772.

Setubal, J.C. et al. (2009) Genome sequence of *Azotobacter vinelandii*, an obligate aerobe specialized to support diverse anaerobic metabolic processes. *Journal of Bacteriology*. 191 (14), pp. 4534-4545.

Shakya, M. et al. (2020) Standardized phylogenetic and molecular evolutionary analysis applied to species across the microbial tree of life. *Scientific Reports*. 10 (1), p. 1723.

Sierra, G. (1960) Hemolytic effect of a glycolipid produced by *Pseudomonas aeruginosa*. *Antonie van Leeuwenhoek*. 26 (1), pp. 189-192.

da Silva, D.P. et al. (2014) Bacterial multispecies studies and microbiome analysis of a plant disease. *Microbiology (United Kingdom)*. 160 (part 3), pp. 556–566.

Sinclare, W.A. (1967) Decline of hardwoods: possible causes. Intergovernmental Panel on Climate Change (ed.) *Climate Change 2013 - The Physical Science Basis*. Cambridge, Cambridge University Press, 1–30.

Singh, P.P. et al. (1999) Biological control of Fusarium wilt of cucumber by chitinolytic bacteria. *Phytopathology*. 89 (1), pp. 92-99.

Skogman, M.E., Vuorela, P.M. and Fallarero, A. (2012) Combining biofilm matrix measurements with biomass and viability assays in susceptibility assessments of antimicrobials against *Staphylococcus aureus* biofilms. *Journal of Antibiotics*. 65 (9), pp. 453-459.

Smith, R.S. and Iglewski, B.H. (2003) *P. aeruginosa* quorum-sensing systems and virulence. *Current Opinion in Microbiology*. 6 (1), pp. 56-60.

Soutar, C.D. and Stavrinides, J. (2020) Phylogenetic analysis supporting the taxonomic revision of eight genera within the bacterial order *Enterobacterales*. *International Journal of Systematic and Evolutionary Microbiology*. 70 (12), pp. 6524-6530.

Srivastava, A.K., Dev, A. and Karmakar, S. (2018) Nanosensors and nanobiosensors in food and agriculture. *Environmental Chemistry Letters*. 16 (1), pp. 161-182.

Stackebrandt, E. et al. (2002) Report of the ad hoc committee for the re-evaluation of the

species definition in bacteriology. *International Journal of Systematic and Evolutionary Microbiology*. 52 (3), pp. 1043–1047.

Stackebrandt, E. and Ebers, J. (2006) Taxonomic parameter revised: tarnishes gold standards. *Microbiology Today*. pp. 153–155.

Van Der Stoep, N. et al. (2009) Diagnostic guidelines for high-resolution melting curve (HRM) analysis: an interlaboratory validation of BRCA1 mutation scanning using the 96-well LightScanner™. *Human Mutation*. 30 (6), pp. 899-909.

Tayeb, L.A. et al. (2008) Comparative phylogenies of *Burkholderia*, *Ralstonia*, *Comamonas*, *Brevundimonas* and related organisms derived from *rpoB*, *gyrB* and *rrs* gene sequences. *Research in Microbiology*. 159 (3), pp. 169–177.

TAYLOR, J.D. et al. (1996) Identification and origin of races of *Pseudomonas syringae* pv. *phaseolicola* from Africa and other bean growing areas. *Plant Pathology*. 45 (3), pp. 469–478.

Taylor, S. et al. (2011) A practical guide to high resolution melt analysis genotyping a practical guide to high resolution melt analysis genotyping. *Bio-Rad Bulletin*.

Thaxton, C.S., Georganopoulou, D.G. and Mirkin, C.A. (2006) Gold nanoparticle probes for the detection of nucleic acid targets. *Clinica Chimica Acta*. 363 (1-2), pp. 120-126.

Thomas, F.M. (2008) Recent advances in cause-effect research on oak decline in Europe. *CAB.Reviews: Perspectives in Agriculture, Veterinary Science, Nutrition and Natural Resources*. 3 (7).

Thomas, F.M., Blank, R. and Hartmann, G. (2002) Abiotic and biotic factors and their interactions as causes of oak decline in Central Europe. *Forest Pathology*. 32 (4–5), pp. 277–307.

Thomas, F.M. and Büttner, G. (1998) Nutrient relations in healthy and damaged stands of mature oaks on clayey soils: two case studies in northwestern Germany. *Forest Ecology and Management*. 108 (3), pp. 301-319.

Thompson, J.D., Higgins, D.G. and Gibson, T.J. (1994) CLUSTAL W: Improving the sensitivity of progressive multiple sequence alignment through sequence weighting, position-specific gap penalties and weight matrix choice. *Nucleic Acids Research*. 22 (22), pp. 4673–4680.

Thompson, J.P. and Skerman, V.B.D. (1979) *Azotobacteraceae*: the taxonomy and ecology of

the aerobic nitrogen-fixing bacteria. *Azotobacteraceae: the taxonomy and ecology of the aerobic nitrogen-fixing bacteria*. London, Academic Press, 417 pp.

Tindall, B.J. et al. (2010) Notes on the characterization of prokaryote strains for taxonomic purposes. *International Journal of Systematic and Evolutionary Microbiology*. 60 (1), pp. 249–266.

Tomlinson, I., Potter, C. and Bayliss, H. (2015) Managing tree pests and diseases in urban settings: the case of oak processionary moth in London, 2006-2012. *Urban Forestry and Urban Greening*. 14 (2), pp. 286-292.

Toth, I.K. et al. (2003) Soft rot *Erwiniae*: from genes to genomes molecular plant pathology. 4 (1), pp. 17-30.

Toth, I.K., Pritchard, L. and Birch, P.R.J. (2006) Comparative genomics reveals what makes an enterobacterial plant pathogen. *Annual Review of Phytopathology*. 44 (1), pp. 305-336.

Ueda, A. and Saneoka, H. (2015) Characterization of the ability to form biofilms by plant-associated *Pseudomonas* species. *Current Microbiology*. 70 (4), pp. 506-513.

Vaidya, G., Lohman, D.J. and Meier, R. (2011) SequenceMatrix: concatenation software for the fast assembly of multi-gene datasets with character set and codon information. *Cladistics*. 27 (2), pp. 171–180.

Vandamme, P. et al. (1996) Polyphasic taxonomy, a consensus approach to bacterial systematics. *Microbiological Reviews*. 60 (2), pp. 407-438.

VanGuilder, H.D., Vrana, K.E. and Freeman, W.M. (2008) Twenty-five years of quantitative PCR for gene expression analysis. *BioTechniques*. 44 (5), pp. 619-626.

Vansteenkiste, D. et al. (2004) Predispositions and symptoms of *Agilus* borer attack in declining oak trees. *Annals of Forest Science*. 61 (8), pp. 815–823.

Vasudevan, R. (2014) Biofilms: microbial cities of scientific significance. *Journal of Microbiology & Experimentation*. 1 (3), pp. 84-98.

Verhille, S. et al. (1999) Taxonomic study of bacteria isolated from natural mineral waters: Proposal of *Pseudomonas jessenii* sp. nov. and *Pseudomonas mandelii* sp. nov. *Systematic and Applied Microbiology*. 22 (1), pp. 45-58.

Versalovic, J. et al. (1994) Genomic fingerprinting of bacteria using repetitive sequence-

based polymerase chain reaction. *Methods in molecular and cellular biology*. 5 (1), pp. 25–40.

Versalovic, J., Koeuth, T. and Lupski, J.R. (1991) Distribution of repetitive DNA sequences in eubacteria and application to fingerprinting of bacterial genomes. *Nucleic Acids Research*. 19 (24), pp. 6823–6831.

Vinatzer, B.A., Monteil, C.L. and Clarke, C.R. (2014) Harnessing population genomics to understand how bacterial pathogens emerge, adapt to crop hosts, and disseminate. *Annual Review of Phytopathology*. 52 (1), pp. 19-43.

Vincent, M., Xu, Y. and Kong, H. (2004) Helicase-dependent isothermal DNA amplification. *EMBO reports*. 5 (8), pp. 795–800.

Visca, P., Imperi, F. and Lamont, I.L. (2007) Pyoverdine siderophores: from biogenesis to biosignificance. *Trends in Microbiology*. 15 (1), pp. 22-30.

Vorholt, J.A. (2012) Microbial life in the phyllosphere. *Nature Reviews Microbiology*. 10 (12), pp. 828-840.

De Vos, P. et al. (1989) Genotypic relationships and taxonomic localization of unclassified *Pseudomonas* and *Pseudomonas*-like strains by deoxyribonucleic acid:ribosomal ribonucleic acid hybridizations. *International Journal of Systematic Bacteriology*. 39 (1), pp. 35–49.

De Vos, P. et al. (1985) Ribosomal ribonucleic acid cistron similarities of phytopathogenic *Pseudomonas* species. *International Journal of Systematic Bacteriology*. 35 (2), pp. 169-184.

De Vos, P. and De Ley, J. (1983) Intra- and Intergeneric Similarities of *Pseudomonas* and *Xanthomonas* Ribosomal Ribonucleic Acid Cistrons. *International Journal of Systematic Bacteriology*. 33 (3), pp. 487-509.

Vuts, J. et al. (2016) Responses of the two-spotted oak buprestid, *Agrilus biguttatus* (Coleoptera: Buprestidae), to host tree volatiles. *Pest Management Science*. 72 (4), pp. 845-851.

Walker, G.T. et al. (1992) Strand displacement amplification- an isothermal, in vitro DNA amplification technique. *Nucleic acids research*. 20 (7), pp. 1691–1696.

Ward, L.I. and Harper, S.J. (2012) Loop-mediated isothermal amplification for the detection of plant pathogens. *Methods in molecular biology (Clifton, N.J.)*. 862, pp. 161–170.

- Whipps, J.M. (2001) Microbial interactions and biocontrol in the rhizosphere. *Journal of Experimental Botany*. 52 (suppl. 1), pp. 487-511.
- Williams, J.G.K. et al. (1990) DNA polymorphisms amplified by arbitrary primers are useful as genetic markers. *Nucleic Acids Research*. 18 (22), pp. 6531–6535.
- Wilson, I.G. (1997) Inhibition and facilitation of nucleic acid amplification. *Applied and Environmental Microbiology*. 63 (10), pp. 3741-3751.
- Wittwer, C.T. et al. (1997) Continuous fluorescence monitoring of rapid cycle DNA amplification. *BioTechniques*. 22 (1), pp. 130-138.
- Wittwer, C.T. et al. (2003) High-resolution genotyping by amplicon melting analysis using LCGreen. *Clinical Chemistry*. 49 (6), pp. 853-860.
- Woese, C.R. et al. (1984) The phylogeny of purple bacteria: the alpha subdivision. *Systematic and Applied Microbiology*. 5 (3), pp. 315-326.
- Woese, C.R. and Fox, G.E. (1977) Phylogenetic structure of the prokaryotic domain: the primary kingdoms. *Proceedings of the National Academy of Sciences*. 74 (11), pp. 5088–5090.
- Woese, C.R., Kandler, O. and Wheelis, M.L. (1990) Towards a natural system of organisms: Proposal for the domains Archaea, Bacteria, and Eucarya. *Proceedings of the National Academy of Sciences of the United States of America*. 87 (12), pp. 4576-4579.
- Xu, J. et al. (2011) Complete genome sequence of the plant pathogen *Ralstonia solanacearum* strain Po82. *Journal of Bacteriology*. 193 (16), pp. 4261-4262.
- Yamamoto, S. et al. (2000) Phylogeny of the genus *Pseudomonas*: Intrageneric structure reconstructed from the nucleotide sequences of *gyrB* and *rpoD* genes. *Microbiology*. 146 (10), pp. 2385–2394.
- Yamamoto, S. and Harayama, S. (1998) Phylogenetic relationships of *Pseudomonas putida* strains deduced from the nucleotide sequences of *gyrB*, *rpoD* and 16S rRNA genes. *International journal of systematic bacteriology*. 48 Pt 3 (3), pp. 813–9.
- Yan, Y. et al. (2008) Nitrogen fixation island and rhizosphere competence traits in the genome of root-associated *Pseudomonas stutzeri* A1501. *Proceedings of the National Academy of Sciences of the United States of America*. 105 (21), pp. 7564-7569.
- Yarza, P. et al. (2008) The All-Species Living Tree project: A 16S rRNA-based phylogenetic tree

of all sequenced type strains. *Systematic and Applied Microbiology*. 31 (4), pp. 241–250.

Yoon, S.H. et al. (2017) Introducing EzBioCloud: A taxonomically united database of 16S rRNA gene sequences and whole-genome assemblies. *International Journal of Systematic and Evolutionary Microbiology*. 67 (5), pp. 1613–1617.

Young, J.M. and Park, D.-C. (2007) Probable synonymy of the nitrogen-fixing genus *Azotobacter* and the genus *Pseudomonas*. *International Journal of Systematic and Evolutionary Microbiology*. 57 (12), pp. 2894–2901.

Zarraonaindia, I. et al. (2015) The soil microbiome influences grapevine-associated microbiota. *mBio*. 6 (2).

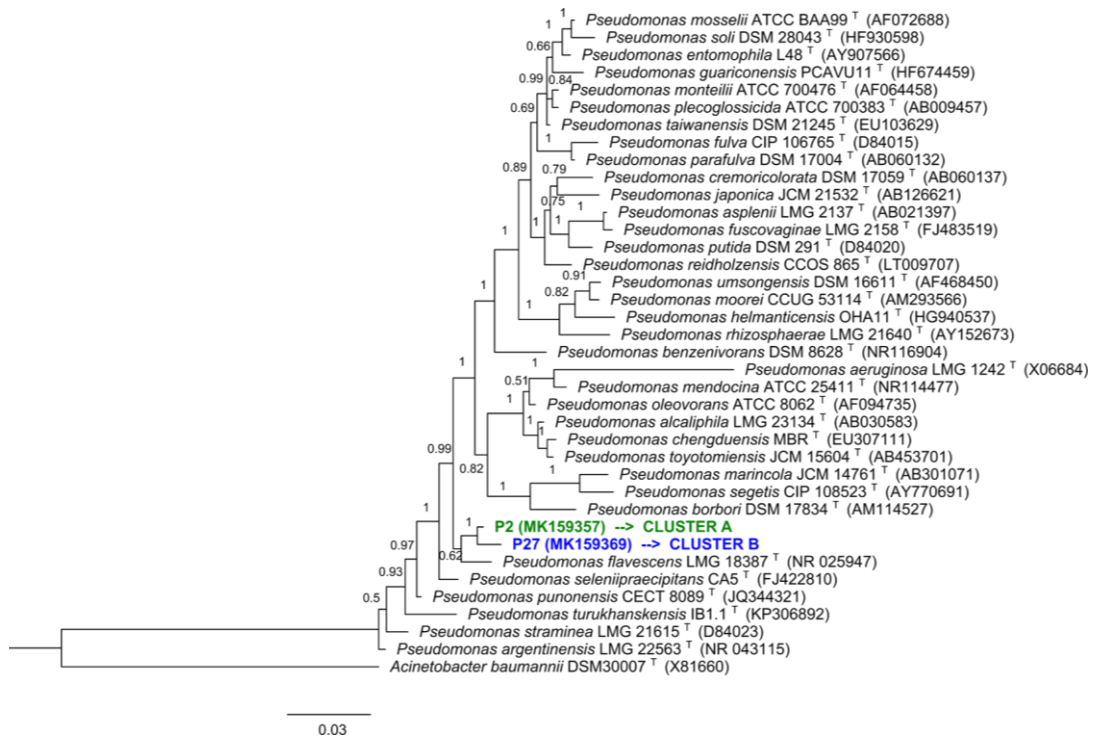
Zhang, L. et al. (2015) *Pseudomonas zhaodongensis* sp. nov., Isolated from saline and alkaline soils. *International Journal of Systematic and Evolutionary Microbiology*. 65 (Pt 3), pp. 1022–1030.

Zhang, Z. et al. (2000) A greedy algorithm for aligning DNA Sequences. *Journal of Computational Biology*. 7 (12), pp. 203–214.

Zhaxybayeva, O. et al. (2009) On the chimeric nature, thermophilic origin, and phylogenetic placement of the *Thermotogales*. *Proceedings of the National Academy of Sciences of the United States of America*. 106 (14), pp. 5865–5870.

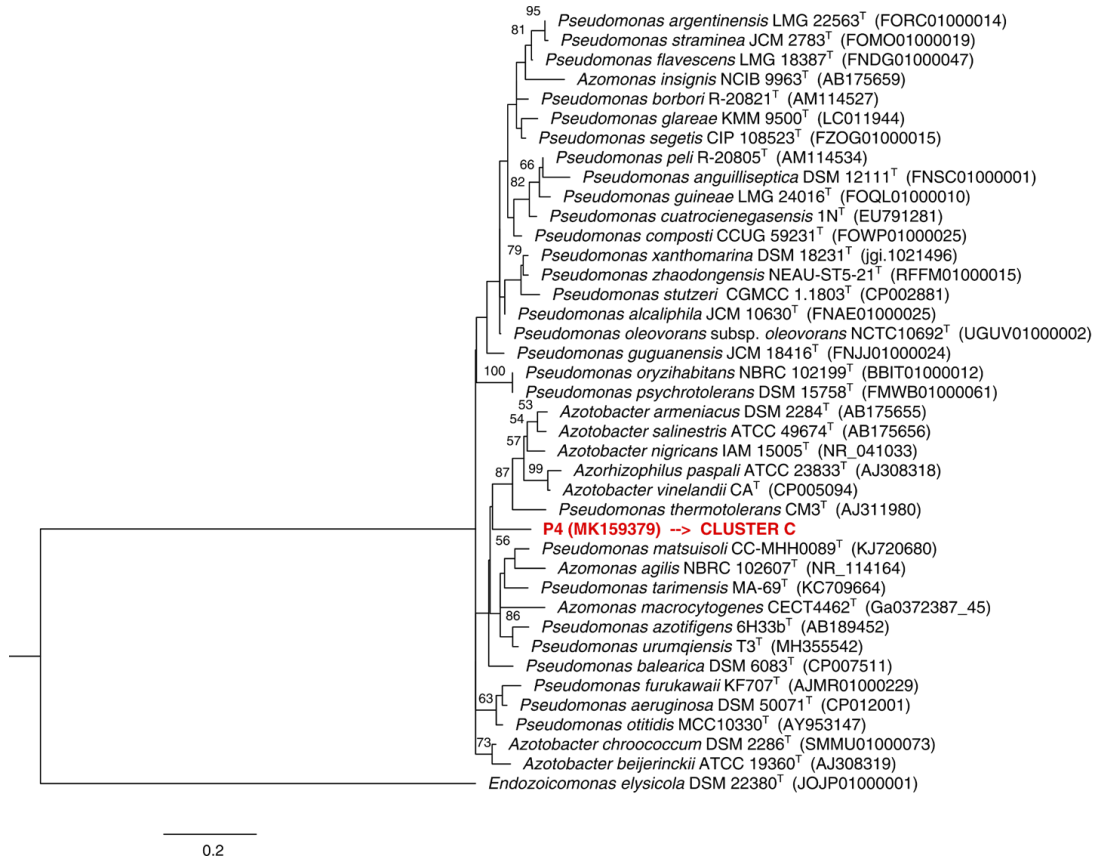
Zuckerlandl, E. and Pauling, L. (1965) Molecules as documents of evolutionary history. *Journal of theoretical biology*. 8 (2), pp. 357–366.

Appendix I: Bayesian 16S rRNA phylogenetic tree of the AOD-associated strains representatives of clusters A and B, 35 closest phylogenetic neighbours, and the outgroup *Acinetobacter baumannii*.



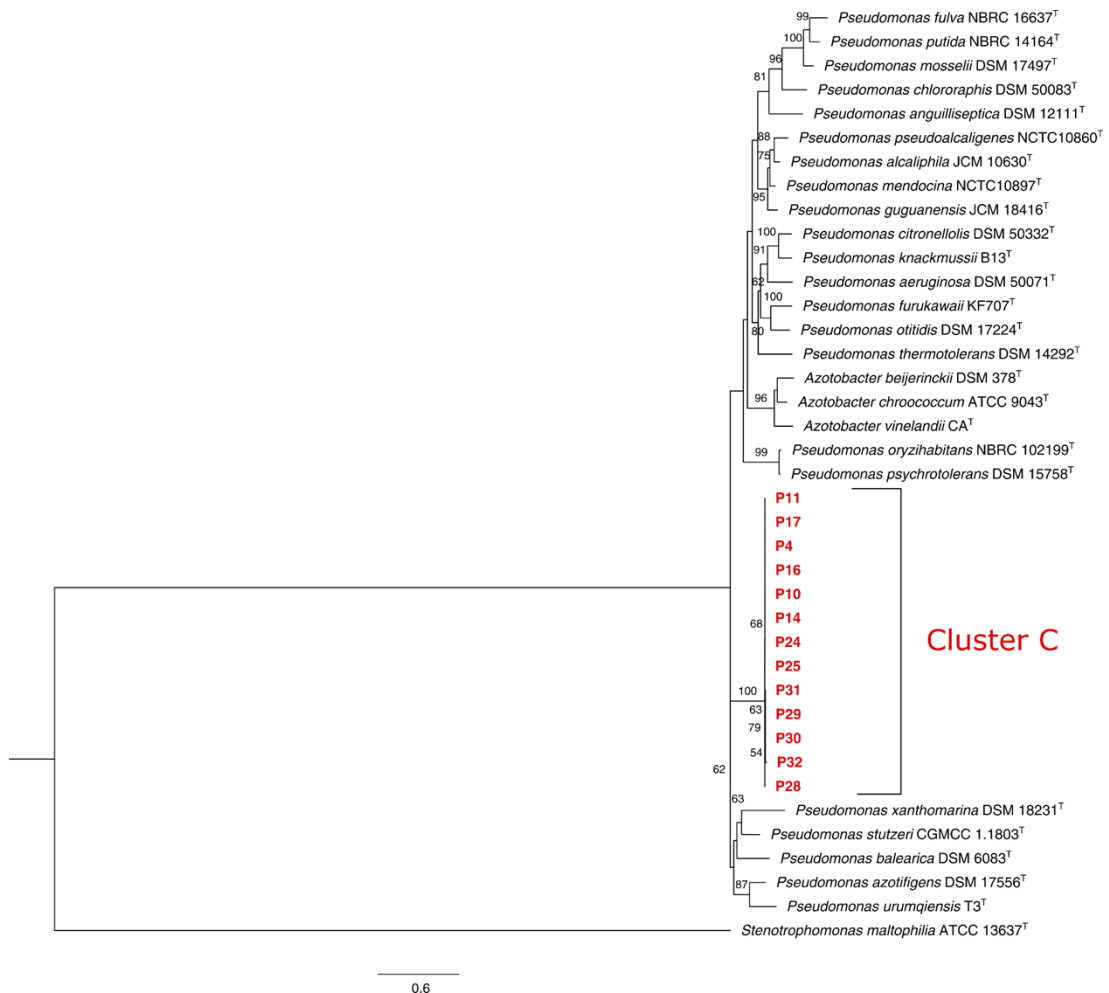
Appendix I: Bayesian 16S rRNA phylogenetic tree of the AOD-associated strains representatives of clusters A and B, 35 closest phylogenetic neighbours and the outgroup *Acinetobacter baumannii*. Phylogenetic relationships amongst the strains were inferred from a dataset of partial 16S rRNA gene nucleotide sequences (1399 bp), using the program MrBayes. Posterior probabilities lower than 0.5 were removed from the branches. The scale bar indicates the nucleotide substitutions per site. Species names, strain numbers and GenBank accession numbers are shown next to the branches. Strains representative of clusters A and B in green and blue, respectively. ^T = type strain.

APPENDIX II: Maximum likelihood 16S rRNA gene phylogenetic tree of the AOD-associated strain representative of cluster C, 38 closest phylogenetic neighbours, and the outgroup *Endozoicomonas elysicola*.



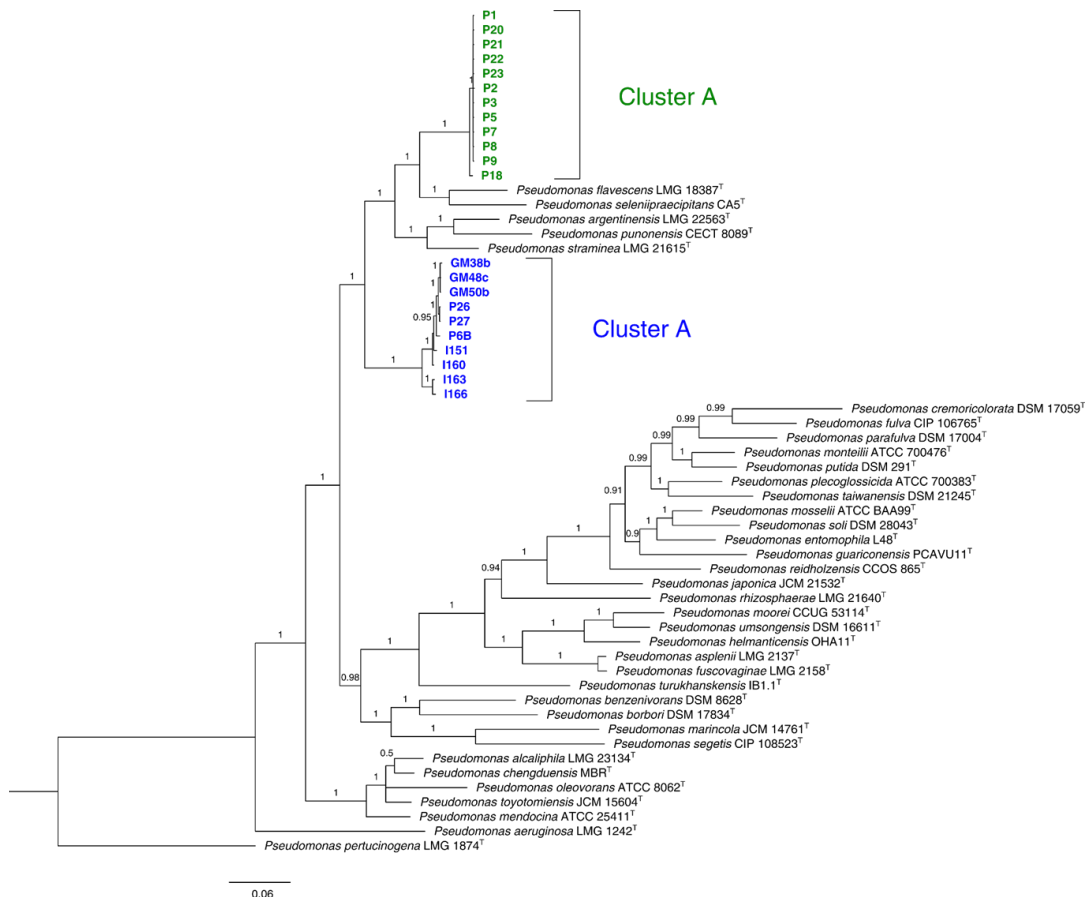
Appendix II: Maximum likelihood 16S rRNA gene phylogenetic tree of the AOD-associated strain representative of cluster C, 38 closest phylogenetic neighbours and the outgroup *Endozoicomonas elysicola*. Phylogenetic relationships amongst the strains were inferred from a dataset of partial 16S rRNA gene nucleotide sequences (1367 bp), using the program PhyML. Bootstrap values were obtained from 1000 replicates and values below 50 % are considered low support and were removed from the branches. The scale bar indicates the nucleotide substitutions per site. Species names, strain numbers and GenBank accession numbers are shown next to the branches. Strain representative of cluster C in red. ^T = type strain.

APPENDIX III: Maximum likelihood MLSA phylogenetic tree of the concatenated gene sequences *gyrB*, *rpoB* and *rpoD*, obtained from the AOD-associated strains in cluster C, 25 closest phylogenetic neighbours, and the outgroup *Stenotrophomonas maltophilia*.



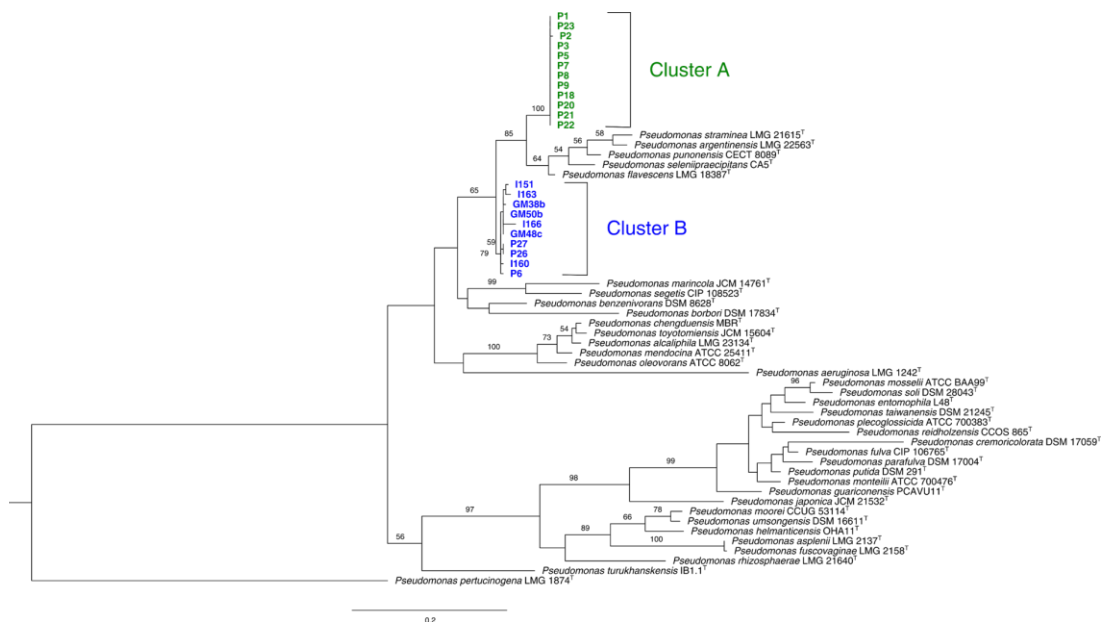
Appendix III: Maximum likelihood MLSA phylogenetic tree of the concatenated gene sequences *gyrB*, *rpoB* and *rpoD*, obtained from the AOD-associated strains in cluster C, 25 closest phylogenetic neighbours and the outgroup *Stenotrophomonas maltophilia*. Phylogenetic relationships amongst the strains were inferred from a dataset of partial concatenated *gyrB*, *rpoB* and *rpoD* nucleotide sequences (771, 753 and 651 bp long respectively), using the program PhyML Bootstrap values were obtained from 1000 replicates and values below 50 % are considered low support and were removed from the branches. The scale bar indicates the nucleotide substitutions per site. Species names and strain numbers are shown next to the branches and accession numbers are available in **Appendix VII**. Cluster C in red. ^T = type strain.

APPENDIX IV: Bayesian MLSA phylogenetic tree of the concatenated gene sequences *gyrb*, *rpob* and *rpod*, obtained from AOD-associated strains in clusters A and B, 35 closest phylogenetic neighbours and the outgroup *Pseudomonas pertucinogena*.



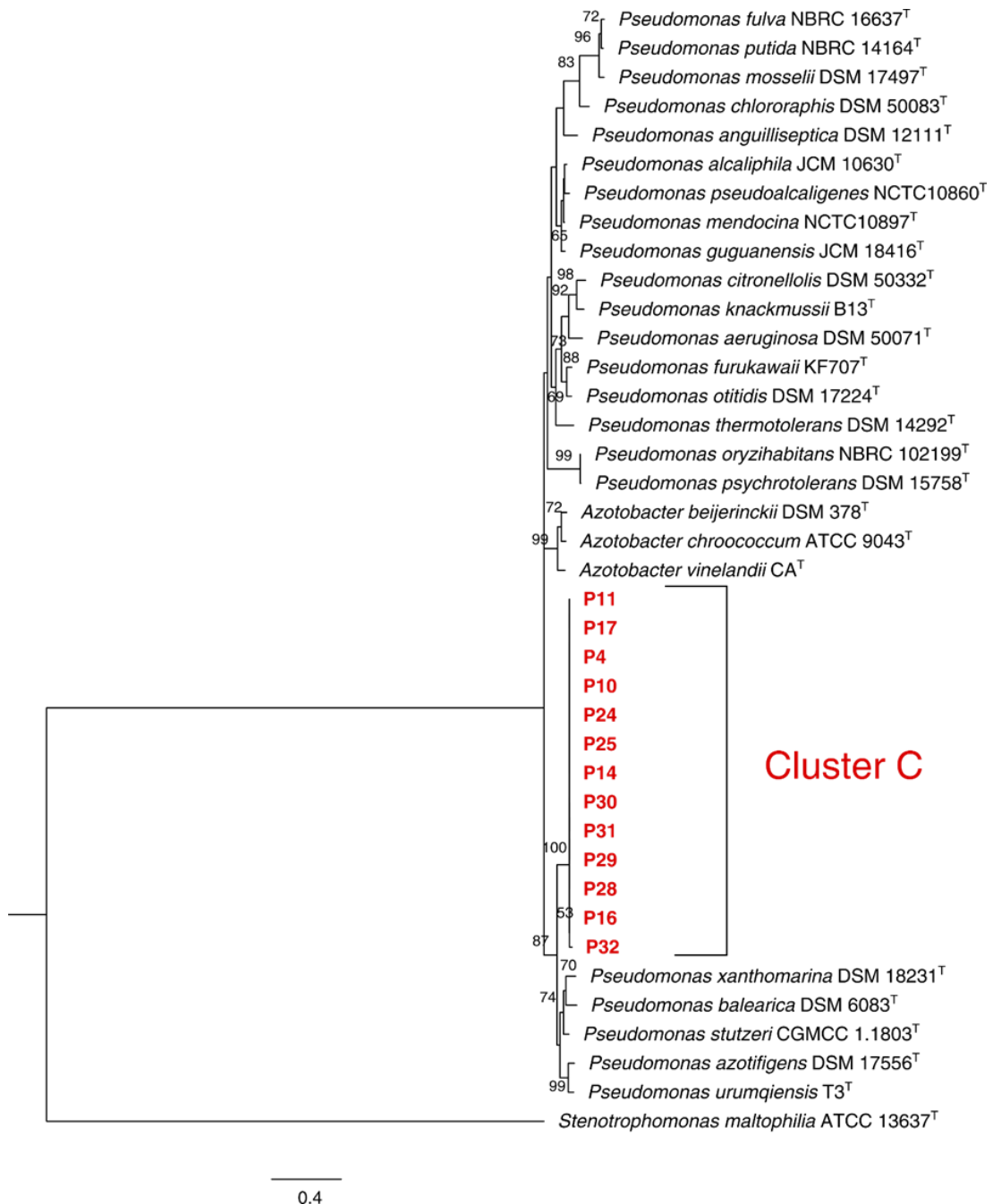
Appendix IV: Bayesian MLSA phylogenetic tree of the concatenated gene sequences *gyrB*, *rpoB* and *rpoD*, obtained from AOD-associated strains in clusters A and B, 35 closest phylogenetic neighbours and the outgroup *Pseudomonas pertucinogena*. Phylogenetic relationships amongst the strains were inferred from a dataset of partial concatenated *gyrB*, *rpoB* and *rpoD* nucleotide sequences (765, 750 and 657 bp long respectively), using the program MrBayes. Posterior probabilities lower than 0.95 are considered low support. Values lower than 0.5 were removed from the branches. The scale bar indicates the nucleotide substitutions per site. Species names and strain numbers are shown next to the branches and accession numbers are available in **Appendix VII**. Clusters A and B in green and blue, respectively. ^T = type strain.

APPENDIX V: Maximum likelihood MLSA phylogenetic tree of the concatenated amino acid sequences *gyrB*, *rpoB* and *rpoD*, obtained from AOD-associated strains in clusters A and B, 35 closest phylogenetic neighbours and the outgroup *Pseudomonas pertucinogena*.



Appendix V: Maximum likelihood MLSA phylogenetic tree of the concatenated amino acid sequences *gyrB*, *rpoB* and *rpoD*, obtained from AOD-associated strains in clusters A and B, 35 closest phylogenetic neighbours and the outgroup *Pseudomonas pertucinogena*. Phylogenetic relationships amongst the strains were inferred with the program PhyML, using a dataset of 724 amino acid sequences translated from partial concatenated *gyrB*, *rpoB* and *rpoD* nucleotide sequences. Bootstrap values were obtained from 1000 replicates and values below 50 % are considered low support and were removed from the branches. The scale bar indicates the amino acid substitutions per site. Species names and strain numbers are shown next to the branches and accession numbers are available in **Appendix VII**. Clusters A and B in green and blue, respectively. ^T = type strain.

APPENDIX VI: Maximum likelihood MLSA phylogenetic tree of the concatenated amino acid sequences *gyrB*, *rpoB* and *rpoD*, obtained from the AOD-associated strains in cluster C, 25 closest phylogenetic neighbours and the outgroup *Stenotrophomonas maltophilia*.



Appendix VI: Maximum likelihood MLSA phylogenetic tree of the concatenated amino acid sequences *gyrB*, *rpoB* and *rpoD*, obtained from the AOD-associated strains in cluster C, 25 closest phylogenetic neighbours and the outgroup *Stenotrophomonas maltophilia*.

Phylogenetic relationships amongst the strains were inferred with the program PhyML, using a dataset of 718 amino acid sequences translated from partial concatenated *gyrB*, *rpoB* and *rpoD* nucleotide sequences. Bootstrap values were obtained from 1000 replicates and values below 50 % are considered low support and were removed from the branches. The scale bar indicates the nucleotide substitutions per site. Species names and strain numbers are shown next to the branches and accession numbers are available in **Appendix X**. Cluster C in red. [†] = type strain.

APPENDIX VII: GenBank accession numbers for the MLSA trees of the AOD-associated *Pseudomonas*.

Appendix VII: GenBank accession numbers for the housekeeping genes *gyrB*, *rpoD* and *rpoB*, used in the multilocus sequence analysis (MLSA) of the AOD-associated isolates belonging to the species *Pseudomonas daroniae* sp. nov., *Pseudomonas dryadis* sp. nov., *Pseudomonas kirkieae* sp. nov., and their closest related neighbours (Bueno-Gonzalez et al., 2019, 2020).

Species and strain (MLSA clusters A and B and neighbours)	<i>gyrB</i> gene	<i>rpoD</i> gene	<i>rpoB</i> gene
<i>Pseudomonas daroniae</i> sp. nov. FRB 228 ^T	MK293898	MK293876	MK293920
<i>Pseudomonas daroniae</i> sp. nov. P1A	MK293899	MK293877	MK293921
<i>Pseudomonas daroniae</i> sp. nov. P3A	MK293900	MK293878	MK293922
<i>Pseudomonas daroniae</i> sp. nov. P5A	MK293901	MK293879	MK293923
<i>Pseudomonas daroniae</i> sp. nov. P7A	MK293902	MK293880	MK293924
<i>Pseudomonas daroniae</i> sp. nov. P8A	MK293903	MK293881	MK293925
<i>Pseudomonas daroniae</i> sp. nov. P9A	MK293904	MK293882	MK293926
<i>Pseudomonas daroniae</i> sp. nov. P18A	MK293905	MK293883	MK293927
<i>Pseudomonas daroniae</i> sp. nov. P20A	MK293906	MK293884	MK293928
<i>Pseudomonas daroniae</i> sp. nov. P21A	MK293907	MK293885	MK293929
<i>Pseudomonas daroniae</i> sp. nov. P22A	MK293908	MK293886	MK293930
<i>Pseudomonas daroniae</i> sp. nov. P23A	MK293909	MK293887	MK293931
<i>Pseudomonas dryadis</i> sp. nov. FRB 230 ^T	MK293910	MK293888	MK293932
<i>Pseudomonas dryadis</i> sp. nov. P6B	MK293911	MK293889	MK293933

<i>Pseudomonas dryadis</i> sp. nov. P26B	MK293912	MK293890	MK293934
<i>Pseudomonas dryadis</i> sp. nov. GM38b	MK293913	MK293891	MK293935
<i>Pseudomonas dryadis</i> sp. nov. GM48c	MK293914	MK293892	MK293936
<i>Pseudomonas dryadis</i> sp. nov. GM50b	MK293915	MK293893	MK293937
<i>Pseudomonas dryadis</i> sp. nov. I151	MK293916	MK293894	MK293938
<i>Pseudomonas dryadis</i> sp. nov. I160	MK293917	MK293895	MK293939
<i>Pseudomonas dryadis</i> sp. nov. I163	MK293918	MK293896	MK293940
<i>Pseudomonas dryadis</i> sp. nov. I166	MK293919	MK293897	MK293941
<i>Pseudomonas aeruginosa</i> LMG 1242 ^T	AB039386	AB039607	AJ717442
<i>Pseudomonas alcaliphila</i> LMG 23134 ^T	FN554167	FN554448	AJ717463
<i>Pseudomonas argentinensis</i> LMG 22563 ^T	FORC01000003.1:486796-489213	FORC01000005.1:82027-83874	FN554728
<i>Pseudomonas asplenii</i> LMG 2137 ^T	AB039455	AB039593	AJ717432
<i>Pseudomonas benzenivorans</i> DSM 8628 ^T	FNCT01000008.1:146807-149224	FNCT01000009.1:33941-35788	HE800506
<i>Pseudomonas borbori</i> DSM 17834 ^T	NZ_FOWX01000035.1:36826-39243	FOWX01000004.1:197393-199240	FN554730
<i>Pseudomonas chengduensis</i> MBR ^T	FMZQ01000001.1:220568-222988	FMZQ01000021.1:58578-60425	NZ_FMZQ01000028.1:4558-8631
<i>Pseudomonas cremoricolorata</i> DSM 17059 ^T	FN554181	FN554462	AJ717476
<i>Pseudomonas entomophila</i> L48 ^T	NC_008027:4346-6766	NC_008027:435570-437420	NC_008027:502974-507047
<i>Pseudomonas flavescens</i> LMG 18387 ^T	NZ_FNDG01000003.1:373257-375674	FNDG01000008.1:238853-240697	NZ_FNDG01000011.1:8358-12431
<i>Pseudomonas fulva</i> CIP 106765 ^T	AB039395	AB039586	AJ717419

<i>Pseudomonas fuscovaginae</i> LMG 2158 ^T	FN554185	FN554467	AJ717433
<i>Pseudomonas guariconensis</i> PCAVU11 ^T	HF674462	HF674460	HF674461
<i>Pseudomonas helmanticensis</i> OHA11 ^T	HG940516.1	HG940517.1	HG940518.1
<i>Pseudomonas japonica</i> JCM 21532 ^T	GQ996725	HE577795	HE577800
<i>Pseudomonas marincola</i> JCM 14761 ^T	NZ_FPBC01000007.1:163356-165773	NZ_FPBC01000018.1:45643-47487	NZ_FPBC01000015.1:104030-108103
<i>Pseudomonas mendocina</i> ATCC 25411 ^T	AJ633103.1	AJ633567.1	KF029437.1
<i>Pseudomonas monteilii</i> ATCC 700476 ^T	FN554205	FN554488	AJ717455
<i>Pseudomonas moorei</i> CCUG 53114 ^T	AM293560	FN554489	FN554742
<i>Pseudomonas mosselii</i> ATCC BAA-99 ^T	FN554207	FN554491	FN554744
<i>Pseudomonas oleovorans</i> ATCC 8062 ^T	AB039396	AB039601	AJ717461
<i>Pseudomonas parafulva</i> DSM 17004 ^T	FN554216	FN554500	AJ717471
<i>Pseudomonas pertucinogena</i> LMG 1874 ^T	DQ350613	FN554502	AJ748153
<i>Pseudomonas plecoglossicida</i> ATCC 700383 ^T	FN554218	FN554503	AJ717456
<i>Pseudomonas punonensis</i> CECT 8089 ^T	FRBQ01000001.1:1393758-1396175	NZ_FRBQ01000007.1:81640-83487	NZ_FRBQ01000017.1:3832-7905
<i>Pseudomonas putida</i> DSM 291 ^T	NC_021505:4197-6617	NC_021505:495867-497717	NC_021505.1:563026-567099
<i>Pseudomonas reidholzensis</i> CCOS 865 ^T	LT009711	LT009713	LT009712
<i>Pseudomonas rhizosphaerae</i> LMG 21640 ^T	FN554224	FN554510	FN554755
<i>Pseudomonas segetis</i> CIP 108523 ^T	NZ_FZOG01000003.1:166161-168578	NZ_FZOG01000008.1:46337-48181	NZ_FZOG01000011.1:7650-11723
<i>Pseudomonas seleniipraecipitans</i> LMG 25475 ^T	HE800485.1	HE800501.1	HE800517.1
<i>Pseudomonas soli</i> DSM 28043 ^T	HF930595.1	HF930597	HF930596

<i>Pseudomonas straminea</i> LMG 21615 ^T	AB039410	AB039600	FN554758
<i>Pseudomonas taiwanensis</i> DSM 21245 ^T	FJ418634	HE577796	HE577797
<i>Pseudomonas toyotomiensis</i> JCM 15604 ^T	AB494447	AB548145	AB548147
<i>Pseudomonas turukhanskensis</i> IB1.1 ^T	LT219440.1	LT219439.1	LT219438.1
<i>Pseudomonas umsongensis</i> DSM 16611 ^T	NIWU01000003.1:104882-107299	NIWU01000003.1:648596-650443	NIWU01000006.1:306493-310566
Species and strain (MLSA cluster C and neighbours)	<i>gyrB</i> gene	<i>rpoD</i> gene	<i>rpoB</i> gene
<i>Pseudomonas kirkliae</i> sp. nov. FRB 229 ^T =PW136 ^T =P4C ^T	MN044407	MN044420	MN044394
<i>Pseudomonas kirkliae</i> sp. nov. P10C= PW153	MN044408	MN044421	MN044395
<i>Pseudomonas kirkliae</i> sp. nov. P11C=PW155 ai)	MN044409	MN044422	MN044396
<i>Pseudomonas kirkliae</i> sp. nov. P14C= PW158 a)	MN044410	MN044423	MN044397
<i>Pseudomonas kirkliae</i> sp. nov. P16C=PW160 bi)b	MN044411	MN044424	MN044398
<i>Pseudomonas kirkliae</i> sp. nov. P17C=PW164 bi)a	MN044412	MN044425	MN044399
<i>Pseudomonas kirkliae</i> sp. nov. P24C=PW214	MN044413	MN044426	MN044400
<i>Pseudomonas kirkliae</i> sp. nov. P25C=PW211 b)	MN044414	MN044427	MN044401
<i>Pseudomonas kirkliae</i> sp. nov. P28C=S40	MN044415	MN044428	MN044402
<i>Pseudomonas kirkliae</i> sp. nov. P29C=SB22b	MN044416	MN044429	MN044403
<i>Pseudomonas kirkliae</i> sp. nov. P30C=SB60b	MN044417	MN044430	MN044404
<i>Pseudomonas kirkliae</i> sp. nov. P31C=SB61b	MN044418	MN044431	MN044405
<i>Pseudomonas kirkliae</i> sp. nov. P32C=SB65	MN044419	MN044432	MN044406
<i>Azotobacter beijerinckii</i> DSM 378 ^T	FOFJ01000003	FOFJ01000015	FOFJ01000074

<i>Azotobacter chroococcum</i> ATCC 9043 ^T	SJAA01000080	SJAA01000042	SJAA01000040
<i>Azotobacter vinelandii</i> CA ^T	CP005094	NC_021149	NC_021149
<i>Endozoicomonas elysicola</i> DSM 22380 ^T	JOJP01000001	JOJP01000001	JOJP01000001
<i>Pseudomonas aeruginosa</i> DSM 50071 ^T	CP012001	CP012001	CP012001
<i>Pseudomonas alcaliphila</i> JCM 10630 ^T	FNAE01000002	FNAE01000005	FNAE01000016
<i>Pseudomonas anguilliseptica</i> DSM 12111 ^T	FNSC01000001	FNSC01000001	FNSC01000001
<i>Pseudomonas azotifigens</i> DSM 17556 ^T	FN554174	AUDU01000018	AUDU01000086
<i>Pseudomonas balearica</i> DSM 6083 ^T	CP007511	AB039605	CP007511
<i>Pseudomonas chlororaphis</i> DSM 50083 ^T	UYXS01000009	UYXS01000008	UYXS01000010
<i>Pseudomonas citronellolis</i> DSM 50332 ^T	PISI01000007	PISI01000020	PISI01000035
<i>Pseudomonas fulva</i> NBRC 16637 ^T	BBIQ01000001	BBIQ01000001	BBIQ01000012
<i>Pseudomonas furukawaii</i> KF707 ^T	LC187275	AJMR01000115	AJMR01000041
<i>Pseudomonas guguanensis</i> JCM 18416 ^T	FNJJ01000008	FNJJ01000018	FNJJ01000012
<i>Pseudomonas knackmussii</i> B13 ^T	HG322950	HG322950	HG322950
<i>Pseudomonas mangiferae</i> DMKU BBB3-04 ^T	VJOY01000011	VJOY01000005	VJOY01000021
<i>Pseudomonas mendocina</i> NCTC10897 ^T	LR134290	LR134290	LR134290
<i>Pseudomonas mosselii</i> DSM 17497 ^T	JHYW01000009	JHYW01000005	JHYW01000046
<i>Pseudomonas nosocomialis</i> A31/70 ^T	LT601025	HE573725	QLAE01000058
<i>Pseudomonas oryzihabitans</i> NBRC 102199 ^T	BBIT01000005	BBIT01000024	BBIT01000030
<i>Pseudomonas otitidis</i> DSM 17224 ^T	FOJP01000007	FOJP01000001	FOJP01000039
<i>Pseudomonas pseudoalcaligenes</i> NCTC10860 ^T	UGUW01000004	UGUW01000004	UGUW01000004
<i>Pseudomonas psychrotolerans</i> DSM 15758 ^T	FMWB01000002	FMWB01000007	FMWB01000040

<i>Pseudomonas putida</i> NBRC 14164 ^T	AP013070	AP013070	AP013070
<i>Pseudomonas stutzeri</i> CGMCC 1.1803 ^T	CP002881	CP002881	CP002881
<i>Pseudomonas thermotolerans</i> DSM 14292 ^T	KB822616	KB822621	KB822612
<i>Pseudomonas urumqiensis</i> T3 ^T	RBZQ01000008	RBZQ01000003	RBZQ01000009
<i>Pseudomonas xanthomarina</i> DSM 18231 ^T	FQXA01000001	FQXA01000009	FQXA01000004

T = type strain.

APPENDIX VIII: Phenotypic characteristics of the AOD-associated strains in cluster A, B and C, and their closest neighbours, obtained with the tests API 20NE, API CH 50 and BIOLOG GN2.

Appendix VIII: Phenotypic characteristics of the AOD-associated *Pseudomonas* in cluster A, B and C, and their closest neighbours, obtained with the tests API 20NE, API CH 50 and Biolog GN2.

API 20 NE, characteristic:	1	2	3	4	5	6	7	8	9	10	11	12	13	14	15	16	17	18
Nitrate reduction to nitrites (nitrification)	-	-	-	-	-	-	-	+	-	+	-	-	-	-	-	-	-	-
Nitrate reduction to nitrogen (denitrification)	-	-	-	-	-	-	-	-	-	+	-	-	-	-	+	-	+	+
Indole production	-	-	-	-	-	-	-	-	-	-	-	-	-	-	-	-	-	-
Acidification from D-glucose	-	-	-	-	-	-	-	-	-	-	-	-	-	-	-	-	-	-
Arginine dihydrolase	-	-	-	-	-	-	-	-	-	-	-	-	-	-	-	-	-	-
Urease	-	-	-	-	-	-	-	-	-	-	-	-	-	-	-	-	-	-
Esculin hydrolysis (β -glucosidase)	-	-	-	-	-	-	-	-	-	-	-	-	-	-	-	-	-	-
Gelatin hydrolysis (protease)	-	-	-	-	-	-	-	-	-	-	-	-	-	-	-	-	-	-
β -galactosidase	-	-	-	-	-	-	-	-	-	-	-	-	-	-	-	-	-	-
Assimilation D-glucose	+	+	+	+	+	+	+	+	+	+	+	-	-	-	+	+	+	+
Assimilation L-arabinose	+	+	+	-	-	-	+	+	+	+	+	-	-	-	-	-	-	-
Assimilation D-mannose	+	+	+	+	+	+	+	+	+	+	+	-	-	-	-	-	-	-
Assimilation D-mannitol	+	+	+	+	+	+	+	+	+	+	+	-	-	-	-	+	-	+
Assimilation N-acetyl-glucosamine	-	-	-	-	-	-	-	-	-	-	-	-	-	-	-	-	-	-

Assimilation D-maltose	-	-	-	-	-	-	-	-	-	-	-	-	-	-	-	+	-	+	+
Assimilation potassium gluconate	+	+	+	+	+	+	+	+	+	+	+	-	-	-	-	+	+	+	+
Assimilation caprate	+	+	+	+	+	+	+	+	+	+	+	+	+	+	+	+	+	+	-
Assimilation adipate	-	-	-	-	-	-	-	-	-	-	-	-	-	-	-	-	-	-	-
Assimilation malate	+	+	+	+	+	+	+	+	+	+	+	+	+	+	+	+	+	+	+
Assimilation citrate	+	+	+	+	+	+	+	+	+	+	+	-	-	-	-	+	+	-	-
Assimilation phenyl-acetate	-	-	-	-	-	-	-	-	-	-	-	-	-	-	-	-	-	-	-

API 50 CH, acid from:	1	2	3	4	5	6	7	8	9	10	11	12	13	14	15	16	17	18	
Control	-	-	-	-	-	-	-	-	-	-	-	-	-	-	-	-	-	-	-
Glycerol	+	+	+	+	w+	+	+	+	-	+	w+	-	-	-	+	-	+	+	
Erythritol	-	-	-	-	-	-	-	-	-	-	-	-	-	-	-	-	-	-	-
D-arabinose	-	-	-	-	-	-	-	-	-	-	-	-	-	-	-	-	-	-	-
L-arabinose	+	+	+	-	-	-	+	+	+	+	+	-	w+	-	+	-	-	-	
D-ribose	-	-	-	-	-	-	-	w+	-	-	-	-	-	w+	w+	-	-	-	
D-xylose	-	-	-	-	-	-	-	+	-	-	-	-	-	-	+	-	-	-	
L-xylose	-	-	-	-	-	-	-	-	-	-	-	-	-	-	-	-	-	-	
D-adonitol	-	-	-	-	-	-	-	-	-	-	-	-	-	-	-	-	-	-	
Methyl-βD-xylopyranoside	-	-	-	-	-	-	-	-	-	-	-	-	-	-	-	-	-	-	
D-galactose	+	+	+	-	-	-	+	+	+	+	+	-	w+	-	+	-	-	-	
D-glucose	+	+	+	+	+	+	+	+	+	+	+	w+	-	-	+	w+	+	+	
D-fructose	+	+	+	+	+	+	+	+	+	+	+	-	-	-	+	w+	+	+	
D-mannose	+	+	+	+	+	+	+	+	+	+	+	-	-	-	+	-	-	-	

L-sorbose	-	-	-	-	-	-	-	-	-	-	-	-	-	-	-	-	-	-
L-rhamnose	-	-	-	-	-	-	-	-	-	-	-	-	-	-	-	-	-	-
Dulcitol	-	-	-	-	-	-	-	-	-	-	-	-	-	-	-	-	-	-
Inositol	-	-	-	-	-	-	-	-	-	-	-	-	-	-	-	-	-	-
D-mannitol	+	+	+	+	+	+	+	+	+	+	+	-	-	-	W+	W+	-	+
D-sorbitol	-	-	-	-	-	-	-	-	-	-	-	-	-	-	-	-	-	-
Methyl- αD-mannopyranoside	-	-	-	-	-	-	-	-	-	-	-	-	-	-	-	-	-	-
Methyl-αD-glucofuranoside	-	-	-	-	-	-	-	-	-	-	-	-	-	-	-	-	-	-
N-acetylglucosamine	-	-	-	-	-	-	-	-	-	-	-	-	-	-	-	-	-	-
Amygdalin	-	-	-	-	-	-	-	-	-	-	-	-	-	-	-	-	-	-
Arbutin	-	-	-	-	-	-	-	-	-	-	-	-	-	-	-	-	-	-
Esculin ferric citrate	-	-	-	-	-	-	-	-	-	-	-	-	-	-	-	-	-	-
Salicin	-	-	-	-	-	-	-	-	-	-	-	-	-	-	-	-	-	-
D-cellobiose	-	-	-	-	-	-	-	-	-	-	-	-	-	-	-	-	-	-
D-maltose	-	-	-	-	-	-	+	+	-	-	-	-	-	-	W+	-	+	+
D-lactose	-	-	-	-	-	-	-	-	-	-	-	-	-	+	-	-	-	-
D-melibiose	-	-	-	-	-	-	-	+	-	-	-	-	-	-	+	-	-	-
D-saccharose (sucrose)	-	-	-	-	-	-	+	-	-	-	-	-	-	-	-	-	-	-
D-trehalose	-	-	-	-	-	-	+	+	-	-	-	-	-	-	W+	-	-	+
Inulin	-	-	-	-	-	-	-	-	-	-	-	-	-	-	-	-	-	-
D-melezitose	-	-	-	-	-	-	-	-	-	-	-	-	-	-	-	-	-	-
D-raffinose	-	-	-	-	-	-	-	-	-	-	-	-	-	-	-	-	-	-
Amidon (starch)	-	-	-	-	-	-	-	-	-	-	-	-	-	-	+	-	+	-
Glycogen	-	-	-	-	-	-	-	-	-	-	-	-	-	-	+	-	+	-

Xylitol	-	-	-	-	-	-	-	-	-	-	-	-	-	-	-	-	-	-
Gentiobiose	-	-	-	-	-	-	-	+	-	-	-	-	-	-	+	-	-	-
D-turanose	-	-	-	-	-	-	-	-	-	-	-	-	-	-	-	-	-	-
D-lyxose	w+	w+	+	w+	w+	w+	-	-	-	-	-	-	-	-	-	-	-	-
D-tagatose	-	-	-	-	-	-	-	-	-	-	-	-	-	-	-	-	-	-
D-fucose	-	-	-	w+	+	w+	-	+	-	-	-	-	-	-	+	-	w+	-
L-fucose	-	-	-	-	-	-	-	-	-	-	-	-	-	-	-	-	-	-
D-arabitol	w+	w+	+	w+	w+	w+	+	+	+	+	+	-	-	-	-	w+	-	+
L-arabitol	-	-	-	-	-	-	-	-	-	-	-	-	-	-	-	-	-	-
Potassium gluconate	-	-	-	-	-	-	-	-	-	-	-	-	-	-	-	-	-	-
Potassium 2-ketogluconate	-	-	-	-	-	-	-	-	-	-	-	-	-	-	-	-	-	-
Potassium 5-ketogluconate	-	-	-	-	-	-	-	-	-	-	-	w+	w+	w+	-	-	-	-

Biolog GN2, oxidation of:	1	2	3	4	5	6	7	8	9	10	11	12	13	14	15	16	17	18
Water	-	-	-	-	-	-	-	-	-	-	-	-	-	-	-	-	-	-
α-cyclodextrin	-	-	-	-	-	-	-	-	-	-	-	-	-	-	-	-	-	-
Dextrin	w+	w+	+	+	w+	+	w+	-	w+	w+	w+	-	-	+	+	+	+	+
Glycogen	w+	w+	+	-	w+	w+	w+	-	w+	w+	w+	w+	-	+	+	+	+	-
Tween 40	-	-	-	-	w+	w+	-	-	-	w+	-	-	+	+	+	+	+	-
Tween 80	-	-	-	-	w+	w+	-	-	-	w+	-	+	+	+	+	+	+	-
N-acetyl-D-galactosamine	-	-	-	-	-	-	-	-	-	-	-	-	-	-	-	-	-	-
N-acetyl-D-glucosamine	-	-	-	-	-	-	-	-	-	-	-	-	-	-	-	-	-	-
Adonitol	-	-	-	-	-	-	-	-	-	-	-	-	-	-	-	-	-	-

L-arabinose	+	+	+	+	+	+	+	+	+	+	+	+	+	+	+	+	+	+
D-arabitol	+	w+	+	+	+	+	+	w+	w+	+	+	-	-	-	-	-	-	-
D-cellobiose	-	-	-	-	-	-	-	-	-	-	-	-	-	-	w+	-	-	-
i-erythritol	-	-	-	-	-	-	-	-	-	-	-	-	-	-	-	-	-	-
D-fructose	+	+	+	w+	+	w+	+	-	w+	+	w+	-	-	-	+	-	w+	-
L-fucose	-	-	-	-	-	-	-	-	-	-	-	-	-	-	-	-	-	-
D-galactose	+	+	+	-	-	-	+	+	+	+	+	-	-	-	-	-	-	-
Gentiobiose	-	-	-	-	-	-	-	-	-	-	-	-	-	-	-	-	-	-
α -D-glucose	+	+	+	+	+	+	+	+	+	w+	w+	-	-	-	+	-	+	-
m-inositol	-	-	-	-	-	-	-	-	-	-	-	-	-	-	-	-	-	-
α -D-lactose	-	-	-	-	-	-	-	-	-	-	-	-	-	-	-	-	-	-
Lactulose	-	-	-	-	-	-	-	-	-	-	-	-	-	-	-	-	-	-
Maltose	-	-	-	-	-	-	-	-	-	-	-	-	-	-	+	-	+	-
D-mannitol	+	+	+	+	+	+	+	+	+	+	+	-	-	-	-	+	-	-
D-mannose	+	+	+	w+	w+	+	+	-	-	+	w+	-	-	-	w+	-	-	-
D-melibiose	-	-	-	-	-	-	-	-	-	-	-	-	-	-	-	-	-	-
β -methyl-D-glucoside	-	-	-	-	-	-	-	-	w+	-	-	-	-	-	-	-	-	-
D-psicose	w+	w+	-	-	-	-	w+	-	w+	w+	-	-	-	-	-	-	-	-
D-raffinose	-	-	-	-	-	-	-	-	-	-	-	-	-	-	-	-	-	-
L-rhamnose	-	-	-	-	-	-	-	-	-	-	-	-	-	-	-	-	-	-
D-sorbitol	-	-	-	-	-	-	-	-	-	-	-	-	-	-	-	-	-	-
Sucrose	-	-	-	-	-	-	+	-	-	-	-	-	-	-	-	-	-	-
D-trehalose	-	-	-	-	-	-	+	+	-	-	-	-	-	-	-	-	-	-
Turanose	-	-	w+	-	w+	-	-	-	-	w+	-	-	-	-	+	-	-	-

Xylitol	-	-	-	-	-	-	-	-	-	-	-	-	-	-	-	-	-	-
Pyruvic acid methyl ester	+	+	+	+	+	+	+	+	+	+	+	+	+	+	+	+	+	-
Succinic acid mono-methyl ester	+	+	+	+	+	+	+	+	+	+	w+	+	+	+	+	+	+	-
Acetic acid	+	+	+	+	+	+	+	-	w+	+	-	+	+	+	+	+	+	-
<i>Cis</i> -aconitic acid	+	+	+	+	+	+	+	+	+	+	+	-	-	-	+	+	+	-
Citric acid	+	+	+	+	+	+	+	+	+	+	+	-	-	-	+	+	+	-
Formic acid	+	w+	+	-	+	+	w+	-	w+	w+	w+	-	-	-	+	+	+	-
D-galactonic acid lactone	-	-	-	-	-	-	-	-	-	w+	-	-	-	-	-	-	-	-
D-galacturonic acid	+	+	+	-	-	-	-	+	+	+	+	-	-	-	-	-	-	-
D-gluconic acid	+	+	+	-	-	-	+	+	+	+	+	-	-	-	+	+	+	-
D-glucosaminic acid	-	-	-	-	-	-	-	-	-	-	-	-	-	-	-	-	-	-
D-glucuronic acid	+	+	+	-	-	-	-	+	+	+	+	-	-	-	-	-	-	-
α -hydroxybutyric acid	-	-	+	-	w+	w+	-	-	w+	w+	-	+	+	+	+	w+	+	-
β -hydroxybutyric acid	+	+	-	-	+	w+	+	w+	+	+	+	-	-	-	+	+	+	-
γ -hydroxybutyric acid	+	+	+	+	+	+	+	w+	+	+	w+	-	-	-	-	-	-	-
<i>p</i> -hydroxy-phenylacetic acid	-	-	-	-	-	-	-	-	-	-	-	-	-	-	-	-	-	-
Itaconic acid	+	+	+	+	+	+	+	+	+	+	+	-	-	-	+	+	+	-
α -ketobutyric acid	-	-	w+	-	w+	-	-	-	w+	-	-	+	+	+	+	+	+	-
α -ketoglutaric acid	+	+	+	+	+	+	+	+	+	+	+	+	+	+	+	+	+	-
α -ketovaleric acid	-	-	w+	-	-	-	-	-	-	-	-	-	-	-	+	w+	+	-
D,L-lactic acid	+	+	+	+	+	+	+	+	+	+	+	+	+	+	+	+	+	-
Malonic acid	-	-	-	-	-	-	w+	-	+	-	-	-	-	-	+	-	+	-
Propionic acid	-	-	+	w+	+	w+	-	-	-	w+	-	+	+	+	+	+	+	-
Quinic acid	+	+	+	+	+	+	+	+	+	-	+	-	-	-	-	-	-	-

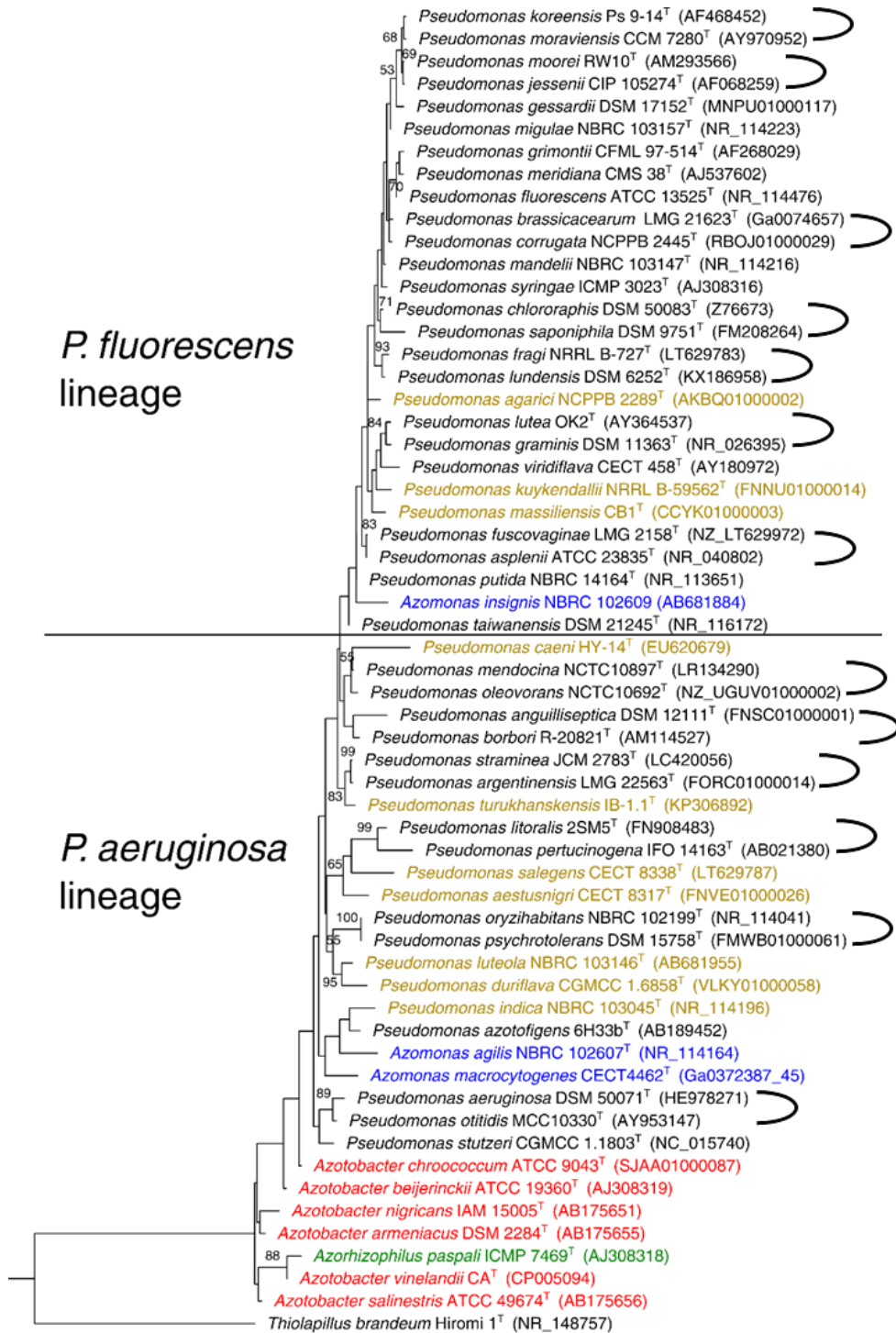
D-saccharic acid	+	-	+	-	-	-	+	-	+	+	-	-	-	-	-	+	-	-
Sebacic acid	-	-	-	-	-	-	-	-	-	-	-	-	-	-	+	+	-	-
Succinic acid	+	+	+	+	+	+	+	-	+	+	+	+	+	+	+	+	+	-
Bromosuccinic acid	+	+	+	+	+	+	+	+	+	+	+	+	+	+	+	+	+	-
Succinamic acid	+	+	+	+	w+	w+	+	-	+	w+	+	+	+	+	-	+	+	-
Glucuronamide	+	+	+	-	-	-	-	-	+	+	+	-	-	-	-	-	-	-
L-alaninamide	w+	w+	w+	-	-	-	-	-	w+	w+	+	+	+	+	+	+	+	-
D-alanine	+	+	+	w+	w+	w+	-	-	w+	+	w+	+	+	+	+	+	+	-
L-alanine	+	+	+	w+	w+	w+	+	-	+	+	+	+	+	+	+	+	+	-
L-alanyl-glycine	-	-	-	-	-	-	-	-	w+	w+	w+	-	-	-	-	-	-	-
L-asparagine	+	+	+	-	+	w+	+	+	+	+	+	+	+	+	+	+	+	-
L-aspartic acid	+	+	+	+	+	+	+	+	+	+	+	+	+	+	-	-	+	-
L-glutamic acid	+	+	+	+	+	+	+	+	+	+	+	+	+	+	+	+	+	-
Glycyl-L-aspartic acid	-	-	-	-	-	-	-	-	-	-	-	-	-	-	-	-	-	-
Glycyl-L-glutamic acid	-	-	-	-	-	-	-	-	-	-	w+	-	-	-	-	-	-	-
L-histidine	-	-	-	-	-	-	-	-	-	-	-	-	-	-	-	-	-	-
Hydroxy-L-proline	+	+	+	+	+	+	+	-	+	+	+	-	-	-	-	-	w+	-
L-leucine	-	-	-	-	-	-	-	-	-	-	-	-	-	-	+	-	+	-
L-ornithine	-	-	-	-	-	-	-	-	-	-	-	-	-	-	-	-	-	-
L-phenylalanine	-	-	-	-	-	-	-	-	-	-	-	-	-	-	-	-	-	-
L-proline	+	+	+	+	+	+	+	+	+	+	+	+	+	+	+	+	-	+
L-pyroglutamic acid	+	+	+	-	w+	w+	+	+	+	+	+	-	-	-	+	+	-	-
D-serine	-	-	-	-	-	-	-	-	-	-	-	-	-	+	-	-	-	-
L-serine	+	+	+	w+	w+	+	+	-	+	+	+	-	-	-	+	-	-	-

L-threonine	-	-	-	-	-	-	-	-	W+	+	-	-	-	-	+	-	W+	-
D,L-carnitine	+	-	W+	-	-	-	W+	W+	-	W+	W+	-	-	-	-	-	W+	-
γ-aminobutyric acid	+	+	+	+	+	+	+	+	+	+	+	-	-	+	-	+	-	-
Urocanic acid	-	-	-	-	-	-	+	-	W+	-	+	-	-	-	-	-	-	-
Inosine	-	-	-	-	-	-	-	-	-	-	-	-	-	-	-	-	-	-
Uridine	-	-	-	-	-	-	-	-	-	-	-	-	-	-	-	-	-	-
Thymidine	-	-	-	-	-	-	-	-	-	-	-	-	-	-	-	-	-	-
Phenyethylamine	-	-	-	-	-	-	-	-	-	-	-	-	-	-	-	-	-	-
Putrescine	-	-	W+	-	-	-	+	+	+	W+	W+	-	-	-	-	-	-	-
2-aminoethanol	+	+	+	-	-	W+	+	+	+	+	-	+	+	+	-	-	W+	-
2,3-butanediol	-	W+	-	-	-	W+	W+	-	-	-	-	-	-	-	-	-	+	-
Glycerol	+	+	+	+	+	+	+	W+	W+	W+	W+	-	-	-	+	-	+	-
D,L, α-glycerol phosphate	W+	W+	+	-	-	-	W+	-	W+	W+	W+	-	-	-	-	-	-	-
α-D-glucose-1-phosphate	-	-	-	-	-	-	-	-	-	-	-	-	-	-	-	-	-	-
D-glucose-6-phosphate	-	-	-	-	-	-	-	-	-	W+	-	-	-	-	+	-	-	-

(1) Cluster A: strain P2, (2) cluster A: strain P9, (3) cluster A: strain P18, (4) cluster B: strain P27, (5) cluster B: strain P6, (6) cluster B: strain P26, (7) *Pseudomonas flavescens* LMG 18387^T, (8) *Pseudomonas argentinensis* LMG 22563^T, (9) *Pseudomonas punonensis* LMG 26839^T, (10) *Pseudomonas seleniipraecipitans* LMG 25475^T, (11) *Pseudomonas straminea* LMG 21615^T, (12) cluster C: strain P4, (13) cluster C: strain P28, (14) cluster C: strain P30, (15) *Pseudomonas stutzeri* LMG 11199^T, (16) *Pseudomonas azotifigens* LMG 23662^T, (17) *Pseudomonas balearica* LMG 18376^T, (18) *Pseudomonas xanthomarina* LMG 23572^T

^T = type strain. +: 100 % of strains positive; -: 100 % of strains negative; w+: 100 % of strains weakly positive.

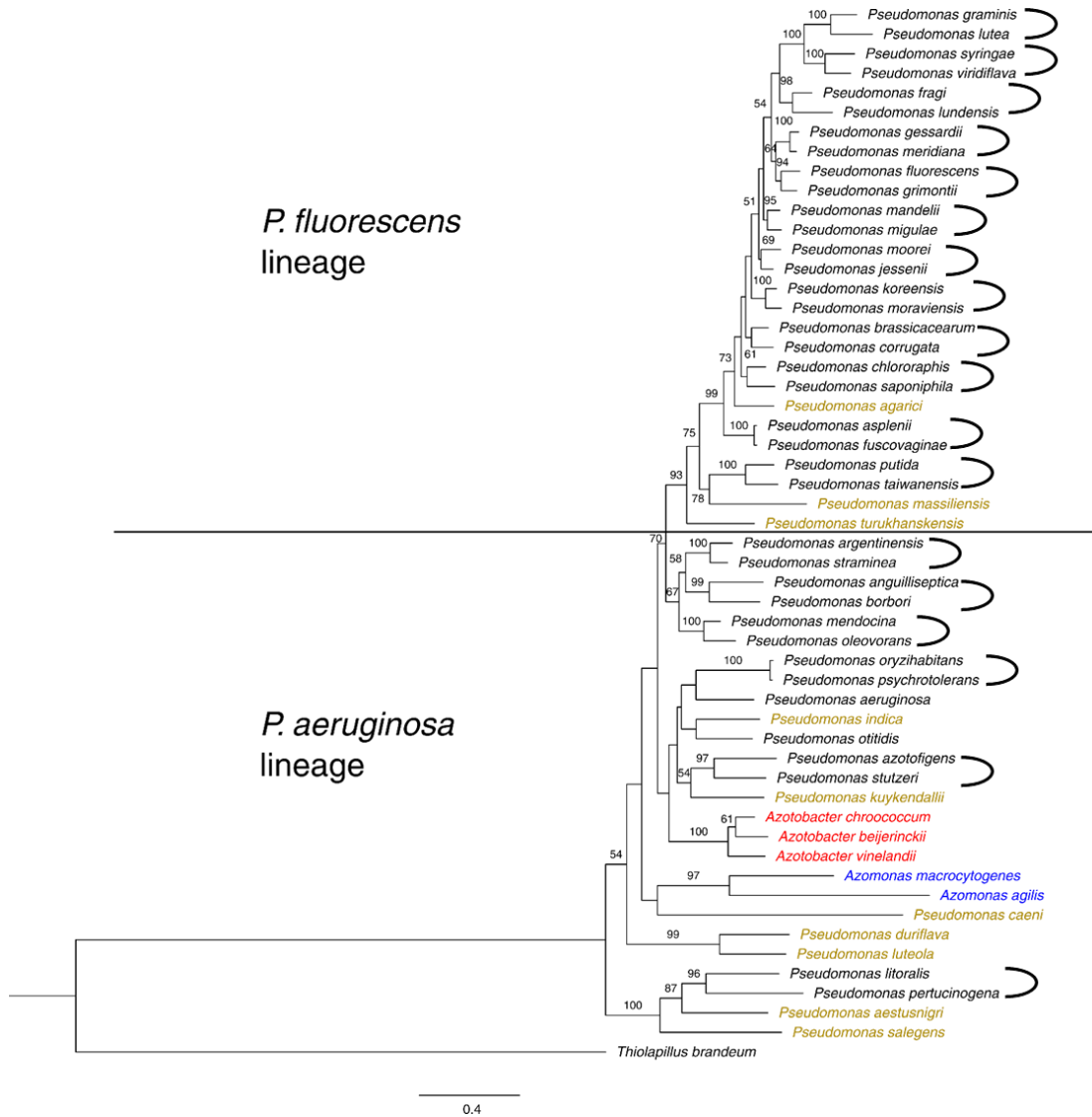
APPENDIX IX: ML 16S rRNA phylogenetic tree of selected *Pseudomonas* species, and all available members of *Azotobacter*, *Azomonas* and *Azorhizophilus*.



0.2

Appendix IX: ML 16S rRNA phylogenetic tree of selected *Pseudomonas* species, and all available members of *Azotobacter*, *Azomonas* and *Azorhizophilus*. The species included in this study were the representatives from each of the 19 *Pseudomonas* groups described in Gomila *et al.* (2015), an extra species per group, the 10 *Pseudomonas* outliers of the genus (in brown), 6 *Azotobacter* species (in red), 3 *Azomonas* species (in blue), the *Azorhizophilus* species (in green), and the outgroup, *Thiolapillus brandeum*. Phylogenetic relationships amongst the 59 strains were inferred from a dataset of partial nucleotide sequences 1328 bp long using the program PhyML. Bootstrap values were obtained from 1000 replicates and values below 50 % are considered low support and were removed from the branches. The scale bar indicates the nucleotide substitutions per site. Species names and strain numbers are shown next to the branches. \supset = pairs formed by the *Pseudomonas* species representative of each of Gomila's groups, and the extra species from the same group (Gomila *et al.*, 2015). $^{\text{T}}$ = type strain.

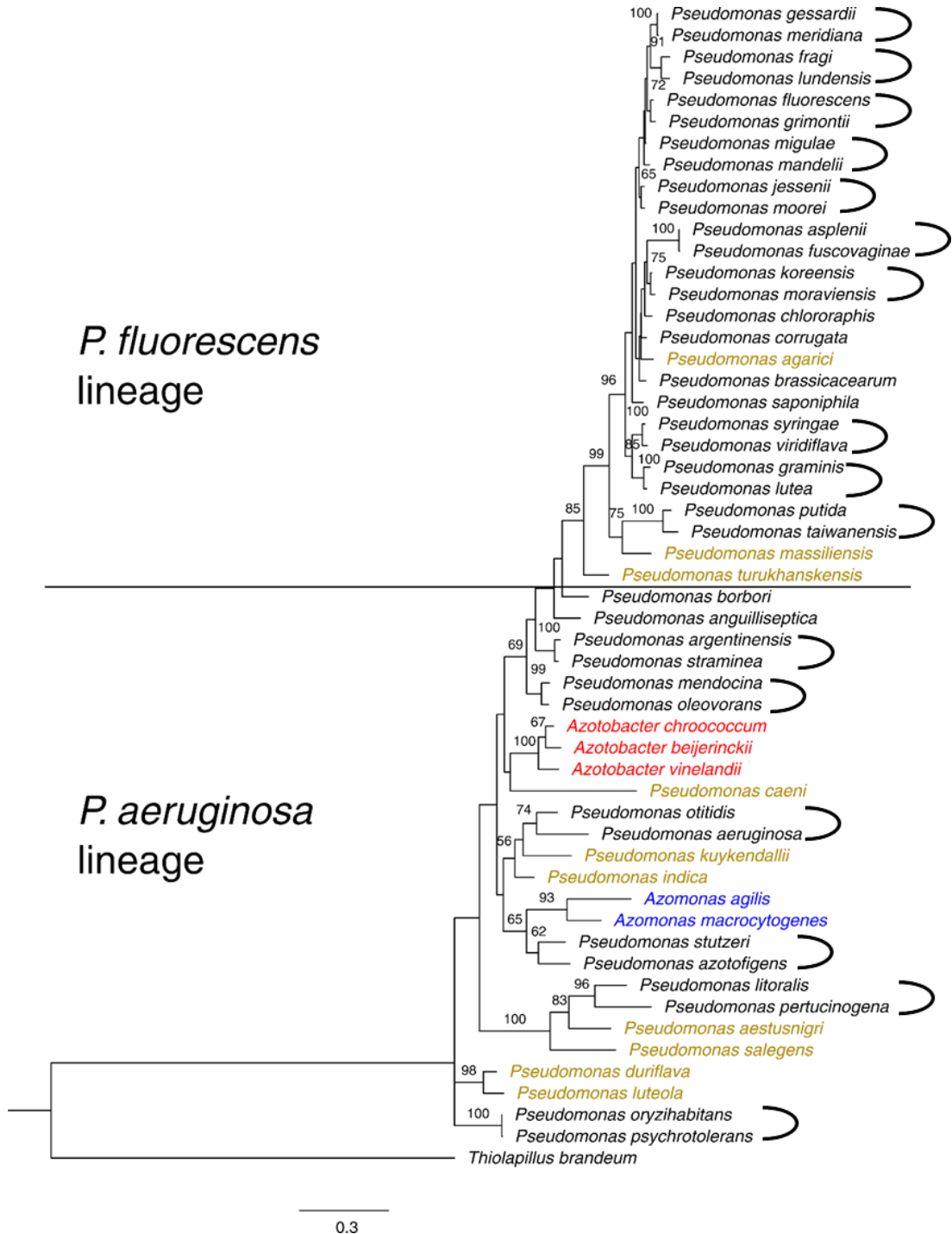
APPENDIX X: ML MLSA phylogenetic tree of selected *Pseudomonas* species, and all available members of *Azotobacter*, *Azomonas* and *Azorhizophilus*.



Appendix X: ML MLSA phylogenetic tree of selected *Pseudomonas* species, and all available members of *Azotobacter*, *Azomonas* and *Azorhizophilus*. The species included in this study were the representatives from each of the 19 *Pseudomonas* groups described in Gomila *et al.* (2015), an extra species per group, the 10 *Pseudomonas* outliers of the genus (in brown), 3 *Azotobacter* species (in red), 2 *Azomonas* species (in blue), and the outgroup, *Thiopillius brandeum*. Phylogenetic relationships amongst the 54 strains were inferred from a dataset of partial concatenated concatenated *gyrB* – 807 bp, *rpoB* – 915 bp and *rpoD* – 759 bp genes, using the program PhyML. Bootstrap values were obtained from 1000 replicates and values below 50 % are considered low support and were removed from the branches. The scale bar

indicates the nucleotide substitutions per site. Species names are shown next to the branches, strains and accession numbers are available in **Appendix X**. \supset = pairs formed by the *Pseudomonas* species representative of each of Gomila's groups, and the extra species from the same group (Gomila et al., 2015). $^{\text{T}}$ = type strain.

APPENDIX XI: ML MLSA phylogenetic tree of selected *Pseudomonas* species, and all available members of *Azotobacter*, *Azomonas* and *Azorhizophilus*.



Appendix XI: ML MLSA phylogenetic tree of selected *Pseudomonas* species, and all available members of *Azotobacter*, *Azomonas* and *Azorhizophilus*. The species included in this study were the representatives from each of the 19 *Pseudomonas* groups described in Gomila et

al. (2015), an extra species per group, the 10 *Pseudomonas* outliers of the genus (in brown), 3 *Azotobacter* species (in red), 2 *Azomonas* species (in blue), and the outgroup, *Thiolapillus brandeum*. Phylogenetic relationships amongst the 54 strains were inferred using the program PhyML. The dataset were 54 amino acid sequences (827 amino acids long), translated from the concatenated genes *gyrB*, *rpoB* and *rpoD*. Bootstrap values were obtained from 1000 replicates and values below 50 % are considered low support and were removed from the branches. The scale bar indicates the nucleotide substitutions per site. Species names are shown next to the branches, strains and accession numbers are available in APPENDIX X. \supset = pairs formed by the *Pseudomonas* species representative of each of Gomila's groups, and the extra species from the same group (Gomila et al., 2015). ^T = type strain.

APPENDIX XII: Genbank accession numbers for the 16S rRNA genes used for the 16S rRNA sequence analysis, and for the housekeeping genes *gyrB*, *rpoB* and *rpoD*, used in the MLSA, performed to study the phylogenetic relationships amongst the genera: *Pseudomonas*, *Azotobacter*, *Azomonas* and *Azorhizophilus*.

Appendix XII: GenBank accession numbers for the 16S rRNA genes used for the 16S rRNA sequence analysis, and for the housekeeping genes *gyrB*, *rpoB* and *rpoD*, used in the MLSA performed to study the phylogenetic relationships amongst the genera: *Pseudomonas*, *Azotobacter*, *Azomonas* and *Azorhizophilus*. The strains chosen are the representative species from each of the *Pseudomonas* groups according to Gomila *et al.* (2015), in blue, and another member of each of the groups. In addition, all *Pseudomonas* outliers and all available *Azotobacter*, *Azomonas* and *Azorhizophilus* strains were added to the analysis. ^T = type.

	Species	16S rRNA (strain and accession)	<i>gyrB</i> (strain and accession)	<i>rpoB</i> (strain and accession)	<i>rpoD</i> (strain and accession)
<i>P. fluorescens</i> lineage	<i>P. fluorescens</i>	ATCC 13525 ^T (NR_114476)	ATCC 13525 ^T (LT907842)	ATCC 13525 ^T (LT907842)	ATCC 13525 ^T (LT907842)
	<i>P. grimontii</i>	CFML 97-514 ^T (AF268029)	CIP 106645 ^T (FN554188)	CIP 106645 ^T (AJ717439)	CIP 106645 ^T (FN554470)
	<i>P. gessardii</i>	DSM 17152 ^T (MNPU01000117)	DSM 17152 ^T (MNPU01000041)	DSM 17152 ^T (MNPU01000034)	DSM 17152 ^T (MNPU01000009)
	<i>P. meridiana</i>	CMS 38 ^T (AJ537602)	CIP 108465 ^T (FN554203)	CIP 108465 ^T (FN554740)	CIP 108465 ^T (FN554485)

<i>P. fragi</i>	NRRL B-727 ^T (LT629783)	NRRL B-727 ^T (LT629783)	NRRL B-727 ^T (LT629783)	NRRL B-727 ^T (LT629783)
<i>P. lundensis</i>	DSM 6252 ^T (KX186958)	DSM 6252 ^T (JYKY01000016)	DSM 6252 ^T (JYKY01000022)	DSM 6252 ^T (JYKY01000028)
<i>P. jessenii</i>	CIP 105274 ^T (AF068259)	DSM 17150 ^T (NIWT01000005)	DSM 17150 ^T (NIWT01000010)	DSM 17150 ^T (NIWT01000005)
<i>P. moorei</i>	RW10 ^T (AM293566)	RW10 ^T (AM293560)	CCUG 53114 ^T (FN554742)	CCUG 53114 ^T (FN554489)
<i>P. koreensis</i>	Ps 9-14 ^T (AF468452)	LMG 21318 ^T (FN554194)	LMG 21318 ^T (FN554737)	LMG 21318 ^T (FN554476)
<i>P. moraviensis</i>	CCM 7280 ^T (AY970952)	DSM 16007 ^T (FN554206)	DSM 16007 ^T (FN554743)	DSM 16007 ^T (FN554490)
<i>P. mandelii</i>	NBRC 103147 ^T (NR_114216)	NBRC 103147 ^T (BDAF01000048)	NBRC 103147 ^T (BDAF01000029)	NBRC 103147 ^T (BDAF01000023)
<i>P. migulae</i>	NBRC 103157 ^T (NR_114223)	NBRC 103157 ^T (BDAG01000001)	NBRC 103157 ^T (BDAG01000010)	NBRC 103157 ^T (BDAG01000005)
<i>P. chlororaphis</i>	DSM 50083 ^T (Z76673)	DSM 50083 ^T (UYXS01000009)	DSM 50083 ^T (UYXS01000010)	DSM 50083 ^T (UYXS01000008)
<i>P. saponiphila</i>	DSM 9751 ^T (FM208264)	DSM 9751 ^T (HE800483)	DSM 9751 ^T (HE800515)	DSM 9751 ^T (FNTJ01000001)
<i>P. corrugata</i>	NCPPB 2445 ^T (RBOJ01000029)	NCPPB 2445 ^T (RBOJ01000096)	NCPPB2445 ^T (RBOJ01000064)	NCPPB2445 ^T (RBOJ01000090)
<i>P. brassicacearum</i>	LMG 21623 ^T (Ga0074657)	LMG 21623 ^T (Ga0074657)	LMG 21623 ^T (Ga0074657)	LMG 21623 ^T (Ga0074657)
<i>P. asplenii</i>	ATCC 23835 ^T (NR_040802)	ATCC 23835 ^T (LT629777)	ATCC 23835 ^T (LT629777)	ATCC 23835 ^T (LT629777)

	<i>P. fuscovaginae</i>	LMG 2158 ^T (NZ_LT629972)	LMG 2158 ^T (FN554185)	LMG 2158 ^T (AJ717433)	LMG 2158 ^T (FN554467)
	<i>P. syringae</i>	ICMP 3023 ^T (AJ308316)	ICMP 3023 ^T (LJRK01000078)	ICMP 3023 ^T (LJRK01000035)	ICMP 3023 ^T (LJRK01000140)
	<i>P. viridiflava</i>	CECT 458 ^T (AY180972)	ICMP 2848 ^T (LKEH01000023)	ICMP 2848 ^T (LKEH01000046)	ICMP 2848 ^T (LKEH01000048)
	<i>P. lutea</i>	OK2 ^T (AY364537)	LMG 21974 ^T (FOEV01000001)	LMG 21974 ^T (FOEV01000026)	LMG 21974 ^T (FN554480)
	<i>P. graminis</i>	DSM 11363 ^T (NR_026395)	DSM 11363 ^T (FOHW01000005)	DSM 11363 ^T (FOHW01000028)	DSM 11363 ^T (FOHW01000007)
	<i>P. putida</i>	NBRC 14164 ^T (NR_113651)	NBRC 14164 ^T (AP013070)	NBRC 14164 ^T (AP013070)	NBRC 14164 ^T (AP013070)
	<i>P. taiwanensis</i>	DSM 21245 ^T (NR_116172)	DSM 21245 ^T (HE800487)	DSM 21245 ^T (AUEC01000049)	DSM 21245 ^T (AUEC01000022)
<i>P. aeruginosa</i> lineage	<i>P. anguilliseptica</i>	DSM 12111 ^T (FNSCO1000001)	DSM 12111 ^T (FNSCO1000001)	DSM 12111 ^T (FNSCO1000001)	DSM 12111 ^T (FNSCO1000001)
	<i>P. borbori</i>	R-20821 ^T (AM114527)	DSM 17834 ^T (FOWX01000035)	DSM 17834 ^T (FOWX01000052)	DSM 17834 ^T (FOWX01000004)
	<i>P. straminea</i>	JCM 2783 ^T (LC420056)	JCM 2783 ^T (FOMO01000001)	JCM 2783 ^T (FOMO01000017)	JCM 2783 ^T (FOMO01000013)
	<i>P. argentinensis</i>	LMG 22563 ^T (FORC01000014)	LMG 22563 ^T (FN554170)	LMG 22563 ^T (FN554728)	LMG 22563 ^T (FN554451)
	<i>P. aeruginosa</i>	DSM 50071 ^T (HE978271)	DSM 50071 ^T (CP012001)	DSM 50071 ^T (CP012001)	DSM 50071 ^T (CP012001)
	<i>P. otitidis</i>	MCC10330 ^T (AY953147)	DSM 17224 ^T (FOJP01000007)	DSM 17224 ^T (FOJP01000039)	DSM 17224 ^T (FOJP01000001)

	<i>P. oleovorans</i>	NCTC10692 ^T (NZ_UGUV01000002)	NCTC10692 ^T (UGUV01000002)	NCTC10692 ^T (UGUV01000002)	NCTC10692 ^T (UGUV01000002)
	<i>P. mendocina</i>	NCTC10897 ^T (LR134290)	NCTC10897 ^T (LR134290)	NCTC10897 ^T (LR134290)	NCTC10897 ^T (LR134290)
	<i>P. oryzihabitans</i>	NBRC 102199 ^T (NR_114041)	NBRC 102199 ^T (BBIT01000005)	NBRC 102199 ^T (BBIT01000030)	NBRC 102199 ^T (BBIT01000024)
	<i>P. psychrotolerans</i>	DSM 15758 ^T (FMWB01000061)	DSM 15758 ^T (FMWB01000002)	DSM 15758 ^T (FMWB01000040)	DSM 15758 ^T (FMWB01000007)
	<i>P. stutzeri</i>	CGMCC 1.1803 ^T (NC_015740)	CGMCC 1.1803 ^T (CP002881)	CGMCC 1.1803 ^T (CP002881)	CGMCC 1.1803 ^T (CP002881)
	<i>P. azotofigens</i>	6H33b ^T (AB189452)	DSM 17556 ^T (FN554174)	DSM 17556 ^T (FN554729)	DSM 17556 ^T (AUDU01000018)
	<i>P. pertucinogena</i>	NBRC 14163 ^T (AB680571)	JCM 11590 ^T (DQ350613)	LMG 1874 ^T (AJ717441)	LMG 1874 ^T (FN554502)
	<i>P. litoralis</i>	2SM5 ^T (FN908483)	2SM5 ^T (LT629748)	2SM5 ^T (LT629748)	2SM5 ^T (LT629748)
Outliers	<i>P. agarici</i>	NCPPB 2289 ^T (AKBQ01000002)	NCPPB 2289 ^T (JH730892)	NCPPB 2289 ^T (AKBQ01000001)	NCPPB 2289 ^T (JH730859)
	<i>P. indica</i>	NBRC 103045 ^T (NR_114196)	NBRC 103045 ^T (BDAC01000026)	NBRC 103045 ^T (BDAC01000045)	NBRC 103045 ^T (BDAC01000009)
	<i>P. luteola</i>	NBRC 103146 ^T (AB681955)	NBRC 103146 ^T (BDAE01000001)	NBRC 103146 ^T (BDAE01000048)	NBRC 103146 ^T (BDAE01000022)
	<i>P. duriflava</i>	CGMCC 1.6858 ^T (VLKY01000058)	CGMCC 1.6858 ^T (VLKY01000002)	CGMCC 1.6858 ^T (VLKY01000034)	CGMCC 1.6858 ^T (VLKY01000003)
	<i>P. caeni</i>	HY-14 ^T (EU620679)	DSM 24390 ^T (ATXQ01000007)	DSM 24390 ^T (ATXQ01000015)	DSM 24390 ^T (ATXQ01000003)
	<i>P. turukhanskensis</i>	IB-1.1 ^T (KP306892)	IB-1.1 ^T (LT219440)	IB-1.1 ^T (LT219439)	IB-1.1 ^T (LT219438)

	<i>P. massiliensis</i>	CB1 ^T (CCYK01000003)	CB1 ^T (CCYK01000005)	CB1 ^T (CCYK01000007)	CB1 ^T (CCYK01000004)
	<i>P. kuykendallii</i>	NRRL B-59562 ^T (FNNU01000014)	NRRL B-59562 ^T (FNNU01000007)	NRRL B-59562 ^T (FNNU01000011)	NRRL B-59562 ^T (FNNU01000001)
	<i>P. aestusnigri</i>	CECT 8317 ^T (FNVE01000026)	CECT 8317 ^T (FNVE01000006)	CECT 8317 ^T (FNVE01000022)	CECT 8317 ^T (FNVE01000004)
	<i>P. salegens</i>	CECT 8338 ^T (LT629787)			
Azotobacter, Azomonas and Azorhizophilus	<i>Azotobacter beijerinckii</i>	ATCC 19360 ^T (AJ308319)	DSM 378 ^T (FOFJ01000003)	DSM 378 ^T (FOFJ01000074)	DSM 378 ^T (FOFJ01000015)
	<i>Azotobacter chroococcum</i>	ATCC 9043 ^T (SJAA01000087)	ATCC 9043 ^T (SJAA01000080)	ATCC 9043 ^T (SJAA01000040)	ATCC 9043 ^T (SJAA01000042)
	<i>Azotobacter vinelandii</i>	CA ^T (CP005094)	CA ^T (CP005094)	CA ^T (CP005094)	CA ^T (CP005094)
	<i>Azomonas macrocytogenes</i>	CECT 4462 ^T (Ga0372387_45)	CECT 4462 ^T (Ga0372387_05)	CECT 4462 ^T (Ga0372387_04)	CECT 4462 ^T (Ga0372387_01)
	<i>Azomonas agilis</i>	NBRC 102607 ^T (NR_114164)	DSM 375 ^T (VLKG01000011)	DSM 375 ^T (VLKG01000014)	DSM 375 ^T (VLKG01000009)
Outgroup	<i>Thiolapillus brandeum</i>	Hiromi 1 ^T (NR_148757)	Hiromi 1 ^T (AP012273)	Hiromi 1 ^T (AP012273)	Hiromi 1 ^T (AP012273)
No MLSA genes data available	<i>Azomonas insignis</i>	NBRC 102609 (AB681884)			
	<i>Azotobacter armeniacus</i>	DSM 2284 ^T (AB175655)			
	<i>Azotobacter nigricans</i>	IAM 15005 ^T (AB175651)			
	<i>Azotobacter salinestris</i>	ATCC 49674 ^T (AB175656)			

	<i>Azorhizophilus paspali</i>	ICMP 7469 ^T (AJ308318)			
--	-------------------------------	-----------------------------------	--	--	--

APPENDIX XIII: Presence/absence chart of phytopathogenic virulence factors in the genomes of AOD-associated *Pseudomonas* and other *Pseudomonas* species.

Appendix XIII: Presence/absence chart of phytopathogenic virulence factors in the genomes of AOD-associated *Pseudomonas* and other *Pseudomonas* species. Data obtained from the VFAnalyzer in the Virulence Factors of Pathogenic Bacteria database (Liu et al., 2019). Some of the values for related genes are lower than the values of genes found in the genome because several copies from the same gene were found in the genome.

Virulence factors	Related genes	1	2	3	4	5	6	7	8	9	10	11	12	13	14	15	16	17	18	19
Adherence																				
Type IV pili biosynthesis	24	19	17	11	+	+	+	21	11	22	14	12	23	11	11	11	+	18	19	19
Type IV pili twitching motility related proteins	10	8	8	2	+	+	+	+	6	6	6	8	9	6	6	6	8	6	6	6
Lipopolysaccharide O-antigen	1	2	6	-	+	+	+	+	-	-	-	-	-	-	-	-	-	-	-	-
Flagella	46	45	+	44	+	45 / 1*	+	+	+	+	+	+	+	+	+	+	+	+	+	+
Flp type IV pili	4	-	+	+	-	-	-	-	-	-	-	-	-	-	-	-	-	-	-	-
Mannose-sensitive hemagglutinin (Msh) pilus, type IV pili	2	-	-	+	-	-	-	-	-	-	-	-	-	-	-	-	-	-	-	-
Polar flagella	1	+	+	+	-	-	-	-	-	-	-	-	-	-	-	-	-	-	-	-
Antimicrobial activity																				
Phenazines biosynthesis	17	-	-	-	+	16	+	+	-	-	-	-	-	-	-	-	-	-	-	-
Antiphagocytosis																				
Alginate biosynthesis	13	3	3	4	+	+	+	+	+	+	+	+	+	+	+	+	+	4	+	+

Alginate regulation	12	1 0	1 0	8	+	+	+	+	9	9	9	9	1 1	9	9	9	1 1	10	10	10
Capsular polysaccharide	1	+	+	+	-	-	-	-	-	-	-	-	-	-	-	-	-	-	-	-
Capsule	5	+	-	+	-	-	-	-	-	-	-	-	-	-	-	-	-	-	-	-
Biosurfactant																				
Rhamnolipid biosynthesis	3	-	-	-	+	2	+	+	-	-	-	1	-	-	-	-	-	-	-	-
Enzyme																				
Hemolytic phospholipase C	1	-	-	-	+	+	+	+	-	-	-	-	-	-	-	-	-	-	-	-
Non-hemolytic phospholipase C	1	-	-	-	+	+	+	+	-	-	+	-	-	-	-	-	-	-	-	-
Phospholipase C	1	-	-	-	+	+	+	+	-	-	-	-	-	-	-	-	-	-	-	-
Phospholipase D	1	-	-	-	-	-	+	+	-	-	-	-	-	-	-	-	-	-	-	-
Iron uptake																				
Pyoverdine	16	1	1 4	1 7	+	+	+	+	1 2	-	+	-	-	1 0	1 2	1 3	-	-	-	-
Pyoverdine receptors	1	9	5	1 5	-	3	-	-	+	-	-	-	-	+	+	-	-	+	+	-
Pyochelin	10	-	-	-	-	-	-	-	3	-	-	-	-	-	-	-	-	+	-	+
Pyochelin receptor	1	-	-	+	+	15	+	+	-	1 0	14	1 4	3	-	-	-	-	12	12	11
Achromobactin biosynthesis and transport	8	9	9	-	+	+	+	+	-	+	+	+	+	-	-	-	-	+	+	+
Yersiniabactin	9	-	-	3	+	+	+	+	-	-	9	-	-	-	-	-	-	2	-	2
Enterobactin transport	1	+	+	-	-	-	-	-	-	-	-	-	-	-	-	-	-	-	-	-
Ferrous iron transport	1	+	+	+	-	-	-	-	-	-	-	-	-	-	-	-	-	-	-	-
Heme utilization	1	+	+	+	-	-	-	-	-	-	-	-	-	-	-	-	-	-	-	-
Iron/managanease transport	3	+	+	+	-	-	-	-	-	-	-	-	-	-	-	-	-	-	-	-
Iron acquisition																				

Enterobactin siderophore	1	-	-	+	-	-	-	-	-	-	-	-	-	-	-	-	-	-	-	-	-	
Protease																						
Elastase	2	-	-	-	+	+	+	+	-	-	-	-	-	-	-	-	-	-	-	-	-	
Alkaline protease	1	-	-	-	+	+	+	+	+	+	+	+	-	-	-	-	-	-	-	+	+	
Protease IV	1	-	-	-	+	+	+	+	-	-	-	-	-	-	-	-	-	-	-	-	-	
Quorum sensing																						
N-(butanoyl)-L-homoserine lactone QS system	2	-	-	-	+	+	+	+	-	-	-	-	-	-	-	-	-	-	-	-	-	
N-(3-oxo-dodecanoyl)-L-homoserine lactone QS system	2	-	-	-	+	+	+	+	-	-	-	1	-	-	-	-	-	-	-	-	-	
N-(3-oxo-hexanoyl)-L-homoserine lactone QS system	2	-	-	-	-	-	-	-	-	-	-	-	-	-	-	-	-	-	+	+	+	
Acylhomoserine lactone synthase	1	+	+	+	+	+	+	+	+	+	+	+	+	+	+	+	+	+	+	+	+	
Regulation																						
GacS/GacA two-component system	2	+	+	+	+	+	+	+	+	+	+	+	+	+	+	+	+	+	+	+	+	
Secretion system																						
Type III secretion system (T3SS)	1	+	+	-	-	-	-	-	-	-	-	-	-	-	-	-	-	-	-	-	-	
<i>P. aeruginosa</i> T3SS	36	2	2	-	3	3	-	+	+	-	-	-	-	-	-	-	-	-	-	-	-	
<i>P. aeruginosa</i> T3SS translocated effectors	4	-	-	-	3	-	3	3	-	-	-	-	-	-	-	-	-	-	-	-	-	
<i>P. syringae</i> T3SS	32	-	-	-	-	-	-	-	-	-	-	-	-	-	-	-	-	-	27	26	+	
Harpins, pilus-associated proteins and other candidate T3SS helpers	6	-	-	-	-	-	-	-	-	-	-	-	-	-	-	-	-	-	4	4	5	
<i>P. syringae</i> T3SS effectors	81	2	2	2	-	-	-	-	-	-	-	-	-	-	-	-	-	-	30 / 3	23 / 1	47 / 6	
Hcp secretion island-1 encoded type VI secretion system (H-T6SS)	21	+	+	1	+	+	+	+	-	-	20	2	2	0	0	9	8	7	-	6	10	5

EPS type II secretion system	2	-	+	-	-	-	-	-	-	-	-	-	-	-	-	-	-	-	-	-
T4SS effectors	1	+	+	+	-	-	-	-	-	-	-	-	-	-	-	-	-	-	-	-
Toxin																				
Exotoxin-A (ETA)	1	-	-	-	-	+	-	-	-	+	1/ 1	-	-	-	-	-	-	-	-	-
Phytotoxin coronatine	20	1	2	1	+	-	+	+	-	-	-	-	-	-	-	-	-	-	-	-
Phytotoxin phaseolotoxin	21	-	-	-	-	-	-	-	-	-	-	-	-	-	-	-	-	-	-	+
Phytotoxin syringopeptin	3	-	-	-	-	-	-	-	-	-	-	-	-	-	-	-	-	+	-	-
Phytotoxin syringomycin	7	-	-	-	-	-	-	-	-	-	-	-	-	-	-	-	-	-	+	-
Hydrogen cyanide production	3	-	-	-	-	-	-	-	+	-	-	-	-	-	-	-	-	-	+	-
TccC-type insecticidal toxins	1	-	-	-	+	+	+	+	+	+	+	-	-	-	-	-	-	-	-	-
Exolysin	2	-	-	-	-	-	-	-	+	+	-	-	-	1	+	+	-	+	+	+
Alpha-hemolysin	1	-	+	+	-	-	-	-	-	-	-	-	-	-	-	-	-	-	-	-
Amino acid and purine metabolism																				
Purine synthesis	1	+	+	+	-	-	-	-	-	-	-	-	-	-	-	-	-	-	-	-
Efflux pump																				
AcrAB	1	+	+	+	-	-	-	-	-	-	-	-	-	-	-	-	-	-	-	-
Endotoxin																				
Lipooligosaccharide	1	+	+	+	-	-	-	-	-	-	-	-	-	-	-	-	-	-	-	-
Stress adaptation																				
Catalase	1	-	+	-	-	-	-	-	-	-	-	-	-	-	-	-	-	-	-	-
Catalase-peroxidase	1	+	+	+	-	-	-	-	-	-	-	-	-	-	-	-	-	-	-	-
Superoxide dismutase SodCI	1	+	+	+	-	-	-	-	-	-	-	-	-	-	-	-	-	-	-	-
Others																				
O-antigen	2	+	+	+	-	-	-	-	-	-	-	-	-	-	-	-	-	-	-	-
Virulence-associated proteins	1	-	+	-	-	-	-	-	-	-	-	-	-	-	-	-	-	-	-	-

Immune evasion																				
Capsule	8	-	+	-	-	-	-	-	-	-	-	-	-	-	-	-	-	-	-	-

1. *Pseudomonas daroniae* sp. nov. P2^T, QJUH00000000, 2. *Pseudomonas dryadis* sp. nov. P27^T, QJUN00000000, 3. *Pseudomonas kirkieae* sp. nov. P4^T, QJUO00000000, 4. *Pseudomonas aeruginosa* LESB58, NC_011770, 5. *Pseudomonas aeruginosa* PA7, NC_009656, 6. *Pseudomonas aeruginosa* PAO1, NC_002516, 7. *Pseudomonas aeruginosa* UCBPP-PA14, NC_008463, 8. *Pseudomonas entomophila* L48, NC_008027, 9. *Pseudomonas fluorescens* Pf0-1, NC_007492, 10. *Pseudomonas fluorescens* Pf-5, NC_004129, 11. *Pseudomonas fluorescens* SBW25, NC_012660, 12. *Pseudomonas mendocina* ymp, NC_009439, 13. *Pseudomonas putida* GB-1, NC_010322, 14. *Pseudomonas putida* KT2440, NC_002947, 15. *Pseudomonas putida* W619, NC_010501, 16. *Pseudomonas stutzeri* A1501, NC_009434, 17. *Pseudomonas syringae* pv. *phaseolicola* 1448A, NC_005773, 18. *Pseudomonas syringae* pv. *syringae* B728a, NC_007005, 19. *Pseudomonas syringae* pv. *tomato* DC3000, NC_004578.

-: All related genes absent.

+: All related genes present.

*45 / 1: 45 related genes present / 1 related gene inactive.

Appendix XIV: Optical density values obtained at 590 nm in the cell attachment assays.

Appendix XIV: Optical density values obtained at 590 nm in the cell attachment assays.

Species	Six-well plate's assay in TSB broth			Tube-coverslip assay in LB broth		
	OD _{590nm}			OD _{590nm}		
	Rep. 1	Rep. 2	Rep. 3	Rep. 1	Rep. 2	Rep. 3
Pda P2 ^T	0.091	0.133	0.055	0.01	0.016	0.016
Pda P9	0.161	0.099	0.092	0.009	0.02	0.041
Pda P18	0.303	0.266	0.224	0.02	0.019	0.019
Pdr P27 ^T	0.167	0.087	0.045	0.014	0.025	0.025
Pdr P6	0.069	0.087	0.045	0.043	0.103	0.033
Pdr P26	0.2	0.166	0.1	0.014	0.028	0.027
<i>P. punonensis</i>	0.569	0.532	0.554	0.033	0.034	0.063
<i>P. flavescens</i>	0.468	0.548	0.458	0.055	0.041	0.041
<i>P. straminea</i>	0.702	0.696	0.66	0.088	0.077	0.077
<i>P. argentinensis</i>	0.221	0.242	0.322	0.071	0.066	0.066
<i>P. seleniipraecipitans</i>	0.133	0.137	0.261	0.054	0.046	0.084
<i>Pph 1302A</i>	0.104	0.074	0.06	0.008	0.003	0.003
<i>P. fulva</i>	0.572	0.547	0.522	0.42	0.206	0.176
NIC	0	0	0	0	0	0
Pki P4 ^T	0.003	0.012	0.011	0.26	0.345	0.39
Pki P28	0.011	0.009	0.01	0.06	0.029	0.011

Species	Tube-coverslip assay in TSB broth		
	OD _{590nm}		
	Rep. 1	Rep. 2	Rep. 3
Pki P4 ^T	0.015	0.016	0.017
Pki P28	0.009	0.014	0.01
Pki P30	0.013	0.013	0.013
<i>P. stutzeri</i>	0.013	0.009	0.009
<i>P. xanthomarina</i>	0.019	0.02	0.027
<i>P. balearica</i>	0.026	0.027	0.016
<i>P. azotifigens</i>	0.015	0.015	0.015
<i>P. fulva</i>	0.132	0.133	0.148
NIC	0	0	0

Pki P30	0.011	0.018	0.017	0.105	0.123	0.147
<i>P. stutzeri</i>	0.01	0.021	0.011	0.013	0.033	0.021
<i>P. xanthomarina</i>	0.01	0.01	0.028	0.016	0.011	0.01
<i>P. balearica</i>	0.079	0.098	0.074	0.088	0.052	0.092
<i>P. azotifigens</i>	0.769	0.641	0.507	0.041	0.04	0.011
<i>P. fulva</i>	0.099	0.088	0.098	0.22	0.232	0.128
NIC	0	0	0	0	0	0

Pda: *Pseudomonas daroniae* sp. nov. Pdr: *Pseudomonas dryadis* sp. nov. Pki: *Pseudomonas kirkieae* sp. nov. Pph: *Pseudomonas syringae* pv. *phaseolicola*. NIC: no inoculum control. Rep. = replicate. ^T = type strain.

Strain numbers: *Pseudomonas flavescens* LMG 18387^T, *Pseudomonas argentinensis* LMG 22563^T, *Pseudomonas punonensis* LMG 26839^T, *Pseudomonas seleniipraecipitans* LMG 25475^T, *Pseudomonas straminea* LMG 21615^T, *Pseudomonas stutzeri* LMG 11199^T, *Pseudomonas azotifigens* LMG 23662^T, *Pseudomonas balearica* LMG 18376^T, *Pseudomonas xanthomarina* LMG 23572^T.